



Statistical descriptions of polydisperse turbulent two-phase flows

Jean-Pierre Minier

EDF, R&D, MFEE, 6 quai Watier, Chatou 78400, France



ARTICLE INFO

Article history:

Accepted 17 October 2016

Available online 11 November 2016

Editor: I. Procaccia

Keywords:

Turbulence

Two-phase flows

Stochastic modeling

Statistical descriptions

ABSTRACT

Disperse two-phase flows are flows containing two non-miscible phases where one phase is present as a set of discrete elements dispersed in the second one. These discrete elements, or ‘particles’, can be droplets, bubbles or solid particles having different sizes. This situation encompasses a wide range of phenomena, from nano-particles and colloids sensitive to the molecular fluctuations of the carrier fluid to inertia particles transported by the large-scale motions of turbulent flows and, depending on the phenomenon studied, a broad spectrum of approaches have been developed.

The aim of the present article is to analyze statistical models of particles in turbulent flows by addressing this issue as the extension of the classical formulations operating at a molecular or meso-molecular level of description. It has a three-fold purpose: (1) to bring out the thread of continuity between models for discrete particles in turbulent flows (above the hydrodynamical level of description) and classical mesoscopic formulations of statistical physics (below the hydrodynamical level); (2) to reveal the specific challenges met by statistical models in turbulence; (3) to establish a methodology for modeling particle dynamics in random media with non-zero space and time correlations. The presentation is therefore centered on organizing the different approaches, establishing links and clarifying physical foundations.

The analysis of disperse two-phase flow models is developed by discussing: first, approaches of classical statistical physics; then, by considering models for single-phase turbulent flows; and, finally, by addressing current formulations for discrete particles in turbulent flows. This brings out that particle-based models do not cease to exist above the hydrodynamical level and offer great interest when combined with proper stochastic formulations to account for the lack of equilibrium distributions and scale separation. In the course of this study, general results for dynamical systems influenced by colored or white noises are established which point to the necessity of developing statistical models for particles in random media from a new standpoint that breaks away from descriptions based only on particle kinetic variables. This is needed to obtain well-posed formulations of particle dispersion by non fully-resolved turbulent flows and suggests also to revisit classical ideas of particle-particle interactions in the presence of a turbulent flow which correlates the dynamics of colliding discrete elements.

© 2016 Elsevier B.V. All rights reserved.

Contents

1. Introduction.....	5
2. The physics of disperse two-phase flows.....	6
2.1. Context and examples.....	6

E-mail address: jean-pierre.minier@edf.fr.

2.1.1.	Two-phase flow patterns	6
2.1.2.	The importance of the disperse two-phase flow regime	7
2.2.	The physical issues at stake	12
2.3.	Particle transport and hydrodynamical equations	12
2.3.1.	Hydrodynamical forces on particles	13
2.3.2.	Brownian effects at the continuum level	15
2.4.	A range of possible descriptions	16
3.	The microscopic, mesoscopic and macroscopic levels of description	17
3.1.	From microscopic to macroscopic descriptions in classical statistical physics	17
3.1.1.	A clear separation of scales	17
3.1.2.	The interest of classical mesoscopic descriptions	18
3.2.	From microscopic to macroscopic descriptions in disperse two-phase flows	19
3.2.1.	A clear separation of information content	19
3.2.2.	The interest of mesoscopic descriptions for single- and two-phase flows	19
4.	Mathematical background and statistical descriptions	21
4.1.	Stochastic processes	22
4.2.	Markovian and non-Markovian processes	23
4.3.	Jump and diffusion stochastic processes	24
4.3.1.	The two building blocks: the Wiener and Poisson processes	24
4.3.2.	Stochastic differential equations	26
4.3.3.	A note on Master Equations	29
4.3.4.	Another note on McKean equations	29
4.4.	From Lagrangian stochastic models to mean-field equations	30
4.5.	Criteria for acceptable probabilistic descriptions	30
4.5.1.	Complete and incomplete probabilistic descriptions	31
4.5.2.	Well-posed and ill-based PDF equations	31
5.	From the atomic to the hydrodynamical levels of description	32
5.1.	Molecular dynamics	32
5.2.	Dissipative Particle Dynamics	33
5.3.	Stochastic Rotation Dynamics	34
5.4.	Lattice Boltzmann methods	35
5.5.	Smoothed particle hydrodynamics	36
5.6.	Smoothed Dissipative Particle Dynamics	38
5.7.	Summary and classification	39
6.	Statistical descriptions of single-phase turbulence	40
6.1.	The Kolmogorov picture of turbulent flows	40
6.2.	The microscopic level: Direct numerical simulation	42
6.3.	The macroscopic level: Reynolds-averaged Navier–Stokes models	43
6.3.1.	Eddy-viscosity models	44
6.3.2.	Reynolds-stress models	44
6.4.	One mesoscopic approach: the large eddy simulation method	45
6.5.	Fine- and coarse-grained models at the mesoscopic level	47
6.5.1.	Probability density function approaches	48
6.5.2.	Filtered density function approaches	49
6.5.3.	Hybrid approaches and towards full particle simulations	50
6.6.	Summary and classification	51
6.7.	Similarities and differences with classical statistical physics	52
7.	Review of present disperse two-phase flow statistical models	53
7.1.	Models below the FR-hydrodynamical level of description	54
7.1.1.	Particle-based methods	54
7.1.2.	Lattice-Boltzmann methods	57
7.2.	Models at the FR-hydrodynamical level of description	58
7.2.1.	Brownian dynamics	58
7.2.2.	Direct numerical simulations	59
7.2.3.	SPH/discrete-particle simulations	62
7.3.	Models above the FR-hydrodynamical level of description	63
7.3.1.	The one-particle PDF modeling issue	65
7.3.2.	The kinetic PDF model	65
7.3.3.	The dynamic PDF model	66
7.4.	Summary and important points	68
8.	The challenges of statistical closures for polydisperse turbulent flows	68
8.1.	A double hierarchy for two-phase flow models	69
8.1.1.	Classical BBGKY-like hierarchies	69
8.1.2.	Hierarchies with respect to one-particle state vectors	70
8.2.	The available information: what can and cannot be calculated	70
8.3.	The importance of consistent fluid and particle descriptions	72

8.4.	Summary and relations between present statistical models	72
9.	General modeling tools and statistical closures	73
9.1.	Functional approaches and the Furutsu–Novikov–Donsker theorem	73
9.2.	Probabilistic descriptions of dynamical systems subject to white or colored noises.....	74
9.3.	Adiabatic elimination of fast variables	79
9.3.1.	Canonical overdamped Langevin model	79
9.3.2.	Relations and differences between various parametrizations	82
9.3.3.	General over-damped Langevin model	84
9.3.4.	The incompressibility constraint in the tracer-particle limit	86
9.3.5.	Applications for single-phase turbulent flows	88
9.3.6.	Applications for disperse two-phase turbulent flows	92
9.3.7.	Comments on the fast-variable elimination technique	93
9.4.	The significance of the choice of the particle state vector	93
10.	Probabilistic models for polydisperse two-phase turbulent flows	94
10.1.	Analysis of the kinetic and dynamic PDF models	94
10.1.1.	Kinetic PDF descriptions are incomplete and ill posed	94
10.1.2.	Dynamic PDF descriptions are complete and well posed	96
10.1.3.	The need of new statistical approaches for particle dispersion	96
10.1.4.	Colored noises must be included in the description	97
10.2.	Selection of the particle state vector	99
10.3.	Stochastic closures and local/non-local macroscopic constitutive relations	102
10.4.	A physical analysis of gradient-diffusion models	105
10.5.	Slow and fast variables in numerical formulations	108
10.6.	Particle collision and agglomeration rates	109
10.6.1.	Remarks on kinetic-based approaches and open issues	110
10.6.2.	Revisiting the estimation of particle collision rates	113
10.6.3.	Calculating collision/agglomeration kernels	115
10.7.	Summary	118
11.	Conclusion	118
	Acknowledgments	119
	References	119

Nomenclature

List of abbreviations

BD	Brownian Dynamics
BBGKY	Bogoliubov Born Green Kirkwood Yvon
BGK	Bhatnagar–Gross–Krook
CLT	Central Limit Theorem
DEM	Discrete Element Methods
DF	Distribution Function
DLVO	Derjaguin–Landau–Verwey–Overbeek
DNS	Direct Numerical Simulation
DPD	Dissipative Particle Dynamics
DSMC	Direct Simulation Monte Carlo
FDF	Filtered Density Function
FND	Furutsu–Novikov–Donsker
FPE	Fokker–Planck Equation
FR	Fully-Resolved (used for FR-hydrodynamical level of description)
GLM	Generalized Langevin Model
HI	Hydrodynamical Interactions
LBM	Lattice Boltzmann Method
LD	Langevin Dynamics
LES	Large-Eddy Simulation
LFDF	Lagrangian Filtered Density Function
LGA	Lattice Gas Automaton
lhs	left-hand side
LMDF	Lagrangian Mass Density Function
MD	Molecular Dynamics
MDF	Mass Density Function

NDF	Number Distribution Function
N-S	Navier–Stokes equations
OU	Ornstein–Uhlenbeck
PDE	Partial Differential Equation
PDF	Probability Density Function
RANS	Reynolds Averaged Navier–Stokes (equations)
RSM	Reynolds Stress Model (equivalent to $R_{ij} - \epsilon$ turbulence models)
rhs	right-hand side
SDPD	Smoothed Dissipative Particle Dynamics
SDE	Stochastic Differential Equation
SGS	Sub-Grid scale
SLM	Simplified Langevin Model
SPH	Smoothed Particle Hydrodynamics
SRD	Stochastic Rotation Dynamics

List of main symbols

C_D	Drag coefficient
d_p	Particle diameter [m]
g	Gravitational acceleration [m s^{-2}]
m_p	Particle mass [kg]
μ_f	Fluid dynamic viscosity [Pa s]
ν_f	Fluid kinematic viscosity [$\text{m}^2 \text{s}^{-1}$]
Γ_f	Fluid scalar diffusivity [$\text{m}^2 \text{s}^{-1}$]
κ_f	Fluid thermal conductivity [$\text{m}^2 \text{s}^{-1}$]
Re	Flow Reynolds number
Pe	Flow Peclet number
Re_p	Particle Reynolds number
ρ_f	Fluid density [kg m^{-3}]
ρ_p	Particle density [kg m^{-3}]
t	Time [s]
Θ_f	Fluid temperature [K]
τ_p	Particle relaxation timescale [s]
$\mathbf{U}_f(t, \mathbf{x})$	Fluid velocity field [m s^{-1}]
$\mathbf{u}_f(t, \mathbf{x})$	Fluctuating fluid velocity field [m s^{-1}]
$R_{f,ij} = \langle u_{f,i} u_{f,j} \rangle$	Fluid Reynolds stress tensor [$\text{m}^2 \text{s}^{-2}$]
P_f	Fluid pressure [$\text{kg m}^{-1} \cdot \text{s}^{-2}$]
$\nu_{f,t}$	Fluid eddy- or turbulent viscosity [$\text{m}^2 \text{s}^{-1}$]
\mathbf{U}_p	Particle velocity [m s^{-1}]
\mathbf{U}_r	Fluid velocity relative to the particle [m s^{-1}]
\mathbf{U}_s	Velocity of the fluid seen by particles [m s^{-1}]
\mathbf{x}_p	Particle position [m]
k_B	Boltzmann constant [$\text{m}^2 \text{kg s}^{-2} \text{K}^{-1}$]
K_{Br}	Brownian diffusion coefficient in the particle momentum equation [$\text{m s}^{-3/2}$]
D_p	Einstein diffusion coefficient
η_K	Kolmogorov length scale [m]
u_K	Kolmogorov velocity scale [m s^{-1}]
τ_K	Kolmogorov timescale [s]
k_f	Fluid turbulent kinetic energy [$\text{m}^2 \text{s}^{-2}$]
ϵ_f	Dissipation of the fluid turbulent kinetic energy [$\text{m}^2 \text{s}^{-3}$]
L_f	Length scale of the large-scale fluid turbulent motions [m]
u_f	Velocity scale of the large-scale fluid turbulent motions [m s^{-1}]
T_L	Lagrangian integral timescale of the fluid [s]

Convention for notations.

Bold symbols represent vectors or matrices.

When we are above the hydrodynamical level of description, particle variables (e.g. position \mathbf{x} and velocity \mathbf{U}) are written with an explicit index f or p to indicate that we are dealing with fluid or discrete particles, while no indexes are used when we are considering a general particle system without explicit reference to the fluid or discrete nature. When we are below the hydrodynamical level of description, no indexes are used for particles (i.e. molecules or macro-molecules).

Apart from the possible indexes f , p or t (for turbulent quantities), Latin letters are used as indexes to indicate spatial coordinates and the Einstein summation convention is applied. Superscripts are used to indicate particle labels when a set of particles are considered and the Einstein summation convention does not apply to these superscripts.

1. Introduction

Polydisperse two-phase flows are made up by discrete elements, or ‘particles’ (solid particles, droplets or bubbles having a wide range of size), embedded in a turbulent fluid flow. These flows play a key role in many applications, from pollutant transport by atmospheric flows for environmental concerns to colloidal particle deposition/resuspension for filtration systems or to design new material-surface properties, as well as in spray cooling used in several industrial processes [1,2]. There is thus considerable impetus to develop satisfactory models of the physics involved in these situations. At the same time, disperse two-phase flows exhibit complex phenomena related to the fundamental particle-turbulence and particle-particle interactions. In turn, particle-particle interactions encompass various sub-phenomena such as particle collisions, particle agglomeration/fragmentation for solid discrete elements (a process involving interface-chemistry effects) or coalescence/breakup for droplets and bubbles (a process involving surface tension effects). At the crossroads between applications and fundamental analysis, modeling disperse two-phase flows remains an open subject that raises challenging theoretical questions in Statistical Mechanics.

As for the methods in classical statistical physics ranging from molecular dynamics to the hydrodynamical level and in single-phase turbulent flows, the aim is to come up with reduced statistical descriptions of two-phase flows that contain enough information to address practical situations of interest. In polydisperse two-phase flows, particle inertia (or other characteristic responses to fluid changes) can vary over several orders of magnitude and the expression of averaged particle properties through constitutive relations is difficult. This means that attempts at deriving statistical closures must be based on fine-grained descriptions. At the hydrodynamical level, it is also possible to simulate explicitly all the degrees of freedom since the basic equations are known. However, for a large number of particles embedded in a high Reynolds-number turbulent flow, the number of degrees of freedom is huge and, though valuable to provide insights, these approaches are limited to simple situations. This explains that the issue is to build intermediate descriptions, based on stochastic models, for a reduced set of variables attached to the particles.

Even a cursory look at the available literature reveals that a wide range of methods have been developed, such as Dissipative Particle Dynamics (DPD), Langevin Dynamics (LD) or Brownian Dynamics (BD), Lattice-Boltzmann Method (LBM), Discrete Element Methods (DEM), or Probability Density Function (PDF) methods, to name just a few samples. Each approach is formulated with respect to a certain level of description and it is not, at first sight, easy to see if the principles behind these methods can be carried over to other situations corresponding to different scales. Furthermore, even within the class of models that simulate explicitly discrete particles, some formulations describe the complete set of particles while others are developed in terms of one-particle PDFs only. This question is further compounded by specific theoretical issues arising in disperse two-phase flows. For example, if particle collisions in a fluid flow are described with a classical kinetic, or Boltzmann, formulation, it can be wondered whether the molecular-chaos assumption is still valid for particles that are correlated since they are transported by the same underlying fluid. Another issue is whether there are correspondences between kinetic-based PDF formulations that rely on functional approaches, such as the Furutsu-Novikov theorem [3], and stochastic models derived from the adiabatic elimination of fast variables in dynamic-based PDF approaches [1,4,5]. The diversity in the situations concerned and the variety of existing models can be an obstacle to trans-disciplinary approaches if a hierarchical structure, or organization, of these methods is lost. A picture of the relations between various modeling formulations is therefore needed.

This article is essentially concerned with disperse two-phase flow modeling. With respect to this theme, it has several specific objectives:

- (i) To present a unified framework in which statistical descriptions developed for the ‘particle phase’ are discussed in relation with the level of description to which they correspond;
- (ii) To analyze modeling tools and how they are applied to simulate particle dynamics in random media depending on the choice of the variables attached to each particle;
- (iii) To bring out the remaining challenges for particle dynamics in turbulent flows.

However, following the arguments given above, it is best to cast these objectives into a more general framework that includes models starting at the molecular level of description and those developed for single-phase turbulent flows. It is indeed important to show that these issues have roots in corresponding formulations in classical statistical physics and are present at different levels of description. For this reason, a first choice made in this work is to build the analysis of the models for disperse turbulent two-phase flows by relating, or contrasting, them with formulations below, or at, the hydrodynamical level of description. A second choice is to present, within reasonable limits, a self-contained study which explains that, for example, the relevant characteristics of stochastic formulations and the technique of fast-variable elimination are elaborated. In line with the overall aim, which is to set up links between models and analyzing their physical foundations, a third choice is to put the emphasis not so much on the respective predictive abilities of the models but rather on their formulation, the physics contained (or left out), and on building a coherent overview.

This article is organized as follows. The basic features of the physics involved in disperse two-phase flows are presented in Section 2, along with a reminder of the fundamental equations at the hydrodynamical level of description. The notions of microscopic, mesoscopic and macroscopic levels of description, extended to include single- and two-phase turbulent flows, are introduced in Section 3 while the mathematical aspects of stochastic modeling are addressed in Section 4. The models operating between molecular dynamics and the hydrodynamical level are organized in Section 5 and the different modeling approaches developed for single-phase flow turbulence are presented in Section 6. Then, present statistical descriptions of particles in turbulent flows are discussed in Section 7. Based on these descriptions, the specific challenges met by models for particle-laden turbulent flows are analyzed in Section 8. This leads to a detailed study of the statistical techniques used as modeling tools which is developed in Section 9. These modeling tools are applied to investigate the physical foundations of current formulations in Section 10. Finally, conclusions and open issues are brought out in Section 11.

2. The physics of disperse two-phase flows

The purpose of this section is to provide an introduction to the main characteristics of disperse two-phase flows represented in the models studied in later sections. Even with this limited ambition, this is a difficult task since all the intricate details of fluid turbulence are compounded by the dynamics of a second phase. In that sense, our aim is to set the stage for the discussions to come by bringing out relevant aspects of disperse turbulent two-phase flows and by drawing a first picture in terms of fundamental interactions and levels of description.

This is done by considering a range of practical situations in Section 2.1, before developing a first analysis of the physics involved in Section 2.2. A reference hydrodynamical formulation is described in Section 2.3 and remarks on the different ways to address disperse two-phase flows are made in Section 2.4.

2.1. Context and examples

Nature being the ultimate guide and teacher, the essential features of polydisperse two-phase turbulent flows are best introduced with a selection of practical situations. These illustrations are also useful to bring out the range of challenging issues in real-life circumstances involving multi-phase flows.

2.1.1. Two-phase flow patterns

As it transpires from their name, two-phase flows refer to flows in which two non-miscible phases (solid, liquid, gas) are present, whereas single-phase flows refer to situations in which only one phase (necessarily fluid) is flowing. Starting from that definition, things start to branch out into various categories.

For instance, if we consider a two-phase flow with two non-miscible fluid phases such as a gas–liquid flow, one of the key points is how the interface between the two phases is geometrically distributed. This is of direct importance for momentum, heat and mass transfers occurring at the interface since the magnitude of these exchanges is proportional to the interface area. Experimental observations of the interface between air and water in an upward co-current flow in a vertical pipe are displayed in Fig. 1. It is seen that there are several configurations, usually called bubbly, slug, churn and annular flows, etc., where the interface between the two phases has very different characteristics. Each of these situations is referred to as a ‘two-phase flow pattern’ and the issue is to predict the pattern of a given two-phase flow as well as the changes from one ‘flow regime’ to another one when gas and liquid velocities, volumetric fractions, or other flow conditions, evolve. In the first regime (named ‘dispersed bubbly’ in Fig. 1), one phase is found as a set of small discrete elements dispersed in a continuous medium (in the present case, air bubbles in the water flow): this corresponds to a ‘disperse two-phase flow’. Although only partially visible, note that there are small liquid droplets embedded in the gas core flowing in the center of the pipe in the annular regime. Therefore, the central part of the annular pattern involves also a disperse two-phase flow, while there is a continuous liquid film along the walls which corresponds to a ‘separate two-phase flow’ between this liquid film and the gas/droplet core.

Transitions between two-phase flow regimes are found in the case of boiling water flowing in steam generator pipes (see Fig. 2(a)). As revealed by the shape of the heat flux curve in Fig. 2(b), the onset of nucleate boiling increases heat exchanges between the wall and the bulk of the flow, leading to higher values of the heat flux coefficient as more and more bubbles are created (from small preexisting gas-filled cavities in the wall surface through the process of heterogeneous nucleation). Yet, when the critical heat flux is reached, boiling is so intense that a vapor film starts to form above the wall surface, limiting further heat exchanges (this corresponds to the Leidenfrost effect [7]). In a heat-flux controlled situation, this induces sudden steps in the wall-surface temperature that put the material resistance at risk (which explains alternative names, such as the burn-out or dry-out crisis). The critical heat flux is therefore associated to a departure from nucleate boiling (DNB) in the liquid boundary layer along the wall surface and to a departure from the (bubbly) disperse two-phase flow existing initially in the vicinity of the wall (cf. the visualizations in Fig. 2(b)).

As particles are found as discrete elements, a particle-laden flow is always a disperse two-phase flow. Note that the notion of two-phase flow patterns is also present for gas–solid flows, especially in the context of fluidization at a macroscopic level, when a two-fluid description is chosen for the gas and particle system, see Fig. 3.

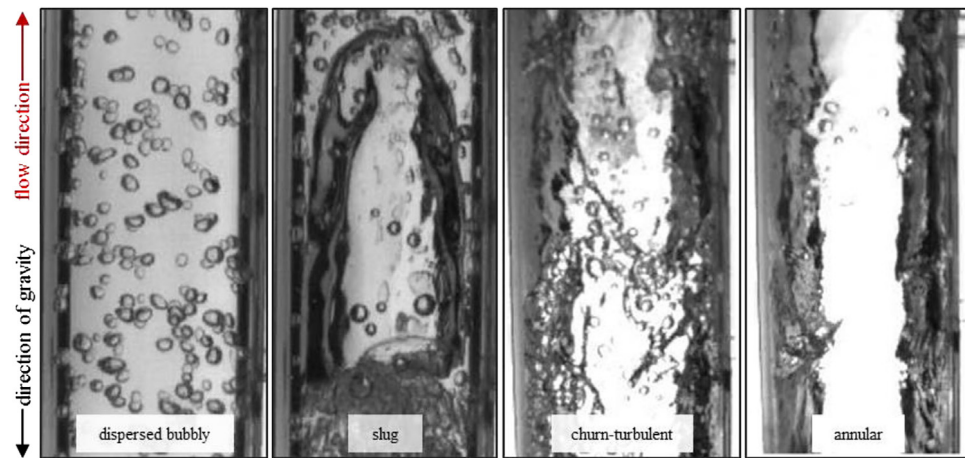


Fig. 1. Two-phase flow patterns: experimental observations of various two-phase flow patterns in an upward co-flowing air–water flow in a vertical pipe. Source: Reproduced from [6].

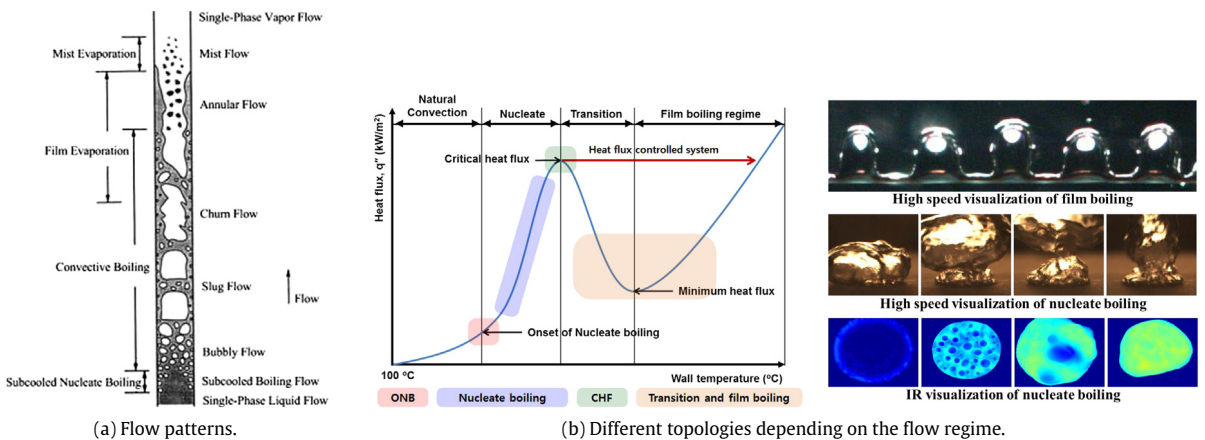


Fig. 2. Relations between two-phase flow patterns and heat transfer: (a) Sketch of two-phase regimes for a boiling liquid rising in a vertical tube; (b) Plot of the heat flux as a function of the wall temperature and visualization of the different boiling regimes. Source: <http://ahnlab.incheon.ac.kr>.

2.1.2. The importance of the disperse two-phase flow regime

One advantage of the subject of disperse two-phase flows is that many applications happen at the human scale and can be observed in daily-life phenomena. One very familiar example concerns the ‘molecule of life’, H₂O, under its different forms (ice, water, vapor). As illustrated in Fig. 4(a), the water cycle involves various two-phase flow situations, among which an air/ocean interface (representative of a separate two-phase flow) and precipitation (with evaporation and condensation leading to the formation of clouds and rain). It is evident that rain droplets are discrete elements falling through a continuous air flow (see Fig. 4(b)) and that these droplets have a range of diameters (or typical sizes when they depart from sphericity): this is an example of a ‘polydisperse two-phase flow’.

Predicting the raindrop size distribution is important to relate remote sensing observations to reliable precipitation estimations for a range of prime questions in hydrology as well as for environmental concerns [8]. In that sense, capturing properly the polydisperse nature of raindrops formed in clouds and falling through the atmosphere is the subject of current research [7,9–11]. This is a challenging issue in physics involving nucleation processes (the formation of rain droplets in clouds) and the interaction between drop shapes and their dynamics as they fall to the ground: the deformation of falling raindrops is illustrated in Fig. 5(a) while the fragmentation of a drop, which results in complex raindrop size and speed distributions [10,11], is shown in Fig. 5(b).

Bubble dynamics is of importance in a range of situations where the issue is not limited to the inception of the bubbly regime (or departure from it) but concerns also the evolution of these bubbles and, especially, whether they grow or collapse in the flow. This corresponds to the problem of cavitation where bubble collapse on material surfaces (such as turbine blades,

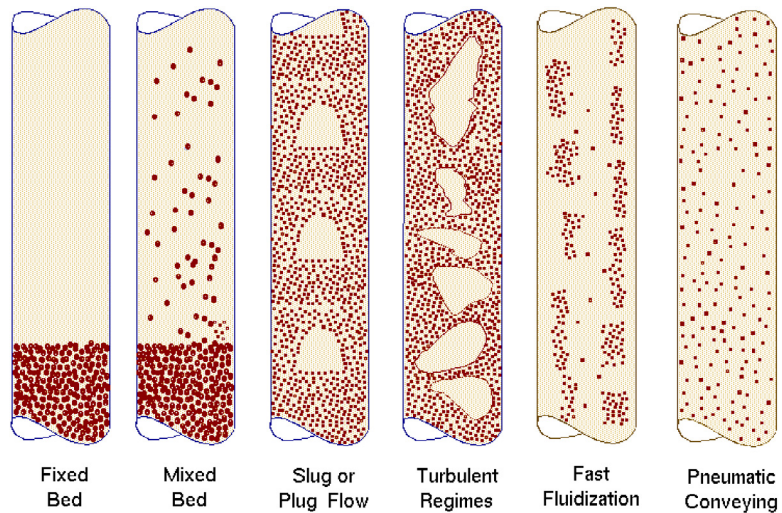
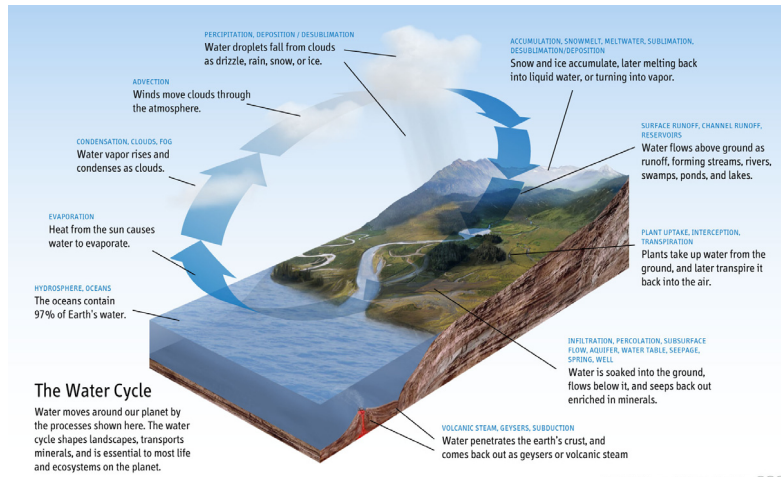


Fig. 3. Illustration of two-phase flow patterns in gas–solid fluidization.
Source: Protto Project



(a) Water cycle in the atmosphere.



(b) Falling rain drops.

Fig. 4. A familiar polydisperse two-phase flow: (a) Sketch of the water cycle in the atmosphere (source: Wikipedia); (b) Rain droplets of various shapes and sizes falling to the ground (source: LibertyMeadows).

propellers, etc.) can lead to severe erosion. However, to avoid associating disperse two-phase flows only with material hazards or engineering issues, more recreational examples are shown in Fig. 6. In Fig. 6(a), small bubbles created in the wake of a playful dolphin reveal the instantaneous fluid flow structures (in particular, depression zones since bubbles are essentially governed by fluid pressure-gradients). As mentioned, the history of these individual polydispersed bubbles can play a significant role. This is the case of champagne bubbles which grow (due to dissolved carbon dioxide) as they move upwards from the bottom of a champagne flute (see Fig. 6(b)). It is now known that bubble growth and bubble trajectories create liquid motions that have an influence on the gas release and flavor of the champagne (this is just a foretaste of more interesting investigations that can be found, for instance, in [12,13]).

Once they are formed, the growth and collapse of bubbles/droplets are not due only to their interaction with local fluid conditions (the instantaneous fluid pressure at bubble locations, the content of specific chemical elements, etc.) but can be governed also by their interactions with neighboring drops or bubbles. This is referred to as coalescence for bubbles and droplets (sometimes coagulation for droplets) while the opposite phenomenon is break-up. In the context of small solid particles, these processes are called agglomeration (or aggregation) and fragmentation. A beautiful illustration of the complex phenomenon of drop coalescence is shown in Fig. 7(a), which reveals the highly distorted intermediate shapes of

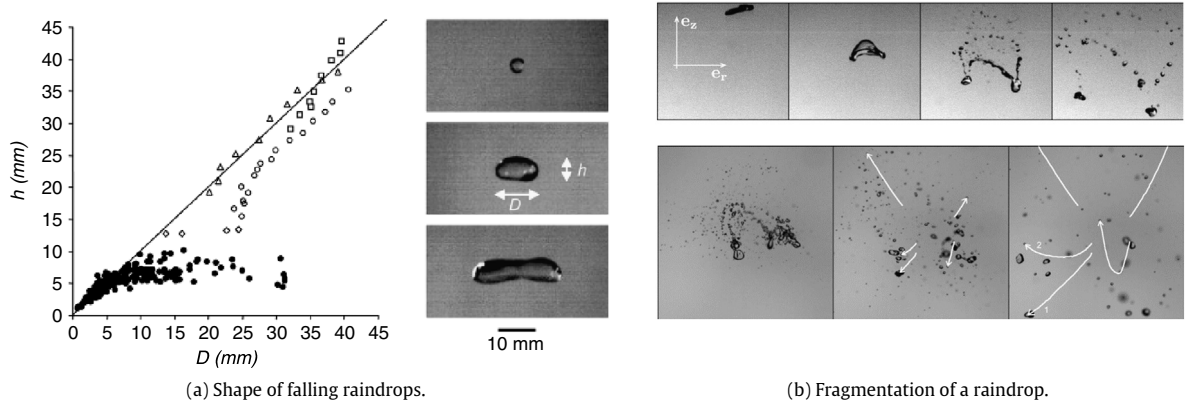


Fig. 5. Evolution of falling raindrop shapes and sizes: (a) Departure from spherical shapes measured by the height h compared to the equatorial diameter D (the empty symbols are for stationary states while the empty ones are for larger globules taken at different times). Reprinted from [9] with permission from IOP Publishing; (b) Fragmentation of an initially spherical drop first flatten into a pancake shape before bursting into a number of fragments. The consecutive snapshots reveal the complicated dynamics of these fragments whose trajectories are indicated by the white arrows. Reprinted from [11].

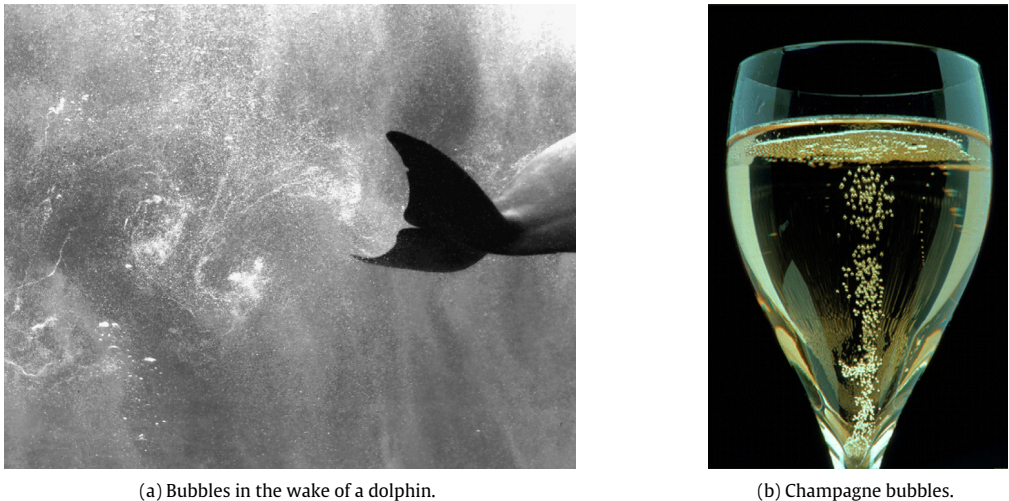
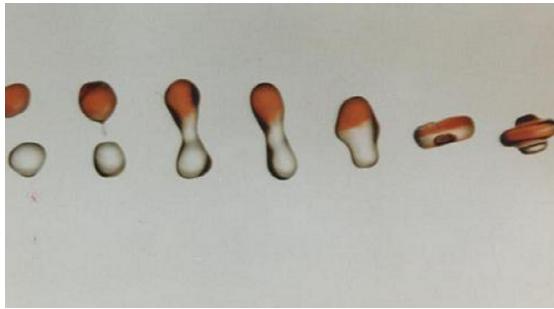


Fig. 6. Illustration of bubble dynamics in a flow: (a) Vapor bubbles created in the wake of a dolphin swimming in the ocean can grow or collapse depending on the instantaneous fluid pressure field. Reprinted from [14]; (b) Champagne bubbles displaying an interaction between bubble growth and their dynamics as they rise to the surface. Reprinted from [15] with permission from American Chemical Society.

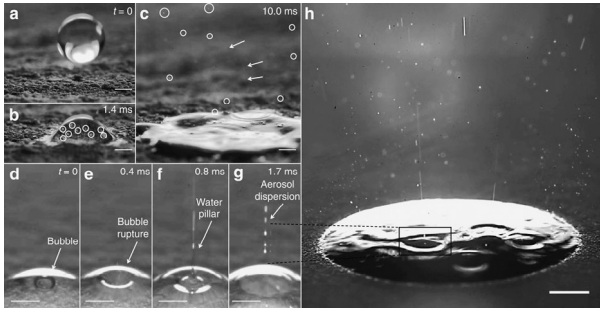
the interface as two droplets merge. The interaction of droplets with a boundary surface can also create satellite droplets through a complex process that increases the polydispersity of the disperse phase (see Fig. 7(b) where satellite drops are indicated as aerosols) [16,17].

Still referring to examples from Earth Science, another illustration of interest for our study is provided by volcanic eruptions and ash-particle dispersion in the atmosphere. Two-phase flows play a central role in current scenarios of volcanic eruptions. First, the de-pressurization in the chimney connecting the magma chamber to the volcano crater allows bubble nucleation to be triggered in the liquid magma resulting in the formation of a bubbly regime whose lower density drives the flow upwards by buoyancy forces (see Fig. 8(a)). Second, as the bubbly magma flow rises in the chimney, it drags a set of particles which makes it, at that stage, a three-phase flow. After the fragmentation limit, or if we consider only the erupting cloud billowing in the atmosphere, we have essentially a stream of hot gases carrying particles. The volcanic cloud contains various particles (rocks, ash, pumices, etc.) with a range of sizes and densities and, due to the high velocities imparted by the eruption, is therefore a manifestation of a polydisperse turbulent two-phase flow. The spread of the volcanic cloud, illustrated in Fig. 8(b), is a large-scale example of particle dispersion.

Given the impact of volcanic clouds (for instance, their capacity to bring air traffic to a halt due to small soot particles sticking to the blades of aircraft turbines), predicting how such volcanic plumes spread in the atmosphere is of paramount



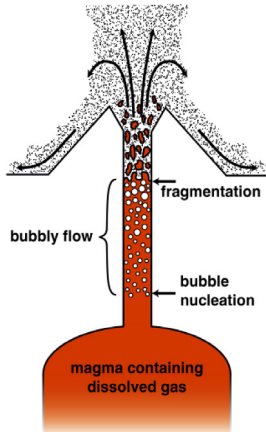
(a) Coalescence between two drops.



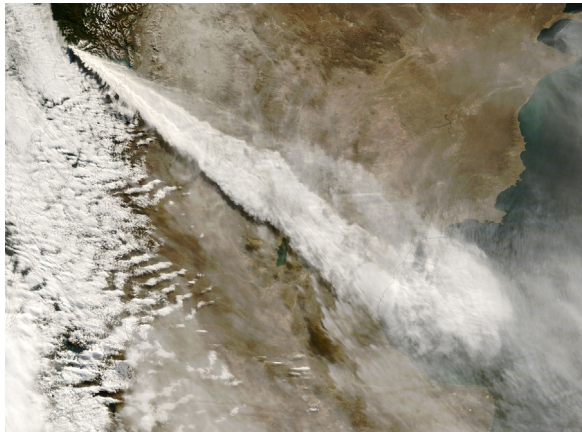
(b) Small aerosols created by the impact of a drop.

Fig. 7. Complex droplet-droplet and droplet-surface interactions leading to polydispersity: (a) Coalescence between two droplets through a complex interface mechanism that creates a large droplet (source: www.mie.utoronto.ca); (b) Experimental observation of the impact of a drop on a surface with smaller droplets, or aerosols, being formed.

Source: Reprinted from [17].



(a) Magma chamber.



(b) Large-scale dispersion in the atmosphere.

Fig. 8. Two-phase flows in volcanic eruptions: (a) Formation of a liquid/gas two-phase flow rising in the chimney from the magma chamber and gas/solid two-phase flow near the crater; (b) Large-scale example of particle dispersion as the volcanic cloud spreads in the atmosphere (credit: NASA).

importance. As for champagne bubbles rising in a flute, particles released in a volcanic cloud are not necessarily inert and can be subject to complex growth processes due to their interaction with the local hot/cold environment as well as with other particles through aggregation and fragmentation mechanisms (see Fig. 9(a)). In consequence, particles contained in a volcanic cloud are not necessarily tracer-particles having negligible inertia with respect to the carrier air flow (*i.e.* the prevailing winds at the volcano site) and can have their own dynamics with particles depositing either by sedimentation or by fluid transport (see Fig. 9(b)). In some situations, ash particle deposition occurs through specific features, such as finger-deposition patterns [18].

Another example from Earth Science concerns colloidal suspensions and their role in the formation of river deltas. This involves now a liquid flow carrying colloids whose interactions are well described by physico-chemical interactions, as in the DLVO theory whose main characteristics are illustrated in Fig. 10(a) (see comprehensive presentations in [20,21]). In a low-salt-content environment, the Debye length (the screening length of the repulsive double-layer interactions, or electrostatic repulsion, shown in Fig. 10(a)) is large enough to keep colloids well separated and, thus, prevent the attractive van der Waals forces from taking over: this means that colloidal suspensions are stable in river water. However, contact with high-salt-content sea water reduces this Debye length allowing the colloids to agglomerate and form larger-size particles, as represented in Fig. 10(b). As agglomeration goes on, particle inertia becomes high enough for these particles (actually, these agglomerates) to sediment, which means that the colloidal suspension has become unstable, as shown in Fig. 11(a). In the context of river water reaching an ocean (where colloids go therefore from low-salt conditions to high-salt ones), the resulting silt deposition over long periods of time explains the formation of river deltas, see Fig. 11(b).

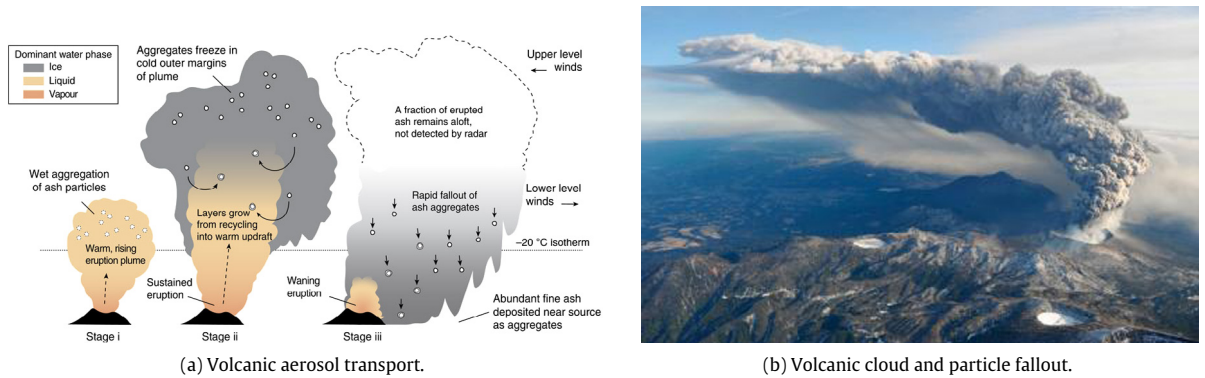


Fig. 9. A (gas-solid) polydisperse two-phase flow at work in volcanic clouds: (a) Small volcanic ‘aerosols’, or particles, are released in the atmosphere and can undergo complex growth processes. Reprinted from [19]; (b) Observation of volcanic particle transport by winds and potential fallouts after an eruption (credit: USGS).

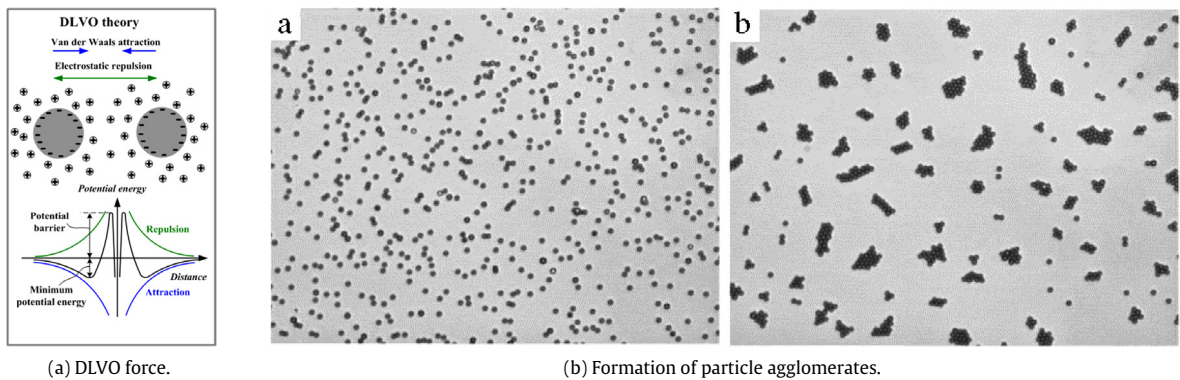


Fig. 10. The role of two-phase flows in the formation of river deltas: (a) Colloids are transported with negligible inertia by the flow but colloid-colloid interactions change when different salt-content conditions are met, as explained by the DLVO theory (source: Wikipedia); (b) Formation of particle agglomerates with growing sizes and inertia as time evolves.

Source: Reprinted from [22] with permission from APS.

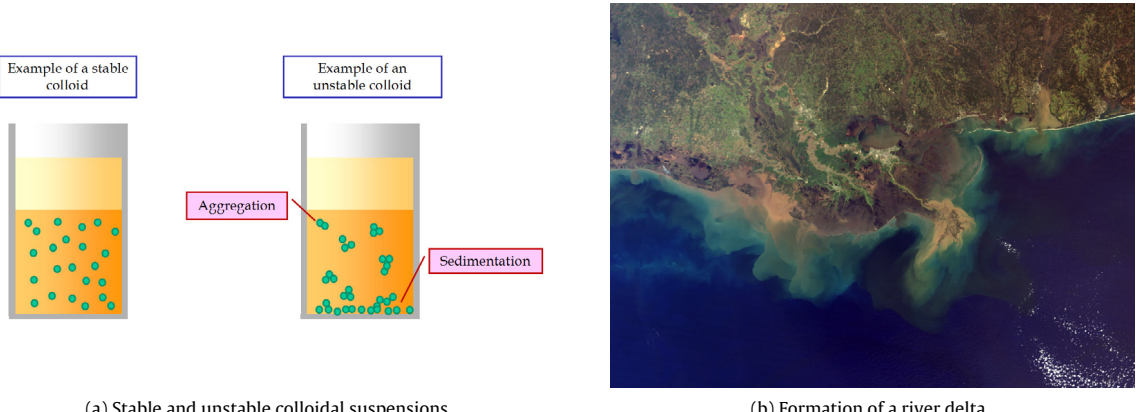


Fig. 11. The role of two-phase flows in the formation of river deltas: (a) The formation of agglomerates can trigger deposition leading to unstable colloidal suspensions (source: Wikipedia); (b) The resulting silt deposition forms delta beds (credit: NASA).

2.2. The physical issues at stake

In the examples presented in Section 2.1, the disperse phase is made up by droplets, bubbles or solid particles. However, regardless of the thermodynamical phase (liquid, gas, solid) under which discrete elements are found, we refer to them as ‘particles’ for the sake of keeping a simple terminology since the nature of these particles is obvious in each situation.

Drawing on the previous illustrations, we can say that there are basically two mechanisms at play in disperse two-phase flows. The first one refers to the transport of separate particles by fluid motions, as well as the interactions of these particles with their local surrounding which can lead to a change of their diameter or other defining characteristics (*i.e.* the particle inner compositions, temperature, etc.). The second mechanism refers to direct particle–particle influences, such as (solid) particle collision and agglomeration, droplet or bubble coalescence. This overall picture can be cast in a simple framework in terms of fundamental interactions. Indeed, from the analysis of the different mechanisms, it is seen that there are two fundamental interactions: *particle–fluid* and *particle–particle interactions*.

As many flows are wall-bounded, a third interaction (*particle–surface interaction*) can also be present, especially in particle deposition and resuspension problems. Comprehensive studies of particle deposition have recently analyzed the interplay between these three interactions (see [2,23,24] and also [5, section 6.1]). The physics of particle–surface interactions is intricate (see [20,25]), the influence of surface heterogeneity (such as surface roughness) is still challenging, and our understanding of the inner morphology of large deposits or aggregates remains uncertain. Nevertheless, the modifications due to the presence of a wall can be regarded as external to the coupled fluid and particle system. Furthermore, following the above-mentioned result that particle deposition can be cast in existing modeling frameworks, treating the specific details of particle–wall interactions would not modify significantly the discussions to come. For these reasons, we consider essentially the issues raised by particle–fluid and particle–particle interactions in the rest of this paper and refer readers to the recent literature on particles in wall-bounded turbulent flows.

In the scope of the present article, the treatment of particle–particle interactions calls for some simplifications. The specifics of bubble/droplet coalescence or particle agglomeration are extremely intricate (and fascinating) and a detailed presentation of each phenomenon would require a comprehensive monograph of its own. This can be guessed by looking at the complex distortion of the shape of the interface in the situation displayed in Fig. 7(a) which involves strong surface-tension effects when two drops coalesce (see [26–28]) or at the structure of colloid agglomerates in the case illustrated in Fig. 11(a) which involves fractal dimensions to express the complex inner structures as agglomerates grow (see [29]). Similarly, the various resistance motions that describe the contact between solid particles are important to study granular matter (some details are provided in Section 7.2.2 for methods coming from contact mechanics). However, the common feature of these phenomena is that particles must first collide before undergoing coalescence, agglomeration, or even break-up and fragmentation induced by impacts. In the present work, we consider therefore that particle–particle interactions refer essentially to ‘particle collisions’, that is to the process through which two (or more) particles are brought into contact. As such, particle–particle interaction does not need further elaborations and the issues are mostly to derive collision rates or to account for them depending on the modeling approach (this is discussed in Section 8.2), as well as to include the effect of the underlying carrier fluid flow in the formulation of probabilistic descriptions (this is addressed in Section 10.6). On the other hand, particle–fluid interaction and particle transport need to be introduced and a reference description corresponding to the hydrodynamical approach is now developed.

2.3. Particle transport and hydrodynamical equations

In a hydrodynamical approach, the governing equations of the fluid (or continuous) phase are the continuity, the Navier–Stokes and the transport equations for a set of scalar fields which gathers the relevant species mass fractions $\phi_f(t, \mathbf{x}) = (\phi_{f,l})_{l=1,\dots,N_s}$ to which an equation for the fluid enthalpy is added, along with an equation of state for compressible flows. In the following, we consider essentially constant-property flows, for which these equations are [30]

$$\frac{\partial U_{f,k}}{\partial x_k} = 0, \quad (1a)$$

$$\frac{\partial U_{f,i}}{\partial t} + U_{f,k} \frac{\partial U_{f,i}}{\partial x_k} = -\frac{1}{\rho_f} \frac{\partial P_f}{\partial x_i} + v_f \frac{\partial^2 U_{f,i}}{\partial x_k \partial x_k}, \quad (1b)$$

$$\frac{\partial \phi_{f,l}}{\partial t} + U_{f,k} \frac{\partial \phi_{f,l}}{\partial x_k} = \Gamma_f \frac{\partial^2 \phi_{f,l}}{\partial x_k \partial x_k} + S_{f,l}, \quad (1c)$$

where $\mathbf{U}_f(t, \mathbf{x})$ and $P_f(t, \mathbf{x})$ are the fluid velocity and pressure fields respectively, ρ_f the fluid density, v_f its kinematic viscosity and Γ_f the scalar diffusivity. In Eq. (1c), the last term on the rhs (right-hand side) is a reactive source term $S_{f,l} = \hat{S}_{f,l}(\phi_f(t, \mathbf{x}))$ where $\hat{S}_{f,l}$ are known functions. In the present work, we are not directly interested in the characteristics of the chemistry involved in reactive flows (see [31,32]) and we do not need to specify the expressions of such reactive source terms. The significant point is, however, that these terms are obtained from the instantaneous scalar variables ϕ_f through a (usually) non-linear but given relation. An important consequence is developed in Section 3.2.2.

It can be noted that the Navier–Stokes equation in Eq. (1b) is written as for a single-phase flow and, being the description of the fluid instantaneous velocity field, is valid at locations \mathbf{x} where no particles are present at time t . Using a velocity scale

u_f and a length scale L_f for the fluid flow, the relative importance of the diffusion terms on the rhs of Eqs. (1b) and (1c) with respect to the convective ones on the lhs (left-hand side) of both equations is assessed through two non-dimensional parameters which are the Reynolds and Peclet numbers (noted Re and Pe respectively), defined by

$$Re = \frac{u_f L_f}{\nu_f}, \quad Pe = \frac{u_f L_f}{\Gamma_f}. \quad (2)$$

The equations are complemented by the corresponding ones for particle dynamics. However, the expressions of the hydrodynamical forces acting on particles embedded in a fluid flow do not, at present, have the same level of validity (and confidence) as the Navier–Stokes equations for the fluid phase. Therefore, a slightly more detailed presentation is given.

2.3.1. Hydrodynamical forces on particles

Since we are dealing with a disperse phase, it is natural to follow a Lagrangian point of view and the governing equations for particle dynamics are obtained by applying the fundamental laws of classical mechanics for each particle carried by a turbulent flow

$$\frac{d\mathbf{x}_p}{dt} = \mathbf{U}_p, \quad (3a)$$

$$m_p \frac{d\mathbf{U}_p}{dt} = \mathbf{F}_{f \rightarrow p} + \mathbf{F}_{p \rightarrow p} + \mathbf{F}_{ext}, \quad (3b)$$

$$I_p \frac{d\Omega_p}{dt} = \mathbf{M}_{f \rightarrow p} + \mathbf{M}_{p \rightarrow p}, \quad (3c)$$

where \mathbf{x}_p is the location of the particle center of mass, m_p the mass of the particle, I_p the moment of inertia and \mathbf{U}_p and Ω_p the translational and rotational velocities, respectively. In Eqs. (3b)–(3c), $\mathbf{F}_{f \rightarrow p}$ and $\mathbf{M}_{f \rightarrow p}$ represent the forces and torques exerted by the fluid on the particle, $\mathbf{F}_{p \rightarrow p}$ and $\mathbf{M}_{p \rightarrow p}$ and \mathbf{F}_{ext} the forces and torques due to the particle–particle interactions and \mathbf{F}_{ext} forces due to external fields such as gravity. As mentioned above, we do not develop specifically the forces and torques due to particle–particle interactions and concentrate essentially on the action of the fluid onto the particles in this section.

The first equation, Eq. (3a), shows that particle transport is treated without approximation by Lagrangian approaches [31,1] and the issue is to express the forces exerted by a turbulent flow on an embedded particle. In spite of numerous studies, it cannot be said that this question has been completely solved, even if a state-of-the-art formulation has emerged. Present formulations retain the so-called drag, lift, added-mass and Basset forces (see [33–35]) which are added to the gravity force, but the expression of these forces can vary according to different authors. The lift force creates special difficulties. Indeed, several expressions have been proposed but each of these expressions has been obtained in a specific or asymptotic situation. This results in a catalog of widely different formulations [1,33,23] and there is, at the moment, no well-established consensus about a unique expression. In the opinion of the present author, the expression of the ‘optimal lift force’ in McLaughlin’s works (see for instance [36,37]) provides the most general expression available. The expression of the Basset force is also still debated and, consequently, present models for these two forces cannot be regarded as being reliable enough. Furthermore, we are more interested in a general and well-accepted form to develop probabilistic approaches, though it is worth remembering that, in some cases, the expression of the forces on a particle can be generalized. For these reasons, we choose to leave out the lift and Basset forces.

For small spherical particles with diameters $d_p \sim \eta_K$ where η_K is the Kolmogorov length scale which represents the smallest length scale for fluid motions in a turbulent flow (see Section 6.1 and [38,39,30] for more elaborate discussions), the reference formulation of the particle momentum equation is derived in [34] and can be written as

$$m_p \frac{d\mathbf{U}_p}{dt} = \frac{\pi d_p^3}{6} \rho_f \frac{D\mathbf{U}_s^V}{Dt} + \frac{\pi d_p^3}{6} (\rho_p - \rho_f) \mathbf{g} + \frac{1}{2} \frac{\pi d_p^2}{4} \rho_f C_D |\mathbf{U}_s^S - \mathbf{U}_p| (\mathbf{U}_s^S - \mathbf{U}_p) + \frac{\pi d_p^3}{6} \rho_f C_A \left(\frac{D\mathbf{U}_s^V}{Dt} - \frac{d\mathbf{U}_p}{dt} \right), \quad (4)$$

where D/Dt refers to the derivative along a fluid–particle trajectory

$$\frac{D}{Dt} = \frac{\partial}{\partial t} + U_{f,k} \frac{\partial}{\partial x_k}. \quad (5)$$

In Eq. (4), ρ_p is the particle density while \mathbf{U}_s^S and \mathbf{U}_s^V stand for the fluid velocities averaged over the surface S_p and the volume V_p of the particle respectively

$$\mathbf{U}_s^S = \frac{1}{S_p} \int_{S_p} \mathbf{U}_f(t, \mathbf{r}_S) d\mathbf{r}_S, \quad (6)$$

$$\mathbf{U}_s^V = \frac{1}{V_p} \int_{V_p} \mathbf{U}_f(t, \mathbf{r}_V) d\mathbf{r}_V. \quad (7)$$

These velocities are expressed by a series expansion around the ‘velocity’ at the particle center, which introduces the notion of the velocity of the fluid seen, $\mathbf{U}_s(t) = \mathbf{U}_f^{ud}(t, \mathbf{x}_p(t))$

$$\mathbf{U}_s^S \simeq \widehat{\mathbf{U}}_s + \frac{d_p^2}{24} (\nabla^2 \mathbf{U}_f^{ud})(t, \mathbf{x}_p(t)), \quad (8)$$

$$\mathbf{U}_s^V \simeq \widehat{\mathbf{U}}_s + \frac{d_p^2}{40} (\nabla^2 \mathbf{U}_f^{ud})(t, \mathbf{x}_p(t)). \quad (9)$$

The notation $\mathbf{U}_f^{ud}(t, \mathbf{x}_p(t))$ is used for the ‘undisturbed velocity field’ that would exist if the particle were not present at the location $\mathbf{x} = \mathbf{x}_p(t)$ at time t (see [34,35] and discussions in [1]) and the last terms added to \mathbf{U}_s on the rhs of the above equations correspond to the so-called Faxen terms [33–35]. In Eq. (4), the first two terms on the rhs correspond to the fluid acceleration and to the buoyancy force while the third term is the general form of the drag force written with the drag coefficient C_D and the fourth term is the added-mass force. The added-mass force is also expressed with an added-mass coefficient C_A (usually taken simply as $C_A = 1/2$) and is a function of the difference between the acceleration of the fluid seen (along its own trajectory) and the particle acceleration while the drag force is expressed in terms of the velocity slip $\mathbf{U}_s^S - \mathbf{U}_p$.

For small particles (say $d_p \leq \eta_K$), the Faxen terms can be neglected. This corresponds to the important point-wise approximation for particles and a classical form of the particle momentum equation is obtained as

$$m_p \frac{d\mathbf{U}_p}{dt} = \frac{\pi d_p^3}{6} \rho_f \frac{D\mathbf{U}_s}{Dt} + \frac{\pi d_p^3}{6} (\rho_p - \rho_f) \mathbf{g} + \frac{1}{2} \frac{\pi d_p^2}{4} \rho_f C_D |\mathbf{U}_s - \mathbf{U}_p| (\mathbf{U}_s - \mathbf{U}_p) + \frac{\pi d_p^3}{6} C_A \rho_f \left(\frac{D\mathbf{U}_s}{Dt} - \frac{d\mathbf{U}_p}{dt} \right). \quad (10)$$

The velocity of the fluid seen is now given as the local instantaneous value of the fluid velocity at the same time and at the particle position, which means that $\mathbf{U}_s(t) = \mathbf{U}_f(t, \mathbf{x}_p(t))$ where $\mathbf{U}_f(t, \mathbf{x})$ represents the fluid velocity field (without having to separate undisturbed and disturbed fluid velocity fields).

In most laboratory, industrial or environmental flows, the Kolmogorov scale is in the range of [50 μm, 1 mm]. This means that small particles or droplets having a diameter of less than, say, 30 μm are usually well below Kolmogorov scales and that the point-wise approximation is quite reasonable. Furthermore, for particles heavier than the fluid $\rho_p \gg \rho_f$, it can be shown that the drag force is the dominant force [1,34,35] and the particle momentum equation is then reduced to

$$\frac{d\mathbf{U}_p}{dt} = \frac{\mathbf{U}_s - \mathbf{U}_p}{\tau_p} + \mathbf{g} \quad (11)$$

where the drag force is written so as to bring out the particle relaxation timescale τ_p

$$\tau_p = \frac{\rho_p}{\rho_f} \frac{4 d_p}{3 C_D |\mathbf{U}_r|}. \quad (12)$$

This timescale is the key notion for particle transport and a measure of particle inertia. More precisely, τ_p stands for the timescale over which particle velocities adjust to the local fluid velocity seen. In the Stokes regime, which is valid when $Re_p \leq 1$ (with Re_p the particle Reynolds number defined by $Re_p = |\mathbf{U}_r| d_p / v_f$, where $\mathbf{U}_r = \mathbf{U}_s - \mathbf{U}_p$), the drag coefficient is $C_D = 24/Re_p$. In that case, the drag force retrieves the classical form $\mathbf{F}_{f \rightarrow p}^{Drag} = 3\pi \rho_f v_f d_p \mathbf{U}_r$ and the particle relaxation timescale is given by the well-known expression

$$\tau_p = \frac{\rho_p}{\rho_f} \frac{d_p^2}{18 v_f}. \quad (13)$$

For general values of Re_p , the drag coefficient is obtained through empirical correlations and an often-retained formula is [33,40]

$$C_D = \begin{cases} \frac{24}{Re_p} [1 + 0.15 Re_p^{0.687}] & \text{if } Re_p \leq 1000, \\ 0.44 & \text{if } Re_p \geq 1000. \end{cases} \quad (14)$$

This correlation is for isolated particles or when particle concentration is not high enough for collective effects, which represent hydrodynamical influences of each particle on its neighbors and is often called the ‘wake effect’, to be significant. In this hydrodynamical description, particle wake effects have to be accounted for with modified correlations based, for example, on the local particle volumetric fraction [33].

For the vast majority of cases involving particles or droplets in a turbulent flow, the preceding expressions provide a satisfactory description and can be deemed sufficient to capture the influence of fluid flows on particle dynamics. For diameters larger than the Kolmogorov length scale, it is seen from the general form of the particle momentum equation, cf. Eq. (4), and the expressions given in Eqs. (6)–(7) that a non-negligible particle size induces a filtering effect and that fluid velocity fluctuations with length scales smaller than d_p tend to be smoothed out and act as an underlying noise. In some cases, particle inertia is high enough (due to the density ratio $\rho_p/\rho_f \gg 1$) so that these particles become ‘bullet-like particles’ for which the influence of the underlying fluid flows can be treated, as a first approximation, as noise. This is however a

questionable simplification when particles are such that their inertia remains smaller than the characteristic timescale of the fluid turbulent motions while being much larger than the Kolmogorov length scale. In these situations, refined analyses are needed. Interesting proposals can be found, for example, in [41,42] where the basic form given in Eq. (11) is retained but where the definition of the particle relaxation timescale τ_p is revisited by dividing velocity fluctuations as slow and fast (depending on the value of their timescale with respect to τ_p) and considering that the fluid molecular viscosity is to be substituted by an ‘effective’ or ‘turbulent viscosity’. Specific details on this analysis and on the resulting scaling of particle velocity can be found in [42] and the literature cited therein. In the context of the present section, it is however interesting to note that investigations on particle dynamics involve right from the outset notions such as the Kolmogorov theory of turbulence, slow and fast variables and the connection between rapidly-varying fluctuations and eddy-viscosity concepts or gradient-diffusion closures. These aspects are at the core of the present article and are addressed in detail in later sections.

As an example of the above point, the point-wise approximation is not always valid for bubbly flows as bubbles tend to have larger sizes. Moreover, the added-mass force becomes important for bubbles whose density ρ_p is much smaller than the fluid one ($\rho_p \ll \rho_f$), while it can be also relevant for small sediments in a liquid medium when $\rho_p \sim \rho_f$. If the added-mass force is retained in the particle momentum equation, the notion of the particle relaxation timescale still holds and simple manipulations of Eq. (4) show that the expression of τ_p is slightly modified to give (in the Stokes regime)

$$\tau_p = \left(\frac{\rho_p + C_A \rho_f}{\rho_f} \right) \frac{d_p^2}{18 \nu_f}. \quad (15)$$

As with the extension of the particle relaxation timescale to account for added-mass effects, an extended version where the fluid pressure-gradient term is kept can be derived from Eq. (4) using the high Reynolds form of the Navier–Stokes equation (also called the Euler equation)

$$\frac{D\mathbf{U}_s}{Dt} = -\frac{1}{\rho_f} \nabla P_f + \mathbf{g}, \quad (16)$$

which gives the extended particle momentum equation

$$\frac{d\mathbf{U}_p}{dt} = -\frac{1}{\rho_p} \left(\frac{1 + C_A}{1 + C_A \rho_f / \rho_p} \right) \nabla P_f + \frac{\mathbf{U}_s - \mathbf{U}_p}{\tau_p} + \mathbf{g}. \quad (17)$$

Even when added-mass forces are disregarded (*i.e.* $C_A = 0$), the extended particle momentum equation takes the form

$$\frac{d\mathbf{U}_p}{dt} = -\frac{1}{\rho_p} \nabla P_f + \frac{\mathbf{U}_s - \mathbf{U}_p}{\tau_p} + \mathbf{g}, \quad (18)$$

with a pressure-gradient contribution that is not necessarily negligible when $\rho_p \gg \rho_f$. Consequently, the form of the particle momentum equation given in Eq. (17) or (18) is useful for sediments and bubbles for which the fluid pressure-gradient is an important driving force, as illustrated by the examples in Fig. 6.

When lift forces are not considered, the particle rotation Ω_p plays no role in the particle dynamics and is usually left out (especially, in the particle point-wise approximation). There are, however, some situations where particle rotation needs to be treated, as in some models for particle–particle contact (see an example in Section 7.2.2). For these applications, the torque due to the friction forces of the fluid is, in the Stokes regime, expressed by

$$\mathbf{M}_{f \rightarrow p} = \pi \rho_f v_f d_p^3 \left(\frac{1}{2} \boldsymbol{\omega}_f - \boldsymbol{\Omega}_p \right), \quad (19)$$

where $\boldsymbol{\omega}_f$ is the fluid vorticity vector at the particle position.

2.3.2. Brownian effects at the continuum level

Hydrodynamical forces do not tell the whole story for small particles sensitive to molecular effects and Brownian motion. These ‘small-enough particles’ are usually defined as colloids for which the settling velocity induced by gravity in a fluid at rest is counterbalanced by the random velocities imparted by the collisions between this (Brownian) particle and the fluid molecules: basically, colloidal particles do not sediment. This corresponds to the example given in Fig. 11 where sedimentation occurs only when agglomeration is triggered and when particles become large enough (or with strong-enough inertia). Using a one-dimensional formulation in the direction aligned by gravity and making use of the equipartition theorem of statistical physics, we get that colloidal particles have a diameter d_p such that

$$\sqrt{\frac{k_B \Theta_f}{m_p}} \sim \tau_p g \implies d_p \simeq \left(\frac{\rho_f^2 v_f^2}{\rho_p^3 g^2} k_B \Theta_f \right)^{1/7}, \quad (20)$$

where k_B is the Boltzmann constant and Θ_f the fluid temperature. This shows that colloidal particles have typically a diameter of the order of a few microns ($d_p \leq 1–2 \mu\text{m}$) while, for $d_p \geq 5–10 \mu\text{m}$, particles are called inertial and Brownian effects can be neglected.

A straightforward way to include Brownian effects at the hydrodynamical level is to add a white-noise term into the particle momentum equation which becomes a generalization of the historical Langevin equation. In that case, the particle equations take the form (see [1,5])

$$d\mathbf{x}_p(t) = \mathbf{U}_p(t) dt, \quad (21a)$$

$$d\mathbf{U}_p(t) = \frac{\mathbf{U}_s(t) - \mathbf{U}_p(t)}{\tau_p} dt + \mathbf{g} dt + K_{Br} d\mathbf{W}(t). \quad (21b)$$

It is seen that the particle momentum equation has been turned into a stochastic differential equation (SDE) that is properly introduced only in Section 4. Yet, in the present context, it is sufficient to think of the increments of the (vector-valued) Wiener process, i.e. $d\mathbf{W}(t)$, as representing independent noise terms. In Eq. (21b), the stochastic diffusion coefficient K_{Br} is obtained by using again that, in a fluid at rest, the particle kinetic energy is constant and given by the equipartition of energy. This corresponds to the most basic (and simplest) form of the so-called fluctuation–dissipation theorem [43] which yields that

$$K_{Br} = \sqrt{\frac{2 k_B \Theta_f}{m_p \tau_p}}. \quad (22)$$

Therefore, K_{Br} decreases as $d_p^{-5/2}$ when the particle diameter is increased and becomes negligible for inertial particles while it should be retained in the colloidal range.

It is also immediate to show that the Langevin description in Eqs. (21) retrieves the Einstein diffusion coefficient as a limit case. This is worked out by considering the long-time limit, or the situation when τ_p becomes small with respect to an observation timescale Δt , and is referred to as the ‘elimination of fast variables’. Indeed, when $\tau_p \ll \Delta t$, the particle velocity can be eliminated in Eq. (21b) and the limit system consists in a diffusion model for particle positions [44]

$$d\mathbf{x}_p(t) = \mathbf{U}_s(t) dt + (\tau_p K_{Br}) d\mathbf{W}(t), \quad (23)$$

where it is seen that the white-noise term in Eq. (21b) has been shifted to the particle position equation. The diffusion coefficient corresponding to this SDE is

$$D_p = \frac{1}{2} (\tau_p K_{Br})^2 = \frac{k_B \Theta_f}{3\pi \rho_f v_f d_p}, \quad (24)$$

which is indeed the expression of the Einstein diffusion coefficient. In this derivation, we have used two results which are in anticipation of developments to come. First, the expression of the diffusion coefficient D_p is derived from the correspondence between the Langevin SDEs and the Fokker–Planck equation in sample space which is recalled in Section 4 and, in particular, in Section 4.3.2. Second, the notion of fast-variable elimination will be shown to be a central point in the analysis of probabilistic models and a detailed presentation is given in Section 9.3.

The evolution equations in Eqs. (21) generalizes the hydrodynamical equations given before. Indeed, this form is valid for inertial particles (for which K_{Br} is negligible) as well as for colloidal particles (for which gravity is negligible). Therefore, Eqs. (21) can be retained as the reference evolution equations for particle dynamics in a hydrodynamical approach. If the extended version in Eq. (17) with the fluid pressure-gradient is preferred, then Eq. (21b) is replaced by the corresponding extended version and, in that case, the equations that express the hydrodynamical description of particle dynamics become

$$d\mathbf{x}_p(t) = \mathbf{U}_p(t) dt, \quad (25a)$$

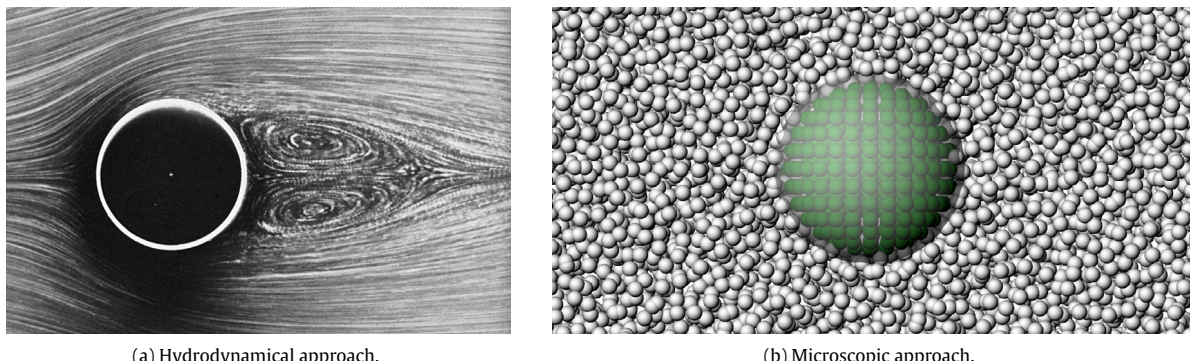
$$d\mathbf{U}_p(t) = - \left(\frac{1}{\rho_p} \left[\frac{1 + C_A}{1 + C_A \rho_f / \rho_p} \right] \nabla P_f \right) dt + \frac{\mathbf{U}_s(t) - \mathbf{U}_p(t)}{\tau_p} dt + \mathbf{g} dt + K_{Br} d\mathbf{W}(t). \quad (25b)$$

This is the basic form of the particle momentum equation for inert particles (without rotation). When electro- or thermophoresis phenomena are present, new terms need to be added since these effects are due to external driving forces whereas turbo-phoresis is already accounted for in the above formulation. These points are discussed in [5, section 2.3].

2.4. A range of possible descriptions

In this section, we have introduced a description where the fluid phase is represented by the instantaneous Navier–Stokes equations, Eqs. (1), and particles by their momentum equation, Eqs. (25) or the simplified form in Eqs. (21). However this does not constitute the fundamental level of description but a reference one among a range of possible formulations.

For example, even if we retain a hydrodynamical approach for the fluid phase, different choices can be made for the particle phase. Following the one adopted in Section 2.3, we can choose to make a point-wise approximation, in which case the drag coefficient must be input including the (potential) collective effect due to hydrodynamical influences between particles (the wake effect). If we decide to describe the real particle shapes and calculate the exact flow around them (see the illustration shown in Fig. 12(a)), then the drag force can be obtained as an output by integrating the elementary forces due to fluid stresses all along particle surfaces. In that case, the wake effect is a result of the approach (at the price of having a fluid resolution much finer than particle diameters).



(a) Hydrodynamical approach.

(b) Microscopic approach.

Fig. 12. Two levels of description for a spherical particle embedded in a flow: (a) A hydrodynamical description with fluid streamlines (from [45]); (b) A finer-grained description where molecules, or macro-molecules, are explicitly simulated to describe the fluid phase (reprinted from [46] with permission from Springer).

Whatever the choice for the way particle shapes are treated, this remains a hydrodynamical formulation since the fluid phase is still described by the Navier–Stokes equations and forces are derived from continuous-mechanics stress tensors. It is, however, possible to opt for other choices for the fluid phase. For instance, one can resort to a molecular-based description of the fluid phase. In that case, drag coefficients are obtained as macroscopic outputs and the interactions between the fluid and embedded particles result from the elementary forces between the fluid molecules (or macro-molecules) and either the colloid particle itself or the sub-particles (the ‘particle molecules’) into which it is decomposed, as illustrated in Fig. 12(b). Similarly, Brownian motion is an input in the hydrodynamical formulation (through the coefficient K_{Br} and the use of a white-noise term represented by the increments of the Wiener process in Eq. (21b) or (25b)) whereas it would be a result of microscopic simulations with explicit interactions between fluid and particle molecules.

These issues, related to what can be calculated and what must be given, are addressed in Section 8.2 once models have been discussed in Sections 5–7. Meanwhile, we have already started to use terms such as a ‘level of description’, ‘microscopic’ or ‘macroscopic’ formulations. Since the purpose of the present article is to discuss statistical approaches, these notions must be clarified to pave the way for later discussions. This is done in Section 3.

3. The microscopic, mesoscopic and macroscopic levels of description

A wide range of approaches have been developed for particle dynamics in turbulent flows. These models have different premises and produce different types of results. Phrased differently, they correspond to different ‘levels of description’ and ‘information content’.

In their analysis, the first step consists in recognizing at which level of description each method is operating. The same is, of course, true for the various models developed for classical statistical physics which spans the levels of description between atom/molecule simulations to hydrodynamical formulations. To fulfill the objective of the present article, which is to bring out the thread of continuity between classical statistical physics and descriptions of particles in turbulent flows as well as the specific challenges raised by the latter, it is important to cast these approaches in a single framework. This is not done to compare them in terms of quality (which is best or which is to be discarded?) but to link the different formulations (to what level of description do they correspond and what is their information content?).

For that purpose, it proves useful to take up the notions of microscopic, mesoscopic and macroscopic formulations that are classical in statistical physics (see for instance [47–49]) and give them an extended definition in terms of information content.

3.1. From microscopic to macroscopic descriptions in classical statistical physics

3.1.1. A clear separation of scales

In classical statistical physics, the differences between levels of description are understood in terms of the time and space scales and the road from microscopic to macroscopic formulations follows coarse-graining procedures that rely on the large separation between these scales. Further characteristics of microscopic, mesoscopic and macroscopic formulations in the context of classical statistical physics are given in Section 5 when specific models are introduced, but the main ideas can already be presented.

At the *microscopic level*, descriptions are developed for individual atoms or molecules and by computing explicitly all the interactions between these molecules. The corresponding space and time scales are therefore given by the averaged dynamic of a molecule, *i.e.* its mean free path and inter-collision time and the description is referred to as Molecular Dynamics (MD).

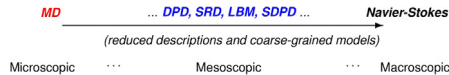


Fig. 13. Different approaches from molecular dynamics methods to hydrodynamical formulations represented by the Navier–Stokes equations corresponding to the microscopic, mesoscopic and macroscopic levels of description in classical statistical physics.

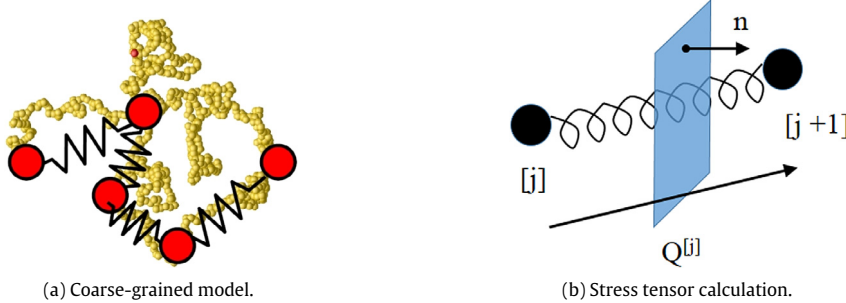


Fig. 14. A mesoscopic description of polymers in fluid (the Rouse model): (a) A coarse-grained description is proposed with beads and springs; (b) The contribution of the spring forces to the stress tensor is deduced.

At the other extreme of the spectrum, that is at the *macroscopic level*, the collective behavior of a great number of molecules is averaged locally to give rise to the hydrodynamical level of description, represented by the Navier–Stokes equations, Eqs. (1), or similar formulations pertaining to continuum mechanics. The huge separation of scales between the microscopic and macroscopic levels of descriptions implies that the smallest time and space scales in fluid dynamics and in turbulence, such as the Kolmogorov scales (see Section 6.1), are still orders of magnitude larger than the microscopic ones. This allows to develop formulations where details of the microscopic dynamics are replaced by stochastic models. These approaches form the *mesoscopic level* of description which is intermediate between the microscopic and macroscopic ones. A variety of models have been proposed at that level, for example Dissipative Particle Dynamics (DPD), Stochastic Rotation Dynamics (SRD), Smoothed Dissipative Particle Dynamics (SDPD) which is an offspring of DPD and Smoothed Particle Hydrodynamics (SPH), etc. in terms of modeled interacting particles or Lattice Boltzmann Method (LBM) in terms of the corresponding (N - or one-particle) distribution functions (DF) in sample space. Further details are provided in Section 5 but, in the context of the present section, these models are only mentioned to illustrate the microscopic, mesoscopic and macroscopic levels of description in the frame of classical statistical physics. The general picture is sketched in Fig. 13 where the arrow indicates the reduction of information contained in the formulations as we go from atomistic to hydrodynamical descriptions.

3.1.2. The interest of classical mesoscopic descriptions

Compared to microscopic approaches, mesoscopic models resolve less information but, as they can be simulated over larger time and space domains (due to the reduction of the number of degrees of freedom), they remain tractable for many applications. On the other hand, compared to macroscopic ones, these mesoscopic formulations contain more information and, consequently, tend to be more expensive to simulate. One interest is that they still reproduce the effects of microscopic fluctuations that are averaged out at the macroscopic level but their key advantage is that they allow complex constitutive relations to be obtained from consistent physical descriptions rather than through empirical correlations.

An interesting example is polymeric fluids (a special case of ‘complex fluids’) where the difficulty is to obtain satisfactory expressions of the stress tensor. Using the above terminology, we are concerned with a closure problem at the macroscopic level and the issue is to come up with accurate rheological laws. In Newtonian fluids, one can use the well-known linear law that relates the stress tensor to the strain rate through the fluid viscosity coefficient (which, as a transport coefficient, is a trace of the fluid microscopic details at the hydrodynamical level). This is indeed Newton’s law from which these fluids derive their name and we obtain a closed macroscopic description, *i.e.* the Navier–Stokes equations. However, for non-Newtonian fluids, such a direct macroscopic approach turns out to be a major obstacle. In that case, it proves useful to ‘step back’ to a mesoscopic description that consists in simulating explicitly a large number of polymers in the fluid flow but whose exact dynamics is replaced by a stochastic model (for a complete description of the following, readers are referred to [50] and, especially, to the introduction of this book).

As shown in Fig. 14(a), the construction of such a mesoscopic model is realized by, first, coarse-graining an actual polymer into a simplified description in terms of N beads connected by springs and, second, by proposing a stochastic model to simulate the dynamics of these bead-and-spring polymer model in fluid flows. Once this is achieved, the stress tensor due to polymers is directly evaluated (see the sketch in Fig. 14(b)). More precisely, to calculate the stress tensor a surface

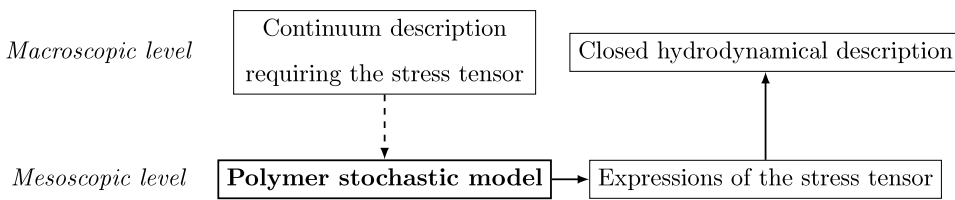


Fig. 15. Representation of the modeling approach based on the formulation of mesoscopic models to derive closed formulations at the macroscopic level.

element, the contribution from the polymers is derived from the virial approach, or the Kramers–Kirkwood expression, which yields

$$\tau_{\text{polymer}} = n_p \sum_{j=1}^{N-1} \langle \mathbf{Q}^{[j]}(t) \mathbf{F}_S^{[j]}(t) \rangle + N n_p k_B \Theta_f \mathbb{1} \quad (26)$$

with $\langle \cdot \rangle$ the ensemble average, n_p the polymer concentration, $\mathbf{F}_S^{[j]}(t)$ the force on the spring labeled $[j]$ at time t and $\mathbf{Q}^{[j]} = \mathbf{r}^{[j+1]} - \mathbf{r}^{[j]}$ the spring distance between the beads $[j+1]$ and $[j]$ whose positions are $\mathbf{r}^{[j+1]}$ and $\mathbf{r}^{[j]}$ respectively (see the derivation in [50, section 4.1.2]). The polymer stress tensor τ_{polymer} is then added to the Newtonian one due to the solvent to give the expression of the total stress at the macroscopic level.

More details of this approach, referred to as Brownian Dynamics (BD), are given in Section 7.2.1 but, for the present discussion, it is worth pointing out that the stress tensor is extracted without approximation from the available information. In other words, the introduction of a mesoscopic model (the bead–spring model) allows a tractable calculation of the stress tensor, derived from an underlying description in a physically-consistent manner, which is input to close the macroscopic equations. This methodology is represented in Fig. 15.

3.2. From microscopic to macroscopic descriptions in disperse two-phase flows

3.2.1. A clear separation of information content

In single-phase and disperse two-phase flow turbulence, the modeling task bears similarities with the previous situation. Indeed, we start with the fundamental equations describing the instantaneous behavior of the fluid and particles at the hydrodynamical level, which are composed of the Navier–Stokes equations for the fluid phase supplemented with the fundamental particle momentum equation (once a selection of the forces acting on particles has been made). Following the statistical approach to turbulence [30,38,39], the aim is to derive a closed set of equations for averaged fluid and particle properties. At first sight, it appears that the fundamental equations could be related to a microscopic level of description while the description in terms of averaged variables (over turbulence fluctuations) could be associated with a macroscopic one. With the previous definitions of microscopic, mesoscopic and macroscopic levels of description in terms of time and space scales, this remains however a loose analogy since there is precisely no such scale separation in turbulence modeling (both for the single-phase and two-phase cases). Nevertheless, it was proposed in [1] to carry out this idea from classical statistical physics to turbulent disperse two-phase flow modeling by introducing an extended definition whereby the three different levels of description are characterized by their ‘information content’. Since then, this approach has proved helpful as a guiding framework (see for instance [1,5,51]).

To quantify the notion of information content, the new definitions of the microscopic, mesoscopic and macroscopic levels of description are expressed with respect to the degrees of freedom resolved in each formulation. More precisely, it is proposed to define a *microscopic formulation* as an approach where all the degrees of freedom are calculated; a *mesoscopic formulation* as an approach where a reduced number of degrees of freedom are simulated; and a *macroscopic formulation* as an approach where averaged relations are obtained.

With the current statistical approach to turbulence modeling, macroscopic descriptions are represented by relations between moments (in a way similar to instantaneous fluid fields being averages over molecular motions), see Sections 6.3 and 6.4. In that sense and though they lie ‘in-between’ deterministic formulations at the microscopic and macroscopic levels, it is not surprising that mesoscopic approaches are made up by stochastic models or by their equivalent formulations in sample space in terms of probability density functions (PDFs) or filtered density functions (FDFs) which can be used in combination with Reynolds Averaged Navier–Stokes (RANS) or with Large Eddy Simulation (LES), as described in Section 6.5. The general modeling picture is represented in Fig. 16.

3.2.2. The interest of mesoscopic descriptions for single- and two-phase flows

On the modeling front, closure issues for reactive turbulent single-phase flows (see [30, chapter 12]) and polydisperse two-phase turbulent flows (see [1,5,52]) are the counterparts of the example of the stress-tensor closure for polymeric fluids. Therefore, mesoscopic models are also of interest since they allow constitutive relations and, thus, closed macroscopic formulations to be obtained. To illustrate this point, we consider successively the two cases of reactive turbulent single-phase and of polydisperse turbulent two-phase flows.



Fig. 16. Different approaches from the instantaneous field equations to averaged ones for turbulent single-phase and dispersed two-phase flows corresponding to the extended definitions of the microscopic, mesoscopic and macroscopic levels of description in terms of information content.

In turbulent reactive flows, the microscopic level is made up by the Navier–Stokes equation and by the transport equations for a set of scalars $\phi_f = (\Theta_f, c_1, \dots, c_{N_s})$ characterizing the combustion processes involved in the situations which are studied, cf. Eqs. (1). The macroscopic level is made up by the mean scalar equations which, following the direct macroscopic modeling approach, are derived by applying the averaging operator to the microscopic equations. For constant-property fluids and in the limit of high Peclet numbers, this yields

$$\frac{\partial \langle \phi_{f,l} \rangle}{\partial t} + \langle U_{f,k} \rangle \frac{\partial \langle \phi_{f,l} \rangle}{\partial x_k} = - \frac{\partial \langle u_{f,k} \phi'_{f,l} \rangle}{\partial x_k} + \langle \hat{S}_{f,l}(\phi_f) \rangle \quad (27)$$

where the terms on the rhs of Eq. (27) involve the mean chemical source term $\langle \hat{S}_{f,l}(\phi_f) \rangle$ and the scalar turbulent flux $\langle u_{f,k} \phi'_{f,l} \rangle$ which is the correlation between the fluctuating velocity components ($u_{f,k} = U_{f,k} - \langle U_{f,k} \rangle$) and the fluctuating scalar ($\phi'_{f,l} = \phi_{f,l} - \langle \phi_{f,l} \rangle$). At the macroscopic level, these two terms are unclosed. Since the chemical source terms $\hat{S}_{f,l}(\phi_f)$ are known but (usually) non-linear functions of the set of scalars ϕ_f (for instance, through the Arrhenius law for the exponential dependence of kinetic rates with respect to the fluid temperature), we are faced with the problem of having to express $\langle \hat{S}_{f,l}(\phi_f) \rangle$ with the only information available at the macroscopic level, which consists in a limited number of moments of the scalars: $\langle \hat{S}_{f,l}(\phi_f) \rangle \stackrel{?}{=} \mathcal{F}_l(\langle \phi_f \rangle, \dots, \langle (\phi_f)^m \rangle)$. In most cases, such direct closure attempts turn out to be intractable [30,31,53]. Similar concerns arise with the scalar turbulent flux. However, it can be noted that these two terms are closed and treated without approximation if the one-point velocity–scalar joint PDF $p_f(t, \mathbf{x}; \mathbf{V}_f, \psi_f)$ is known, since we have

$$\langle \hat{S}_{f,l}(\phi_f) \rangle(t, \mathbf{x}) = \int \hat{S}_{f,l}(\psi_f) p_f(t, \mathbf{x}; \psi_f) d\psi_f, \quad (28a)$$

$$\langle U_{f,k} \phi_f \rangle(t, \mathbf{x}) = \int V_{f,k} \psi_f p_f(t, \mathbf{x}; \mathbf{V}_f, \psi_f) d\mathbf{V}_f d\psi_f. \quad (28b)$$

If we want to treat the chemical source term $\langle \hat{S}_{f,l}(\phi_f) \rangle$ and the turbulent fluxes $\langle u_{f,k} \phi'_{f,l} \rangle$ without approximation, these relations show that, at minima, $p_f(t, \mathbf{x}; \mathbf{V}_f, \psi_f)$ must be known. It is also seen that, if we want to treat only the chemical source term without approximation, the one-point scalar PDF $p_f(t, \mathbf{x}; \psi_f)$ (the marginal of $p_f(t, \mathbf{x}; \mathbf{V}_f, \psi_f)$) must be available. In that case, the turbulent fluxes have to be closed by making an assumption, for example by resorting to a gradient-diffusion model. A further remark is that additional information provided by multi-point PDFs, such as the two-point velocity–scalar PDF $p(t, \mathbf{x}^1, \mathbf{x}^2; \mathbf{V}_f^1, \psi_f^1, \mathbf{V}_f^2, \psi_f^2)$ or even a N -point velocity–scalar PDF $p(t, \mathbf{x}^i; \mathbf{V}_f^i, \psi_f^i)$ (with $i = 1, \dots, N$), is not needed if we choose to describe only one-point scalar moments.

Similar concerns arise for discrete particles embedded in turbulent flows. This situation encompasses the one described above since particles can be subjected to their own combustion processes, e.g. burning coal particles (see the description of a mesoscopic model for mixed coal and biomass particles in co-firing furnaces given in [5, section 5.2.2]) or fuel droplets in combustion engines, etc. However, even the simple situation of inert particles involves difficult closure issues at the macroscopic level for polydisperse particles. As we are now dealing with a system made up by two phases (the fluid and the set of discrete particles), the microscopic level of description consists in the Navier–Stokes equations for the fluid, Eqs. (1), supplemented with the particle momentum equation, for example the simplified form given in Eq. (21b). The macroscopic level of description corresponds again to a set of transport equations for mean particle properties, such as the particle mass concentration $\rho_p \alpha_p(t, \mathbf{x})$ where $\alpha_p(t, \mathbf{x})$ is the mean volumetric fraction occupied by the particle phase at (t, \mathbf{x}) and the mean velocity fields $\langle \mathbf{U}_p \rangle(t, \mathbf{x})$. The direct application of the averaging operator to the microscopic equations gives the first two moments equations which are (as demonstrated later in Section 4.4, see also the complete derivations in [1,54]):

$$\frac{\partial (\alpha_p \rho_p)}{\partial t} + \frac{\partial [\alpha_p \rho_p \langle U_{p,j} \rangle]}{\partial x_j} = 0, \quad (29a)$$

$$\alpha_p \rho_p \frac{\partial \langle U_{p,i} \rangle}{\partial t} + \alpha_p \rho_p \langle U_{p,j} \rangle \frac{\partial \langle U_{p,i} \rangle}{\partial x_j} = - \frac{\partial [\alpha_p \rho_p \langle u_{p,i} u_{p,j} \rangle]}{\partial x_j} + \alpha_p \rho_p \left\langle \left(\frac{U_{s,i} - U_{p,i}}{\tau_p} \right) \right\rangle. \quad (29b)$$

At this macroscopic level, we are faced with the task of having to express the particle kinetic tensor, $\langle u_{p,i} u_{p,j} \rangle$, as a function of one-point moments. As for scalars, a gradient-diffusion model could be assumed to close the particle kinetic tensor. Yet, this first task is compounded by a second one due to the last term on the rhs of the mean particle momentum equation in Eq. (29b). Like the mean chemical source term in Eq. (27), this term is unclosed for polydisperse particles. Indeed, τ_p is a known but non-linear function of \mathbf{U}_s , \mathbf{U}_p , d_p and we have to come up with a closed expression of $\langle (U_{s,i} - U_{p,i})/\tau_p \rangle$ as a function of $\langle U_{s,i} \rangle$, $\langle U_{p,i} \rangle$, $\langle d_p \rangle$ (note that a closed expression for $\langle \tau_p \rangle$ already induces similar difficulties).

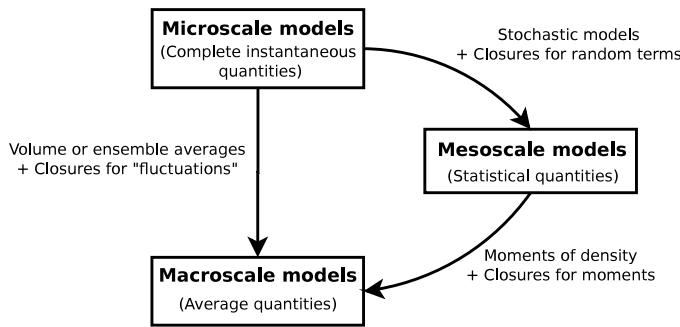


Fig. 17. Relations between the microscopic, mesoscopic and macroscopic levels of description and their interest for closure issues.
Source: Reprinted from [2] with permission from Elsevier.

The issues of the treatment of the mean chemical source term and of the mean drag force term in the mean particle momentum equation show that, for single-phase and disperse two-phase turbulent flows, it is too difficult to close directly at the macroscopic level through constitutive relations between macroscopic variables. It is also seen that these situations are similar to the problem of the stress tensor in polymeric fluids, and that formulations in terms of microscopic, mesoscopic and macroscopic levels of description defined by their information content are helpful to reveal the thread of continuity between these situations. The road towards closed macroscopic formulations is sketched in Fig. 17 (see [51] and [30, chapter 12]) and brings out the interest of going through mesoscopic formulations.

Several conclusions can be drawn from the previous examples:

- (1) For single-phase and disperse two-phase turbulent flows, the mesoscopic levels of description correspond essentially to PDF models whose name translate the fact that they simulate the PDF of a set of variables that define the particle state vector. PDF models for single-phase turbulent flows are introduced in Section 6.5 while PDF models for disperse two-phase flows are first discussed in Section 7.3 and, then, investigated throughout Sections 9 and 10. The notion of the particle state vector is discussed in Sections 8.1, 9.4, 10.1 and 10.2;
- (2) Once a mesoscopic approach is selected, it is essential to be aware of the information that can be extracted and the information that remains external. This is exemplified in Section 8.2;
- (3) When incomplete mesoscopic descriptions are retained (or when direct macroscopic closures are attempted), gradient-diffusion models are often used for unclosed fluxes. This assumption is analyzed at the end of Section 9.3 where a paragraph is dedicated to gradient-diffusion models for turbulent scalar fluxes and in Section 10.3 for the particle kinetic tensor. Given its importance, this issue is taken up in Section 10.4.

It is seen that the vast majority of models developed at the mesoscopic level of description are stochastic models. To gain a better understanding of the models reviewed in Sections 5–7 and to address the specific issues appearing for probabilistic descriptions of particles in turbulent flows studied in Sections 9 and 10, it is useful to establish a sound mathematical background on stochastic processes. This is done in Section 4.

4. Mathematical background and statistical descriptions

There is now a rich literature on stochastic processes. This does not, however, make the situation necessarily easier for newcomers in this field as they are faced with a forest of strange terms (Monte Carlo methods, PDF models, Stochastic Differential Equations, white noises, Langevin, Fokker–Planck, Liouville and even so-called Master Equations, etc.), without any obvious hierarchy between these different aspects. To get one's bearings in this domain, it is useful to make a distinction between 'stochastic calculus', where the purpose is to investigate the mathematical properties of stochastic processes and set up rigorous manipulation rules, and 'stochastic modeling', where the aim is to use stochastic processes as modeling tools for various issues in physics, chemistry and engineering. Up to recently, this two-faced portrait was reflected, on the one hand, in a dense mathematical literature not always accessible to readers with a physical standpoint (see, among others, [55–58]), and in a variety of separate applications in physics without reference to a common framework on the other hand (see some historical accounts in [43,59,60]).

In the last decades, this situation has improved thanks to reference textbooks addressing the range of applications in physics from a unified perspective [43,50,59]. In the present author's opinion, Öttinger's book [50] provides an excellent presentation with the right compromise between mathematical rigor and physical descriptions. It is telling that this detailed account grew out of a single physical study, namely the simulation of polymeric fluids outlined in Section 3.1.2. However, only stochastic diffusion processes were considered and this text can be complemented with Gardiner's handbook [43]. In Fluid Dynamics, this middle-of-the-road approach between mathematics and physics has been also developed and a number

of reviews are available where relevant aspects of stochastic processes, regarded as modeling tools, are covered. This can be found in [31] and in [30, chapter 12] for single-phase turbulent flows and in [1, section 2] as well as in [5, 52, 60] for disperse turbulent two-phase flows.

For these reasons, we limit ourselves to presenting only the key aspects of stochastic processes of interest for the analysis of stochastic models for particles in turbulent flows. Yet, the presentation is not too sketchy. This is done to emphasize the underlying message that “mathematical details” should not be overlooked if one is to ensure that physical models have solid roots. It will be seen in Sections 9 and 10 that, at the core of the discussions about colored and white noises and well- or ill-posed descriptions, are questions related to the Markov nature of stochastic processes and to a proper handling of stochastic diffusion processes. In anticipation of these analyses, we start with the rigorous definition of a stochastic process in Section 4.1 before addressing the central distinction between Markov and non-Markov processes in Section 4.2. The fundamental class of jump-diffusion processes is presented in Section 4.3 while the general methodology from Lagrangian stochastic models to mean-field equations is recalled in Section 4.4. This leads to the important discussion in Section 4.5 in which useful criteria to assess probabilistic models are set up.

4.1. Stochastic processes

Definition of a stochastic process. A stochastic process, noted as \mathbf{Z} or $(\mathbf{Z}(t), t \geq 0)$, is a family of random variables indexed by a parameter which is usually time (with $t \in [0; T_{\max}]$, where T_{\max} is an end time with the possible value $T_{\max} = +\infty$). In the following, we consider vector-valued stochastic processes in \mathfrak{N}^d (where d is the dimension) and we denote the values in the corresponding sample space by \mathbf{z} .

Key characteristics. To understand the essential characteristics of a stochastic process, it is useful (and even necessary) to introduce the rigorous definition that extends the mathematical one for random variables, whereby \mathbf{Z} is a family of measurable functions $\mathbf{Z}(t)$ on an underlying probability space Ω equipped with a σ -algebra \mathcal{F} and a probability measure \mathbb{P} . This gives that \mathbf{Z} as a measurable function of two variables:

$$\begin{aligned} [0; T_{\max}] \times (\Omega, \mathcal{F}, \mathbb{P}) &\longrightarrow (\mathfrak{N}^d, \mathcal{B}^d) \\ (t, \omega) &\longmapsto \mathbf{Z}(t, \omega), \end{aligned} \quad (30)$$

where \mathcal{B}^d is the Borel σ -algebra for \mathfrak{N}^d obtained as the d -tensorial-product of the Borel σ -algebra for \mathfrak{N} . The first interest of this definition is to show that there are two ways to characterize a stochastic process:

- (1) For each fixed value of t , $\mathbf{Z}(t)$ (also noted \mathbf{Z}_t) is a vector-valued random variable

$$\begin{aligned} (\Omega, \mathcal{F}, \mathbb{P}) &\longrightarrow (\mathfrak{N}^d, \mathcal{B}^d) \\ \omega &\longmapsto \mathbf{Z}_t(\omega), \end{aligned} \quad (31)$$

with a probability density function (PDF) $p(t; \mathbf{z})$, assuming that the probability measure $\mathbb{P}_{\mathbf{Z}_t}$ of the random variable $\mathbf{Z}(t)$ has a density with respect to the Borel measure $d\mathbf{z}$. This corresponds to the ‘PDF point of view’ where the purpose is to derive the PDF equation satisfied by $p(t; \mathbf{z})$ in sample space.

- (2) For each fixed value of ω , indicating a subset of the sigma algebra \mathcal{F} or one ‘elementary event’, the resulting time function

$$\begin{aligned} [0; T_{\max}] &\longrightarrow (\mathfrak{N}^d, \mathcal{B}^d) \\ t &\longmapsto \mathbf{Z}_\omega(t), \end{aligned} \quad (32)$$

defines a trajectory, or a sample path, of the stochastic process. This corresponds to the ‘trajectory point of view’ where the purpose is to write the time-evolution equations of these ‘particles’ (which represent samples of the PDF and are used in Monte Carlo estimations) in physical space.

The second interest of the rigorous definition of stochastic processes is that the explicit reference to σ -algebras allows to quantify the intuitive notions of the information content (the information resolved by one description) and level of description introduced in Section 3. More precisely, fine- and coarse-grained descriptions are seen to correspond to different embedded σ -algebras, or sub- σ -algebras (see detailed illustrations in [50, chapter 2.1.1]). Furthermore, this is the only way to properly explain conditional expectations defined, not by fixing the value of another random variable, but with respect to sub- σ -algebras (see [50, chapter 2.1.4]) as the correct formulation of partially-resolved information.

For a stochastic process, there is always more information in the trajectories than in its PDF. However, since we are interested in approximating statistics derived from a stochastic process (which corresponds to an approximation in law or to an approximation of the PDF in a weak sense), we can loosely refer to an equivalence between the PDF and trajectory points of view. Nevertheless, this gives further support to the trajectory point of view which is often adopted in the rest of the article.

The law of a stochastic process. Knowing the law of a random variable $\mathbf{Z}(t)$ (at a given time) is equivalent to saying that we know its PDF $p(t; \mathbf{z})$ or, in a weak sense, that we know the value of a large number of samples. Indeed, Monte Carlo estimations yield that for N samples $(\mathbf{Z}^{(k)}(t))_{k=1,\dots,N}$, we have

$$p(t; \mathbf{z}) \simeq p_N(t; \mathbf{z}) = \frac{1}{N} \sum_{k=1}^N \delta(\mathbf{z} - \mathbf{Z}^{(k)}(t)) \quad (33)$$

where the approximation $p(t; \mathbf{z}) \simeq p_N(t; \mathbf{z})$ is in the weak (or distribution) sense since, for any statistics $\langle Q(\mathbf{Z}(t)) \rangle$ obtained from the random variable $\mathbf{Z}(t)$ (with Q a smooth-enough function), we can write that

$$\langle Q(\mathbf{Z}(t)) \rangle = \int Q(\mathbf{z}) p(t; \mathbf{z}) d\mathbf{z} \simeq \int Q(\mathbf{z}) p_N(t; \mathbf{z}) d\mathbf{z} = \frac{1}{N} \sum_{k=1}^N Q(\mathbf{Z}^{(k)}(t)). \quad (34)$$

However, knowing a stochastic process is not equivalent to knowing the family of its one-time PDFs ($p(t; \mathbf{z}), t \geq 0$) since it entails, for example, knowing also the joint laws of joint random variables $\mathbf{Z}(t)$ and $\mathbf{Z}(t')$ at any times t and t' , etc. Using the trajectory point of view, it is seen that to carry out the reasoning developed for the law of vector-valued random variables to stochastic processes implies to regard a stochastic process as a trajectory-valued random variable and, consequently, to handle the related space of functions ($t \mapsto \mathbf{Z}_\omega(t)$) with a σ -algebra and a probability measure (see [50, chapter 2.3.1]). This notion of the law of a stochastic process is then easier to understand in a discrete setting: simply speaking, knowing the law of a stochastic process is equivalent to the knowledge of the joint PDF $p(t_1, \mathbf{z}_1; t_2, \mathbf{z}_2, \dots; t_N, \mathbf{z}_N)$ for any set of N times and for any values of the chosen times (t_1, t_2, \dots, t_N). It is thus clear that the amount of information required is huge and, in particular, much larger than the sole access to the one-time PDF functions $p(t, \mathbf{z})$.

4.2. Markovian and non-Markovian processes

Markov processes. The notion of Markov processes is the direct extension of the theory of deterministic dynamical systems in classical mechanics, where the knowledge of an initial condition (at a time t_0) and of the rate of change is enough to predict the future of a dynamical system. Carried to the world of probabilistic descriptions, this is formulated in terms of conditional PDFs with the same ideas based on the present (i.e. $t = t_0$), the past (i.e. $t < t_0$) and the future (i.e. $t > t_0$). Loosely speaking, a Markov process is a stochastic process for which ‘knowledge of the whole past’ or ‘knowledge of the present’ amounts to the same for predicting the future (in a probabilistic sense). A rigorous definition requires adapted-sigma algebras [50,55] but, for our purpose, it is sufficient to illustrate the Markov property of a stochastic process in a discrete setting by writing that

$$p(t_{n+1}, \mathbf{z}_{n+1} | (t_n, \mathbf{z}_n; t_{n-1}, \mathbf{z}_{n-1}; \dots; t_1, \mathbf{z}_1)) = p(t_{n+1}, \mathbf{z}_{n+1} | t_n, \mathbf{z}_n) \quad (35)$$

where t_n represents here the present time while t_{n+1} stands for the future and (t_{n-1}, \dots, t_1) for the past, while \mathbf{z}_i is the value of the process at $t = t_i$ (i.e. $\mathbf{Z}(t_i) = \mathbf{z}_i$). An important element is that the condition entering the conditional PDF, written as (t_n, \mathbf{z}_n) in Eq. (35), represents in fact the *whole information known* at the present time $t = t_n$. For example, if we consider a system upon which an external action is exerted, then this action must be fully determined by the knowledge of (t_n, \mathbf{z}_n) for the Markov property to be valid.

The fundamental property of Markov processes is that the law of the stochastic process is completely determined from the knowledge of only two functions: $p(t_0, \mathbf{z}_0)$ which represents an initial PDF condition and $p(t, \mathbf{z} | t_0, \mathbf{z}_0)$ which is the conditional or transition PDF from a state \mathbf{z}_0 at $t = t_0$ to a state \mathbf{z} at a later time t . This transition PDF plays the role of the time rate of change in classical mechanics and is the central quantity. Indeed, all the N -time PDFs are easily reconstructed by the application of the Chapman–Kolmogorov equation (or chain-rule) [43,50,61]

$$p(t, \mathbf{z} | t_0, \mathbf{z}_0) = \int p(t, \mathbf{z} | t_1, \mathbf{z}_1) p(t_1, \mathbf{z}_1 | t_0, \mathbf{z}_0) d\mathbf{z}_1, \quad (36)$$

which demonstrates that information on the complete law of the process is retrieved.

Important relations are obtained from the Infinitesimal Operator defined by

$$\mathcal{L}_t g(\mathbf{z}) = \lim_{dt \rightarrow 0} \frac{\langle (g(\mathbf{Z}_{t+dt}) | \mathbf{Z}_t = \mathbf{z}) \rangle - g(\mathbf{z})}{dt}, \quad (37)$$

which ‘measures’ the effect of a conditional increment of the Markov process over a test function g (note that this a characterization in a weak sense). In particular, it can be shown [43,50,55] that the transitional PDF $p(t, \mathbf{z} | t_0, \mathbf{z}_0)$ is the solution of two mirrored equations corresponding to whether we fix the end condition (t, \mathbf{z}) and track the evolution backward in time to possible past values (t_0, \mathbf{z}_0) or whether we fix the initial condition (t_0, \mathbf{z}_0) and observe the evolution as time t evolves in the future. In the first case, this corresponds to the Kolmogorov backward equation written as

$$\begin{cases} \frac{\partial p(t, \mathbf{z} | t_0, \mathbf{z}_0)}{\partial t_0} + \mathcal{L}_{t_0} [p(t, \mathbf{z} | t_0, \mathbf{z}_0)] = 0, \\ p(t, \mathbf{z} | t_0, \mathbf{z}_0) = \delta(\mathbf{z} - \mathbf{z}_0) \quad t_0 \rightarrow t. \end{cases} \quad (38)$$

In the second case, the evolution equation corresponds to the Kolmogorov forward equation

$$\begin{cases} \frac{\partial p(t, \mathbf{z} | t_0, \mathbf{z}_0)}{\partial t} = \mathcal{L}_t^\perp [p(t, \mathbf{z} | t_0, \mathbf{z}_0)], \\ p(t, \mathbf{z} | t_0, \mathbf{z}_0) = \delta(\mathbf{z} - \mathbf{z}_0) \quad t \rightarrow t_0, \end{cases} \quad (39)$$

where \mathcal{L}_t^\perp stands for the adjoint operator of \mathcal{L}_t . The fact that the complete law of a Markov process can be reconstructed from the Chapman–Kolmogorov relation in Eq. (36) means that the evolution equation for the transition PDF lives up to its

name of a ‘Master Equation’ (ME) [59,62]. This terminology refers essentially to the Kolmogorov forward equation since, from a physical point of view, we are usually considering the time evolution of a dynamical system from an observed initial state at a given time t_0 . However, as seen from the two adjoint Kolmogorov equations, any model developed in terms of a Markov process yields naturally information on both the forward and backward problems. A further remark is that this well-established formulation implies to treat a Markov stochastic process either from a backward or from a forward standpoint. The difference of sign in front of the operators in Eqs. (38) and (39) gives a hint that attempts at deriving formulations where some variables (say (z_1, \dots, z_r) with $r < d$) of a (general) vector-valued stochastic process are treated in a forward approach while others (say (z_{r+1}, \dots, z_d)) would be treated in a backward one are not likely to be well posed. This remark is of some significance for the analysis of kinetic formulations of particles in partially-resolved turbulent flows, as seen in Section 10.1.1. *Non-Markovian processes.* Based on the PDF point of view mentioned above, it is always possible to consider the one-time PDF $p(t, \mathbf{z})$ of the family of random variables $\mathbf{Z}(t)$, or the transition PDF $p(t, \mathbf{z} | t_0, \mathbf{z}_0)$, from which one-time statistical moments can be derived (through the definition of the related distribution function, see Section 4.4). However, when the Markov property breaks down, not much can be said about a stochastic process. In particular, it is not possible to reconstruct further information from the sole knowledge of the one-time PDF. One can still write an evolution equation for this one-time PDF (or the transition one) $p(t, \mathbf{z})$, for example of the form

$$\frac{\partial p(t, \mathbf{z})}{\partial t} = \mathcal{G}[p(t, \mathbf{z})] \quad (40)$$

where \mathcal{G} is an operator, but this equation cannot be considered as the equivalent of a ME [62].

The lack of Markovianity induces further serious limitations. For example, when investigating path properties of dynamical systems influenced by external colored noises, Markovianity is an almost necessary road, as can be seen for instance in [63,64] for a study of exit times in the simplest linear situation or in [65] for a study of activation rates in a bistable system. Indeed, non-Markovianity implies that a complete probabilistic description cannot be obtained as easily and requires, in general, much more sophisticated techniques. These points are further analyzed in Section 9 and, especially, in Section 9.2.

4.3. Jump and diffusion stochastic processes

Following the remark on the higher information content of the trajectories of a stochastic process, the theory of jump-diffusion stochastic processes is best addressed from the trajectory point of view. Once these trajectories are properly defined, the corresponding PDF equations in sample space are derived. The general formulation of the stochastic differential equations (SDEs) for the trajectories of a jump-diffusion process rests upon two building blocks which are the Poisson and Wiener processes. The essential properties of these two fundamental stochastic processes are given first in Section 4.3.1 before building the general expression in Section 4.3.2 where PDF equations are stated.

4.3.1. The two building blocks: the Wiener and Poisson processes

The Poisson process. The Poisson process is the canonical model for random discrete, or count, events. In these processes, there is a very small probability to have one event but each event implies a significant change represented by a jump (multiple jumps at one time are not possible). The trajectories of the Poisson process are therefore piecewise constant with jumps (having a step of one unity in the standard Poisson process) occurring at random times [43,57]. Typical properties are illustrated in Fig. 18.

The increments of the Poisson process, $\Delta N(t) = N(t + \Delta t) - N(t)$, are stationary and independent. A Poisson process is characterized by its intensity λ which stands for the mean value of the number of events per unit time (thus with the dimension of a frequency [s^{-1}]) and the number of events in a time interval $[t, t + \Delta t]$ is a Poisson random variable

$$\mathbb{P}[\Delta N(t) = k] = \frac{(\lambda \Delta t)^k}{k!} e^{-\lambda \Delta t} \quad (41)$$

from which it derives that the mean and variance of $\Delta N(t)$ are linear with respect to Δt

$$\langle \Delta N(t) \rangle = \lambda \Delta t \quad \langle (\Delta N(t) - \langle \Delta N(t) \rangle)^2 \rangle = \lambda \Delta t. \quad (42)$$

In any finite interval, the individual events (the times at which the Poisson process jumps) are uniformly distributed. This property explains that the Poisson process is often regarded as the ‘reference distribution’ for uniformly-distributed discrete events: for example, if we distribute a number of particles in an interval with a uniform distribution, then the number of particles found in a small bin of length Δx is a Poisson distribution with a mean equal to $\lambda \Delta x$ (where λ is here a density with respect to length and has the dimension [m^{-1}]). In practice, this explains that measured particle distributions are often compared to this reference one and that any deviation from the Poisson law is regarded as the manifestation of an underlying order (a non-uniform law for the individual particle distribution).

Given the discontinuous nature of the trajectories, there are typically two ways to simulate a Poisson process. The first method is based on the waiting times (the time intervals between successive random jumps) and, since values are constant

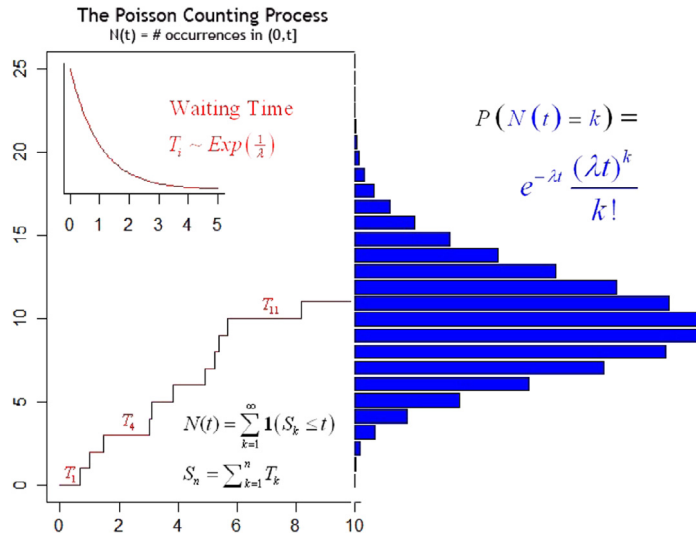


Fig. 18. Some properties of the Poisson process $N(t)$: example of one trajectory of the process jumping at random times T_i , which follow an exponential distribution and the resulting pdf of $N(t)$ at each time t being a Poisson distribution.
Source: Reprinted from [66] with permission from Springer.

between jumps, the idea is to go directly from one event to the next one. These waiting times are random variables following an exponential distribution with the same intensity λ :

$$\mathbb{P}[T_i = t] = \lambda e^{-\lambda t} \Rightarrow \langle T_i \rangle = \frac{1}{\lambda}, \quad (43)$$

and are generated before applying the unit-one jump (*i.e.* $\Delta N(t) = 1$) or any more general event when considering generalized Poisson processes (see below in Section 4.3.2). This is the algorithmic form under which stochastic particle systems used to simulate collision and agglomeration events are presented, as will be seen in Section 10.6 (further discussions and examples can be found in [5, section 6.2] and in the literature mentioned there). This first method imposes to handle variable time steps and, when other phenomena are present, it may be preferred to use the second method where a Poisson process is simulated at fixed times. Whereas in the first method the jumps are always of unit one since we go from one jump to the next one using random time intervals, the second method is based on the simulation of the number of possible events occurring in fixed time intervals. When the time interval Δt is much smaller than the relevant timescale $1/\lambda$ (*i.e.* $\lambda \Delta t \ll 1$), the statistics of the increments, which follow the Poisson distribution given in Eq. (41), have the simplified expression:

$$\begin{aligned} \mathbb{P}[\Delta N(t) = 0] &\simeq 1 - \lambda \Delta t \\ \mathbb{P}[\Delta N(t) = 1] &\simeq \lambda \Delta t \\ \mathbb{P}[\Delta N(t) = k] &= 0 \quad (k \geq 2). \end{aligned} \quad (44)$$

The Wiener process. First introduced (in an heuristic way) by Einstein in 1905 and later put on solid mathematical grounds by Wiener in 1921, the Wiener process is the canonical model of Brownian motion [43,50]. It has been the subject of comprehensive studies (see for example [56]) in which its specific (and often surprising) properties have been investigated, and is the cornerstone of the construction of stochastic differential equations [55,57,58]. Based on this accumulated knowledge, the Wiener process is defined by the following three properties:

- (i) The process has independent increments, *i.e.* $(W(t_3) - W(t_2))$ and $(W(t_1) - W(t_0))$ are independent when $t_0 < t_1 < t_2 < t_3$;
- (ii) The trajectories of the process are continuous functions (almost everywhere);
- (iii) The increments of the Wiener process $(W(t_2) - W(t_1))$ are centered Gaussian random variables and with a variance equal to $(t_2 - t_1)$.

From these characteristics, it results that the Wiener process W is a Gaussian, Markov process, with zero mean and a covariance equal to $\langle W(t)W(t') \rangle = \min(t, t')$. Its Gaussian transitional PDF is the solution of the heat equation (this point is extended by defining stochastic diffusion processes in Section 4.3.2). The trajectories of the Wiener process are continuous and, in contrast to the Poisson process, they represent continuous evolutions where there is a near-one chance that modifications happen but with small changes. The most important properties are that the trajectories of the Wiener

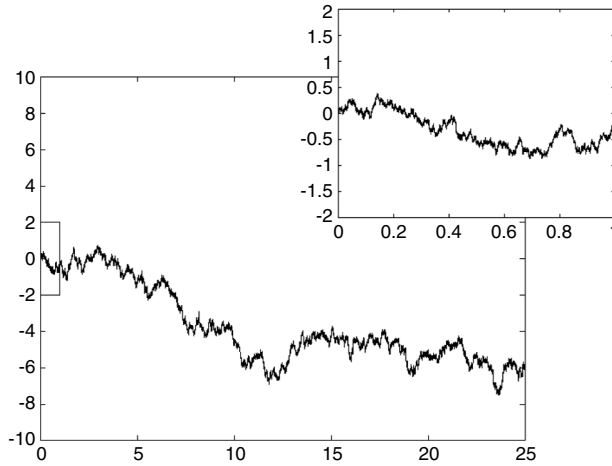


Fig. 19. One trajectory of the Wiener process showing a continuous but ragged profile. The window, where a zoom of the trajectory is displayed, indicates the self-similar nature and the (infinitely) fast fluctuations of the trajectories of the Wiener process.
Source: Reprinted from [66] with permission from Springer.

process are non-differentiable at any point and have unbounded total variations in any interval. Furthermore, the increments $dW(t) = dW(t + dt) - W(t)$ are stationary and independent with successive moments

$$\langle dW(t) \rangle = 0, \quad \langle (dW(t))^2 \rangle = dt, \quad \langle (dW(t))^n \rangle = o(dt) \quad \forall n > 2. \quad (45)$$

The linear variation of the variance of the increments $\langle (dW(t))^2 \rangle$ with respect to dt is of paramount importance in the development of stochastic calculus [55,57,58]. This property reflects the non-differentiable nature of the trajectories of the Wiener process (for differentiable processes, the variance of the increments varies as dt^2) or, in other terms, expresses that the ‘velocity’ of a Brownian particle is infinite at any instant (and, thus, does not exist). Yet, the smoothing property of the integration operator allows to identify the integration of Gaussian white noise to the Wiener process [1,50,60] or, loosely speaking, to say that the ‘derivative of the Wiener process’ represents Gaussian white noise. The non-differentiability and infinite total variation of the trajectories of the Wiener process have deep consequences for the construction of the stochastic integral, as recalled below. A typical example of a trajectory of the Wiener process is displayed in Fig. 19 which illustrates the wildly varying nature of the trajectories at any scale. Yet, when averaged over a large number of trajectories, these wild fluctuations corresponds to the smooth, but irreversible, diffusion of the PDF.

4.3.2. Stochastic differential equations

To present the main characteristics of the SDEs for jump–diffusion processes, a one-dimensional setting is sufficient since there is no special difficulty in generalizing to the d -dimensional case. For this reason, the main notions are presented for a one-dimension stochastic process and directly stated for a vector-valued one. Furthermore, the case of stochastic diffusion processes (with continuous trajectories) is presented first before including jumps in the general formulation.

Using the trajectory standpoint, the purpose is to give a meaning to the equation of the trajectories of a dynamical system represented by the one-dimensional process Z

$$\frac{dZ(t)}{dt} = A(t, Z(t)) + B(t, Z(t)) \zeta(t) \quad (46)$$

when ζ becomes a Gaussian white-noise process. The key idea is to give sense not to the above differential form but to its integrated formulation which, using the identification of $\int_0^t \zeta(s) ds$ with a white-noise process, i.e. $\zeta_t dt = dW_t$, is given by

$$Z(t) = Z(t_0) + \underbrace{\int_{t_0}^t A(t_s, Z(s)) ds}_{\text{regular integral}} + \underbrace{\int_{t_0}^t B(s, Z(s)) dW(s)}_{\text{stochastic integral}}. \quad (47)$$

If the usual Riemann–Stieltjes approach can be used for the regular integral, the stochastic one requires a special definition (due to the fact that the trajectories of W are of infinite total variation). For a non-anticipating process X , the stochastic integral is properly defined in the Ito sense as

$$\int_{t_0}^t B(s, Z(s)) dW_s = \text{ms-} \lim_{N \rightarrow \infty} \sum_{i=1}^N B(t_i, Z(t_i)) (W(t_{i+1}) - W(t_i)) \quad (48)$$

where $(t_i)_{i=1,N}$ represents a partition of the interval $[0; t]$ (with $t_1 = 0$ and $t_{N+1} = t$) and where the limit is to be understood as a limit in the mean-square sense [50,55,57,58] and not any more as a convergence trajectory by trajectory. With these clarifications, the equations for the trajectories of a one-dimensional stochastic process are completely defined. Written in incremental form as a short-hand notation, they are usually referred to as Langevin equations in the physics literature

$$dZ(t) = A(t, Z(t)) dt + B(t, Z(t)) dW(t), \quad (49)$$

and the corresponding PDF equation in sample space is the Fokker–Planck equation (FPE)

$$\frac{\partial p(t, z | t_0, z_0)}{\partial t} = -\frac{\partial [A(t, z) p(t, z | t_0, z_0)]}{\partial z} + \frac{1}{2} \frac{\partial^2 [B^2(t, z) p(t, z | t_0, z_0)]}{\partial z^2}. \quad (50)$$

Note that an initial condition for the trajectories $Z(t_0) = z_0$ (with z_0 being a fixed number) is translated into the initial condition $p(t, z | (t_0, z_0)) = \delta(z - z_0)$ when $t \rightarrow t_0$ for the PDF. The FPE is one example of a forward Kolmogorov equation, cf. Eq. (39), and corresponds to the infinitesimal operator \mathcal{L}_t

$$\mathcal{L}_t(\cdot) = A(t, z) \frac{\partial [\cdot]}{\partial z} + \frac{1}{2} B^2(t, z) \frac{\partial^2 [\cdot]}{\partial z^2}. \quad (51)$$

Given the form of the Fokker–Planck equation as a convection–diffusion equation (thus the name given to stochastic diffusion processes), the functions A and B are referred to as the drift and diffusion coefficients, respectively. Note that, whatever the sign of B , the diffusion coefficient entering the PDF equation is B^2 and is therefore always positive or null (which further justifies its name of diffusion coefficient).

The correspondence between Langevin and Fokker–Planck equations is easily extended to the multi-dimensional case. For instance, the SDEs written for a d -dimensional process $\mathbf{Z} = (Z_1, \dots, Z_d)$ are

$$dZ_i(t) = A_i(t, \mathbf{Z}(t)) dt + B_{ij}(t, \mathbf{Z}(t)) dW_j(t), \quad (52)$$

with $(W_j)_{j=1,d}$ a set of d independent Wiener processes. In Eq. (52), the drift $\mathbf{A} = (A_i)$ is now a vector while the diffusion $\mathbf{B} = (B_{ij})$ is a matrix. It is straightforward to show that the corresponding Fokker–Planck equation is

$$\frac{\partial p(t, \mathbf{z} | t_0, \mathbf{z}_0)}{\partial t} = -\frac{\partial [A_i(t, \mathbf{z}) p(t, \mathbf{z} | t_0, \mathbf{z}_0)]}{\partial z_i} + \frac{1}{2} \frac{\partial^2 [D_{ij}(t, \mathbf{z}) p(t, \mathbf{z} | t_0, \mathbf{z}_0)]}{\partial z_i \partial z_j}, \quad (53)$$

where $\mathbf{D} = \mathbf{B}\mathbf{B}^\perp$ (or $D_{ij} = B_{ik}B_{jk}$) is a symmetric definite-positive matrix. As in the one-dimensional case, the positivity of \mathbf{D} justifies the reference to a diffusive nature induced by the rapidly-varying terms, $B_{ij}(t, \mathbf{Z}(t)) dW_j(t)$, in Eq. (52). The fact that several matrices \mathbf{B} can correspond to the same diffusion matrix \mathbf{D} expresses the loose equivalence between the trajectory and PDF points of view. In an approximation in law, note that only the value of \mathbf{D} is significant.

The physical meaning of the coefficients A and B in the Langevin and Fokker–Planck equations are further revealed by considering the statistics of the conditional increments (using a simple one-dimensional version), which are:

$$\langle \Delta Z | Z(t) = z \rangle = A(t, z) \Delta t, \quad (54a)$$

$$\langle (\Delta Z)^2 | Z(t) = z \rangle = B^2(t, z) \Delta t. \quad (54b)$$

As displayed in Fig. 20, it is seen that the drift term, $A(t, z)$, governs the mean evolution of the conditional increments of the process, while the diffusion coefficient, $B(t, z)$, governs the spread of the conditional increments around its mean value.

From the properties of the Wiener process, it is clear that the increments ΔW_t over a time step Δt are indeed Gaussian random variables. Apart from the case of Brownian motion itself (where $A = 0$ and $B = 1$), the simplest example of a stochastic diffusion process is the Ornstein–Uhlenbeck (OU) process whose trajectories can be written as

$$dZ(t) = -\frac{Z(t)}{\tau} dt + K dW(t), \quad (55)$$

where the timescale τ and the diffusion coefficient K are constant. This leads immediately to Z being a Gaussian process whose characteristics are easily worked out (see [43,50]). This is, however, a special case of the general form of the SDEs for a stochastic diffusion process given in Eq. (52) and this has led to repeated confusion with respect to the nature of the Gaussian hypothesis made in the construction of stochastic diffusion processes. As clarified by the relations in Eqs. (54) in a discrete setting, only the conditional increments $\Delta Z | (Z(t) = z)$ of the process Z are assumed to follow a Gaussian spread over the small time interval Δt . In the special case where the diffusion coefficient is constant and the drift linear, as for the case of an OU process, the stochastic process Z is indeed Gaussian. Yet, in the general situation when $B(t, z)$ is not constant, the Gaussian hypothesis applies only to the conditional increments and the resulting process Z can deviate from Gaussianity. Though this point has been clarified [1,5,60], it is worth emphasizing that the observation of non-Gaussian distributions does not invalid models based on stochastic diffusion processes.

Still using the trajectory point of view, the SDEs for a jump–diffusion process are

$$dZ(t) = A(t, Z(t)) dt + B(t, Z(t)) dW(t) + C(t, Z(t)) dN(t), \quad (56)$$

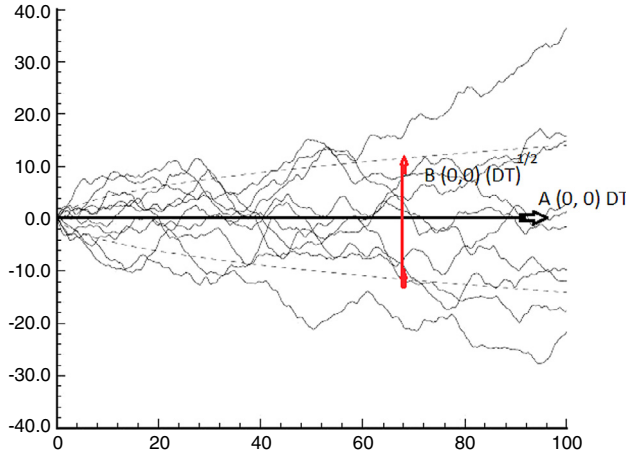


Fig. 20. Some conditional trajectories of a stochastic diffusion process, or Langevin equations, illustrating the physical meaning of the drift and diffusion coefficients.

Source: Reprinted from [66] with permission from Springer.

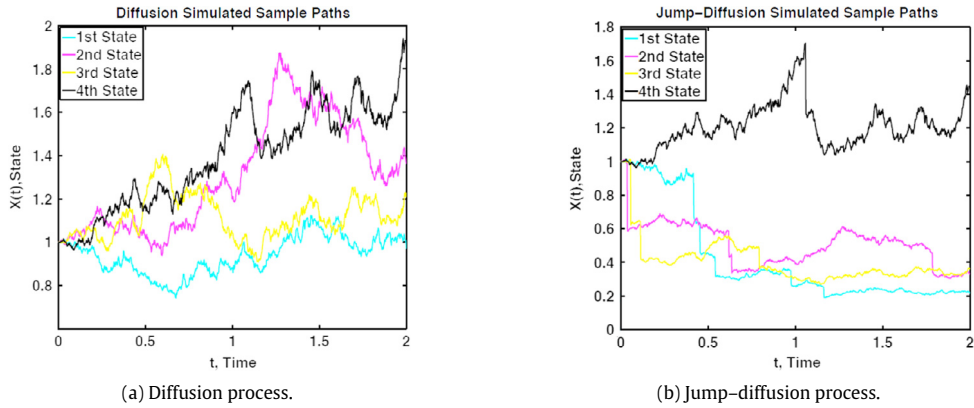


Fig. 21. Representation of trajectories of: (a) A diffusion process; (b) A jump–diffusion process.
Source: Reprinted from [66] with permission from Springer.

where N a Poisson process with intensity λ and $C(t, Z(t))$ represents the amplitude of the jumps. The jumps contribute to the statistics of the conditional increments over a time step Δt and Eqs. (54) become

$$\langle \Delta Z \mid Z(t) = z \rangle = A(t, z) \Delta t + C(t, z) \lambda \Delta t, \quad (57a)$$

$$\langle (\Delta Z)^2 \mid Z(t) = z \rangle = B^2(t, z) \Delta t + C^2(t, z) \lambda \Delta t. \quad (57b)$$

The introduction of jumps is illustrated in Fig. 21(a) which displays sample paths of a diffusion process and in Fig. 21(b) which shows similar sample paths for a jump–diffusion process, revealing the discontinuous nature of the trajectories and their diffusive behavior between successive jumps.

From the properties of the Poisson process, we know that, over an infinitesimal time increment dt , the increments of $N(t)$ can take only two possible values

$$\mathbb{P}[dN(t) = k] = (1 - \lambda dt) \delta_{k,0} + \lambda dt \delta_{k,1} \Rightarrow \langle (dN(t))^m \rangle = \lambda dt \quad \forall m. \quad (58)$$

Thus, the Poisson jumps contribute to any order in dt (while it is interesting to remember that the increments of the Wiener process contributes only to the second order in dt). The SDEs of a jump–diffusion process can be further generalized by considering random amplitudes for the jumps (this is referred to as a compound Poisson process), which gives

$$dZ(t) = A(t, Z(t)) dt + B(t, Z(t)) dW(t) + C(t, Z(t), Q) dN(t), \quad (59)$$

where Q_t is an independent random variable (in particular, independent of N_t). For such a general jump–diffusion process, the law of the random jumps is expressed by

$$W(y | t, z) = W(y | Z(t) = z) = \mathbb{P}[C = y | Z(t) = z] \lambda, \quad (60)$$

where the probability \mathbb{P} refers to the law of the independent random variable Q_t . Then, the equation satisfied by the transitional PDF $p(t, z | t_0, z_0)$ is

$$\begin{aligned} \frac{\partial p(t, z | t_0, z_0)}{\partial t} &= -\frac{\partial [A(t, z) p(t, z | t_0, z_0)]}{\partial x} + \frac{1}{2} \frac{\partial^2 [B^2(t, z) p(t, z | t_0, z_0)]}{\partial x^2} \\ &+ \int [W(z | t, y) p(t, y | t_0, z_0) - W(y | t, z) p(t, z | t_0, z_0)] dy. \end{aligned} \quad (61)$$

This is the form referred to as the Chapman–Kolmogorov PDF equation in [43]. The relation of this PDF equation with classical PDF equations is discussed in more details elsewhere [1], while generalizations to the multi-dimensional case are straightforward.

4.3.3. A note on Master Equations

It is known that the cumulative effects of many small jumps can be replaced by a stochastic diffusion process (this is the basis of random walk formulations). This has led to believe that jump processes constitute more fundamental building blocks and that diffusion processes are mere approximations of them. In classical statistical physics, this vision is supported by the discrete nature at the microscopic level of description (nature is made of atoms; discrete energy levels in atoms; etc.), as recalled in Section 3. This may explain that the name of Master Equation is sometimes attributed to Eq. (61) with $A = B = 0$ but not to the mixed jump–diffusion formulation (when $A \neq 0$ or $B \neq 0$).

However, this interpretation is not valid for the extended definitions of the microscopic and macroscopic levels of description introduced in Section 3. In that case, the ‘elementary level’ involves a mixture of continuous fields (the fluid phase) and a set of discrete particles. Thus, stochastic diffusion processes are typically used to represent particle dispersion by continuous fluid motions while jump ones refer to collisions or other particle–particle interactions. In that sense, diffusion and jump processes reflect two aspects of the same phenomenon and are to be regarded as complementary, but equivalent, models working at the same level of description. Consequently, the complete formulation in Eq. (61) is considered as the true Master Equation.

4.3.4. Another note on McKean equations

In Section 4.3.2, we have followed the classical formulation of SDEs where the drift and diffusion coefficients depend only on the variable Z . There are, however, many situations in physics where this approach needs to be extended to the case where the coefficients depend also on statistics derived from the set of particles. Though this distinction is not always mentioned in physically-oriented texts, it is important to be aware that this represents an extension of the well-established Langevin–Fokker–Planck framework described previously.

Such generalized stochastic processes are called McKean processes in the mathematical literature or, to use a more physical terminology, ‘processes with mean-field interactions’ (an account is given in [50, section 3.3.4]). Using a one-dimensional formulation (the extension to the multi-dimensional case is straightforward) and a diffusion process without jumps for the sake of simplicity, this means that the evolution equation for the trajectories of the process has now the general form

$$dZ(t) = A(t, Z(t), \langle \mathcal{F}(Z(t)) \rangle) dt + B(t, Z(t), \langle \mathcal{G}(Z(t)) \rangle) dW, \quad (62)$$

where $\langle \mathcal{F}(Z(t)) \rangle$ and $\langle \mathcal{G}(Z(t)) \rangle$ stand for statistics on the random variable $Z(t)$. These processes can also be understood as ‘weakly interacting processes’ since, by introducing classical Monte Carlo estimations of the statistics, the extended formulation of the evolution of the trajectory labeled (i) can be expressed as

$$dZ^{(i)}(t) = A\left(t, Z^{(i)}(t), \frac{1}{n} \sum_{j=1}^n \mathcal{F}(Z^{(j)}(t))\right) dt + B\left(t, Z^{(i)}(t), \frac{1}{n} \sum_{j=1}^n \mathcal{G}(Z^{(j)}(t))\right) dW, \quad (63)$$

where we have $\text{ms} - \lim_{n \rightarrow \infty} \frac{1}{n} \sum_{j=1}^n \mathcal{F}(Z^{(j)}(t)) = \langle \mathcal{F}(Z(t)) \rangle$. This property is related to the notion of the propagation of chaos, which is discussed in Sections 5.4 and 10.6.

The theory developed for the definition of SDEs as well as the derivation of the PDF equation remain valid but the FPE, which is an extension of Eq. (50), is written as

$$\frac{\partial p(t, z | t_0, z_0)}{\partial t} = -\frac{\partial [A(t, z, \mathcal{H}_A(p)) p(t, z | t_0, z_0)]}{\partial z} + \frac{1}{2} \frac{\partial^2 [B^2(t, z, \mathcal{H}_B(p)) p(t, z | t_0, z_0)]}{\partial z^2} \quad (64)$$

to exhibit the dependence of the drift and diffusion coefficients with p . Note that Eq. (64) is now a non-linear equation with respect to the transitional PDF of the process.

4.4. From Lagrangian stochastic models to mean-field equations

In the present work, we adopt a Lagrangian point of view to build probabilistic descriptions, which means that the physical modeling steps are essentially expressed by the choice of a Lagrangian model. Once this is done, a well-established road, based on proper relations between Lagrangian and Eulerian probabilistic descriptions, is then followed to derive the corresponding mean-field equations. Since this formalism has been presented in [1,4,5,30,31], only the milestones along this PDF road are recalled.

In the application to particle dynamics in fluid flows, particle positions are always explicitly described. We use therefore the decomposition $\mathbf{Z} = (\mathbf{x}_p, \mathbf{z}_c)$ where the particle location is always present and where \mathbf{z}_c stands for the complementary part of the chosen process. In sample space, the corresponding variables are noted $\mathbf{z} = (\mathbf{y}_p, \mathbf{z}_c)$. Starting from the unconditional Lagrangian PDF $p_p^L(t; \mathbf{y}_p, \mathbf{z}_c)$ and using M_p for the total mass of the discrete particles in the domain, the Lagrangian and Eulerian mass density functions (MDFs) for the disperse phase are defined by

$$F_p^L(t; \mathbf{y}_p, \mathbf{z}_c) = M_p p_p^L(t; \mathbf{y}_p, \mathbf{z}_c), \quad (65a)$$

$$F_p^E(t, \mathbf{x}; \mathbf{z}_c) = F_p^L(t; \mathbf{y}_p = \mathbf{x}, \mathbf{z}_c) = \int F_p^L(t; \mathbf{y}_p, \mathbf{z}_c) \delta(\mathbf{y}_p - \mathbf{x}) d\mathbf{y}, \quad (65b)$$

while the same relations hold for the continuous phase by using the total fluid mass M_f and the Lagrangian and Eulerian MDFs $F_f^L(t; \mathbf{y}_f, \mathbf{z}_c)$ and $F_f^E(t, \mathbf{x}; \mathbf{z}_c)$ respectively (it is only the nature of the variables selected for \mathbf{Z} that can differ between the two phases but the formalism is the same, see the synthetic formulation in [4]). When collating Lagrangian and Eulerian MDFs, the key difference is that particle position is a variable in the Lagrangian formulation while it is a parameter in the Eulerian one. Note that this is a one-way procedure where the Eulerian MDF (or distributions) is derived from the Lagrangian one.

In the following, we concentrate essentially on the disperse phase. Once the Eulerian MDF is defined, particle mean field properties can be extracted. For a particle variable written as $H_p(t; \mathbf{z}_c)$, its average $\langle H_p \rangle$ (which is a field variable), is defined as

$$\alpha_p(t, \mathbf{x}) \rho_p \langle H_p \rangle(t, \mathbf{x}) = \int H_p(t; \mathbf{z}_c) F_p^E(t, \mathbf{x}; \mathbf{z}_c) d\mathbf{z}_c, \quad (66)$$

where ρ_p is the particle density and $\alpha_p(t, \mathbf{x})$ is the mean particle volumetric fraction. The fluctuating component is then expressed as $h_p = H_p - \langle H_p \rangle$. It is worth emphasizing that α_p is a rigorously-defined probabilistic quantity that represents the average presence of one phase at a given location and should not be confused, in the present framework, with volumetric averages. In a discrete sense, when we handle N stochastic particles, the definitions of Lagrangian and Eulerian MDFs are directly carried out to yield

$$F_{p,N}^L(t; \mathbf{y}_p, \mathbf{z}_c) = \sum_{i=1}^N m_p^{(i)} \delta(\mathbf{y}_p - \mathbf{x}_p^{(i)}) \delta(\mathbf{z}_c - \mathbf{z}_c^{(i)}) \quad (67)$$

$$F_{p,N}^E(t, \mathbf{x}; \mathbf{z}_c) = F_{p,N}^L(t; \mathbf{y}_p = \mathbf{x}, \mathbf{z}_c) \quad (68)$$

where $m_p^{(i)}$ is the mass of the particle labeled (i) . This shows that in a small volume around location \mathbf{x} where averages are estimated as the ensemble averages over the N_x^p particles present in that volume, we get the equivalent of Favre, or mass-weighted, averages

$$\langle H_p \rangle(t, \mathbf{x}) \simeq \langle H_p \rangle_N = \frac{\sum_{i=1}^{N_x^p} m_p^{(i)} H_p(t; \mathbf{z}_c^{(i)}(t))}{\sum_{i=1}^{N_x^p} m_p^{(i)}}. \quad (69)$$

For incompressible single-phase flows, the same relations are valid and correspond to the limit case where we are handling notional fluid particles (or samples of the PDF) having the same mass $m_f^{(i)} = m_f$, $\forall i$ and with $\alpha_f(t, \mathbf{x}) = 1$ from the incompressibility constraint (see comprehensive accounts in [30,31,67]).

Whether we consider a Lagrangian PDF for a Markov process, as in Eq. (39), or for a non-Markov process, as in Eq. (40), it follows from the definitions of the relations given in Eqs. (65) that the Eulerian MDF satisfies the same evolution equation as the Lagrangian MDF. From the application of this PDF methodology to the fundamental particle momentum equations, we can then obtain rigorously the particle mean-field equations that were already given in Eqs. (29) for the first two moments, *i.e.* the particle concentration $\rho_p \alpha_p(t, \mathbf{x})$ and the mean velocity $\langle \mathbf{U}_p \rangle(t, \mathbf{x})$.

4.5. Criteria for acceptable probabilistic descriptions

It is useful to set up criteria to analyze whether an approach proposed for particles in turbulent flows can be regarded as an acceptable probabilistic description. These criteria are not selected with respect to the precision of practical predictions but are meant to assess consistency issues for probabilistic models.

Indeed, the well-established but (apparently) longer road that goes from the definition of a Markov process to its transitional PDF, the forward and backward equations and formulations as in Eq. (56) (or Eq. (61) for the PDF), is not always

followed and short-cut approaches are sometimes attempted. For instance, in several physically-oriented approaches, the equation for the one-time PDF is derived directly from the ‘fine-grained PDF’ $\mathcal{P}(t; \mathbf{z})$ defined as $\mathcal{P}(t; \mathbf{z}) = \delta(\mathbf{Z}(t) - \mathbf{z})$ with $p(t; \mathbf{z}) = \langle \mathcal{P}(t; \mathbf{z}) \rangle$ (see a detailed presentation of the manipulations of such fine-grained PDFs in [30]). For example, using the relation $\langle \mathbf{A} \mathcal{P}(t; \mathbf{z}) \rangle = \langle \mathbf{A} | (\mathbf{Z}(t) = \mathbf{z}) \rangle p(t; \mathbf{z})$ for a random variable \mathbf{A} , the following evolution equation

$$\frac{d\mathbf{Z}(t)}{dt} = \mathbf{A}(t), \quad (70)$$

yields the open, or unclosed, PDF equation

$$\frac{\partial p(t; \mathbf{z})}{\partial t} = - \frac{\partial}{\partial z_k} [\langle A_k | \mathbf{Z}(t) = \mathbf{z} \rangle p(t; \mathbf{z})], \quad (71)$$

which can be closed by proposing expressions for the unknown ‘fluxes’ on the rhs of Eq. (71). Once this is done, it can however be wondered whether this constitutes a proper probabilistic description of the phenomenon that is studied. For this purpose, two criteria are proposed.

4.5.1. Complete and incomplete probabilistic descriptions

From the knowledge of the one-time PDF, or even the transitional PDF $p(t; \mathbf{z} | t_0; \mathbf{z}_0)$, the first criterion consists in asking that we can reconstruct information on the complete law of the stochastic process \mathbf{Z} .

From the analysis carried out in Sections 4.1 and 4.2, it follows that this amounts to requiring that the stochastic process be a Markov stochastic process. As demonstrated there, knowledge of the equation satisfied by the transitional PDF (the forward Kolmogorov equation) is sufficient to build a complete description for the stochastic process and, therefore, of the physical phenomenon represented by this process. On the other hand, non-Markov processes constitute incomplete probabilistic descriptions, in the sense that they provide limited information and that the complete law cannot be retrieved.

At this stage, it is worth recalling that the Markov property is essentially due to the modeling standpoint. *Markovianity depends on the standpoint.* A very classical example helps to bring out the relation between Markovianity and the definition of the stochastic processes. This example can be found in several references (see, for instance, [59,62,68], often about the historical Kramers equation) and is only briefly recalled here. Let us consider a one-dimensional stochastic process Z whose trajectories follow the evolution equations

$$\frac{dZ(t)}{dt} = A(t, Z(t)) + B(t, Z(t))\xi(t) \quad (72)$$

where ξ is an external noise acting on Z and $A(t, z)$ and $B(t, z)$ given functions. If ξ takes independent values and is a stationary Gaussian process, it corresponds to a Gaussian white-noise and, from the properties given in Section 4.3.1, ξ can be written in terms of the increment of a Wiener process W as $dW(t) = \xi(t)dt$, leading to the SDE in the Itô sense [50,55]

$$dZ(t) = A(t, Z(t))dt + B(t, Z(t))dW(t). \quad (73)$$

Since the increments $dW(t)$ are independent, the future can be predicted based on present values and, consequently, Z is a Markov process. However, when ξ is a Gaussian ‘colored noise’, that is with a non-zero correlation time τ , it is immediate to see that Z is no longer a Markov process. To simulate this colored Gaussian noise, we can use a simple OU process [43]

$$d\xi(t) = -\frac{\xi(t)}{\tau} dt + \sqrt{\frac{2\langle \xi^2 \rangle}{\tau}} dW(t). \quad (74)$$

With the help of this equation, it is obvious that, while Z is not Markovian, the joint process (Z, ξ) is indeed a Markovian process [43,59,61]. In spite of its simplicity, this example embodies a key aspect: Markovianity is not a characteristic of a physical system but the consequence of the description that we retain for this system. It does not manifest an intrinsic property of a dynamical system but reflects a modeling point of view.

4.5.2. Well-posed and ill-based PDF equations

Several mesoscopic formulations are developed with the main purpose to obtain a set of macroscopic equations, or some macroscopic information as in the example of the stress tensor for polymers in Section 3.1.2 or the particle kinetic tensor in Section 3.2.2. In that case, the inability to reconstruct the complete law of the stochastic process that is simulated is not a major obstacle, since the purpose of the equation for the one-time PDF $p(t; \mathbf{z})$ is to derive a set of mean-field equations with the formalism presented in Section 4.4. However, the validity of the resulting set of mean-field equations rests upon the validity of this PDF equation.

This is raised as the second criterion, in which it is required that a proposed PDF equation, of the general form indicated in Eq. (40), be a well-posed partial-differential equation in sample space. By this, we mean that the Cauchy problem has a unique solution and that, in particular, two solutions corresponding to two different initial conditions converge as $t \rightarrow +\infty$. To that effect, it proves interesting to introduce the notion of the relative entropy defined as

$$H(p_2 | p_1) = - \int \ln \left(\frac{p_2}{p_1} \right) p_1(t; \mathbf{z}) d\mathbf{z} \quad (75)$$

for two PDFs $p_1(t; \mathbf{z})$ and $p_2(t; \mathbf{z})$. This relative entropy is also known as the ‘information gain’ or ‘Kullback–Leibler divergence’ [69]. In Information Theory, it represents the information lost when p_2 is used instead of p_1 to describe the system represented by \mathbf{Z} . Since $H(p_2 | p_1)$ is always positive and acts as a pseudo-measure to control the distance between two PDFs [70,71], it is used as a Lyapunov functional to assess whether two solutions converge to the same limit one. This is the approach followed in [61, chapter 6.1] to demonstrate the well-posed nature of Fokker–Planck equations and has been recently applied to analyze different PDF models for particles in turbulent flows (see [52] whose results are used later in Section 10.1).

This well-posed criterion appears as a minimal requirement for a PDF equation to be meaningful. Through its formulation, what is at stake is the guarantee that macroscopic descriptions derived from such PDF equations can be regarded as acceptable ones.

5. From the atomic to the hydrodynamical levels of description

We start our journey through scales, information contents and statistical challenges with the methods ranging from molecular dynamics to hydrodynamics. Using the terminology introduced in Section 3, this is referred to as the realm of classical statistical physics.

Strictly speaking, these methods are not within the scope of our study and are therefore not presented in great detail. However, introducing their characteristic features is useful to bring out the similarities and differences with the statistical descriptions of particles in turbulent flows described in later sections. For the same reason, we do not attempt to paint a comprehensive picture by drawing every formulation that has been devised but choose to discuss some representative ones. Along the same line, it is worth emphasizing that the purpose is not to compare these methods in terms of their predictive quality or applicability but merely to set up a reference framework.

Molecular Dynamics is briefly addressed in Section 5.1, while some mesoscopic methods are considered in Sections 5.2–5.6. The main purpose of this section is represented by the classification proposed in Section 5.7 and the discussions therein.

5.1. Molecular dynamics

In this study, the basic microscopic level is Molecular Dynamics which describes a fluid as a stream of interacting atoms/molecules treated as non-interpenetrating hard spheres. This notion of a fundamental level of description is, of course, relative since thinking of atoms and molecules as small spheres is quite macroscopic with respect to quantum mechanical descriptions. This is, nevertheless, the relevant one in our context in that it sets the stage for all the formulations to follow.

The traditional model in MD considers conservative inter-particle forces that derive from a two-body potential, which means that the total energy of the fluid system is the sum of all the pair potentials. The most-frequent choice is the Lennard-Jones potential (also called the 12-6 potential) given by

$$\Phi_{LJ}(r) = 4e_0 \left[\left(\frac{\sigma}{r} \right)^{12} - \left(\frac{\sigma}{r} \right)^6 \right], \quad (76)$$

where r is the distance between two particles, e_0 is the depth of the potential well and σ the distance at which the potential is zero (particles are strongly repulsive when $r \leq \sigma$), as represented in Fig. 22(a). MD is then formulated as a N -body problem (with N the number of atoms or molecules considered) and the equations of motion are obtained by applying the fundamental principle of classical mechanics, which gives

$$\frac{d\mathbf{x}^{[i]}}{dt} = \mathbf{U}^{[i]}, \quad (77a)$$

$$m^{[i]} \frac{d\mathbf{U}^{[i]}}{dt} = \sum_{\substack{j=1,N \\ j \neq i}} \mathbf{F}^{[j] \rightarrow [i]} = - \sum_{\substack{j=1,N \\ j \neq i}} \nabla \Phi_{LJ}(|\mathbf{x}^{[j]} - \mathbf{x}^{[i]}|) \quad (77b)$$

with $\mathbf{F}^{[j] \rightarrow [i]}$ the force of the particle labeled $[j]$ on the particle $[i]$ ($i, j = 1, \dots, N$), and $m^{[i]}$, $\mathbf{x}^{[i]}$ and $\mathbf{U}^{[i]}$ the mass, position and velocity of the particle $[i]$, respectively. This is represented in Fig. 22(b) to show that all two-body forces are accounted for. Due to the stiff profile of the Lennard-Jones potential, this ‘exact’ treatment induces very severe constraints of the time and space spans that can be covered.

Since we keep track of all the interactions, the evolution equations are deterministic. In sample space, this means that we are handling a N -particle PDF, or a MDF, in a $6N$ dimensional space since the degrees of freedom of the complete system correspond to the vector-valued variable \mathbf{Z} made up by the positions and velocities of all the particles,

$$\mathbf{Z} = (\mathbf{x}^{[1]}, \mathbf{U}^{[1]}; \dots; \mathbf{x}^{[i]}, \mathbf{U}^{[i]}; \dots; \mathbf{x}^{[N]}, \mathbf{U}^{[N]}). \quad (78)$$

By noting $\mathbf{z} = (\mathbf{y}^{[i]}, \mathbf{V}^{[i]})_{i=1,N}$ the corresponding variable in sample space, the PDF $p(t, \mathbf{z})$ is the solution of a Liouville equation

$$\frac{\partial p}{\partial t} + \sum_{i=1}^N V_k^{[i]} \frac{\partial p}{\partial y_k^{[i]}} + \sum_{i=1}^N \frac{\partial}{\partial V_k^{[i]}} \left[\left(\sum_{j \neq i}^N F_k^{[j] \rightarrow [i]}(\mathbf{y}^{[j]} - \mathbf{y}^{[i]}) \right) p \right] = 0, \quad (79)$$

where the Einstein summation convention is used for space coordinates (i.e. $k \in \{1, 2, 3\}$) but not for particle labels.

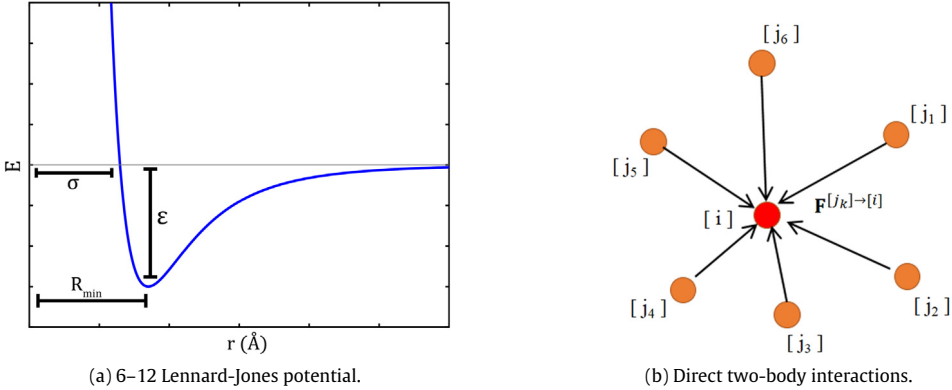


Fig. 22. Representation of particle interactions in Molecular Dynamics: (a) Profile of the classical 6–12 Lennard-Jones potential with ϵ the potential well, R_{\min} the separation at which this minimum is reached and σ the distance at which the potential is zero (i.e. the molecule diameter is the hard-sphere model); (b) Sketch of the direct approach where each two-body interaction between atoms/molecules is accounted for.

For our purpose, the important element is that MD introduces the kinetic approach where each particle is described by its position and velocity: $\mathbf{Z}^{[i]} = (\mathbf{x}^{[i]}, \mathbf{U}^{[i]})$. In keeping with the vision of atoms/molecules in void and with dynamic evolutions governed by conservative forces deriving from a potential, note that this is an exact description. Note also that MD contains the traditional image of molecules undergoing free flights and collisions, which is retrieved when the pair potential is simplified to a step function in the hard-sphere model ($\Phi_{LS} \simeq \Phi_{hs}$ where $\Phi_{hs} = +\infty$ when $r = \sigma$ and $\Phi_{hs} = 0$ when $r > \sigma$).

5.2. Dissipative Particle Dynamics

Ever since the first propositions in [72,73], rapidly followed by reformulations in [74,75] where the method took its basic form, Dissipative Particle Dynamics has met with considerable success and there is now a vast literature dedicated to studying its properties (see, for instance, reviews in [76–78]). Among the various mesoscopic models, DPD comes closest to MD since it is formulated in terms of pairwise interactions between a set of particles (see Fig. 23(b)). The method is also a good example of the coarse-graining procedure in that the DPD particles represents clusters of atoms or molecules.

The leading idea is that clumping molecules into DPD particles removes the details of the fast degrees of freedom leaving only a noise term, while the stiff pair-potential of MD becomes a soft repulsive one between clusters (see Fig. 23(a)). The principle of DPD is therefore expressed by the following equations

$$\frac{d\mathbf{x}^{[i]}}{dt} = \mathbf{U}^{[i]}, \quad (80a)$$

$$m^{[i]} \frac{d\mathbf{U}^{[i]}}{dt} = \sum_{\substack{j=1,N \\ j \neq i}} \left(\mathbf{F}_C^{[j] \rightarrow [i]} + \mathbf{F}_D^{[j] \rightarrow [i]} + \mathbf{F}_R^{[j] \rightarrow [i]} \right), \quad (80b)$$

where each force $\mathbf{F}^{[j] \rightarrow [i]}$ is decomposed into the sum of three terms: $\mathbf{F}_C^{[j] \rightarrow [i]}$ is a soft repulsive conservative force that accounts for ‘pressure’ between DPD particles while $\mathbf{F}_D^{[j] \rightarrow [i]}$ and $\mathbf{F}_R^{[j] \rightarrow [i]}$ are the dissipative and random terms, respectively. The introduction of these last two terms reflects what is done to model Brownian motion (see Section 2.3.2) where the cumulative effects of the fast fluid molecular motions lead to the Langevin formulation with the sum of (purely) dissipative and random terms. The explicit form of the DPD mesoscopic model is therefore translated by the SDEs:

$$d\mathbf{x}^{[i]} = \mathbf{U}^{[i]} dt, \quad (81a)$$

$$m^{[i]} d\mathbf{U}^{[i]} = \sum_{\substack{j=1,N \\ j \neq i}} \mathbf{F}_C^{[j] \rightarrow [i]}(\mathbf{x}^{[ij]}) dt + \sum_{\substack{j=1,N \\ j \neq i}} \left(-\gamma \omega(\mathbf{x}^{[ij]}) (\mathbf{e}^{[ij]}. \mathbf{U}^{[ij]}) \mathbf{e}^{[ij]} dt + \sqrt{2k_B \Theta_f \gamma \omega(\mathbf{x}^{[ij]})} \mathbf{e}^{[ij]} dW^{[ij]} \right), \quad (81b)$$

where $\mathbf{U}^{[ij]} = \mathbf{U}^{[i]} - \mathbf{U}^{[j]}$ is the relative velocity, $\mathbf{x}^{[ij]} = \mathbf{x}^{[i]} - \mathbf{x}^{[j]}$ the relative position, and $\mathbf{e}^{[ij]} = \mathbf{x}^{[ij]} / r^{[ij]}$ (with $r^{[ij]} = |\mathbf{x}^{[ij]}|$ the relative distance) the unit vector linking particle [i] to particle [j]. In Eq. (81b), $W^{[ij]}$ represents a Wiener process (independent for each particle pair) with $W^{[ij]} = -W^{[ji]}$ so that the total particle momentum is conserved, while γ is a friction coefficient and $\omega(\mathbf{x}^{[ij]})$ a weight function. As shown in Fig. 23(a), simple models are usually retained for the soft potential, for example:

$$\mathbf{F}_C^{[j] \rightarrow [i]} = \begin{cases} a^{[ij]} (1 - r^{[ij]} / r_c) e^{[ij]} & \text{if } r^{[ij]} \leq r_c, \\ 0 & \text{if } r^{[ij]} \geq r_c, \end{cases} \quad (82)$$

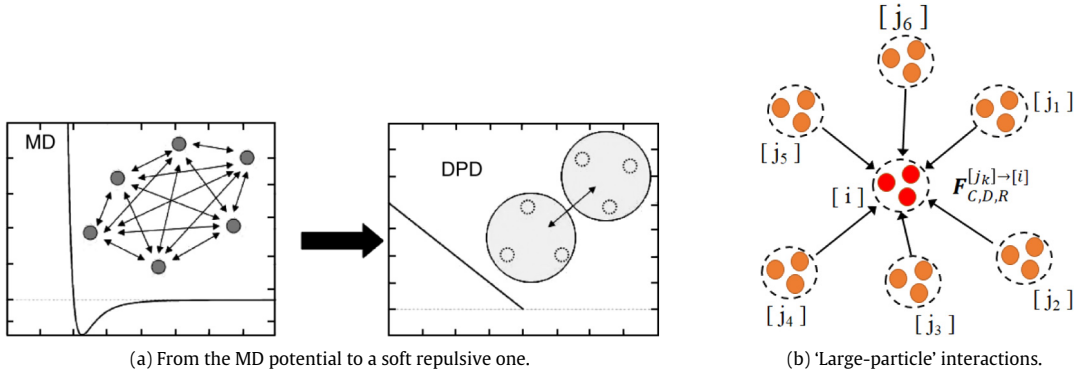


Fig. 23. Representation of the particle interactions in Dissipative Particle Dynamics: (a) The stiff MD potential is summed up to give a soft repulsive potential between molecular clusters (reprinted from [77] with permission from John Wiley and Sons); (b) DPD is still a N -particle direct interaction approach but each particle represents a mesoscopic particle (a cluster of molecules).

where $a^{[ij]}$ is the repulsion parameter between particle $[i]$ and particle $[j]$ that determines the strength of the soft repulsion force. This expression shows that the conservative force is local in space (only neighboring particles interact) and, therefore, that DPD basically simulates compressible fluids. A local property for the weight function $\omega(\mathbf{x}^{[ij]})$ is also assumed, through similar expressions

$$\omega(\mathbf{x}^{[ij]}) = \begin{cases} (1 - r^{[ij]} / r_c)^s & \text{if } r^{[ij]} \leq r_c, \\ 0 & \text{if } r^{[ij]} \geq r_c. \end{cases} \quad (83)$$

From this description, a few remarks can be made:

- (i) The existence of an equilibrium distribution (*i.e.*, the canonical distribution) with the corresponding equipartition theorem allows to close the diffusion coefficient of the stochastic diffusion process used in Eq. (81b) with the simplest case of the fluctuation-dissipation theorem, yielding the term $\sqrt{2k_B\Theta_f\gamma}\omega$ in the expression of $\mathbf{F}_R^{[j]\rightarrow[i]}$;
- (ii) The parameters of the models are γ , $a^{[ij]}$, r_c and the exponent s in Eq. (83), from which relations to the macroscopic fluid properties, such as the equation of state as well as the compressibility and viscosity coefficients and the Schmidt number, are derived (see comprehensive discussions in [74,75,77,79,80]).

DPD is an example of a bottom-up mesoscopic approach. Strictly speaking, this is not entirely true since, in practice, the parameters are often tuned so as to obtain the desired macroscopic properties. However, the formulation in terms of pairwise interacting coarse-grained particles and the spirit of the method are clearly developed in that sense.

5.3. Stochastic Rotation Dynamics

Another popular mesoscopic approach is Stochastic Rotation Dynamics whose detailed presentations can be found in [81–83]. Depending on the specifics of the algorithm, SRD is also referred to as Multi-Particle Collision Dynamics (MPCD), but the terminology of SRD is more telling and is retained here.

SRD is a particle-based method where particle positions and velocities are continuous variables. As noted in [82,83], this approach is line with the principles of the Direct Simulation Monte Carlo (DSMC) method introduced by Bird more than fifty years ago (see [84]). Indeed, the simulation is based on the succession of streaming and collisions steps during each time step Δt . In the streaming step, particles are convected with their own velocities without colliding, as in DSMC. Then, a grid is introduced and particles are sorted into cells (with a typical size Δx). The main difference with DSMC is that the collision step consists in a simplified treatment where particle velocities are updated with

$$\mathbf{U}^{[i]}(t + \Delta t) = \mathbf{U}^{[i]}(t) + \mathcal{R} \cdot (\mathbf{U}^{[i]}(t) - \mathbf{U}^{[\alpha]}(t)), \quad (84)$$

where $\mathbf{U}^{[\alpha]}(t)$ is the center-of-mass velocity in the cell noted $[\alpha]$ and is calculated as the average over the particles located in this cell at time t . In its basic form, \mathcal{R} is a rotation operator with a fixed angle β but around a random axis. This is done independently in each cell and at each time step.

Some characteristics can be put forward:

- (i) SRD does not describe pair interactions but is an attempt to account directly for the cumulative effects of many collisions. It is a collective treatment (rotation around the local mean velocity and by the same amount for particles belonging to the same cell);

- (ii) Whereas DPD is a continuous-in-time stochastic model, SRD is a discrete-time approach of particle dynamics where Δt plays a direct role in the model. Though particle locations and velocities are continuously distributed, the space discretization in cells and, in particular, the mesh size Δx are also explicit parts of the model;
- (iii) As a result, SRD leads to transport coefficients (viscosity, Schmidt number, etc.) that depend on Δt and Δx .

SRD is an example of a top-down mesoscopic model in that details of the microscopic formulation (MD) are clearly skipped. It is a rapid and efficient N -particle mesoscale method that accounts simply for collisional macroscopic effects while reproducing thermal fluctuations in the resulting hydrodynamical limit when a large number of time steps are repeated.

5.4. Lattice Boltzmann methods

Most mesoscale models are stochastic particle-based approaches. Using the terminology of Section 4, this corresponds to the trajectory point of view. Yet, it is also possible to follow the PDF point of view in which models are developed in sample space in terms of the PDF of the variables retained to describe a physical system. For mesoscopic descriptions of fluids, the remark made at the end of Section 5.1 shows that the kinetic approach based on particle (atom/molecule) position and velocity is relevant for molecular phenomena. This is the basis of the kinetic theory whose typical formulation consists in a PDF equation in sample space and the reference model in that category is the Lattice Boltzmann Method which grew out of earlier attempts made with Lattice Gas Automaton (LGA). Note that we refer simply to PDFs rather than to the traditional notion of distribution functions (DF), such as the usual number distribution function (NDF) or the MDF, since these notions have already been related in Section 4.4 (in the following, we consider in fact Eulerian PDFs for kinetic variables from which all DFs are deduced by proper normalizations).

A second noteworthy difference is that present particle-based models simulate the N -particle (Lagrangian) PDF whereas LGA and LBM calculate the one-particle (Eulerian) PDF. Therefore, LBM is based right from the outset on the molecular chaos hypothesis which is at the core of the Boltzmann equation (the name of the method is a constant reminder of that fact). Indeed, the molecular chaos assumption is central to show that the PDF (or DF) in the Boltzmann equation $p^{[1]}$ is actually the one-particle marginal density of the N -particle distribution. This is referred to as the ‘propagation of chaos’ property which is formulated as

$$\lim_{N \rightarrow +\infty} p_N^{[k]}(t; \mathbf{x}^{[1]}, \mathbf{V}^{[1]}, \dots, \mathbf{x}^{[k]}, \mathbf{V}^{[k]}) = \prod_{i=1}^k \lim_{N \rightarrow +\infty} p_N^{[1]}(t; \mathbf{x}^{[i]}, \mathbf{V}^{[i]}) \quad (85)$$

where $p_N^{[k]}$ is the k -particle marginal density from the N -particle system. The term propagation means that, if the property is satisfied at $t = 0$, then it holds at $t > 0$, which allows $p^{[1]}$ to be identified with the one-particle marginal density of the particle system $p^{[1]} = \lim_{N \rightarrow +\infty} p_N^{[1]}$. This point is well covered in a recent review, see [85] and references therein.

LBM is a well-known and widely used method and there are several detailed presentations on this approach (see, for instance, [78,86] and the literature quoted there). For this reason, we only provide an outline of the approach.

LGA and LBM are based on a description of molecular dynamics as being made up by successions of free flights and collisions. As in the DSMC and SRD methods, they rely on a sequence of streaming and collision steps and use also a grid, referred to as a lattice since it is typically a cubic lattice. However, in contrast to DSMC and SRD, the variables which are handled are grid-based and the collision step is formulated quite differently. In LGA, the variables attached to a lattice site $\mathbf{x}^{[\alpha]}$ are the occupation numbers $n_i(t, \mathbf{x}^{[\alpha]})$ where the index i refers to discrete particle velocity values, traditionally noted as \mathbf{c}_i , and which are the discrete vectors connecting the site $[\alpha]$ to its neighbors. This means that particle transport is represented by a jump from one site to a neighboring one at each time step Δt . In LGA, these occupation numbers are Boolean and, therefore, the method was an attempt to mimic closely molecular collisions. In that sense, mirroring the formulation of DPD from MD, LGA can be thought as a bottom-up approach but was faced with an exponential wall of computational complexity due to the nature of this collision operator.

To cut a simplified picture, LBM was devised with the same key ingredients of a lattice-based formulation but directly for the one-particle PDF (or DF) and with a top-down approach. As in LGA, velocity is not a continuously-distributed variable and only a discrete set of velocities linked to the lattice (reflected in names such as the D3Q19 model, see Fig. 24(a)) are simulated. The difference with LGA is that the occupation numbers are replaced by the distribution functions, or by the lattice-based (Eulerian) PDFs, noted $p_i^{[1]}(t, \mathbf{x}^{[\alpha]})$ which represent the density of fluid molecules having the velocity \mathbf{c}_i at the lattice site $\mathbf{x}^{[\alpha]}$ at time t . The LBM is expressed by the following dynamical evolution

$$p_i^{[1]}(t + \Delta t, \mathbf{x}^{[\alpha]} + \mathbf{c}_i \Delta t) = p_i^{[1]}(t, \mathbf{x}^{[\alpha]}) + C_{ij} \left(p_j^{[1]}(t, \mathbf{x}^{[\alpha]}) - p_j^{eq}(t, \mathbf{x}^{[\alpha]}) \right), \quad (86)$$

where C_{ij} stands for the collision operator. It is seen that LBM is expressed as a locally linear relaxation towards an equilibrium distribution p_j^{eq} and the most popular form of the relaxation matrix is given by the Bhatnagar–Gross–Krook (BGK) model where $C_{ij} = -\delta_{ij}/\tau_{BGK}$ with τ_{BGK} the relaxation timescale. More elaborated forms can use multiple relaxation timescales and the equilibrium distribution can be constructed based solely on symmetry requirements and conservation laws of hydrodynamics (LBM is clearly a top-down formulation).

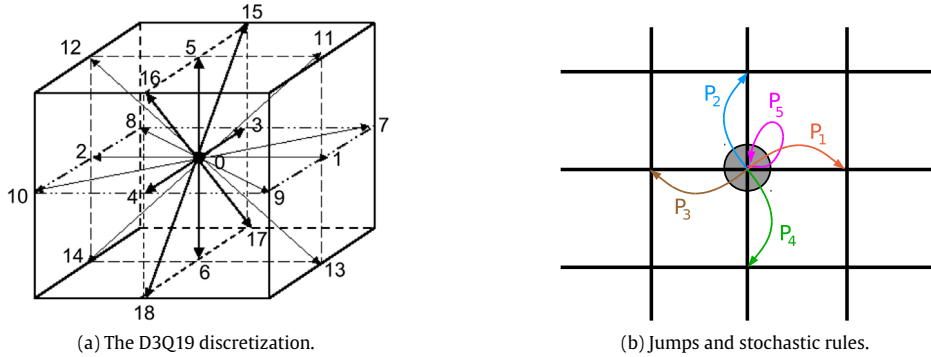


Fig. 24. Representation of the grid-based formulation of Lattice Boltzmann Method: (a) The D3Q19 scheme which indicates the discrete set of velocities simulated; (b) Sketch of the grid-based jumps (explicitly simulated in LGA and accounted for in LBM).

With respect to LBM, the following points are worth considering:

- (i) Contrary to DSMC and SRD which use a grid to isolate local groups of particles, LBM is an entirely grid-based numerical method;
- (ii) The formulation in terms of distribution functions means that the mean free path is not dictated by the lattice (as in LGA) or by the inter-particle mean distance in particle-based methods and is a free parameter;
- (iii) Its typical formulation requires to know (or to postulate) the equilibrium distribution and the relaxation timescale, as exemplified by the BKK model;
- (iv) Thermal fluctuations are not naturally included, though progress has been made in that respect (see discussions in [78,87]);
- (v) Connections with other methods is less easy than with particle-based formulations, for example when discrete colloids are embedded in a fluid (see Section 7);
- (vi) Particle transport is not well treated by grid-based discrete-jump processes. This is not necessarily important for molecular modeling since this is essentially a collision-dominated regime but raises some questions for dilute particle systems in turbulent flows, as seen in Section 10.

5.5. Smoothed particle hydrodynamics

As it transpires from its name, Smoothed Particle Hydrodynamics (SPH) is a method designed to operate at the hydrodynamical level of description. In the context of this section, SPH is therefore not a mesoscopic approach but a macroscopic one. Due to the use of a spatial smoothing operator applied to the hydrodynamical equations, it is even a ‘more macroscopic version’ than the Navier–Stokes equations. It is however important to introduce its characteristics at this stage to understand the ideas behind hybrid formulations, such as the Smoothed Dissipative Particle Dynamics method presented in Section 5.6. This is also the first sign that, contrary to an usual belief, particle-based descriptions do not stop to exist when the hydrodynamical (or continuum) level is reached. In that sense, SPH is a pivotal approach which opens the possibility to build bridges with the methods for single-phase flow turbulence to be addressed in Section 6.

The method originated in the 1970s for astronomical simulations (see [88,89]) and has been growing ever since with current applications for free-surface flows and multi-phase (*i.e.* fluid–fluid) flows where the straightforward way with which interfaces is handled is attractive compared to traditional grid-based discretizations (see detailed presentations in [90,91]). Indeed, SPH is a purely particle (or grid-free) method that approximates a fluid field, say $\phi(t, \mathbf{x})$, through three typical steps:

$$\hat{\phi}(t, \mathbf{x}) = \int_{\Omega} \phi(t, \mathbf{x}') W(\mathbf{x}' - \mathbf{x}, h) d\mathbf{x}', \quad (87a)$$

$$\hat{\phi}(t, \mathbf{x}^{[i]}) \simeq \sum_{j=1}^N \phi(t, \mathbf{x}^{[j]}) W^{[ij]}(h) \Omega^{[j]}, \quad (87b)$$

$$\phi(t, \mathbf{x}^{[i]}) \simeq \hat{\phi}(t, \mathbf{x}^{[i]}). \quad (87c)$$

The first step in Eq. (87a) involves a filtering operation with a spatially-invariant smoothing kernel $W(\mathbf{x}', \mathbf{x}, h) = W(\mathbf{x}' - \mathbf{x}, h)$ where h is the size of its compact support (see Fig. 25). Note that, to keep the traditional notation, the smoothing kernel is still noted W in the various SPH equations developed below but should not be confused with the Wiener process. In the second step, a discrete approximation is used to transform the volume integration over the whole flow domain Ω into a sum implying N ‘fluid particles’ that, for consistency reasons with preceding formulations, are still labeled as $[i]$ with an associated

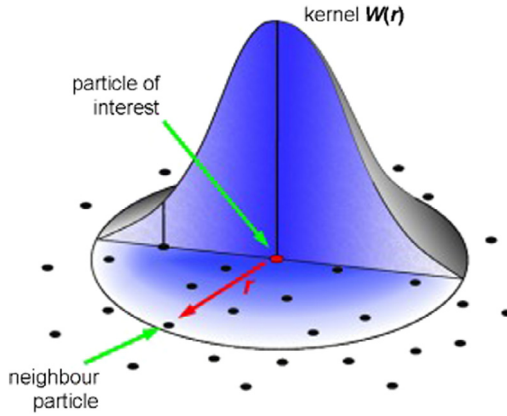


Fig. 25. Representation of the particle-based formulation of Smoothed Particle Hydrodynamics: a typical profile is indicated for the smoothing kernel whose compact support means that each particle is only interacting with its neighbors. As pressure is given by the local density, SPH is a multi-body particle scheme.

volume $\Omega^{[i]}$ (the traditional notation in SPH is with indices a and b), while $W^{[ij]}(h)$ is a short-hand notation for $W(\mathbf{x}^{[i]} - \mathbf{x}^{[j]}, h)$. The last step indicates that the initial field value at a particle location is approximated by the smoothed one (thus, the name of the method). In spite of its apparent trivial nature, this last step should not be overlooked as it implies that we are handling regularized versions of the hydrodynamical fields, which explains the above comment on the macroscopic characteristic of SPH. This has also consequences when considering turbulent flows and the absence of sub-kernel information (see Section 6).

The interest of using a smoothing kernel is that spatial variations are predicted around each particle position, allowing gradients to be calculated as gradients of the kernel (from an integration-by-part formula). For the field $\phi(t, \mathbf{x})$ considered above, this leads to

$$(\nabla\phi)(t, \mathbf{x}^{[i]}) = \sum_{j=1}^N \phi(t, \mathbf{x}^{[j]}) (\nabla W)^{[ij]}(h) \Omega^{[j]} \quad (88)$$

where the derivatives are taken with respect to the position of the particle $[i]$. With these identities, the explicit field dependences can be removed and $\phi(t, \mathbf{x}^{[i]})$ is noted as $\phi^{[i]}(t)$, or simply $\phi^{[i]}$, to indicate the $[i]$ -particle attached variable.

The traditional SPH approach consists in starting from a field description, written in terms of Partial Differential Equations (PDE), and in applying the above steps. In doing so, there are often several ways with which a field can be transformed (like a change of variables) before introducing the particle formulation (cf. Eq. (87b)). For instance, particle density can be obtained from

$$\rho^{[i]} = m^{[i]} \vartheta^{[i]} \quad \text{with} \quad \vartheta^{[i]} = \sum_{j=1}^N W^{[ij]}(h), \quad (89)$$

which defines the particle specific volume $\vartheta^{[i]}$ for each SPH particle [92,93]. This leads to differences in the practical expression of SPH models but this point is left to the existing literature on the subject as these variants are dependent on the physical context that is considered (see [91,94,95]).

The Navier–Stokes equations for an incompressible flow are written in a Lagrangian framework (the superscript $+$ is used for the exact equation of a fluid–particle as in [31])

$$\frac{d\mathbf{x}_f^+}{dt} = \mathbf{U}_f^+, \quad (90a)$$

$$\frac{d\mathbf{U}_f^+}{dt} = -\left(\frac{1}{\rho_f} \nabla P_f\right)^+ + (\nu_f \nabla^2 \mathbf{U}_f)^+. \quad (90b)$$

Then, applying the above SPH approach results in a N -interacting ‘large-scale’ fluid–particle model which reads (see [93–95])

$$\frac{d\mathbf{x}_f^{[i]}}{dt} = \mathbf{U}_f^{[i]}, \quad (91a)$$

$$m_f^{[i]} \frac{d\mathbf{U}_f^{[i]}}{dt} = - \sum_{j=1}^N \left(\frac{P_f^{[i]}}{(\vartheta^{[i]})^2} + \frac{P_f^{[j]}}{(\vartheta^{[j]})^2} \right) \nabla W^{[ij]}(h) + \rho_f \nu_f \sum_{j=1}^N \left(\frac{1}{(\vartheta^{[i]})^2} + \frac{1}{(\vartheta^{[j]})^2} \right) \frac{\mathbf{x}_f^{[j]}. \nabla W^{[ij]}(h)}{(r_f^{[ij]})^2} \mathbf{U}_f^{[j]}, \quad (91b)$$

with $r_f^{[ij]} = |\mathbf{x}_f^{[ij]}| = |\mathbf{x}_f^{[i]} - \mathbf{x}_f^{[j]}|$ and where the index f is introduced to indicate that we are considering fluid particles at the hydrodynamical level (this notation is used when we are handling fluid elements from that level of description but not for ‘real mesoscopic’ particles).

A few remarks can be made on SPH formulations:

- (i) As in the mesoscopic models considered previously, only the particles located within the kernel range around the position of a given fluid-particle $[i]$ interact with that particle, showing that SPH is also essentially simulating compressible flows (for considerations about incompressible flows, see a recent analysis in [96]);
- (ii) The SPH model shows similarities with the DPD model introduced in Section 5.2, with the conservative force due to (hydrodynamical) pressure. However, if the equation of state is an outcome of the DPD approach, it is an input in SPH;
- (iii) Since the pressure associated to each particle is dependent on the local value of density obtained from neighboring particles (cf. Eq. (89)), the use of an equation of state and the pressure-gradient force in Eq. (91b) show that we are now dealing with multi-body interactions rather than pairwise ones as in DPD (see Eq. (82)).

SPH is classically viewed as a mathematical formalism that turns an elementary formulation in terms of fields (which are solutions of PDEs) into a particle approximation. As revealed by the presentation in this section, it is also possible to regard SPH particles, not just as approximating moving points, but as real fluid elements having thermodynamic consistency and described as undergoing multi-body interactions. At the hydrodynamical level, these points of view are equivalent. This second presentation is however believed to provide a more fruitful perspective since it points to links with complementary particle systems. A good example of such a combination is a revisited formulation of DPD that is now presented.

5.6. Smoothed Dissipative Particle Dynamics

In our context, SPH is a macroscopic approach but its particle formulation and the correspondences with the DPD models presented in Section 5.2 led to a new mesoscale method in [92], called Smoothed Dissipative Particle Dynamics (SDPD). The name of this hybrid formulation is an indication that it relies on the formalism used in SPH but somewhere ‘below’ the hydrodynamical level (note that the term hydrodynamics is not in the name of the method).

The complete formulation of the SDPD equations can be found in the original paper [92] while the key ideas are summed up in an interesting subsequent overview [97], and the method is currently being developed (see, for instance, [98,99]). The principle behind SDPD is to combine the ability of DPD to reproduce thermal fluctuations and the direct connection of SPH to the Navier–Stokes equations. The method relies on a consistent thermodynamical formulation and the GENERIC framework (a comprehensive account of the latter is in [100]).

Since the complete equations (see Eqs. (63) in [92]) involve many terms whose expressions would obscure the clarity of this presentation, we limit ourselves to giving only the main structure for constant fluid properties (the viscosity ν_f , thermal conductivity κ_f , etc.) and using the SPH notations and formulations in Eqs. (91) (for example, we retain the gradient of the kernel $W^{[ij]}$ and not the function F_{ij} used in [92]). Each particle is now considered as a small thermodynamical system whose characterization requires to use, not only its kinetic energy, but also its volume (i.e. $\mathcal{V}^{[i]} = 1/\vartheta^{[i]}$) and its entropy $S^{[i]}$. A given equation of state, $E^{eq}(m^{[i]}, S^{[i]}, \mathcal{V}^{[i]})$, where E^{eq} is the internal energy, based on the particle volume and entropy allows to derive the pressure and temperature from the classical thermodynamical definitions

$$P^{[i]} = -\frac{\partial E^{eq}}{\partial \mathcal{V}^{[i]}}, \quad \Theta^{[i]} = \frac{\partial E^{eq}}{\partial S^{[i]}}. \quad (92)$$

With these definitions, the (simplified) SDPD model is expressed by the equations, as first stated in [92] and taken up in later works (see for instance [97,99,101])

$$\frac{d\mathbf{x}^{[i]}}{dt} = \mathbf{U}^{[i]}, \quad (93a)$$

$$m^{[i]} \frac{d\mathbf{U}^{[i]}}{dt} = - \sum_{j=1}^N \left(\frac{P^{[i]}}{(\vartheta^{[i]})^2} + \frac{P^{[j]}}{(\vartheta^{[j]})^2} \right) \nabla W^{[ij]}(h) + \frac{5}{3} \mu_f \sum_{j=1}^N \left(\frac{\mathbf{x}^{[ij]}. \nabla W^{[ij]}(h)}{\vartheta^{[i]} \vartheta^{[j]} (r^{[ij]})^2} \right) (\mathbf{U}^{[ij]} + (\mathbf{e}^{[ij]} \cdot \mathbf{U}^{[ij]}) \mathbf{e}^{[ij]}) + \tilde{\mathbf{F}}^{[ij]}, \quad (93b)$$

$$\Theta^{[i]} \frac{dS^{[i]}}{dt} = 2\kappa_f \sum_{j=1}^N \left(\frac{\mathbf{x}^{[ij]}. \nabla W^{[ij]}(h)}{\vartheta^{[i]} \vartheta^{[j]} (r^{[ij]})^2} \right) \Theta^{[ij]} - \frac{5}{6} \mu_f \sum_{j=1}^N \left(\frac{\mathbf{x}^{[ij]}. \nabla W^{[ij]}(h)}{\vartheta^{[i]} \vartheta^{[j]} (r^{[ij]})^2} \right) (\mathbf{U}^{[ij]} \cdot \mathbf{U}^{[ij]} + (\mathbf{e}^{[ij]} \cdot \mathbf{U}^{[ij]})^2) + \Theta^{[i]} \tilde{j}^{[i]}, \quad (93c)$$

where $\Theta^{[ij]} = \Theta^{[j]} - \Theta^{[i]}$. Note that the index f has been dropped since we are operating below the hydrodynamical level of description and SDPD particles are meant to represent meso-scale or macro-molecules. It can be observed that the formulations of the viscous term can have slightly different forms (cf. Eqs. (91b) and (93b)). This is related to the fact that an incompressible flow is sometimes directly assumed (this is the case in the present article and in Eqs. (90)–(91)) whereas a more general expression of the stress tensor involving the dilatability term (i.e. $\nabla \cdot \mathbf{U}_f$) can be retained as in the above SDPD formulation (see a discussion in [93]). In Eqs. (93b) and (93c), $\tilde{\mathbf{F}}^{[ij]}$ and $\tilde{j}^{[i]}$ are random terms due to thermal fluctuations (essentially governed by the thermal energies $k_B \Theta^{[i]}$ and $k_B \Theta^{[j]}$) and $\tilde{\mathbf{F}}^{[ij]}$ can be seen as a revisited expression of the random term in the original DPD models, cf. Eq. (81b).

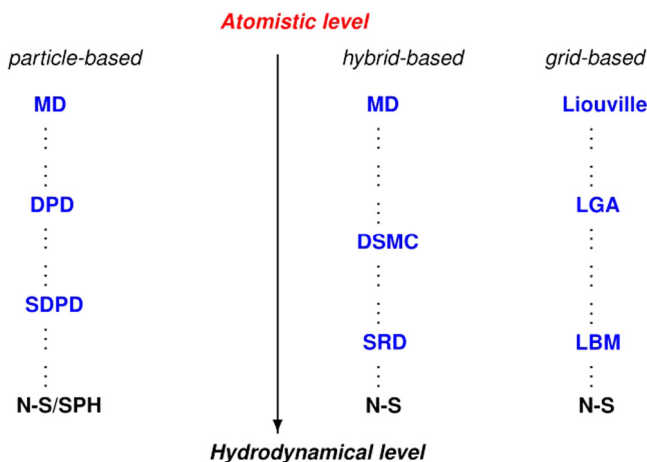


Fig. 26. Organization of the methods from the atomistic level of description represented by Molecular Dynamics (physical space) and Liouville (sample space) formulations to the hydrodynamical level. The downward arrow indicates coarse-graining and a reduction in the information content as less details are resolved.

The following points are interesting to note:

- (i) Compared to the initial DPD models, which were attempts at bottom-up derivations from MD, SDPD is an example of a top-down approach (the equation of state, the fluid viscosity ν_f and thermal conductivity κ_f are given);
- (ii) SPH is a deterministic particle method while SDPD, like DPD, is a stochastic one based on stochastic diffusion processes;
- (iii) SDPD is a particle-based approach consistent with the hydrodynamical equations when thermal fluctuations are disregarded, *i.e.* SDPD=SPH in that limit;
- (iv) The method accounts naturally for thermal fluctuations and represents therefore a model for fluctuating hydrodynamics (due to thermal noise).

5.7. Summary and classification

The different methods presented in this section are organized in Fig. 26, where the downward-pointing arrows indicate a reduction in the information content manifested by a decrease in the number of degrees of freedom. There are three roads starting at the atomic (microscopic) level and leading to the hydrodynamical (macroscopic) one. The first one, labeled grid-based, refers to methods based on grid discretization in sample space (LGA, LBM). The second one, labeled hybrid-based, describes approaches which use a grid to isolate particle sub-groups for collisional treatments (DSMC, SRD) while the column on the left side, labeled particle-based, refers to methods developed only in terms of particle systems.

Several conclusions can be drawn:

- (i) Both the microscopic and macroscopic levels of description are well-established descriptions that can be regarded as being ‘exact’;
- (ii) The MD and hydrodynamical descriptions correspond to deterministic equations while mesoscopic methods are based on stochastic models for particle dynamics;
- (iii) The role of particles and fields is distinct: particle descriptions are at the microscopic and mesoscopic levels while the field description is only at the macroscopic one;
- (iv) The mesoscopic level is a world dominated by particle-based methods. Even in hybrid formulations, the grid plays a secondary role;
- (v) Most methods have a top-down view (*e.g.*, LBM, SRD, SDPD) while few methods follow a bottom-up approach (*e.g.*, LGA, DPD);
- (vi) Many top-down approaches use essentially the scale separation between the microscopic and macroscopic levels in their formulation. Having described random variables and stochastic processes in Section 4, a parallel can be drawn with the situation where one wishes to obtain a Gaussian distribution from the repetition of identical steps. Since the scale separation means that we repeat a large number of identically-distributed small time steps (sub-steps) to go from one macroscopic observation instant to the next one, then the Central Limit Theorem (CLT) ensures that a Gaussian distribution is obtained at the macroscopic level, whatever the details of these (microscopic) sub-steps. This is basically the principle followed in methods such as DSMC, SRD, etc.;
- (vii) However, even in the category of top-down models, SDPD stands out in the sense that it contains an explicit hydrodynamical description set in a particle formulation.



(a) Hot plume.



(b) In the turbulent wake of a windfarm.

Fig. 27. Examples of single-phase turbulent fluid flows exhibiting complex motions: (a) Transition from laminar to turbulent in a hot plume rising in still air (credit: Creative Commons Attribution); (b) Formation and interaction of turbulent wakes in a windfarm (credit: Vattenfall).

Equipped with this basic scheme and first organization of the different methods developed for classical statistical physics, we can address the description of single-phase turbulent flows. This is done in Section 6.

6. Statistical descriptions of single-phase turbulence

At the hydrodynamical level where molecular fluctuations have been averaged out, things get calmer with smooth streamlines but ... only for a little while. As the flow velocity increases, a transition between laminar and turbulent regimes is often observed. This is illustrated in Fig. 27(a) with the example of a rising hot plume: due to buoyancy effects, the hot gas is accelerated upwards until a point (related to a velocity threshold) where the streamlines become agitated and display apparently-chaotic motions. Note that this corresponds to a significant spread of the plume, indicating that the rate of mixing is considerably enhanced when the flow is turbulent. Another typical illustration of turbulence is in the wake of an object and a large-scale example is shown for a wind-farm in Fig. 27(b). The wake produced by the first upstream wind turbines is turbulent and affects downstream turbines with non-negligible impact on the overall performance. Being due to the competition between convection and viscous diffusion, turbulence is not observed in small domains where the smoothing viscous forces dominate and is not an issue, for example, in microfluidic applications. However, in the vast majority of practical and daily-life flows, turbulence is present.

This short presentation follows classical accounts in which turbulence is characterized by its manifestations but is not rigorously defined. Such direct observations are also the best way to understand that turbulence refers to a flow but not to a fluid and also that, though the elementary equations are deterministic, turbulence is regarded as a random phenomena. Given the huge number of degrees of freedom revealed by the classical picture of turbulence recalled in Section 6.1, the direct numerical approaches in Section 6.2 are applicable only to low Reynolds-number flows and simple geometries. Therefore, the quest is to come up with reduced statistical descriptions inline with the extended definition of microscopic, mesoscopic and macroscopic levels of description proposed in Section 3. Modeling approaches developed at various levels are considered in Sections 6.3–6.5 and are organized in Section 6.6.

6.1. The Kolmogorov picture of turbulent flows

The Kolmogorov description of high Reynolds-number turbulent flows has been the pillar of turbulence theory ever since its formulation in two landmark papers in 1941 and 1962, referred to as K41 or K62. This does not mean that all predictions have been confirmed but this theory is undoubtedly the reference one in turbulence and analyses are (nearly) always made with respect to the K41 or K62 pictures. In that sense, the Kolmogorov description provides the ‘zero level’ (playing the same role as the Gaussian or Poisson distributions for continuous- or discrete-valued random variables) with respect to which ‘deviations’ are measured. It is important to emphasize that the Kolmogorov theory is essentially a description of the inertial and dissipative ranges (thus for the structure of ‘small space and time fluctuations’) but not of the large, energy-containing, scales (see the remarks at the beginning of Section 6.3). On the other hand, these notions of large and small scales are meaningful thanks to the Kolmogorov picture, showing again its invaluable merit as a reference theory.

Comprehensive discussions of the Kolmogorov theory can be found in textbooks (see [30,38,39,102]) and in numerous reviews (see [1,67]), to which readers are referred for detailed accounts. In a nutshell, the key ideas are well captured by the earlier description of Richardson (1922) epitomized in his sonnet-like rendering (“Big whorls have little whorls; Which feed on their velocity; And little whorls have lesser whorls; And so on to viscosity”). The reference to ‘whorls’ corresponds to an intuitive, but loosely-defined, decomposition of velocity fluctuations into a range of ‘eddies’ characterized by their

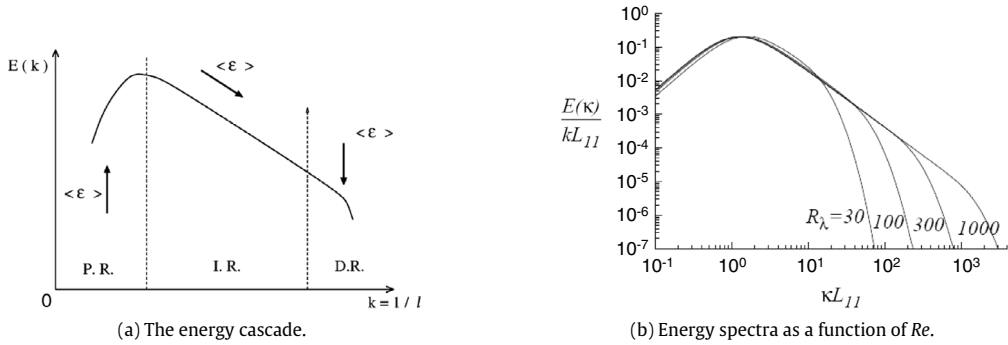


Fig. 28. The Kolmogorov picture of turbulence: (a) Energy is produced at the large scales and is transferred through the inertial range before being dissipated by viscous motions at the same rate $\langle \epsilon_f \rangle$; (b) Evolution of the energy spectra when the Reynolds number based on the Taylor length scale $Re_\lambda \sim Re^{1/2}$ increases.

Source: Reprinted from [30] with permission from Cambridge University Press.

velocity scale $\delta u(l)$ and their timescale $\tau(l)$, where l is the ‘size’ of an eddy. This pictorial description embodies the notion of the energy cascade represented in Fig. 28: energy is produced at the large scales imposed by the geometry of the flow domain or the boundary conditions and is transferred through the inertial range until it is dissipated at the smallest scales by viscous motions.

This qualitative picture was put on solid grounds by Kolmogorov and intuitive ideas were given quantitative expressions with the Kolmogorov similarity hypotheses that introduced the notion of locally isotropic turbulent flows whose motions are characterized statistically by the fluid viscosity ν_f and the kinetic energy dissipation rate ϵ_f (which is taken as being the same as the rate of energy transfer in the inertial range).

The first important outcome of the Kolmogorov theory is to properly characterize the smallest scales of turbulence by their length, velocity, and time scales expressed by

$$\eta_K = \left(\frac{\nu_f^3}{\epsilon_f} \right)^{3/4}, \quad u_K = (\nu_f \epsilon_f)^{1/4}, \quad \tau_K = \left(\frac{\nu_f}{\epsilon_f} \right)^{1/2}. \quad (94)$$

If we introduce L_f and u_f to represent the length and velocity of the large-scale turbulent motions and use the simple scaling $\epsilon_f \sim u_f^3/L_f$, we immediately obtain that the ratios between the length and time scales of the largest to the smallest scales are

$$\frac{L_f}{\eta_K} \sim Re^{3/4}, \quad \frac{T_f}{\tau_K} \sim Re^{1/2}, \quad (95)$$

with $T_f = L_f/u_f$ and $Re = u_f L_f / \nu_f$ the Reynolds number based on the large scales.

The second outcome is to yield scaling relations for the eddy velocity and time scales since, for l in the inertial range (i.e. $L_f \gg l \gg \eta_K$), we get that

$$\delta u(l) = (\epsilon_f l)^{1/3} \sim u_f (l/L_f)^{1/3}, \quad \tau(l) = (l^2/\epsilon_f)^{1/3} \sim \frac{L_f}{u_f} (l/L_f)^{2/3}. \quad (96)$$

For more rigorous applications of the Kolmogorov theory, it is important to be aware that the fundamental formulation was developed not only for spatial correlations but for a space-time region and that it corresponds to a Lagrangian vision. Indeed, the original expression of the locally isotropic hypothesis concerns the statistics of the relative velocity field defined by $\delta \mathbf{U}_f(\tau, \mathbf{r}) = \mathbf{U}_f(t_0 + \tau, \mathbf{x}) - \mathbf{U}_f(t_0, \mathbf{x}_0)$, that is in the reference frame moving with the velocity of a chosen fluid-particle, $\mathbf{U}_f(t_0, \mathbf{x}_0)$, with $\mathbf{r} = \mathbf{x} - \mathbf{x}_0 - \mathbf{U}_f(t_0, \mathbf{x}_0)\tau$ (see the comprehensive discussion in [38, chapter 8]). How kinetic energy is distributed between scales is then assessed with the velocity structure functions.

The most famous application of the theory is for the Eulerian fluid velocity correlations which are characterized by the tensor

$$D_{ij}(t, \mathbf{x}, \mathbf{r}) = \langle \delta U_{f,i}(0, \mathbf{r}) \delta U_{f,j}(0, \mathbf{r}) \rangle, \quad (97a)$$

$$= \langle [U_{f,i}(t, \mathbf{x} + \mathbf{r}) - U_{f,i}(t, \mathbf{x})] [U_{f,j}(t, \mathbf{x} + \mathbf{r}) - U_{f,j}(t, \mathbf{x})] \rangle. \quad (97b)$$

For isotropic conditions, this velocity structure tensor can be written as [30,38,39]

$$D_{ij}(t, \mathbf{x}, \mathbf{r}) = D_{NN}(t, r) \delta_{ij} + [D_{LL}(t, r) - D_{NN}(t, r)] \frac{r_i r_j}{r^2}, \quad (98)$$

and is thus expressed by two scalar functions $D_{LL}(t, r)$ and $D_{NN}(t, r)$ (with $r = |\mathbf{r}|$) which are called the longitudinal and transverse structure functions, respectively. Moreover, the continuity constraint implies that D_{NN} is uniquely determined by D_{LL} , and the second-order velocity structure tensor $D_{ij}(t, \mathbf{x}, \mathbf{r})$ is therefore fully characterized by one scalar function $D_{LL}(t, r)$. In the inertial range, the Kolmogorov similarity hypothesis yields that

$$D_{LL}(t, r) = C_2(\epsilon_f r)^{2/3}, \quad (99)$$

where C_2 is a constant. Note that this is, of course, the same result as the one given in Eqs. (96) since D_{LL} represents $(\delta u(l))^2$ (using again $\epsilon_f \sim u_f^3/L_f$). The Fourier transform of $D_{LL}(t, r)$ gives the (longitudinal) kinetic energy spectrum with the well-known $-5/3$ variation in the inertia range (see Fig. 28(b)). This point has been the subject of numerous experimental and numerical studies ever since the 1960s and detailed discussions can be found in the references mentioned above. When $v_f \rightarrow 0$ (with fixed u_f and L_f), then $Re \rightarrow +\infty$ but the kinetic energy dissipation rate ϵ_f tends towards a finite value which is the only remaining trace of the vanishing viscosity. Smaller and smaller scales are generated and the energy spectrum is stretched to larger and larger wave numbers but with the same slope, as shown in Fig. 28(b).

Though this aspect is more rarely developed, the Kolmogorov theory applies also for the Lagrangian statistical characteristics of velocity differences (the reference presentation remains the one given in [38, chapter 8]). For time differences τ in the inertial ranges (*i.e.* $\tau_K \ll \tau \ll T_f$), the increments $d_\tau \mathbf{U}_f^+ = \mathbf{U}_f^+(t + \tau) - \mathbf{U}_f^+(t)$ of the velocity of a fluid-particle are characterized by the Lagrangian structure tensor $\langle dU_{f,i}^+ dU_{f,j}^+ \rangle$ which is

$$\langle d_\tau U_{f,i}^+ d_\tau U_{f,j}^+ \rangle = D^L(\tau) \delta_{ij}, \quad (100)$$

where a superscript $+$ is used to indicate that we are dealing with the exact equation of a fluid-particle [31] (as already done in Section 5.5), *i.e.* $\mathbf{U}_f^+(t) = \mathbf{U}_f(t, \mathbf{x}_f^+(t))$ with $\mathbf{x}_f^+(t)$ the position of a fluid-particle tracked in the flow, and where $D^L(\tau)$ is also a scalar function (now of time rather than of the distance r) called the Lagrangian velocity structure function. Then, a straightforward application of the Kolmogorov similarity hypothesis gives that

$$D^L(\tau) = C_0 \epsilon_f \tau, \quad (101)$$

where C_0 is a constant. This result is of significance for the development of the Lagrangian stochastic models for single-phase flows considered in Section 6.5 and also for their extension to disperse two-phase flows, as shown in Section 7.3.3. It resurfaces in the physical analysis of Lagrangian formulations developed in Section 10.1.4.

It is interesting to note that, while there is no well-marked separation in terms of length scales, there is a separation in terms of timescales. More precisely, it is seen that $\delta u(l)$ diminishes as l becomes smaller but without any marked decrease between two comparable scales (the decrease is continuous) whereas such a clear-cut distinction exists between a fluid-particle velocity \mathbf{U}_f^+ and its acceleration \mathbf{A}_f^+ . Indeed, fluid-particle velocities are governed by the large-scale motions of a turbulent flow and scale as $(\mathbf{U}_f^+)^2 \sim u_f^2$ with a timescale $T_L \sim T_f = u_f^2/\epsilon_f$, while fluid-particle accelerations are governed by the small-scale motions and scale as $(\mathbf{A}_f^+)^2 \sim \epsilon_f/\tau_K$ with a timescale which is of the order of the Kolmogorov timescale τ_K . This situation plays a central role in the analysis of stochastic models in Section 10.

So far, this outline of the Kolmogorov theory has essentially followed the K41 picture in that the rate of kinetic transfer and dissipation ϵ_f is taken as a parameter rather than as a random variable. In relation with this aspect are the effects due to the intermittency of the flow produced by the inherent transfer processes of turbulence, referred to as ‘inner intermittency’ (to be distinguished from external intermittency due, for example, to large-scale mixing between laminar and turbulent flows). In other words, we have assumed that $\epsilon_f = \langle \epsilon_f \rangle$. While the above picture can be kept as such by substituting ϵ_f by $\langle \epsilon_f \rangle$, especially for second-order moments where the impact of intermittency effects is still small, a refined description based on a log-normal distribution for the dissipation of kinetic energy was developed in the K62 formulation. For this specific point, the basic presentation of the refined similarity hypothesis is in [38, section 25.2] and this question has been investigated in several studies. Since this (interesting) aspect is not within the scope of the present article, readers are referred to the vast literature that has grown on the subject.

6.2. The microscopic level: Direct numerical simulation

With the help of the Kolmogorov picture, we can define the microscopic level of description of single-phase turbulent flows as the complete solution of the Navier-Stokes equations, cf. Eqs. (1). By complete, it is meant that all the fluctuations in space (with wavelengths $l \in [\eta_K ; L_f]$) and in time (with periods $\tau \in [\tau_K ; T_f]$) are captured. This is in line with the extended definition of the microscopic level of description given in Section 3.2 since all the degrees of freedom of a single-phase turbulent flow are explicitly calculated.

In terms of simulations, this corresponds to the Direct Numerical Simulation (DNS) approach where the Navier-Stokes equations are solved numerically without resorting to any turbulence model. In each calculation, only one realization of the flow is produced and statistics are obtained by averaging over several simulations or by using time averaging (for locally stationary flows) or space averaging (for locally homogeneous flows). In that sense, DNS are sometimes referred to as ‘numerical experiments’ whose interest is to get access to difficult-to-measure quantities (such as the kinetic energy dissipation), provide insights, and constitute databases against which macroscopic models can be tested.

The model-free formulation makes DNS the equivalent of MD in classical statistical physics and, as with MD, DNS is a demanding method from a computational point of view. This can be inferred with simple scaling arguments: from Eq. (95), we know that the ratio of the large scales L_f to the smallest ones scales as $L_f/\eta_K \sim Re^{3/4}$ and, consequently, the requirement that all fluctuations be captured implies that the number of grid points must be larger than $(L_f/\eta_K)^3 \sim Re^{9/4}$. This becomes rapidly a severe limitation to computations as Re increases (think about atmospheric flows where Re can reach 10^8). Note that the same is true for fluctuations in time imposing that time steps must be smaller than τ_K , and a careful assessment indicates that the numerical costs of DNS increase as Re^3 [30].

The huge computational costs incurred by the DNS approach are duly put forward in the literature. There is, however, one aspect that is sometimes overlooked in relation with the above-mentioned term of numerical experiments. The underlying question is whether DNS outcomes have really the same status as experimental measurements. In that respect, it can be mentioned that the description of boundary conditions remains often simplified. One typical example is that walls are often considered as perfectly smooth surfaces, down to molecular details, disregarding surface roughness. This is not one aspect that is specifically investigated in this work (following the discussions on the fundamental interactions in Section 2.2) and it may not be a severe limit for single-phase turbulent flows (particularly in the bulk of the flow). Yet, similar points with more important consequences will arise for two-phase flows in Section 7.2. In the opinion of the present author, it is therefore best to think of DNS as being the ‘conditional numerical truth’ (conditioned on the choice of an ideal description for the flow conditions), or as insightful numerical experiments but in an idealized world.

6.3. The macroscopic level: Reynolds-averaged Navier–Stokes models

For single-phase turbulent flows, the macroscopic level of description corresponds to the mean-flow equations. Since the consideration of the mean-velocity field $\langle \mathbf{U}_f \rangle(t, \mathbf{x})$ was initiated by Reynolds (1894), these approaches are referred to as the Reynolds-averaged Navier–Stokes and several terms and equations are named after Reynolds.

Mean-flow evolutions are governed essentially by the large scales where most of the kinetic energy is found and which are determined by the geometry of the flow domain, the inlet and boundary conditions and, possibly, external conditions. There is thus little hope for a universal description and the mean flow is not predicted by the Kolmogorov theory. Furthermore, the averaging process removes most of the instantaneous details of turbulence, leaving only their statistical signature in the averaged quantities that are observed. On the other hand, the energy-containing scales are responsible for mixing as well as large-scale transport and are therefore essential in most practical situations. This is sometimes referred to as ‘engineering concerns’, as if these issues were at variance with, or independent of, the study of the structural nature of turbulent flows. This is not so, as the developments in subsequent chapters will demonstrate, but the formulation of macroscopic equations does not rely directly on the Kolmogorov picture, apart from the central role played by $\langle \epsilon_f \rangle$.

The most direct way to obtain the equation for the mean-velocity field $\langle \mathbf{U}_f \rangle(t, \mathbf{x})$ is to apply the averaging operator to the Navier–Stokes equations, Eqs. (1). With the Reynolds decomposition into a mean and a fluctuating part, $\mathbf{U}_f(t, \mathbf{x}) = \langle \mathbf{U}_f \rangle(t, \mathbf{x}) + \mathbf{u}_f(t, \mathbf{x})$ (which was already used in Eq. (27)), this gives the mean-momentum equation, also called the Reynolds equation, which has the form

$$\frac{\partial \langle U_{f,i} \rangle}{\partial t} + \langle U_{f,j} \rangle \frac{\partial \langle U_{f,i} \rangle}{\partial x_j} + \frac{\partial \langle u_{f,i} u_{f,j} \rangle}{\partial x_j} = -\frac{1}{\rho_f} \frac{\partial \langle P_f \rangle}{\partial x_i} + \nu_f \nabla^2 (\langle U_{f,i} \rangle). \quad (102)$$

In the following, we consider only high Reynolds-number turbulent flows and the mean viscous term can be neglected. Similarly, apart from the remaining finite values of $\langle \epsilon_f \rangle$ (see the discussion in Section 6.1), viscosity-related terms will be neglected since we are not especially interested in the near-wall region where these effects are important or in low Reynolds-number flows (for these aspects, see specific discussions in [30]). The Reynolds equation can then be written as

$$\frac{D_f \langle U_{f,i} \rangle}{Dt} = -\frac{1}{\rho_f} \frac{\partial \langle P_f \rangle}{\partial x_i} - \frac{\partial \langle u_{f,i} u_{f,j} \rangle}{\partial x_j}, \quad (103)$$

where D_f/Dt is the convective derivative due to the mean velocity,

$$\frac{D_f}{Dt} = \frac{\partial}{\partial t} + \langle U_{f,j} \rangle \frac{\partial}{\partial x_j}. \quad (104)$$

From the expression in Eq. (103), it is seen that the application of the averaging operator yields a new tensor, i.e. $R_{f,ij} = \langle u_{f,i} u_{f,j} \rangle$, which is the Reynolds stress (since it plays the role of a stress tensor). At the macroscopic level of description, the Reynolds stress components $R_{f,ij}$ are unknown and need to be expressed in terms of known parameters or variables. This is the classical issue of having to formulate constitutive relations when operating directly at the macroscopic level, as discussed in Section 3.

The two main closures that have been developed at the macroscopic level are: first, to propose an algebraic relation for the Reynolds stresses through the eddy-viscosity concept; second, to write and close the transport equation for each component of the Reynolds $R_{f,ij}$ through Reynolds-stress models (RSM).

In the context of the present article, we are not concerned with how present formulations (or their variants) are built or by analyzing their predictive capacities (these aspects are addressed in [30]). We are interested in RANS formulations as exemplifying the macroscopic level of description for turbulent flows. For these reasons, we limit ourselves to the bare facts of the representative models in the class of eddy-viscosity models and Reynolds stress models.

6.3.1. Eddy-viscosity models

In eddy-viscosity approaches, a local closure (in time and space) is assumed between the Reynolds stress tensor and the rate of strain tensor of the mean flow. This is expressed by

$$\langle u_{f,i} u_{f,j} \rangle = \frac{2}{3} k_f \delta_{ij} - \nu_{f,t} \left(\frac{\partial \langle U_{f,i} \rangle}{\partial x_j} + \frac{\partial \langle U_{f,j} \rangle}{\partial x_i} \right), \quad (105)$$

where $k_f = 1/2 \langle u_{f,i} u_{f,i} \rangle$ is the turbulent kinetic energy and $\nu_{f,t}$ the turbulent viscosity (or ‘eddy-viscosity’).

The most commonly-used eddy-viscosity model is the $k-\epsilon$ model where $\nu_{f,t}$ is given by a local expression in terms of the turbulent kinetic energy k_f and its timescale (taken as $k_f/\langle \epsilon_f \rangle$), which gives $\nu_{f,t} = C_\mu k_f^2/\langle \epsilon_f \rangle$, with C_μ a constant. The name of the method hints to the variables that are explicitly simulated, since the model is based on transport equations for the turbulent kinetic energy k_f and its mean dissipation rate $\langle \epsilon_f \rangle$, which have the form

$$\frac{D_f k_f}{Dt} = \frac{\partial}{\partial x_k} \left(\frac{\nu_{f,t}}{\sigma_{k_f}} \frac{\partial k_f}{\partial x_k} \right) + \mathcal{P}_f - \langle \epsilon_f \rangle, \quad (106)$$

$$\frac{D_f \langle \epsilon_f \rangle}{Dt} = \frac{\partial}{\partial x_k} \left(\frac{\nu_{f,t}}{\sigma_{\epsilon_f}} \frac{\partial \langle \epsilon_f \rangle}{\partial x_k} \right) + C_{\epsilon_f,1} \frac{\mathcal{P}_f \langle \epsilon_f \rangle}{k_f} - C_{\epsilon_f,2} \frac{\langle \epsilon_f \rangle^2}{k_f}, \quad (107)$$

where

$$\mathcal{P}_f = -\langle u_{f,i} u_{f,j} \rangle \partial \langle U_{f,i} \rangle / \partial x_j, \quad (108)$$

is the turbulent kinetic energy production rate. In Eqs. (106)–(107), σ_{k_f} , σ_{ϵ_f} , $C_{\epsilon_f,1}$ and $C_{\epsilon_f,2}$ are constants of the model.

6.3.2. Reynolds-stress models

In Reynolds-stress models (RSM), a local closure for $R_{f,ij}$ is not attempted and the components of the Reynolds stress tensor are obtained as the solutions of their own (modeled) transport equations. These transport equations for $R_{f,ij}$ are obtained from the Navier–Stokes equations and express the work done by the pressure-gradient and viscous forces in the exact instantaneous Navier–Stokes equations. In the high Reynolds-number limit where viscous diffusive terms are neglected and where dissipation is taken as isotropic (this represents one aspect whereby Kolmogorov theory is used through the notion of locally isotropic flows), the resulting (open) form of these equations is written as

$$\frac{D_f \langle u_{f,i} u_{f,j} \rangle}{Dt} = -\frac{\partial T_{f,kij}}{\partial x_k} + \mathcal{P}_{f,ij} + \mathcal{R}_{f,ij}^d - \frac{2}{3} \langle \epsilon_f \rangle \delta_{ij}, \quad (109)$$

where $T_{f,kij}$, $\mathcal{P}_{f,ij}$ and $\mathcal{R}_{f,ij}^d$ are given by

$$T_{f,kij} = \langle u_{f,i} u_{f,j} u_{f,k} \rangle + \langle u_{f,i} p_f \rangle \delta_{jk} + \langle u_{f,j} p_f \rangle \delta_{ik}, \quad (110)$$

$$\mathcal{P}_{f,ij} = -\langle u_{f,i} u_{f,k} \rangle \frac{\partial \langle U_{f,j} \rangle}{\partial x_k} - \langle u_{f,j} u_{f,k} \rangle \frac{\partial \langle U_{f,i} \rangle}{\partial x_k}, \quad (111)$$

$$\mathcal{R}_{f,ij}^d = \left\langle \frac{p_f}{\rho_f} \left(\frac{\partial u_{f,i}}{\partial x_j} + \frac{\partial u_{f,j}}{\partial x_i} \right) \right\rangle. \quad (112)$$

In these equations, $T_{f,kij}$ is called the Reynolds-stress flux, $\mathcal{P}_{f,ij}$ the production tensor and $\mathcal{R}_{f,ij}^d$ the pressure-rate-of-strain tensor. The production terms $\mathcal{P}_{f,ij}$ do not need closure (note that \mathcal{P}_f in Eq. (106) is half the trace of $\mathcal{P}_{f,ij}$ since $k_f = 1/2 R_{f,ii}$). On the other hand, both $T_{f,kij}$ and $\mathcal{R}_{f,ij}^d$ need to be closed. The Reynolds-stress flux contains, first, a triple correlation between the fluctuating velocity components due to the application of the averaging process to the exact convective term and, second, a contribution due to fluctuating pressure–velocity correlations. The original form of the transport equation for $R_{f,ij}$ involves the work done by the fluctuating pressure-gradient force (since $p_f = P_f - \langle P_f \rangle$) and yields directly a contribution which corresponds to the velocity–pressure-gradient tensor

$$\Pi_{f,ij} = -\frac{1}{\rho_f} \left\langle u_{f,i} \frac{\partial p_f}{\partial x_j} + u_{f,j} \frac{\partial p_f}{\partial x_i} \right\rangle, \quad (113)$$

which, by integration by parts, is transformed to give $\mathcal{R}_{f,ij}^d$ and the second contribution to $T_{f,kij}$. The interest of such a decomposition is that the fluid continuity equation implies that $\mathcal{R}_{f,ii}^d = 0$, showing therefore that $\mathcal{R}_{f,ij}^d$ is redistributing (fluctuating kinetic) energy between the components of the Reynolds-stress tensor.

To model $T_{f,kij}$, a gradient-diffusion hypothesis is used with an anisotropic diffusion coefficient of the form

$$T_{f,kij} = -C_{f,s} \frac{k_f}{\langle \epsilon_f \rangle} \langle u_{f,k} u_{f,i} \rangle \frac{\partial \langle u_{f,i} u_{f,j} \rangle}{\partial x_l}, \quad (114)$$

where $C_{f,s}$ is a constant. The most important term in RSMs is the redistribution model for $\mathcal{R}_{f,ij}^d$. The present consensus is to use the LRR-IP (for Launder, Reece and Rodi and Isotropization of Production (IP), respectively) model where

$$\mathcal{R}_{f,ij}^d = -C_{f,R} \frac{\langle \epsilon_f \rangle}{k_f} \left(\langle u_{f,i} u_{f,j} \rangle - \frac{2}{3} k_f \delta_{ij} \right) - C_{f,IP} \left(\mathcal{P}_{f,ij} - \frac{2}{3} \mathcal{P}_f \delta_{ij} \right), \quad (115)$$

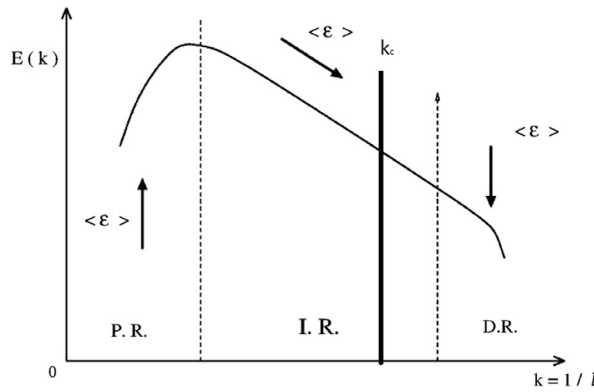


Fig. 29. The Large Eddy Simulation approach: a cut-off length $k_c = 1/\Delta$ is introduced to separate between the large-scale fluid motions that are calculated and the subgrid ones whose effects are replaced by a model.

where $C_{f,R}$ and $C_{f,IP}$ are constants of the model. This expression is referred to as the ‘basic redistribution model’ [30]. On the rhs of Eq. (115), the first part corresponds to the Rotta model which is acting as a return-to-equilibrium driving force for the components of the Reynolds stress tensor while the basic idea of the IP contribution is to assume that rapid pressure gradients tend to increase the Reynolds-stress anisotropy. The modeled transport equations for $R_{f,ij}$ are supplemented with an equation for $\langle \epsilon_f \rangle$, typically Eq. (107), and, for this reason, RSM are also called $R_{ij} - \epsilon$ models (or second-order models).

More details on eddy-viscosity and Reynolds-stress model can be found in [30, chapter 10, chapter 11]. However, a few remarks are in order with respect to the discussions to come:

- (1) The ambition of these macroscopic formulations is limited to the first two one-point moments, $\langle U_{f,i} \rangle(t, \mathbf{x})$ and $\langle u_{f,i} u_{f,j} \rangle(t, \mathbf{x})$. There is no length information and, therefore, no spatial correlation (and, thus, no spectrum) can be calculated;
- (2) The application of the averaging operator generates an open hierarchy between one-point moments: $\langle U_{f,i} \rangle(t, \mathbf{x})$ depends on $\langle u_{f,i} u_{f,j} \rangle(t, \mathbf{x})$ which, in turn, depends on triple correlations $\langle u_{f,i} u_{f,j} u_{f,k} \rangle(t, \mathbf{x})$, and so on;
- (3) It is worth emphasizing that the Reynolds-stress tensor, the triple correlation and the successive one-point velocity correlations appearing in the mean-flow equations arise from the application of the averaging operator to convective transport. They are therefore convective terms but they are treated, fully or partially, as diffusive ones through the use of gradient-diffusion expressions;
- (4) An important difference between the two macroscopic models is that the Reynolds stresses $R_{f,ij}$ depend only on local properties of the mean flow in eddy-viscosity models while they are non-local in RSMs (a first hint of the discussion in Section 10.3);
- (5) The decomposition in terms of mean and fluctuating components does not correspond to a separation between slow- and rapidly-varying variables. Indeed, classical observations (for example in free-shear flows such as jets or mixing layers) indicate that the ratio between the timescale of the mean flow S_f (with $S_f^{-1} = \partial \langle U_f \rangle / \partial x$) and of the turbulent fluctuations represented by $k_f / \langle \epsilon_f \rangle$ can be as high as $S_f k_f / \langle \epsilon_f \rangle \sim 3$. Turbulence is long-lived and fluctuations cannot be regarded as white noises with respect to mean variables.

6.4. One mesoscopic approach: the large eddy simulation method

Though the approach was initiated in the early 1960s for meteorological applications by Smagorinsky, whose name is deeply associated with the method, large-eddy simulation started to take off in the 1990s with the increase of computational resources. Compared to the mean-flow models described above, LES relies more heavily on the Kolmogorov theory. As represented in Fig. 29, the leading idea is to introduce a cut-off length to separate between the large-scales motions that are explicitly computed and the residual ones that are modeled. This is indeed in line with Kolmogorov ideas where only the statistical characteristics of scales lying within the inertial and dissipative ranges can be regarded as universal and have therefore a chance to be replaced by a model.

These ideas are translated into the application of a spatial filtering operation instead of an ensemble averaging one. To that effect, the filtered value, noted $\langle H_f \rangle_{ls}(t, \mathbf{x})$, of a field quantity $H_f(t, \mathbf{x})$ is defined by

$$\langle H_f \rangle_{ls}(t, \mathbf{x}) = \int H_f(t, \mathbf{x}') G(\mathbf{x}', \mathbf{x}) d\mathbf{x}', \quad (116)$$

where $G(\mathbf{x}, \mathbf{x}')$ is the filter function which is, nearly always, taken as a spatially and temporally invariant positive function with a compact support. In other words, $G(\mathbf{x}, \mathbf{x}')$ can be written as $G(\mathbf{x}, \mathbf{x}') \equiv G(\mathbf{x} - \mathbf{x}')$ with the properties $G(\mathbf{x}) \geq 0$ and

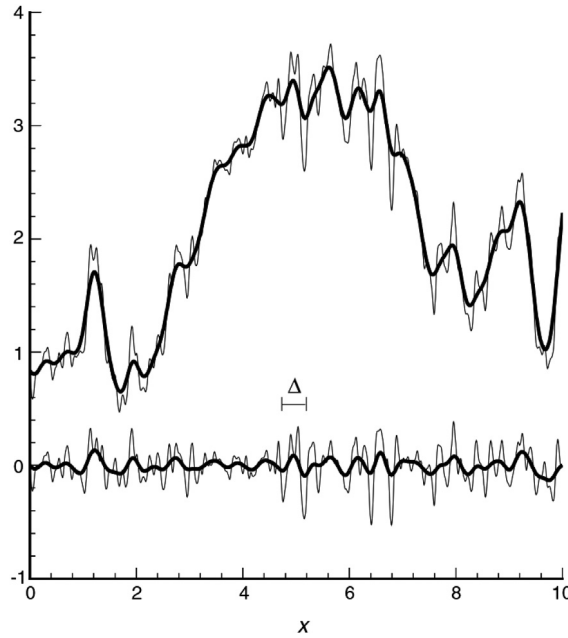


Fig. 30. Illustration of the LES method for a one-dimensional signal: the original signal is the thin line and the thick line corresponds to the filtered one on the top of the figure. The difference between the two is the residual signal that oscillates around zero but the filtered value of these residual motions is not zero, manifesting the lack of idempotence property.

Source: Reprinted from [30] with permission from Cambridge University Press.

$\int G(\mathbf{x})d\mathbf{x} = 1$. With this definition, each variable can be decomposed into a filtered value and a residual one, which for the velocity field is expressed by

$$\mathbf{U}_f(t, \mathbf{x}) = \langle \mathbf{U}_f \rangle_{ls}(t, \mathbf{x}) + \mathbf{u}'_f(t, \mathbf{x}) \quad (117)$$

with $\mathbf{u}'_f(t, \mathbf{x})$ the residual or unresolved part of the velocity field. The difference between the spatial filtering operation and a proper probabilistic averaging is manifested by the loss of the idempotence property since $\langle \mathbf{u}'_f \rangle_{ls}(t, \mathbf{x}) \neq 0$.

In practice, the width of the filter function G is closely related (if not identical) to a mesh size Δ . The best example of that situation is when a box filter function is chosen which, in a one-dimensional formulation, is $G(x) = H(\Delta/2 - |x|)/\Delta$ (with $H(x)$ the Heaviside function). The same is true for traditional filter functions, such as the Gaussian filter or other choices (see [30]). Without having to specify the exact relation, we can thus regard the filter width as being given by the local mesh size. This implies a strong dependence of the LES approach to space discretization into a mesh and an interwoven relation between the formulation of the method and its numerical implementation (which, to some extend, cannot be distinguished anymore). For this reason, the filtered and residual components in Eq. (117) are also referred to as resolved and unresolved respectively, while the unresolved part is usually called the subgrid-scale (SGS) component.

The effects of filtering are illustrated with a one-dimensional signal in Fig. 30. It is seen that the filtered signal follows the trends of the original one but details (which means the short length-scale fluctuations) below the filter size Δ are lost while the filtered values of the residual signal are not zero, due to the lack of the idempotence property. Compared to the original signal, less information is resolved but, compared to a mean value, more information is kept: this indicates that LES approaches are operating at a mesoscopic level of description.

As for the mean-flow equations, the equations for the filtered velocity field are obtained by applying the spatial filtering operation to the Navier–Stokes equations, which gives [30]:

$$\frac{\partial \langle U_{f,i} \rangle_{ls}}{\partial t} + \langle U_{f,j} \rangle_{ls} \frac{\partial \langle U_{f,i} \rangle_{ls}}{\partial x_j} = -\frac{1}{\rho_f} \frac{\partial \langle P_f \rangle_{ls}}{\partial x_i} - \frac{\partial \langle \tau_{f,ij} \rangle_{ls}}{\partial x_j}, \quad (118)$$

where $\langle \tau_{f,ij} \rangle_{ls} = \langle U_{f,i} U_{f,j} \rangle_{ls} - \langle U_{f,i} \rangle_{ls} \langle U_{f,j} \rangle_{ls}$ denotes the residual-stress tensor, also called the subgrid-stress tensor, which, in the LES formalism, plays the role of the Reynolds stress $\langle u_{f,i} u_{f,j} \rangle$. The situation is therefore similar to the Reynolds equation, Eq. (102), in that a model for the subgrid-stress tensor needs to be introduced.

By far, the most-widely used model at present is the Smagorinsky model which is an eddy-viscosity model with the form

$$\langle \tau_{f,ij} \rangle_{ls} = \frac{2}{3} k_f^r \delta_{ij} - v_{f,t}^s \left(\frac{\partial \langle U_{f,i} \rangle_{ls}}{\partial x_j} + \frac{\partial \langle U_{f,j} \rangle_{ls}}{\partial x_i} \right), \quad (119)$$

where $k_f^r = 1/2\langle \tau_{f,ii} \rangle_{ls}$ is the residual kinetic energy and $\nu_{f,t}^S$ the Smagorinsky SGS viscosity coefficient. The specific feature of the model is that the eddy viscosity of the residual motions is explicitly expressed as a function of the mesh size Δ by the relation

$$\nu_{f,t}^S = (C_S \Delta)^2 S_{ls} \quad (120)$$

where C_S is the Smagorinsky constant and S_{ls} the characteristic filtered rate of strain

$$S_{ls} = (2\langle S_{ij} \rangle_{ls} \langle S_{ij} \rangle_{ls})^{1/2}, \quad \text{with } \langle S_{ij} \rangle_{ls} = \frac{1}{2} \left(\frac{\partial \langle U_{f,i} \rangle_{ls}}{\partial x_j} + \frac{\partial \langle U_{f,j} \rangle_{ls}}{\partial x_i} \right). \quad (121)$$

In the basic formulation, C_S is a constant while, in more evolved formulations, various propositions have been put forward to derive local estimates of this ‘constant’ (this corresponds to so-called dynamical models). Similar efforts along that direction are described in [30, chapter 13]. Note that the closed LES formulation, which is made up by Eqs. (118) and (119), does not explicitly require the rate of dissipation of the residual kinetic energy ϵ_f^r , although this one can be estimated by the relation

$$\epsilon_f^r = C_S \frac{(k_f^r)^{3/2}}{\Delta}. \quad (122)$$

Several remarks can be made on this mesoscopic approach:

- (1) The spatial filtering operation means that an Eulerian point of view is still adopted as manifested by a formulation in terms of fields;
- (2) Present LES models assume a deterministic evolution for filtered variables, which is reflected into deterministic closures for the residual-stress tensor. However, although spatial filtering removes some randomness, the filtered velocity $\langle \mathbf{U}_f \rangle_{ls}(t, \mathbf{x})$ is still a random variable and proper accounts of this aspect would greatly benefit from a formulation in terms of sub-sigma algebras (see Section 4). Surprisingly, this question is addressed in few works (see discussions in [53, 103]);
- (3) There is no instantaneous field in LES but, since the large unsteady motions are explicitly computed, the filtered velocity field is an outcome of the method and spatial correlations (due to these large-scale motions) can be extracted. For example, the kinetic energy spectrum (limited to the range of wave numbers that are explicitly computed) is a result and can be compared to the ones obtained from DNS;
- (4) The LES approach is founded in Kolmogorov theory and makes use of the classical picture of the energy cascade through scales and, especially, the distinction between the large, energy-containing, scales and the small scales that are assumed to reach universal properties (conditioned on the values of the large ones);
- (5) Yet, the Kolmogorov theory reveals also that, if there is a distinction between large and small scales, there is no clear-cut separation. In other words, the kinetic energies $(\delta u(l))^2$ and $(\delta u(l'))^2$ as well as the timescales $\tau(l)$ and $\tau(l')$ of two eddies l and l' are of the same order when $l \simeq l'$, indicating that the introduction of a cut-off is artificial;
- (6) In relation with the latter point, the current use of the eddy-viscosity concept to model SGS implies a one-way energy transfer and an underlying vision of SGS as being very fast, purely dissipative, motions even compared to the scales just above the filter cut-off length. The connection between gradient-diffusion, eddy-viscosity, and fast variables is a current theme in this work and is developed in Section 10.4.

As mentioned with point (3) above, the available information is the unsteady filtered velocity field. This represents a multi-point information (to be compared with the formulation of the macroscopic descriptions in terms of one-point moments) but only for large-scale motions (SGS are lost). For mixing and large-scale transport issues, this represents an improvement since the kinetic energy of the residual motions is small but not, for example, for chemical process which are governed by molecular reactions and, therefore, by the smallest scales. More precisely, if we take up the example of the chemical source term in Section 3.2.2, it is seen that no modeling progress has been achieved with LES formulations. This situation explains that other mesoscopic models have been developed with the purpose to reintroduce information on the whole range of fluctuations. These approaches are referred to as PDF and FDF methods and are now presented.

6.5. Fine- and coarse-grained models at the mesoscopic level

PDF and FDF methods derive their names from the information that they produce, which indicates that they aim at simulating the probability density function (PDF) and the filtered density function (FDF), respectively. Compared to the previous approaches, they are formulated in terms of particle systems where stochastic models are used to represent the evolution of the instantaneous variables attached to each particle. Although the interest of these methods is marked for scalar variables when single-phase reactive flows are involved, we essentially concentrate in the following on the dynamical variables which are the positions $\mathbf{x}_f(t)$ and velocities $\mathbf{U}_f(t)$ of a large number of fluid particles.

The connection between the introduction of Lagrangian stochastic models and mean (for PDF) or filtered (for FDF) equations follows the methodology recalled in Section 4.4. This is now a well-established mathematical procedure, especially for PDF methods. In the LES context, the idea introduced by Pope and developed in a series of papers with various co-authors [104–109] is to rely on the spatial filtering of fine-grained PDFs. Loosely speaking, both formulations can indeed be cast into

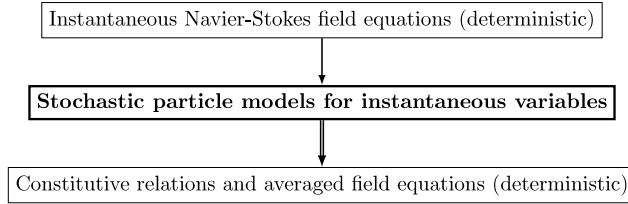


Fig. 31. Representation of the Lagrangian stochastic approach to derive macroscopic models: Reynolds-stress models (for Lagrangian PDF methods) and filtered equations (for Lagrangian FDF methods).

a single framework by considering the application of different ‘operators’ to instantaneous variables. To illustrate that point, we consider a variable $\mathbf{Z}(t)$ represented by a stochastic model. As mentioned at the beginning of Section 4.5, the fine-grained PDF for a sample value \mathbf{z} is defined by $\delta(\mathbf{Z}(t) - \mathbf{z})$. From this initial particle-based information, two distribution functions result from the application of the two operators used in Sections 6.3 and 6.4, that is

$$p(t; \mathbf{z}) = \langle \delta(\mathbf{Z}(t) - \mathbf{z}) \rangle, \quad (123)$$

$$p_{ls}(t; \mathbf{z}) = \langle \delta(\mathbf{Z}(t) - \mathbf{z}) \rangle_{ls}. \quad (124)$$

This is, however, a formal analogy since $p(t; \mathbf{z})$ is a true PDF while $p_{ls}(t; \mathbf{z})$ can only loosely be regarded as such since $\langle \cdot \rangle_{ls}$ is not a proper expectation operator (remember that it does not satisfy the idempotence property). This point is further addressed in Section 6.5.3 but, with this caveat in mind, we nevertheless consider these functions as the ‘measure functions’ to manipulate. The consequence is that the construction of PDF or FDF mesoscopic models rests upon the choice of a Lagrangian stochastic model for $(\mathbf{x}_f(t), \mathbf{U}_f(t))$, as represented in Fig. 31. We can therefore develop a particle description of turbulent flows with a view towards mean- or filtered-flow equations.

The starting point is provided by the Navier–Stokes equations in a Lagrangian formulation which, using the same notations as in Section 6.1, write

$$\frac{dx_{f,i}^+}{dt} = U_i^+, \quad (125a)$$

$$\frac{dU_{f,i}^+}{dt} = -\left(\frac{1}{\rho_f} \frac{\partial \langle P_f \rangle}{\partial x_i}\right)^+ - \underbrace{\left(\frac{1}{\rho_f} \frac{\partial p_f}{\partial x_i}\right)^+}_{\text{to model}} + (\nu_f \Delta u_{f,i})^+, \quad (125b)$$

using the Reynolds decomposition into mean and fluctuating parts (leaving out the mean viscous term $\nu \Delta \langle U_i \rangle$ at high Reynolds-number flows) that is relevant for PDF approaches. As shown in Eq. (125b), the fluctuating pressure-gradient and viscous terms are to be modeled.

6.5.1. Probability density function approaches

A reference stochastic model is the GLM (Generalized Langevin Model) [30,67,110] which represents fluid–particle variables by a stochastic diffusion process with the form

$$dx_{f,i} = U_{f,i} dt, \quad (126a)$$

$$dU_{f,i} = -\frac{1}{\rho_f} \frac{\partial \langle P_f \rangle}{\partial x_i} dt + D_i dt + \sqrt{C_0 \langle \epsilon_f \rangle} dW_i. \quad (126b)$$

The first equation, Eq. (126a) is apparently trivial but the fact that it is equal to Eq. (125a) shows that convective transport is treated without approximation (thanks to the Lagrangian formulation with instantaneous variables). As a result, every term due to convective transport appears in closed form in the resulting mean equations. In Eq. (126b), the diffusion coefficient has an isotropic form, in line with the Kolmogorov theory for Lagrangian statistics presented in Section 6.1 and, in particular, Eq. (101). Still in Eq. (126b), the drift vector \mathbf{D} is written as a generalized return-to-equilibrium term (thus, the name Langevin used for these models) to the local mean velocity, which means that it is modeled as

$$D_i = G_{ij} (U_{f,j} - \langle U_{f,j} \rangle) \quad (127)$$

where the matrix G_{ij} depends on the particle location and on statistics of the fluid flow but not on the particle velocity, i.e. $G_{ij} = G_{ij}(t, \mathbf{x}_f(t), \mathcal{F}[(\mathbf{x}_f, \mathbf{U}_f)])$ where the notation $\mathcal{F}[(\mathbf{x}_f, \mathbf{U}_f)]$ refers to fluid mean quantities either given or calculated from the set of particles and that are interpolated at the particle position. Therefore, in homogeneous flows, G_{ij} depends only on time and Eq. (126b) is a linear model for fluid–particle velocities, while the complete particle system in Eqs. (126) is non-linear in general non-homogeneous situations. This point has been emphasized in several works (see [1,30,67]) and,

for the sake of simplicity of the notations, these dependences are considered as implicit and are not kept in the following equations. A classical decomposition of the matrix G_{ij} is [67,111]

$$G_{ij} = -\left(\frac{1}{2} + \frac{3}{4}C_0\right)\frac{\langle\epsilon_f\rangle}{k_f}\delta_{ij} + G_{ij}^a \quad (128)$$

where the matrix G_{ij}^a represents anisotropic effects and, for reasons that become clear with the mean equations derived below, is subject to the condition $\text{Tr}(\mathbf{G}^a \cdot \mathbf{R}_f) = 0$, with \mathbf{R}_f the Reynolds-stress tensor. For later developments, it is useful to write the drift vector with the Lagrangian timescale T_L as

$$D_i = -\frac{U_{f,i} - \langle U_{f,i} \rangle}{T_L} + G_{ij}^a (U_{f,j} - \langle U_{f,j} \rangle) \quad \text{with} \quad T_L = \frac{1}{\left(\frac{1}{2} + \frac{3}{4}C_0\right)} \frac{k_f}{\langle\epsilon_f\rangle}. \quad (129)$$

As for the matrix G_{ij} , the mean terms are to be understood as being the values of the mean fields at the particle location, for instance $\langle U_{f,i} \rangle = \langle U_{f,i} \rangle(t, \mathbf{x}_f)$.

The mean equations corresponding to the GLM are easily derived by the application of the PDF methodology in Section 4.4. When the mean pressure-gradient is calculated to enforce the continuity condition, the mean fluid continuity equation is respected. Since the drift vector D_i in Eq. (126b) is such that $\langle D_i \rangle = 0$ whatever the choice of the matrix G_{ij} , the formulation in terms of instantaneous fluid-particle positions and velocities as in Eqs. (126) ensures that the high Reynolds-number form of the Reynolds equation, Eq. (103), is always satisfied. Note that the Reynolds-stress tensor $R_{f,ij}$, being a convective effect, is in closed form in a Lagrangian approach. The modeled second-order equations are

$$\frac{D_f \langle u_{f,i} u_{f,j} \rangle}{Dt} = -\frac{\partial \langle u_{f,i} u_{f,j} u_{f,k} \rangle}{\partial x_k} + \mathcal{P}_{f,ij} + \langle u_{f,i} D_j \rangle + \langle u_{f,j} D_i \rangle + C_0 \langle \epsilon_f \rangle \delta_{ij} \quad (130)$$

which, with the decomposition in Eq. (128), can be rewritten as

$$\begin{aligned} \frac{D_f \langle u_{f,i} u_{f,j} \rangle}{Dt} &= -\frac{\partial \langle u_{f,i} u_{f,j} u_{f,k} \rangle}{\partial x_k} + \mathcal{P}_{f,ij} - \left(1 + \frac{3}{2}C_0\right) \frac{\langle\epsilon_f\rangle}{k_f} \left(\langle u_{f,i} u_{f,j} \rangle - \frac{2}{3}k_f \delta_{ij}\right) \\ &\quad + G_{ik}^a \langle u_{f,j} u_{f,k} \rangle + G_{jk}^a \langle u_{f,i} u_{f,k} \rangle - \frac{2}{3} \langle \epsilon_f \rangle \delta_{ij}. \end{aligned} \quad (131)$$

Since the redistribution terms $\mathcal{R}_{f,ij}^d$ are of zero trace, this form explains that one must have $G_{ik}^a \langle u_{f,i} u_{f,k} \rangle = 0$, which is the constraint given above.

It is seen that $G_{ij}^a = 0$ corresponds to the Rotta model while the basic redistribution model in Eq. (115) is retrieved, for instance, with

$$G_{ij}^a = C_{f,1} \frac{\partial \langle U_{f,i} \rangle}{\partial x_j} + C_{f,2} \frac{\mathcal{P}_f}{2k_f} \delta_{ij}, \quad (132)$$

where $C_{f,1}$ and $C_{f,2}$ are constants of the model. These correspondences are studied in detail in [30,111] but are outside the scope of the present article. We are more concerned with the structure of PDF methods and how they fit in the general picture of microscopic, mesoscopic and macroscopic descriptions of single-phase turbulent fluid flows. To that effect, an important remark is in order.

With PDF methods, we are dealing with a particle system akin to the ones considered in Section 5. However, there are no direct particle-particle interactions and, instead, each particle is interacting with the mean fields that they create, as sketched in Fig. 32. In other words, present PDF models are *mean-field stochastic approaches*. Consequently, there is no length information in present PDF formulations. The methods described above are one-point PDF models since they derive from a one-particle (Lagrangian) PDF formulation (cf. the discussion in Section 8.2).

6.5.2. Filtered density function approaches

In the LES context, the modeling issue is also represented by Eqs. (125), but with a decomposition in terms of filtered and residual parts. A representative model, corresponding to the one referred to as the VFDF2 model in [106], is

$$dx_{f,i} = U_{f,i} dt, \quad (133a)$$

$$dU_{f,i} = -\frac{1}{\rho_f} \frac{\partial \langle P_f \rangle_{ls}}{\partial x_i} dt + G_{ij} (U_{f,j} - \langle U_{f,j} \rangle_{ls}) dt + \sqrt{C_0 \epsilon_f^r} dW_i, \quad (133b)$$

where the viscous terms of the filtered velocity is again neglected for high Reynolds-number turbulent flows. In Eq. (133b), the matrix G_{ij} has a form similar to the one used in the PDF context (with $G_{ij}^a = 0$) and is given by

$$G_{ij} = -\left(\frac{1}{2} + \frac{3}{4}C_0\right) \frac{\epsilon_f^r}{k_f^r} \delta_{ij}. \quad (134)$$

In the above closures, C_0 and C_S are the model constants already introduced in Section 6.4, and k_f^r and ϵ_f^r still represent the SGS kinetic energy and dissipation rate, respectively. This means that $k_f^r = 1/2 \langle \tau_{f,ii} \rangle_{ls}$ and that ϵ_f^r is given by Eq. (122).

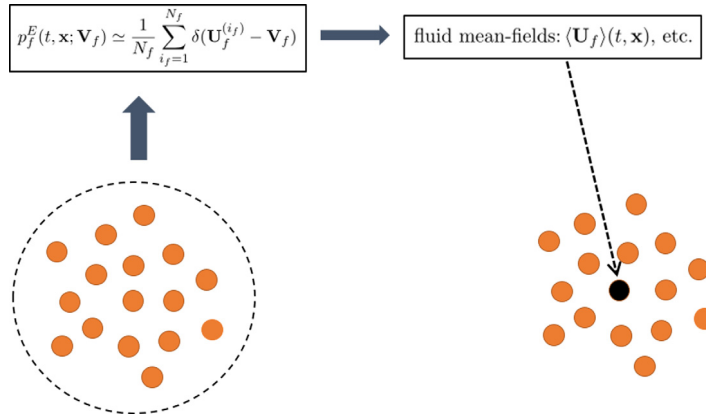


Fig. 32. Representation of the mean-field formulation of one-particle Lagrangian stochastic approaches: in a small volume around a given point, particles interact with the mean fields that they create. This represents therefore multi-body forces (as in SPH) but with weak interactions.

By comparing the particle velocity model in Eq. (133b) with the form in Eqs. (126b) and (128), it is clear that present LES closures are direct extensions of current PDF proposals. Note that the similarity between the particle stochastic systems in Eqs. (126) and (133) is on a par with the similarity between the Reynolds equation closed with the $k-\epsilon$ eddy-viscosity expression and the filtered-momentum equation with the Smagorinsky closure for the SGS-stress tensor. In Eqs. (133), the LES formulation enters the modeling picture through the closure retained for the SGS dissipation rate ϵ_f^r , which is estimated directly from the mesh size (or the filter size) in Eq. (122), rather than from a modeled equation as in Eq. (107).

The connection between the stochastic particle system in Eqs. (133) and filtered quantities, such as the filtered velocity $\langle \mathbf{U}_f \rangle_{ls}$ used in the Langevin model on the rhs of Eq. (133b), is not immediate and even somewhat puzzling at first sight. The correspondence between the two formulations is due to the assumption put forward at the beginning of Section 6.5 that the FDF is treated as a true PDF (see detailed discussions on this formalism in the original papers on the FDF method, especially in [106] as well as a recent analysis in [5, section 7]). In terms of the Eulerian PDFs from which statistics are derived (see Section 4.4), this means that the filtered (Eulerian) fine-grained PDFs is identified with the ‘true’ (Eulerian) PDF from the particle stochastic system (which is the Lagrangian one conditioned on a given location). In other words, it is assumed that

$$p_{f,ls}^E(t, \mathbf{x}; \mathbf{V}_f) = \int \delta(\mathbf{V}_f - \mathbf{U}_f(t, \mathbf{x}')) G(\mathbf{x}' - \mathbf{x}) d\mathbf{x}' \equiv p_f^E(t, \mathbf{x}; \mathbf{V}_f), \quad (135)$$

where the (Eulerian) PDF p_f^E is classically approximated with Monte Carlo estimations,

$$p_f^E(t, \mathbf{x}; \mathbf{V}_f) \simeq \frac{1}{N_x} \sum_{n=1}^{N_x} \delta(\mathbf{U}_f^{(n)}(t) - \mathbf{V}_f), \quad (136)$$

with N_x the number of particles, labeled with (n) , found at time t in a small volume δV_x around point \mathbf{x} . In particular, this shows that the ‘mean’ local particle velocity extracted from the particle system corresponds to the local value of the filtered field velocity field, in the sense that

$$\frac{1}{N_x} \sum_{n=1}^{N_x} U_{f,i}^{(n)} \xrightarrow{\delta V_x \rightarrow 0, N_x \rightarrow +\infty} \langle U_{f,i} \rangle_{ls}. \quad (137)$$

6.5.3. Hybrid approaches and towards full particle simulations

The PDF and FDF models provide more information than the RANS and LES methods respectively, in that the distribution of the fluctuating or SGS velocities is simulated (the same is true for scalars when they are included in the descriptions): they constitute mesoscopic approaches operating at a finer level of description. Compared to the RANS and LES formulations, they also offer new interpretations and open the way for a new paradigm.

Indeed, it is seen that the modeled particle momentum equations, Eq. (126b) or Eq. (133b), imply a combination of particle/field descriptions. Different hybrid formulations can then be devised. For example, one can imagine that a RANS (or LES) calculation is first performed and that the mean (or filtered) fields are provided to the particle method (this is in line with the classical Eulerian/Lagrangian formulation of disperse two-phase flows to be addressed in Section 7). In this vision, particles are simply used to reproduce fluctuations (or SGS variations), around a given mean or filtered value, and there are then redundant fields since the mean (or filtered) fluid velocity field is also produced by the particle simulation. A more important remark is to note that the Reynolds equation (or the filtered) momentum-equation are closed in PDF (or FDF methods) since the Reynolds- (or SGS-) stress tensors result from the particle approach. Consequently, eddy-viscosity

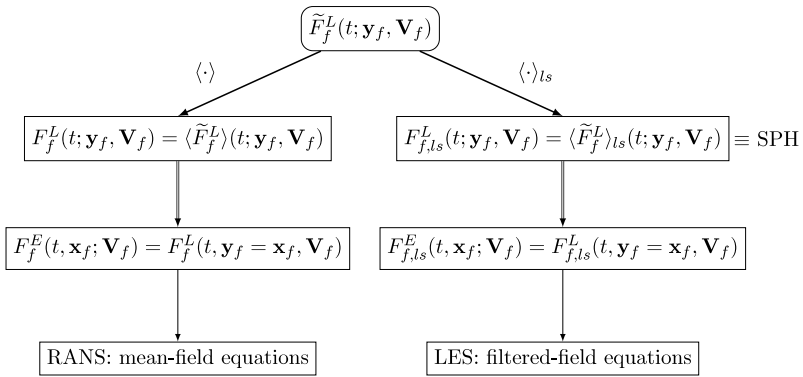


Fig. 33. Sketch of the central role played by the discrete LMDF \tilde{F}_f^L from which the application of different statistical operators yields the Lagrangian and Eulerian MDFs and the resulting macroscopic descriptions.

closures are even in conflict with the Lagrangian models which have been shown to be inherently equivalent to second-order closures. Consequently, a second vision consists in developing consistent hybrid formulations where the particle stochastic model is used to extract the Reynolds stress tensor (or the SGS one) that is fed into the mean (or filtered) equations (see descriptions in [106,112,113]). In that case, the field and particle formulations are consistent with the ‘turbulence model’ given by the Lagrangian description (this allows significant departures from the limitations of eddy-viscosity closures in LES). It can even been considered that the numerical solution of the mean (or filtered) equations is basically providing estimations of the first-order velocity moments with reduced statistical noise to the Lagrangian module, in the spirit of Variance Reduction Techniques (VRT) for Monte Carlo methods [114]. This second hybrid formulation is still rooted in a field description in the sense that particles are introduced as a (Lagrangian) Monte Carlo method to solve the (Eulerian) PDF (or FDF) equations in sample space. This is true with the present formulations of FDF models built from a manipulation of fields.

It is however possible to use only particle descriptions. In [5, section 7], it is proposed to derive FDF models for LES applications from a Lagrangian description in terms of particles, by starting from the discrete Lagrangian Mass Density Function (LMDF). In the context of single-phase turbulent flows, this means that, if we consider the discrete LMDF (already introduced in Eq. (67)) corresponding to a fluid-particle description in terms of positions and velocities

$$\tilde{F}_f^L(t; \mathbf{y}_f, \mathbf{V}_f) = \sum_{n=1}^{N_f} m_f^{(n)} \delta(\mathbf{y}_f - \mathbf{x}_f^{(n)}(t)) \delta(\mathbf{V}_f - \mathbf{U}_f^{(n)}(t)), \quad (138)$$

with, for instance, an equal mass $m_f^{(n)} = \Delta m_f$ assigned to each fluid-particle (in incompressible flows), then the LMDF needed for RANS formulations and the Lagrangian Filtered Density Function (LFDF) needed for LES are retrieved by applying the different ‘statistical operators’, $\langle \cdot \rangle$ and $\langle \cdot \rangle_{ls}$ respectively. This general approach based on the discrete LMDF as the source function is represented in Fig. 33.

As indicated on the rhs of Fig. 33, this methodology retrieves the formulation of SPH (which is, at the moment, a particle-based LES without sub-kernel fluctuations) in terms of a particle system where the particles located within the smoothing kernel range interact directly (see the developments first proposed in [115]). Leaving aside the technical details of the formalism (see [5]), the important element is that an elementary Lagrangian formulation is shown to underlie all the previous mesoscopic models. A further interest is that this approach corresponds, in an asymptotic case, to the SPH formulation without SGS or, to use a more appropriate terminology, sub-kernel fluctuations (see [115]). For our present purpose, these ideas suggest that full-particle approaches open new connections between different methods. Therefore, a picture of the different roads leading from the microscopic to macroscopic levels of description in single-phase turbulence is now proposed.

6.6. Summary and classification

The various methods developed for single-phase turbulent flows are organized in Fig. 34 with a presentation that is similar to the one in Fig. 26. There are however significant differences. In the present case, the microscopic level is made up by the Navier-Stokes equations (that is, by the hydrodynamical description forming the macroscopic level in Fig. 26) while the macroscopic level refers now to the RANS description. This means that both the starting and end points of the modeling road are descriptions in terms of fields.

Not surprisingly, the traditional approach to single-phase turbulence modeling has relied on field-based methods, as represented by the column labeled ‘field-based’ in Fig. 34. Since these methods correspond to grid-based simulations, a reference mesh length Δ is used to indicate the resolution and to emphasize that these methods adopt a spatial point of view translated, for example, in the spatial filtering operation in the LES approach. These approaches follow the direct modeling road represented in Fig. 17: a set of field equations is first derived from the application of a statistical operator (probabilistic

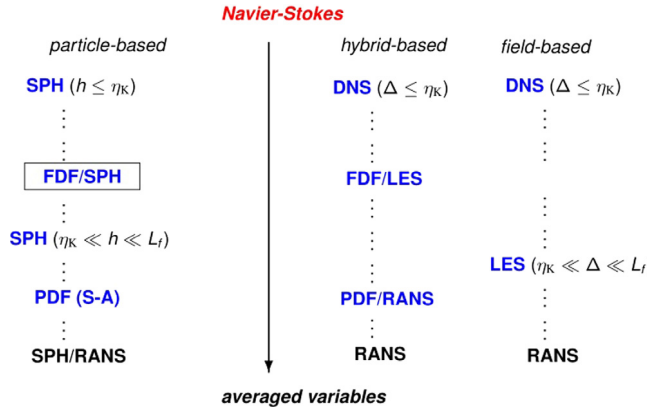


Fig. 34. Organization of the different methods from the hydrodynamical level of description represented by the instantaneous Navier–Stokes equations to the averaged ones represented by the Reynolds ones (RANS). As in Fig. 26, the downward arrow indicates a reduction in the information content.

mean, spatial averaging, etc.); the reduced set of equations contains open terms arising from convection not being treated accurately in Eulerian descriptions that go with field-based methods; then, ‘closure assumptions’ are applied to obtain a closed set of equations. It can be noted that the last step involves typically gradient-diffusion hypothesis, whose ubiquity justifies the analysis proposed in Section 10.4.

In the present case, the new message is expressed by the existence of the two columns labeled ‘particle-based’ and ‘hybrid-based’ in Fig. 34, which manifest that descriptions in terms of particles are still relevant. The role of particles and fields is however less clear-cut than in classical statistical physics (see Section 5) where these notions are distinct, with particles being a fundamental level of description and fields their mean properties observed at a much-larger-grained resolution. In the present situation, referring to ‘fluid particles’ at a hydrodynamical level is more surprising at first sight and, in the PDF and FDF methods described in the Section 6.5, these particles are usually introduced as notional particles or samples of the simulated PDF. As explained in Section 6.5.1, particles interact only through the mean fields that they create and there is no instantaneous or SGS fields in the PDF or FDF methods respectively. This constitutes the hybrid-based formulations indicated in the middle column in Fig. 34 where the particle point of view appears at an intermediate level between the DNS and RANS ones that are still regarded as field descriptions. Note that this corresponds to the indirect modeling road in Fig. 17: a probabilistic description is first established, for example of the instantaneous velocity field; a (Lagrangian) Monte Carlo model is developed for this PDF, or FDF, equation in terms of stochastic or notional particles; a closed set of mean field equations is derived from this description.

It is also possible to regard the stochastic particles in the PDF method as mimicking the dynamics of real fluid particles. This is indicated as PDF (S-A) (for Stand-Alone) in the left column, although there is no real difference in the information content between the PDF/RANS method in the hybrid-based column and the PDF (S-A) one in the particle-based column. It gives a first hint of the possibility to use a full particle-based description right from the (microscopic) outset. Following the remark made at the end of Section 6.5.3, this corresponds, for example, to the SPH approach described in Section 5.5 in which a field description is translated into a large number of interacting fluid particles. Since this method relies on smoothing kernels to calculate gradients (and, thus, to capture length information), the size of the kernel h is indicated to express the resolution of these particle-based simulations. With present formulations, a SPH simulation with a smoothing length lying in the turbulent inertial zone ($\eta_K \ll h \ll L_f$) corresponds to a particle-based LES, albeit one with no sub-kernel model. In Fig. 34, these SPH/LES and the PDF (S-A) methods are put at different vertical levels. This should not be interpreted as stating a hierarchy between the two formulations since the information content is of a different nature: in the SPH/LES model, one calculates the direct but smoothed N -particle interactions yielding a (large-scale) velocity field, while there is no instantaneous field in the PDF formulation but with a probabilistic description of (one-point) velocities. This may explain that there is, at present, a gap in this particle-based column represented by the boxed method called FDF/SPH, indicating that such a formulation has not yet been built. In spite of this missing link, the hybrid- and particle-based columns in Fig. 34 bring out the interplay between particle and field descriptions and show that approaches in terms of particle systems present great practical interest.

6.7. Similarities and differences with classical statistical physics

The organizations in Sections 5.7 and 6.6 bring out similarities and differences between the methods used in classical statistical physics (‘below the hydrodynamical level’) and in single-phase turbulence modeling (‘above the hydrodynamical level’). If we consider the formulations that are continued and those with a broken link, additional remarks can be made.

First, by looking at the form of the basic equations of DPD and SDPD (cf. Eqs. (81) and Eqs. (93), respectively), and of the PDF method (cf. Eqs. (126)), it is clear that there is a continuity between these particle-based formulations. They are based

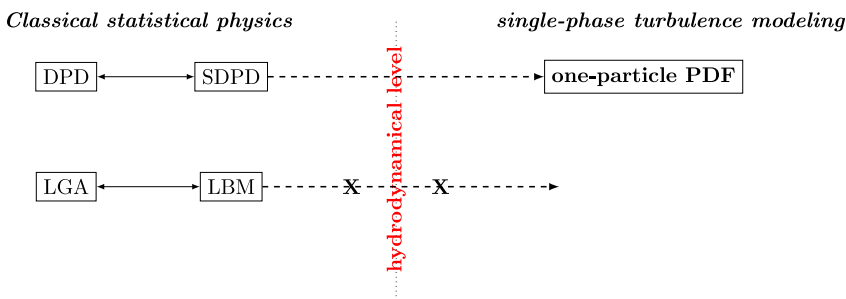


Fig. 35. Continuing or broken links between formulations developed in classical statistical physics and in single-phase turbulence modeling. The hydrodynamical level of description marks a limit and the horizontal crossed or uncrossed dashed lines across that limit indicate whether there is a successor method or not.

on the same particle variables (\mathbf{x}, \mathbf{U}) and with similar models based on a decomposition into conservative (or pressure-like), dissipative and random forces. DPD and SDPD are N -particle PDF method (with a noise due to molecular effects) while PDF methods are in fact one-particle PDF models (with a noise due to turbulent fluctuations). In spite of this difference, it is seen that PDF models are the successors of DPD and SDPD in single-phase turbulence modeling.

On the other hand, it is seen that there is no equivalent of LBM in single-phase turbulence modeling. LBM can, of course, be used as a Navier–Stokes solver and, in that sense, as a tool for DNS approaches but there is no equivalent formulation of the basic LBM ideas for mean and fluctuating velocity variables in turbulence (above the continuum level). This can be traced back to the lack of scale separation in turbulence and to the fact that there is no equilibrium distribution (there is also nothing like the equipartition of energy in turbulence). If one-point velocity PDFs are well approximated by Gaussian ones in homogeneous situations, they deviate from Gaussianity in non-homogeneous ones in a non-universal way (see [15,30]). Thus, relaxation ideas such as in the classical BGK model for LBM cannot be carried to the world of turbulence modeling. These continuing or broken relations are represented in Fig. 35.

A further remark is that, in Fig. 34, Lagrangian PDF (and FDF) models correspond to the separation between bottom-up and top-down formulations. There are indeed two ways to look at such stochastic particle systems:

- (i) The first one consists in proposing a given stochastic model and in regarding this model as validated when the ‘correct RSM’ is retrieved. This corresponds to the top-down view and is the one adopted in Pope’s work (see [30,67,116]). Note that this approach is similar to what is done in the LBM, SDPD, SRD approaches which are often calibrated so as to retrieve transport coefficients pertaining to the hydrodynamical description, such as the Nusselt or Schmidt numbers (see Section 5.7);
- (ii) The second view is to build PDF models from ‘first principles’ by using arguments carried from statistical physics. Few works have been developed along that bottom-up road (see earlier attempts in [117,118]), although it was shown in [119] that present Langevin models can be derived from the application of Onsager’s hypothesis. Note that this view is similar to the first attempts in classical statistical physics (LGA, DPD).

These remarks indicate that, as we move into ‘turbulence modeling’ and what are apparently ‘mere engineering concerns’, rooting new models into a solid theoretical ground can become necessary. This becomes even more the case when discrete particles are added.

7. Review of present disperse two-phase flow statistical models

The overviews in Sections 5 and 6 have revealed that a wide range of methods exist to describe single-phase turbulent flows, from the molecular details of MD to a small set of statistical constitutive relations for averaged flow-properties in RANS models. When particles are added in a flow, this first series of approaches is compounded by a second one related to how we choose to describe particles and their interactions with the carrier fluid phase. To find one’s way in this new domain, two standpoints or guiding assessments are helpful:

- (a) The first one corresponds to the particle size and inertia: for example, small particles such as colloids are sensitive to molecular fluctuations (see the discussions in Section 2.3.2) and it makes sense to retain a finer-than-the-hydrodynamical-level of description (cf. the methods described in Section 5). This is particularly relevant for nanoparticles for which molecular details are important while for colloids in the micro-range a coarser approach based on a hydrodynamical description of the flow and a random-walk model for Brownian effects can be sufficient (this is the formulation in Section 2.3). Along the same line, larger-sized particles, or having an inertia much higher than the fluid, are not dependent on the characteristics of the fluctuations in a turbulent flow and require only some statistical estimations such as time and length scales;

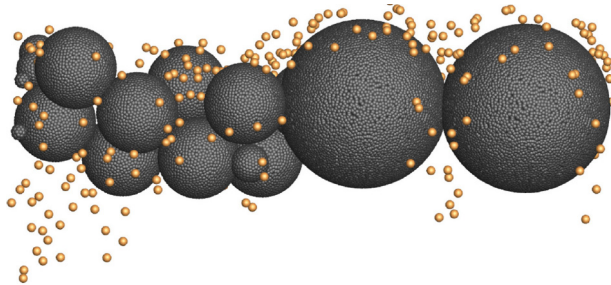


Fig. 36. A particle–particle DPD formulation for colloids in a fluid where discrete particles, or colloids, are immersed in a sea of fluid particles. The small yellow particles represent fluid particles while colloids are represented by the large brown particles.

Source: Reprinted from [120] with permission from Elsevier.

- (b) The second guideline is related to the information content that is sought, for example whether we want to obtain the drag force coefficient as a result or the long-time particle dispersion rate for a given drag force. This was already hinted to in Section 2.4 but we can now address that question in more details.

The main purpose of this section is to introduce the characteristic features of one-particle PDF models that are analyzed in depth in Sections 9 and 10. This is done in Section 7.3. However, to bring out the thread of continuity as well as the differences with the previously-described methods, it is useful to discuss how disperse two-phase flows are modeled in classical statistical physics (in that case, this correspond to colloidal suspensions, as explained above). This is presented in Sections 7.1 and 7.2 where, following the patterns used in Sections 5 and 6, a distinction with respect to the hydrodynamical level of description is made. At this point, a more precise terminology is needed. Indeed, all the methods considered in Section 6 can be regarded as hydrodynamical ones and this single reference is not sufficiently anymore. In the following, we therefore refer to the level of description where all the hydrodynamical degrees of freedom are fully resolved (FR) as the FR-hydrodynamical level.

In that sense, Section 7.1 presents formulations where the carrier fluid flow is simulated with the methods introduced in Section 5 (apart from SPH which, for small enough smoothing kernel lengths, belong to the class of methods at the FR-hydrodynamical level). Then, particle simulations based on fully-resolved flows are outlined in Section 7.2. Drawing on these notions, the reasons behind the development of one-particle PDF models, and their characteristic features are addressed in Section 7.3.

7.1. Models below the FR-hydrodynamical level of description

7.1.1. Particle-based methods

One of the strong points of particle-based methods for fluid flow modeling below the FR-hydrodynamical level is that colloids, polymers or other immersed bodies can be included in the description in a straightforward manner. Indeed, discrete particles (which refer to colloids, polymers, etc.) appear as one particle, or a set of bounded sub-particles, in a stream of fluid (or solvent) particles and fluid–particle, as well as particle–particle, interactions are easily included in the particle scheme developed for the fluid, for example by considering different potentials for fluid–fluid, fluid–particle and particle–particle forces.

The basic principle consists in a Lagrange/Lagrange (or particle/particle) formulation for disperse two-phase flows which, apart from its open framework, allows to obtain a strong coupling between the fluid and the particle phases. It is illustrated in Fig. 36 which shows a number of ‘large-scale particles’ surrounded by a stream of fluid particles represented here by DPD particles (this result is taken from the study in [120] of colloid capture in porous media where there are three types of particles: fluid, colloids and collectors. The particles plotted in this figure are actually colloids and collectors but they can be used to illustrate the notion of a mixture of different particles to represent disperse two-phase flows). Given that both the fluid and the discrete particles are described here in terms of interacting ‘particles’, we refer in the rest of this sub-section to discrete particles immersed in a flow as ‘colloids’ in order to avoid confusion between the fluid particles used in the formulations (as ‘discretized elements’) and the discrete, or physical, particles.

Depending on the details of each method for the fluid, there are various ways with which the fluid–colloid interactions are accounted for and we refer to the burgeoning literature on each formulation for specific discussions (see [72,77,120–126] for DPD, [81–83] for SRD and [99,127,128] for SDPD).

In the particle-based methods to represent a fluid in classical statistical physics (below the FR-hydrodynamical level), various coarse-grained models are used and, similarly, different descriptions have been proposed for discrete particles. In a MD formulation for both phases, each colloid is decomposed into its molecular elements (*i.e.* its atoms or molecules) to form a mixture of interacting particles. This was represented in Fig. 12(b) and the MD formulation in Section 5.1 is readily extended by considering three potentials: ϕ_{ij}^{F-F} , ϕ_{ij}^{F-C} and ϕ_{ij}^{C-C} for the forces between fluid–fluid (F–F), fluid–colloid or

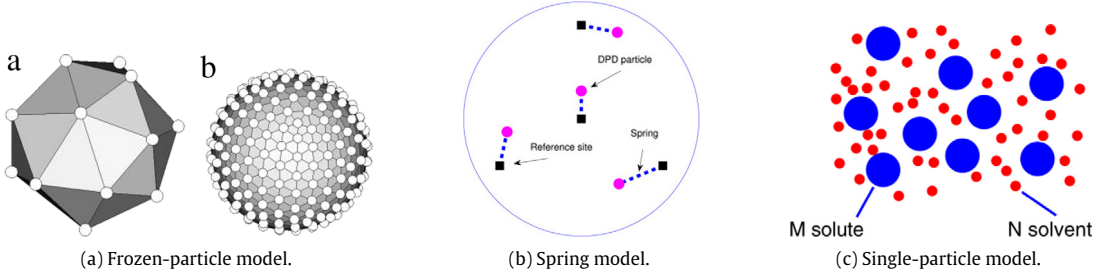


Fig. 37. Different descriptions of a spherical colloid represented as: (a) a collection of bounded fluid particles in the frozen-particle model (reprinted from [122] with permission from AIP); (b) as a set of particles attached through a spring to reference sites subject to solid-body motion in the spring model (reprinted from [126] with permission from Elsevier); (c) as a single discrete (or solute) particle with a different size and inertia from the fluid (or solvent) particles in the single-particle model.

fluid/discrete-particle (F-C) and colloid-colloid (C-C) molecules, respectively. At one degree or another, this idea is retained in the various coarse-grained formulations (either bottom-up or top-down).

Regardless of how the different forces are implemented in each formulation, it is interesting to consider the evolution in the way in which colloids are represented. In the first attempts (see [73]), a colloid was described as a set of bounded fluid particles subject to a solid-body motion only. This is called the frozen-particle model, represented in Fig. 37(a) where a number of fluid particles are linked to form a discrete one, in that case a spherical colloid. These ‘colloidal sub-particles’ take part in the same interaction scheme as the fluid particles but are moved with a solid body motion derived from the sum of the forces on the colloids. This approach has been used in several studies in DPD, SRD or SDPD [122,127,129]. It can be noted that the colloidal sub-particles are treated as fluid particles and follow the same interaction scheme, which means that we are essentially considering neutrally buoyant or low-inertia colloids. Furthermore, it is also clear from Fig. 37(a) that many (fluid) particles are needed to describe a single discrete or colloid one (typically a few hundreds). On the other hand, this approach can be applied for any shape of the immersed body and the tangential forces and resulting rotational motion are captured as a result of the formulation.

Yet, freezing the internal degrees of freedom of the fluid particles making up a colloid by imposing the solid-body motion leads to a loss of thermal energy. In a recent model, it is proposed to retain the idea of using fluid particles to describe each colloid but these fluid particles are attached to reference sites through a spring and can fluctuate while being linked to the colloid. Basically, the first idea of the frozen-particle model is kept but is applied to a few reference sites, or ‘constituent particles’, around which the elementary particles that define a single colloid oscillate. This is represented in Fig. 37(b) and details on this ‘spring model’, which allows internal energy to be maintained, can be found in [126].

A noteworthy evolution of the description of colloids (or discrete particles) that brings us closer to what is currently being done at the FR-hydrodynamical level and above is the single-particle model, represented in Fig. 37(c). Instead of using a collection of fluid particles to define one colloid, each colloid is treated as a single discrete particle having therefore a different size and different properties. This evolution is sketched in Fig. 38.

The interesting aspect of this recent formulation is that, within the general framework of a particle/particle approach to describe the fluid+particle (colloid) system, different dynamical formulations can be implemented for the fluid and the particle phases. This has been essentially developed for the DPD approach (see [120,121,124,125]). Using the presentation given in Section 5.2, this means that the soft repulsive potential with its linear profile for the conservative force (see Eq. (82)) is kept for the fluid-fluid interactions while an exponential force is used to describe the fluid-colloid and colloid-colloid forces (see details in [120,125])

$$\mathbf{F}_{C,F-C}^{[ij]} = \begin{cases} \frac{a_{FC}^{[ij]}}{1 - e^{-b_{FC}^{[ij]}}} \left(e^{-b_{FC}^{[ij]} r^{[ij]}/r_c} - e^{-b_{FC}^{[ij]}} \right) e^{[ij]} & \text{if } r^{[ij]} \leq r_c, \\ 0 & \text{if } r^{[ij]} \geq r_c, \end{cases} \quad (139)$$

where $a_{FC}^{[ij]}$ and $b_{FC}^{[ij]}$ are parameters that determine the fluid-colloid conservative force [120]. Another important element is that shear forces along the colloid surface are no longer captured as in the frozen-particle model. The basic DPD equations are then extended to include shear forces, as illustrated in Fig. 39, by keeping track of the angular momentum of each particle $\mathcal{Q}^{[i]}$, which means that Eqs. (80) are superseded by the following description

$$\frac{d\mathbf{x}^{[i]}}{dt} = \mathbf{U}^{[i]}, \quad (140a)$$

$$m^{[i]} \frac{d\mathbf{U}^{[i]}}{dt} = \sum_{j=1,N} \left(\mathbf{F}_C^{[j] \rightarrow [i]} + \mathbf{F}_D^{[j] \rightarrow [i]} + \mathbf{F}_{Rot}^{[j] \rightarrow [i]} + \mathbf{F}_R^{[j] \rightarrow [i]} \right), \quad (140b)$$

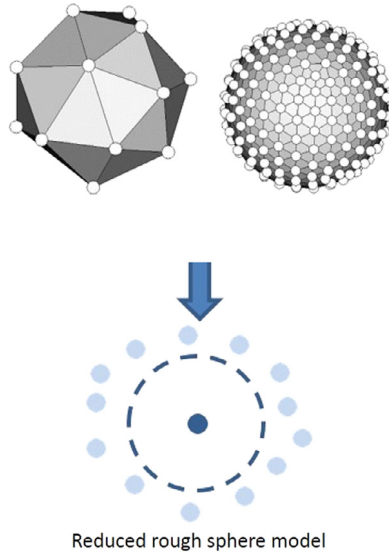


Fig. 38. Evolution of discrete particle representation in particle-based methods below the FR-hydrodynamical level. The collection of the large number of fluid particles making up a discrete colloid in the frozen-particle model is reduced to a single-particle description, also called a ‘rough sphere model’, to which a size corresponding to the excluded volume or the Einstein diffusion coefficient can be assigned.

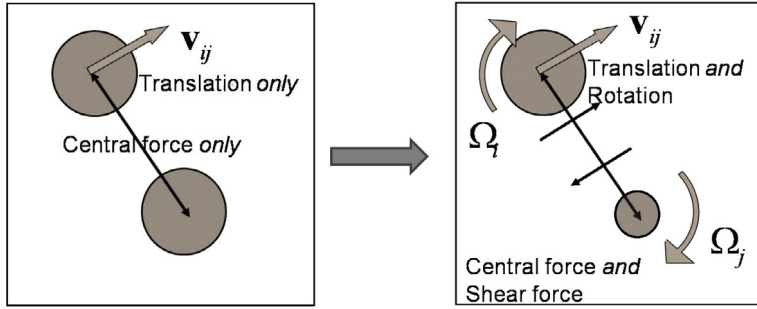


Fig. 39. Extension of the classical DPD formulation to account for shear forces and rotational motion and represent discrete particle motion with the single-particle model.

Source: Reprinted from [130] with permission from IOP Publishing.

$$I^{[i]} \frac{d\Omega^{[i]}}{dt} = \sum_{\substack{j=1,N \\ j \neq i}} \lambda_{ij} \mathbf{x}^{[ij]} \times \mathbf{F}^{[j \rightarrow i]}, \quad (140c)$$

where $I^{[i]}$ is the moment of inertia of the particle labeled $[i]$. In Eq. (140b), the translational dissipative force $\mathbf{F}_D^{[j \rightarrow i]}$ has also an extended expression compared to one given on the rhs of Eq. (81b) to account for central and shear components (see the sketch in Fig. 39), which is

$$\mathbf{F}_D^{[j \rightarrow i]} = -\gamma_{\parallel} \omega(\mathbf{x}^{[ij]})(\mathbf{e}^{[ij]} \cdot \mathbf{U}^{[ij]}) \mathbf{e}^{[ij]} - \gamma_{\perp} \omega(\mathbf{x}^{[ij]}) [\mathbf{U}^{[ij]} - (\mathbf{e}^{[ij]} \cdot \mathbf{U}^{[ij]}) \mathbf{e}^{[ij]}], \quad (141)$$

where γ_{\parallel} and γ_{\perp} are the central and shear friction coefficients respectively, while the rotational force is formulated as

$$\mathbf{F}_{Rot}^{[j \rightarrow i]} = -\gamma_{\perp} \omega(\mathbf{x}^{[ij]}) [\mathbf{x}^{[ij]} \times (\lambda_{ij} \Omega^{[i]} + \lambda_{ji} \Omega^{[j]})]. \quad (142)$$

In Eqs. (140c) and (142), λ_{ij} corresponds to a weight factor to account for the different nature of the particles (the fluid and the colloid particles) and is given by (see [121])

$$\lambda_{ij} = \frac{R^{[i]}}{R^{[i]} + R^{[j]}}, \quad (143)$$

where $R^{[i]}$ is the radius associated to the particle $[i]$. Finally, the random force $\mathbf{F}_R^{[j \rightarrow i]}$ in Eq. (140b) is closed by applying the fluctuation-dissipation relation. This gives a slightly more complicated formulation than in Eq. (81b), due to the introduction

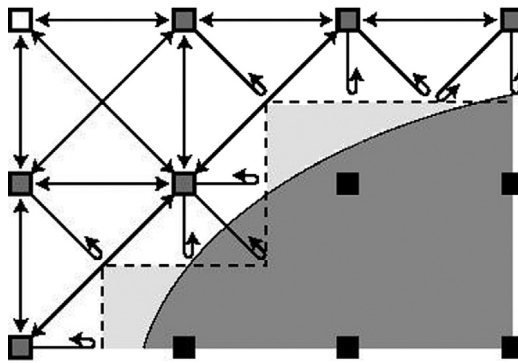


Fig. 40. Representation of a LBM scheme near a solid body surface: the nodes in the solid are shown as black squares and the nodes in the fluid acting as boundary nodes are shown in gray-filled squares.

Source: Reprinted from [134] with permission from Elsevier.

of the two friction coefficients γ_{\parallel} and γ_{\perp} instead of one for a purely central force, but the principle remains the same. The complete expression can be found in the above-mentioned works (for instance, see Eq. (10) in [120]). Through the expression of the moment of inertia ($I^{[i]} = 2m^{[i]}(R^{[i]})^2/5$) and the factor λ_{ij} , it is seen that this extended DPD formulation based on the single-particle approach uses explicitly the radius associated to each 'DPD particle', something that was not clear in the original formulation of the DPD model (see the discussions in [92,97,124]). As represented in Fig. 38, a typical DPD-particle size can be estimated to a formulation of the forces, especially the conservative one through the parameter $a_{FC}^{[i]}$ that governs the strength of the fluid-colloid force (see [120,121,124,125]).

Before turning to different formulations, a few remarks can be made:

- (i) The development of particle-based methods for fluid+colloid systems based on the single-particle model for the colloids means that these formulations are closer to the hydrodynamical description in that we explicit use a physical size attached to each colloid;
- (ii) The new formulations introduce also an explicit difference in the dynamical equations for the fluid and colloid particles, compared to the approach with the frozen-particle model where only type of evolution equations is used;
- (iii) The single-particle model means that the original description of each particle is augmented: instead of the elementary kinetic variables $(\mathbf{x}^{[i]}, \mathbf{U}^{[i]})$, the extended description is now in terms of the position, translational and rotational velocities $(\mathbf{x}^{[i]}, \mathbf{U}^{[i]}, \boldsymbol{\Omega}^{[i]})$ which are still kinetic-based variables;
- (iv) The description of discrete particles (here colloids) was mainly presented with respect to the DPD formulation but is also used in other formulations such as SRD. This gives rise to a number of hybrid models (e.g. SRD/MD or SRD/DPD, see [81, section 5]) but it can be noted that the description retained for the colloids is usually operating at a finer level of description than the one for the fluid particles.

7.1.2. Lattice-Boltzmann methods

In contrast to particle-based methods for the fluid below the FR-hydrodynamical level, developing LBM with discrete particles, such as colloids, polymers or more inertia solid particles, is much more difficult. This is essentially due to the grid-based formulation of the method which makes handling discrete particles trickier since we are in an Eulerian/Lagrangian formulation. Such an issue is common to most grid/particle discretization schemes and coupling the fluid to discrete particles in LBM formulations is not immediate.

A classical approach consists in defining (or mapping) the shape of the discrete particles in the mesh used for LBM and using the surface of the particle as a limiting surface where boundary conditions, i.e. collisions, are imposed for the fluid (see Fig. 40). This gives an exchange of momentum at each time step from which the forces and torques acting on the particle can be deduced (see [131,132], as well as accounts given in [133]). Another possibility that has gained interest is to adopt an hydrodynamical description for the immersed particles and use the equation of motion based on drag and random force, cf. Eqs. (21). Leaving out gravity which is an external force, the terms on the rhs of Eq. (21b) correspond to the total force that the fluid is exerting on the (spherical) particle. From the principle of action and reaction, the force acting on the fluid due to that particle is the same one with an opposite sign

$$\mathbf{F}^{P \rightarrow F} dt = - \left(\frac{\mathbf{U}_s(t) - \mathbf{U}_p(t)}{\tau_p} dt + K_{Br} d\mathbf{W}(t) \right) \quad (144)$$

with K_{Br} given by Eq. (22). This force can be introduced in the collision step of the LBM scheme (see [133,135]) to account for a large number of collisions on the particle surface and to obtain the resulting exchange of momentum.

It can be noted that using a hydrodynamical formulation of the forces on the particles, as in Eq. (144), means that the particle description is coarser than the fluid one, contrary to the situation with the particle-based methods in the preceding section. A grid/particle implementation implies also that the overall scheme is not convenient for moving and potentially deformable immersed objects. Furthermore, it was noted in Section 6.7 that present formulations of LBM do not make them directly transportable to model turbulence. This is even more the case for turbulent two-phase flows since, not only is there no universal equilibrium distribution to which to relax, but there is also no well-established set of averaged moment equations (similar to RANS models in single-phase turbulent flows) which can act as a guideline or even a safeguard. Clearly, it is difficult to apply the ideas of LBM in that context and, for these reasons (without overlooking their interest for situations requiring fluid simulations below the FR-hydrodynamical level), they are not considered in the rest of this article.

7.2. Models at the FR-hydrodynamical level of description

7.2.1. Brownian dynamics

Brownian Dynamics is a well-known method to simulate polymer dynamics and detailed presentations are available in classical textbooks [50,136–138] as well as in the publications describing its applications (see, for example, a recent work [139] and references therein).

As far as the description of the polymers is concerned (see Section 3.1.2), BD is a mesoscopic method but, with respect to the terminology introduced at the beginning of the present section, it is operating at the FR-hydrodynamical level. Indeed, it is developed with the premise that the fluid flow is fully characterized by the knowledge of the velocity field $\mathbf{U}_f(t, \mathbf{x})$. The basic (coarse-grained) bead–spring model for a polymer was already introduced in Section 3.1.2 (see Fig. 14) and we can give now the evolution equations.

Clearly, BD is a particle-based approach and the equations for a bead $[i]$ (with $i = 1, N_b$) belonging to a chain of N_b beads that makes up one polymer have the familiar form

$$\frac{d\mathbf{x}_{pol}^{[i]}}{dt} = \mathbf{U}_{pol}^{[i]}, \quad (145a)$$

$$m_{pol}^{[i]} \frac{d\mathbf{U}_{pol}^{[i]}}{dt} = \mathbf{F}_{pol,D}^{[i]} + \mathbf{F}_{pol,nH}^{[i]} + \mathbf{F}_{pol,R}^{[i]}, \quad (145b)$$

with $m_{pol}^{[i]}$, $\mathbf{x}_{pol}^{[i]}$ and $\mathbf{U}_{pol}^{[i]}$ the mass, position and velocity of the bead $[i]$ of a polymer, respectively, and where $\mathbf{F}_{pol,D}^{[i]}$ is the hydrodynamical drag force, $\mathbf{F}_{pol,nH}^{[i]}$ the sum of all the non-hydrodynamical forces and $\mathbf{F}_{pol,R}^{[i]}$ the random term due to molecular fluctuations. The force $\mathbf{F}_{pol,nH}^{[i]}$ includes the forces due to springs, excluded volume interactions, etc. Its expression is related to special models (such as the finitely extensible nonlinear elastic (FENE) model, the worm-like chain (WLC) model, etc.) used to capture specific effects of polymeric motion, but we refer to the available literature for details as these aspects are outside the scope of the present article.

A feature of BD that is of importance for our purpose is that bead inertia is considered to be very small. This means that Eq. (145b) is typically a stiff SDE and BD is, in fact, formulated in terms of the bead positions only. To work out the evolution equations in the limit of vanishing bead inertia, it is best to start with the case where the drag force on one bead is not influenced by other bead motions. In the BD literature, this is referred to as the ‘free-draining regime’ and, with the above assumptions, the evolution equations are

$$\frac{d\mathbf{x}_{pol}^{[i]}}{dt} = \mathbf{U}_{pol}^{[i]}, \quad (146a)$$

$$m_{pol}^{[i]} \frac{d\mathbf{U}_{pol}^{[i]}}{dt} = -\zeta \left(\mathbf{U}_{pol}^{[i]} - \mathbf{U}_f(t, \mathbf{x}^{[i]}) \right) + \mathbf{F}_{pol,nH}^{[i]} + \mathbf{F}_{pol,R}^{[i]}, \quad (146b)$$

where ζ is the friction coefficient (in the notations of Section 2.3.2, $\zeta = m_{pol}/\tau_p$ with τ_p the bead relaxation timescale which is taken as being the same for all the beads $[i]$). When $\zeta/m_{pol}^{[i]} \rightarrow +\infty$, $\mathbf{U}_{pol}^{[i]}$ becomes a rapidly-varying variable that can be eliminated. This leads to the equation for bead positions which, using proper notations for the resulting SDE, is

$$d\mathbf{x}_{pol}^{[i]} = \mathbf{U}_f(t, \mathbf{x}^{[i]}) dt + \frac{1}{\zeta} \mathbf{F}_{pol,nH}^{[i]} dt + \sqrt{\frac{2k_B\Theta_f}{\zeta}} d\mathbf{W}^{[i]}. \quad (147)$$

Note that this equation is a slightly extended version of the formulation already given in Section 2.3.2, cf. Eq. (23). In sample space, the corresponding description for the PDF $p_{pol}(t; \mathbf{y}^{[1]}, \dots, \mathbf{y}^{[i]}, \dots, \mathbf{y}^{[N_b]})$ is a Fokker–Planck equation whose form is

$$\frac{\partial p_{pol}}{\partial t} = - \sum_{i=1}^{N_b} \left[\frac{\partial}{\partial \mathbf{y}^{[i]}} \cdot \left\{ \left(\mathbf{U}_f(t, \mathbf{y}^{[i]}) + \frac{1}{\zeta} \mathbf{F}_{pol,nH}^{[i]} \right) p_{pol} \right\} + \frac{k_B\Theta_f}{\zeta} \frac{\partial^2 p_{pol}}{\partial \mathbf{y}^{[i]} \partial \mathbf{y}^{[i]}} \right]. \quad (148)$$

However, an important aspect of polymer dynamics is that the motion of other beads has an influence on the hydrodynamical drag force exerted on the bead $[i]$. This is a solvent-mediated force between beads that is referred to as

hydrodynamical interactions (HI). When HI are taken into account, the drag force in Eq. (146b) has a tensorial expression

$$\frac{dx_{pol}^{[i]}}{dt} = \mathbf{U}_{pol}^{[i]}, \quad (149a)$$

$$m_{pol}^{[i]} d\mathbf{U}_{pol}^{[i]} = - \sum_{j=1}^{N_b} \zeta^{[ij]} \left(\mathbf{U}_{pol}^{[j]} - \mathbf{U}_f(t, \mathbf{x}^{[j]}) \right) dt + \mathbf{F}_{pol,nH}^{[i]} dt + \sqrt{2} \sum_{j=1}^{N_b} \sigma^{[ij]} d\mathbf{W}^{[j]}, \quad (149b)$$

where we have used directly a proper notation in terms of SDE (this is the classical Ermak–McCammon model [140]) in which the diffusion matrix $\sigma^{[ij]}$ is, as usual, obtained from the application of the fluctuation–dissipation theorem which gives that $\sigma\sigma^\perp = (k_B\Theta_f)\zeta$. Then, by defining the matrix $D^{[ij]}$ by $\mathbf{D} = (k_B\Theta_f)\zeta^{-1}$, the limit diffusion model for the bead position is [50,136,137]

$$d\mathbf{x}_{pol}^{[i]} = \mathbf{U}_f(t, \mathbf{x}^{[i]}) dt + \sum_{j=1}^{N_b} \frac{\partial D^{[ij]}}{\partial \mathbf{x}^{[j]}} dt + \sum_{j=1}^{N_b} \frac{1}{k_B\Theta_f} D^{[ij]} \cdot \mathbf{F}_{pol,nH}^{[j]} dt + \sqrt{2} \sum_{j=1}^{N_b} \alpha^{[ij]} d\mathbf{W}^{[j]}, \quad (150)$$

where it is straightforward to show that the diffusion matrix α is such that $\alpha\alpha^\perp = \mathbf{D}$. The matrix $D^{[ij]}$ is called the mobility matrix since it expresses the influence of bead [j] on bead [i]. In the free-draining approximation, it is simply given by $D^{[ij]} = (k_B\Theta_f/\zeta)\delta^{[ij]}\delta$ where $\delta^{[ij]}$ and δ are the Kronecker symbols referring to the bead indexes and the three-dimensional coordinates, respectively. To account for HI, this mobility tensor is extended and written as

$$D^{[ij]} = \frac{k_B\Theta_f}{\zeta} (\delta^{[ij]}\delta + \zeta \mathbf{M}^{[ij]}(\mathbf{x}^{[j]} - \mathbf{x}^{[i]})) \quad (151)$$

where $\mathbf{M}^{[ij]}(\mathbf{x})$ is the Green function of the time-independent linearized Navier–Stokes equations, with $\mathbf{M}^{[ij]}(\mathbf{0}) = 0$. This part of the mobility tensor can be taken as the Oseen–Burgers tensor but, to account for the finite size of the beads and for excluded-volume interactions, it is often preferred to use the Rotne–Prager–Yamakawa tensor or some variant of it (see, for instance, detailed explanations in [50, chapter 4.2.1]). The form of this tensor is not within the scope of the present discussion and we refer to the available literature on this question. In sample space, the corresponding PDF equation is, of course, a Fokker–Planck equation which is easily derived from Eq. (150) (see [50]) and is not repeated here.

From the above description, a few characteristic points of BD can be noted:

- (i) Contrary to the methods below the FR-hydrodynamical level, HI are not captured by BD and must be input through the selection of the mobility tensor \mathbf{D} and, especially, with a non-zero choice of the tensor \mathbf{M} in Eq. (151);
- (ii) The resulting model is a stochastic diffusion model but, in the present situation, one ‘stochastic particle’ (or sample of the PDF) corresponds to one polymer, that is to one set of N_b sample positions. In the notations used in the preceding sections, this means that we have $\mathbf{x}_p = (\mathbf{x}_{pol}^{[1]}, \dots, \mathbf{x}_{pol}^{[N_b]})$. Correspondingly, the PDF equation is an equation in a high dimensional space (its dimension is $3N_b$) making direct (or strong) numerical solutions of the Fokker–Planck intractable as soon as $N_b \geq 3$. In that case, the formulation in terms of SDEs gives access, through dynamical Monte-Carlo methods, to a weak solution of the PDF equation;
- (iii) BD corresponds to an asymmetrical description of the fluid+polymer system since the fluid is given as a known field (an Eulerian vision) while the polymers are tracked in a Lagrangian standpoint;
- (iv) Each polymer is described with kinetic variables but, in contrast to all the previous methods which were based on $\mathbf{Z}_{pol} = (\mathbf{x}_{pol}^{[i]}, \mathbf{U}_{pol}^{[i]})_{i=1,N_b}$, we are using a reduced kinetic description in terms of positions only $\mathbf{Z}_{pol} = (\mathbf{x}_{pol}^{[i]})_{i=1,N_b}$;
- (v) The stochastic diffusion model for the bead positions in Eq. (150) is obtained from the elimination of the bead velocities. This is a foretaste of the fast-variable elimination technique that is presented and studied in detail in Section 9.3 and, in particular, in Section 9.3.4 where its application to colloids and polymers resurface.

The last three points, (iii)–(v), have a direct correspondence to some aspects of disperse two-phase turbulent flows, although it will be seen that the absence of an equipartition energy and the related fluctuation–dissipation principle call for deeper investigations.

7.2.2. Direct numerical simulations

For larger-sized particles (that is above the colloidal limit), molecular fluctuations become negligible and we enter the world of deterministic particle methods, as long as the fluid velocity field is fully resolved. At this FR-hydrodynamical level, there are basically two families of approaches which can be introduced by considering the particle equations of motion given in Eqs. (3). Depending on the volume fraction occupied by particles, the fluid–particle or particle–particle interactions can be dominant. This has led to two formulations where the emphasis is put on either of these interactions.

Distinct element methods and granular flows. When the particle volume fraction is high-enough (this remains here a loosely-defined and qualitative limit), particle–particle interactions can be considered as dominant. Between macroscopic bodies (we are above the colloidal limit), this includes van der Waals forces (see [20]) at contact and intricate adhesion forces if particles are deformable. In this ‘collisional regime’, the discrete-element method (DEM) has been developed recently (see [141–143]) to simulate N -particle collisions or close-range interactions in a fluid flow.

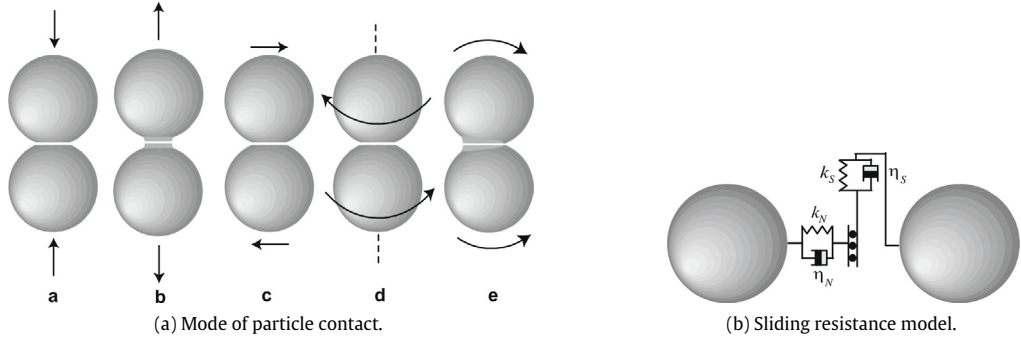


Fig. 41. Representation of particle-particle collisional effects in DEM: (a) different modes of interactions upon contact between two solid particles (normal compression (a), normal extension (b), sliding (c), twisting (d) and rolling (e)); (b) sketch of a spring-dashpot-slider model used to simulate the sliding of interaction.

Source: Reprinted from [142] with permission from Elsevier.

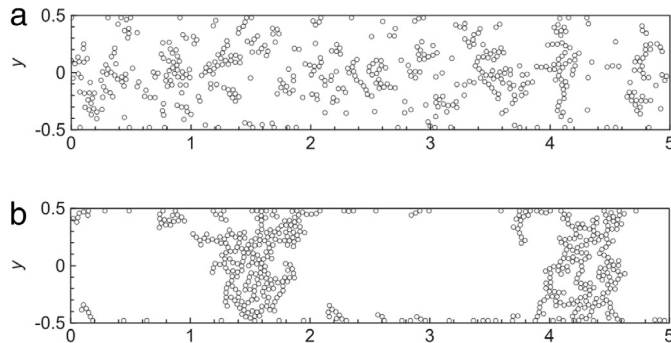


Fig. 42. Simulation of the formation of large-scale aggregates in a two-dimensional channel flow using DEM. Two different strengths of the van der Waals force between particles are used: for a low value, particles form relatively small-sized aggregates that concentrate mostly in the center of the channel (case a); while, for higher adhesive power, large-scale aggregates are formed across the channel height with complex inner structures and building intermittent porous sections in the flow (case d).

Source: Reprinted from [141] with permission from Elsevier.

In the DEM approach, particles are tracked simultaneously in a fluid flow with multiple time-step algorithms to detect collisions (see [142]) but the emphasis of the method is on the treatment of particle-particle collisions. For example, the result of each contact is simulated with a refined approach that considers explicitly the forces and torques due to normal relative motion between colliding particles but also sliding, twisting and rolling motion, as shown in Fig. 41(a). Each contact mode is modeled separately and, for example, sliding motion is represented by a spring-dashpot-slider model illustrated in Fig. 41(b) (see [142]). Note that this is valid only for solid particles and granular matter (obviously, a completely different physics is involved for droplets and bubbles, see the discussion at the end of Section 2.2). In between collisions, particles are tracked in a fluid flow calculated by solving the Navier-Stokes equations modified to account for the exchange of momentum between the fluid and the particles and the reduced volume fraction for the fluid (see discussions in [5]). At the FR-hydrodynamical level, this can, therefore, be regarded as an exact approach.

From this (brief) description of particle-particle interactions upon contact, it is clear that DEM is an attractive formulation with a view towards granular flows and can even be seen as a method pertaining to solid mechanics. In that sense, it is inclined towards contact mechanics, adhesion theory, particle deformation, material properties (particle roughness plays a role), etc. [141–143].

DEM is interesting to study aggregate formation and, for instance, the inner structure of multi-layer deposits (see the discussion on the interest of applying DEM to investigate multi-layer resuspension due to the impact of incoming particles on a previously-deposited layer of particles in [23, section 6.2.2.2]). One example is shown in Fig. 42 which reveals the formation of large-scale aggregates for different ratios of the particle adhesive force relative to their inertia in a channel flow (see [141]).

In the context of the present article, we can regard DEM as a counterpart of MD at the FR-hydrodynamical level, as far as particle-particle interactions are concerned. Indeed, in MD particle-particle (*i.e.* molecule-molecule) forces are described with elaborate potentials (for instance, the LJ potential) while in DEM detailed models are also applied for these particle-particle effects, such as the ones outlined above. However, simplified versions can be used by resorting to the hard-sphere

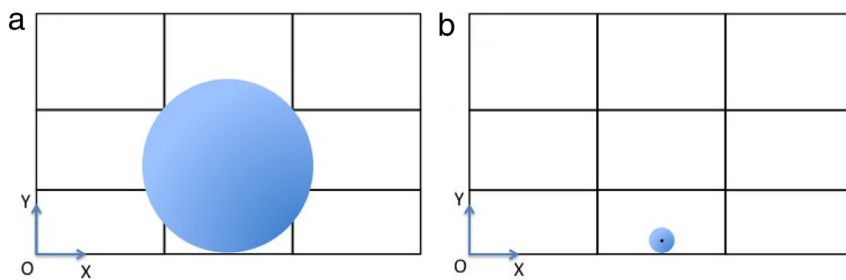


Fig. 43. Particle size with respect to a grid cell: (a) fully-resolved simulation; (b) point-particle simulation.
Source: Reprinted from [144] with permission from Springer.

model. In MD, this gives the free-flight and collision picture at the core of several methods below the FR-hydrodynamical level (see Section 5). Similarly, if we neglect deformation and treat particles as hard spheres, we find also a two-fold picture in terms of particle transport by fluid motions and (simple) elastic collisions.

Away from the world of collision-dominated effects, two caveats are in order. The detection of particle contact with classical algorithms can become difficult for particles that are just above the colloidal limit. This issue is taken up in Section 10.6. Second, for high Reynolds-number turbulent flows, the emphasis is shifted towards fluid-particle interactions (to the best of the author's knowledge, no DEM simulation has yet been performed for fully-developed turbulent flows). *DNS-turbulent flows and particle transport.* In the DNS approach to particle-laden turbulent flows, the emphasis is put on fluid-particle interactions and on particle transport by turbulent motions. There is, in fact, no intrinsic difference with DEM, as the two methods are meant as microscopic formulations at the FR-hydrodynamical level, but DNS approaches are clearly for turbulence-dominated aspects.

DNS formulations for disperse two-phase flows are the direct continuation of the ones mentioned in Section 6.2 for single-phase turbulent flows and, in effect, the same numerical methods are used for the calculation of the fluid phase. In most studies, a relatively dilute regime is considered, whereby the particle volume effect can be neglected (the volume fraction of the continuous phase remains approximately equal to one) but source terms representing momentum exchanges between the fluid and particles are added when the particle mass loading is not negligible.

Traditional approaches to the fluid flow calculation rely on a grid to discretize the Navier-Stokes equations (this corresponds to the field-based formulations discussed in Section 6.6 and in Fig. 34) and, when particles are added, we are dealing with an hybrid Eulerian/Lagrangian approach reflected in a grid/particle formulation. To properly capture the smallest scales of turbulence, the grid size and the time step must be of the order, or smaller, than the Kolmogorov ones (see Section 6.1), i.e. $\Delta \leq \eta_K$ and $\Delta t \leq \tau_K$, respectively. Depending on the diameter of the immersed particles and on the Reynolds number of the flow (since η_K diminishes as Re is increased), different spatial situations can be met (see Fig. 43):

- (a) in the first situation, the particle diameter is larger than the Kolmogorov length scale (taking $\Delta \simeq \eta_K$) and, in that case, the fluid flow is fully resolved around the surface of each particle. This corresponds to the situation where the fluid forces and torques can be deduced from the simulation by integrating fluid friction stresses along the particle surface, as mentioned in Section 2.4. Note also that a particle filters the spatial variations smaller than its diameter;
- (b) in many practical situations of interest, however, particles are smaller than the Kolmogorov scale. Indeed, in most laboratory, industrial or environmental flows, the Kolmogorov scale is in the range [50 μm, 1 mm] and particles or droplets having a diameter of less than, say, 30 μm are then much smaller (as already mentioned in Section 2.3.1). This is the second situation displayed in Fig. 43 which corresponds to the point-wise approximation for particles.

In the point-particle approximation, particles are subject to the whole range of eddies (or spatial variations) but, due to their inertia, temporal fluctuations can be filtered. This is assessed by introducing the Stokes number which is defined as the ratio of the particle relaxation timescale τ_p (see Section 2.3.1 and Eq. (12)) and the Kolmogorov timescale, $St = \tau_p/\eta_K$. An illustration is given in Fig. 44 which shows the energy spectrum of the fluid streamwise velocity component obtained from a DNS in a channel flow at a given location situated in the boundary layer near the wall and where the limit frequency, taken as being $1/St$, is plotted for different particle inertia (different values of τ_p). It is seen that particles with a higher inertia will be explicitly sensitive to a reduced part of the fluid kinetic energy spectrum (the fluctuations above their limit frequency), while time fluctuations well below this limit could be regarded as fast noises. Note however, that there is no well-marked separation and that frequencies over the whole range play different roles.

A noteworthy difference between present DNS methods for particle-laden flows and the DEM introduced previously is that only particle translational velocities are considered since no lift forces are usually considered for small particles. It is also worth underlying that, in spite of continuous effort, no clear and physically well-justified formulation of a general lift force has yet been proposed (see the discussion in Section 2.3 and in a recent account in [5, section 2.1]) which explains that lift forces are usually left out. In other words, DNS approach to disperse two-phase flows are based on Eqs. (3a)–(3b) only.

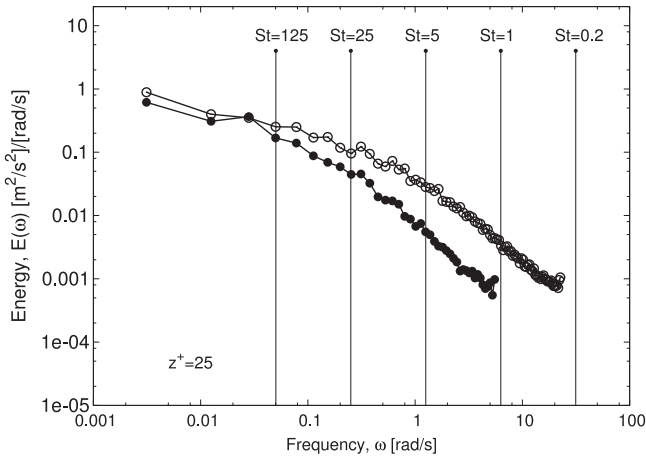


Fig. 44. Time-filtering effects of turbulent fluctuations due to particle inertia, as measured by the Stokes number based on the Kolmogorov timescale $St = \tau_p/\eta_K$. The energy spectrum of the streamwise velocity component of the fluid velocity at a distance $z^+ = 25$ from the wall (the distance is expressed in wall-units, see [30]) is obtained from a DNS in a turbulent channel flow for two Reynolds numbers based on the friction velocity, $Re_\tau = 150$ (\bullet) and $Re_\tau = 300$ (\circ). The particle-inertia filtering effect is represented by plotting the corresponding frequency $1/St$ for different values of the Stokes number (i.e. different values of τ_p).

Source: Reprinted from [144] with permission from Springer.

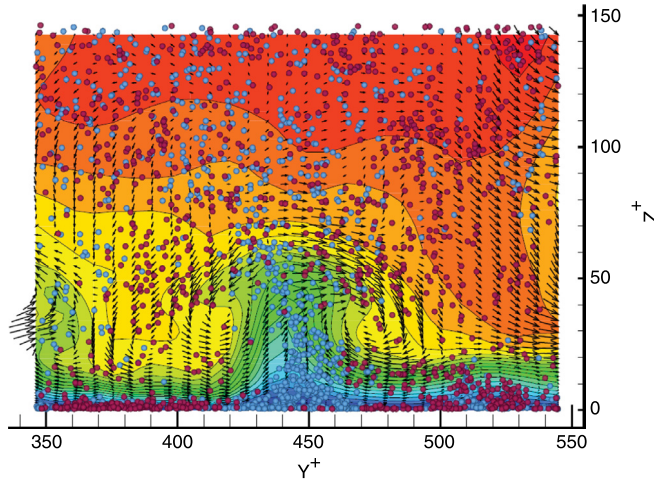


Fig. 45. A front view of particles and structures in the near-wall region of a turbulent channel flow laden with discrete particles. The vectors represent the fluid velocity and the color iso-contours map the values of the stream-wise velocity component.

Source: Reprinted from [147] with permission from Elsevier.

Once a picture is assumed with the selection of the forces acting on the particles, DNS for disperse two-phase are indeed exact formulations at the FR-hydrodynamical level or, to use the terminology introduced in Section 6.2, they embody the ‘conditional numerical truth’. They are invaluable tools to investigate the intricate physics of particle dynamics in turbulent flows. For example, they are useful to study phenomena such as preferential concentration effects and have played a fundamental role in revealing the importance of fluid coherent structures in particle transport in near-wall regions, as shown in Fig. 45 (on these aspects, see the relevant literature and, in particular, [145–147]).

7.2.3. SPH/discrete-particle simulations

In Section 7.1, we have seen that the methods operating below the FR-hydrodynamical level are typically Lagrangian-Lagrangian, or particle-particle, formulations. This corresponds to a consistent description of the two phases, which makes strong coupling between the fluid and the particles easier to handle. On the other hand, BD, DEM and DNS are hybrid methods, based on an Eulerian-Lagrangian standpoint translated into grid-particle formulations. This situation is not surprising since, as mentioned, the classical approaches for fluid flows at, or above, the FR-hydrodynamical level are field-based methods.

However, the analysis carried out in Section 6.6 has also pointed out that particle-based methods, such as SPH, present advantages. One such interest is to develop a consistent formulation of disperse two-phase flows at the FR-hydrodynamical

level since the disperse phase is naturally described in terms of particles. To the author's knowledge, no such particle-particle model has yet been applied at this FR-hydrodynamical level but, to illustrate this possibility and suggest new research directions, we propose the following approach.

Drawing on the particle-particle methods of Section 7.1 with the single-particle model for colloids, the basic principle is to consider a disperse two-phase flow as being a mixture of fluid and discrete particles, called F-particles and D-particles respectively. Then, a SPH description can be retained for the interactions between F-particles, as in Section 5.5, supplemented with the hydrodynamical description of particle motion, as in Section 2.3, in the particle pointwise approximation. It is possible to account for the forces due to the discrete particles on the fluid by adding them as source terms in the Navier-Stokes equations (as in the LBM approach in Section 7.1.2) and by treating them directly with the SPH formalism. To distinguish between different particles, we label the N_f F-particles with Latin indices (e.g. i and j) while Greek ones (e.g. α and β) are used for the N_p D-particles. With these notations, the proposed model for a Lagrangian-Lagrangian method for disperse two-phase flows at the FR-hydrodynamical level is expressed by the following equations

$$\frac{d\mathbf{x}_f^{[i]}}{dt} = \mathbf{U}_f^{[i]}, \quad (152a)$$

$$\begin{aligned} m_f^{[i]} \frac{d\mathbf{U}_f^{[i]}}{dt} = & - \sum_{j=1}^{N_f} \left(\frac{P_f^{[i]}}{(\vartheta^{[i]})^2} + \frac{P_f^{[j]}}{(\vartheta^{[j]})^2} \right) \nabla W^{[ij]}(h) \\ & + \rho_f v_f \sum_{j=1}^{N_f} \left(\frac{1}{(\vartheta^{[i]})^2} + \frac{1}{(\vartheta^{[j]})^2} \right) \frac{\mathbf{x}_f^{[ij]} \cdot \nabla W^{[ij]}(h)}{(r_f^{[ij]})^2} \mathbf{U}_f^{[ij]} \\ & - \sum_{\beta=1}^{N_p} \frac{m_p}{\tau_p} (\mathbf{U}_s^{[\beta]} - \mathbf{U}_p^{[\beta]}) W^{[i\beta]}(h), \end{aligned} \quad (152b)$$

$$\frac{d\mathbf{x}_p^{[\alpha]}}{dt} = \mathbf{U}_p^{[\alpha]}, \quad (152c)$$

$$\frac{d\mathbf{U}_p^{[\alpha]}}{dt} = \frac{1}{\tau_p} (\mathbf{U}_s^{[\alpha]} - \mathbf{U}_p^{[\alpha]}) + \sum_{\beta=1}^{N_p} \mathbf{F}_{p-p}^{[\beta \rightarrow \alpha]} W^{[\alpha\beta]}(h). \quad (152d)$$

In Eq. (152b) and (152d), the velocity of the fluid seen, $\mathbf{U}_s^{[\alpha]}(t)$, is directly obtained from the usual SPH formula (using only fluid particles), and is given by

$$\mathbf{U}_s^{[\alpha]}(t) = \mathbf{U}_f(t, \mathbf{x}_p^{[\alpha]}) = \sum_{j=1}^{N_f} \mathbf{U}_f^{[j]} W^{[\alpha j]}(h). \quad (153)$$

It is seen that this system is a closed model for the fluid and discrete-particle flow where the momentum equations for F- and D-particles are intrinsically different but are coupled through the velocity of the fluid seen. Only translational velocities and a drag force have been retained for the sake of simplicity but a force between discrete particles \mathbf{F}_{p-p} has been added on the rhs of Eq. (152d) to show how the fundamental fluid-fluid, fluid-particle and particle-particle interactions appear in this two-phase SPH formalism for disperse flows. It can be noted that, since F-particles are influenced by neighboring D-particles through the last term on the rhs of Eq. (152b), HI should be captured by the above formulation.

These principles are represented in Fig. 46 which shows that the approach is formulated in terms of two sets of interacting particles (the F-particles in orange and the D-particles in black in Fig. 46(a)) and that the basic scheme is to distinguish between the nature of particles to account for different forces acting on a fluid element (see Fig. 46(b)). It remains to be seen whether these ideas turn out to be fruitful suggestions.

7.3. Models above the FR-hydrodynamical level of description

Above the FR-hydrodynamical level, only limited information on fluid flows is accessible. This corresponds to the mesoscopic and macroscopic methods discussed in Section 6 for single-phase turbulence and used to simulate the carrier-phase flows in the present context of disperse two-phase flows when descriptions above the FR-hydrodynamical level are derived. As seen in Section 6, the macroscopic level corresponds to RANS descriptions, that is to a limited set of transport equations, typically for the first and second one-point moments. The corresponding mean-momentum equation for the particle phase has already been formulated in Section 3.2.2, cf. Eq. (29b), and the set of transport equations for the particle kinetic tensor (the particle equivalent of the Reynolds stress tensor for the fluid) is discussed later in Sections 10.3 and 10.4. The complete structure made up by the first and second-order velocity moments for the fluid and particle phases was studied in detail in previous works (see [154]) and, at this stage, the characterization of this macroscopic level of description of turbulent disperse two-phase flows is clear enough.

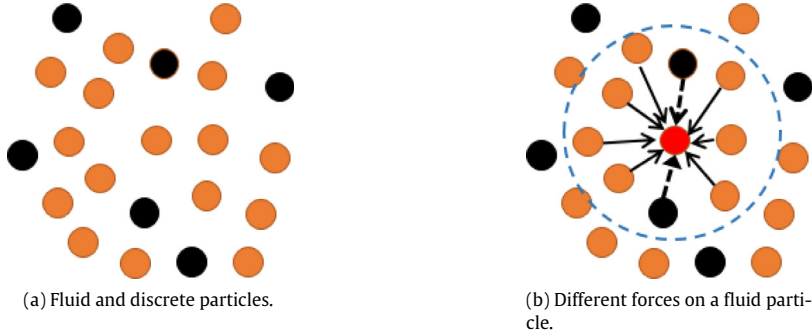


Fig. 46. A particle-particle approach to disperse two-phase flows based on the SPH formalism: (a) A two-phase flow is represented as a mixture of fluid (in orange) and discrete (in black) particles; (b) Sketch of the different forces on one fluid particle (in red) where the dashed-line circle represents the range of the smoothing kernel and the arrows indicate that different forces between F-F and F-D particles are implemented.

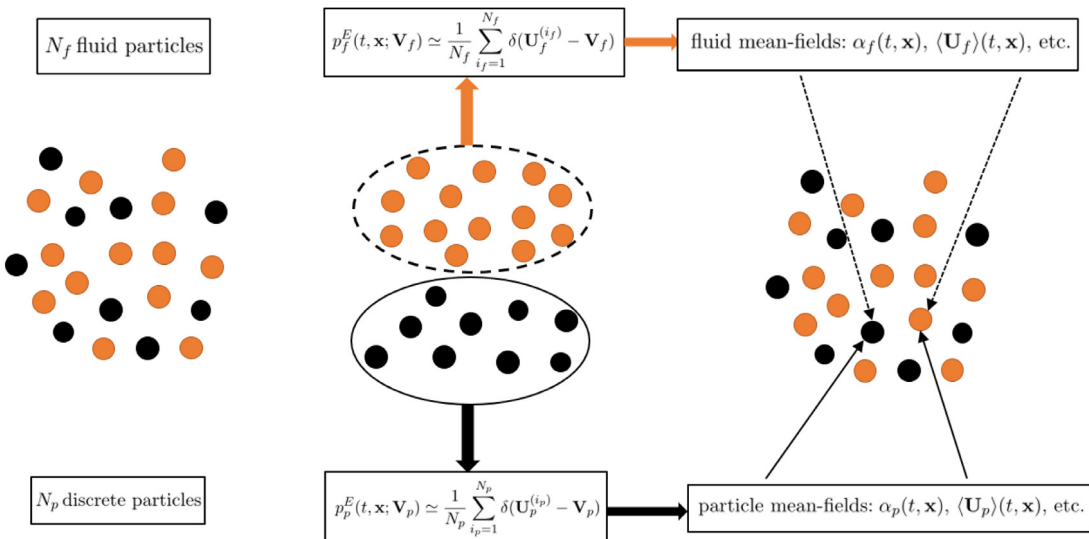


Fig. 47. Representation of mean-field interactions in one-point PDF formulations: N_f fluid and N_p discrete particles are present in a small volume where statistics are calculated. From the two sub-sets made up by the fluid and discrete particles, the two one-point PDFs are approximated and mean-field values are obtained by Monte Carlo estimations. Then, each fluid or discrete particle interacts with the mean fluid- and particle-field values created from the complete set.

For these reasons, we do not need to repeat the complete set of macroscopic equations with all their (intricate) details but we can refer to their structure and, especially, build on some remarks made in the preceding sections to explain the central role played by probabilistic approaches for polydisperse two-phase flow modeling:

1. From the analysis developed in Section 3.2.2, we know that direct closures at the macroscopic level are intractable and that mesoscopic methods are required;
2. Based on the study of the turbulent flow models in Section 6, we observe that these mesoscopic methods are typically probabilistic approaches and, for general inhomogeneous situations, correspond to the one-particle PDF models introduced in Section 6.5;
3. Consequently, it makes sense to consider similar one-particle PDF models for the treatment of the complete fluid and particle system. However, these one-particle PDF models (corresponding to one-point Eulerian PDFs) are basically mean-field approaches, as explained in Section 6.5.1. This means that the interaction scheme between fluid elements and discrete particles is not as in the SPH/discrete-particle model proposed in Section 7.2.3 and illustrated in Fig. 46. In the context of one-point PDF models for the fluid and particle system, the situation is depicted in Fig. 47, which shows that the fluid and discrete ‘notional particles’ interact only indirectly through the mean fields that they create (see discussions in [1, section 8]).

These arguments suggest that the relevant aspect to develop is a probabilistic description of discrete particles in turbulent flows and that, once established, this formulation can be coupled to the available mesoscopic or macroscopic approaches

for the carrier-phase turbulent flows. In the rest of this section, we therefore consider two formulations of one-particle PDF models for discrete particles in turbulent flows predicted with RANS methods.

So far, we have essentially referred to RANS descriptions of turbulent fluid flows. Yet, in Section 6.4, the mesoscopic LES method was introduced and this approach can also be selected for the simulation of the fluid phase. There are then two situations: first, if we disregard sub-grid fluctuations for high-inertia particles (see the sketch in Fig. 44), then LES results can be regarded as DNS ones and we are back into the world of deterministic particle methods as in Section 7.2.2. It was however demonstrated (see [148]) that this is a poor approximation and that subgrid fluctuations of the fluid velocity field need to be accounted for in the description of particle dynamics. Then, the formalism outlined in Section 6.5.3 indicates that ideas developed for RANS can be transported to LES formulations (this has been recently demonstrated by setting up a new probabilistic formalism, see [5, section 7]). We therefore refer essentially to the RANS context in the following, with the underlying understanding that formulations can be extended to include LES approaches.

7.3.1. The one-particle PDF modeling issue

To introduce one-particle PDF models for discrete particles (from now on, an index p is used to emphasize that we are describing discrete particles to be distinguished from fluid ones), it is useful to rewrite the governing equations, cf. Eq. (3a) and Eq. (11), under the slightly different form

$$\frac{d\mathbf{x}_p}{dt} = \mathbf{U}_p, \quad (154a)$$

$$\frac{d\mathbf{U}_p}{dt} = \frac{1}{\tau_p}(\mathbf{U}_s - \mathbf{U}_p) + \mathbf{F}_{ext}, \quad (154b)$$

where a drag force is retained to which a general force \mathbf{F}_{ext} , deriving for example from a potential, is added. Indeed, the form in Eq. (154b) is sufficient to bring out the closure issues and the answers brought by the kinetic and dynamic PDF approaches.

From the formalism recalled in Section 4.4, we know that the derivation of mean-field equations is built on the Lagrangian PDF which, for the kinetic variables $(\mathbf{x}_p, \mathbf{U}_p)$, is $p_p^L(t; \mathbf{y}_p, \mathbf{V}_p)$. The PDF equation satisfied by p_p^L can be derived from Eqs. (154) by manipulating the fine-grained PDF $\mathcal{P}(t; \mathbf{y}_p, \mathbf{V}_p) = \delta(\mathbf{x}_p(t) - \mathbf{y}_p)\delta(\mathbf{U}_p(t) - \mathbf{V}_p)$ since we have that $p(t; \mathbf{y}_p, \mathbf{V}_p) = \langle \mathcal{P}(t; \mathbf{y}_p, \mathbf{V}_p) \rangle$ (see the relations at the beginning of Section 4.5). Using standard techniques (see [1,30,31], the exact but unclosed PDF equation for p_p^L is

$$\frac{\partial p_p^L}{\partial t} + \frac{\partial [V_{p,i} p_p^L]}{\partial y_{p,i}} = -\frac{\partial [F_{ext,i} p_p^L]}{\partial V_{p,i}} + \frac{\partial}{\partial V_{p,i}} \left[\left\langle \frac{V_{p,i}}{\tau_p} | (\mathbf{y}_p, \mathbf{V}_p) \right\rangle p_p^L \right] - \frac{\partial}{\partial V_{p,i}} \left[\left\langle \frac{U_{s,i}}{\tau_p} | (\mathbf{y}_p, \mathbf{V}_p) \right\rangle p_p^L \right]. \quad (155)$$

At the level of a kinetic description, the last term which involves the conditional average value of \mathbf{U}_s/τ_p is unknown and needs to be closed. We are then exactly in the situation described in Section 3.2.2 and it can be noted that the modeling is due to the velocity of the fluid seen \mathbf{U}_s but also to the particle relaxation timescale since τ_p is a function of both \mathbf{U}_p and \mathbf{U}_s , $\tau_p = \mathcal{F}(\mathbf{U}_p, \mathbf{U}_s)$, as shown by the general expression in Eqs. (12) and (14).

Two different answers to this closure issue are brought by the kinetic and dynamic PDF models which are now presented.

7.3.2. The kinetic PDF model

In the kinetic PDF model, only particle position and velocity are retained in the description, which means that we are dealing with the stochastic process made up by $\mathbf{Z}_p = (\mathbf{x}_p, \mathbf{U}_p)$ whose corresponding PDF is $p_p^{L,r}(t; \mathbf{y}_p, \mathbf{V}_p)$. Due to this reduced set of variables (thus, the superscript r used for $p_p^{L,r}$), it can be noted that the complete expression of the particle relaxation time formulated in Eq. (12) cannot be handled since \mathbf{U}_s is external to the chosen description. In practice, one has to approximate τ_p by a constant, that is assume that particles remain in the Stokes regime so that $\tau_p \simeq \tau_p^{st}$ with the Stokes timescale expressed in Eq. (13). With this approximation, the unclosed kinetic PDF equation is written as

$$\begin{aligned} \frac{\partial p_p^{L,r}}{\partial t} + \frac{\partial [V_{p,i} p_p^{L,r}]}{\partial y_{p,i}} &= -\frac{\partial [F_{ext,i} p_p^{L,r}]}{\partial V_{p,i}} + \frac{\partial}{\partial V_{p,i}} \left[\frac{V_{p,i}}{\tau_p^{st}} p_p^{L,r} \right] \\ &\quad - \frac{\partial}{\partial V_{p,i}} \left[\frac{1}{\tau_p^{st}} \langle U_{f,i} \rangle p_p^{L,r} \right] - \frac{\partial}{\partial V_{p,i}} \left[\frac{1}{\tau_p^{st}} \langle u_{s,i} | (\mathbf{y}_p, \mathbf{V}_p) \rangle p_p^{L,r} \right] \end{aligned} \quad (156)$$

where the velocity of the fluid seen has been decomposed as $\mathbf{U}_s = \langle \mathbf{U}_f \rangle(t, \mathbf{x}_p(t)) + \mathbf{u}_s$ with $\mathbf{u}_s(t) = \mathbf{u}_{f,i}(t, \mathbf{x}_p(t))$. Following the remark made in Section 7.3.1 about the difference between the statistics of the fluid and of the fluid seen by discrete particles, it cannot be said that $\langle \mathbf{u}(t, \mathbf{x}_p(t)) \rangle = 0$ even for particles located at a given point, and the (usually) non-zero value of $\langle u_{s,i} \rangle$ is the drift velocity (see [4,5,52,149]).

The closed form of the kinetic PDF equation in sample space is obtained by resorting to the Furutsu–Novikov theorem (which is also called the Furutsu–Novikov–Donsker (FND) relation [39,150–152], a terminology that we retain in the following, see Section 9.1). The explicit derivation is detailed in [3] (see in particular the appendix in [3]). It has been recently

revisited in a detailed study of PDF formulations (see [52]) and is not repeated here. From the application of the FND relation, the resulting closure for the flux in the open kinetic PDF equation, Eq. (156), is

$$\frac{1}{\tau_p^{st}} \langle u_{s,i} | (\mathbf{y}_p, \mathbf{V}_p) \rangle p_p^{L,r} = \kappa_i p_p^{L,r} - \frac{\partial [\lambda_{ij} p_p^{L,r}]}{\partial y_{p,j}} - \frac{\partial [\mu_{ij} p_p^{L,r}]}{\partial V_{p,j}}. \quad (157)$$

In this equation, $\lambda_{ij}(t; \mathbf{y}_p, \mathbf{V}_p)$, $\mu_{ij}(t; \mathbf{y}_p, \mathbf{V}_p)$ and $\kappa_i(t; \mathbf{y}_p, \mathbf{V}_p)$ are referred to as the ‘dispersion tensors’ and are given by

$$\lambda_{ij} = \frac{1}{\tau_p^{st}} \int_0^t \langle \Gamma_{jk}(t, t') R_{f,ik}(t, \mathbf{y}_p; t', \mathbf{x}_p(t')) \rangle_{(\mathbf{y}_p, \mathbf{V}_p)} dt' \quad (158a)$$

$$\mu_{ij} = \frac{1}{\tau_p^{st}} \int_0^t \langle \dot{\Gamma}_{jk}(t, t') R_{f,ik}(t, \mathbf{y}_p; t', \mathbf{x}_p(t')) \rangle_{(\mathbf{y}_p, \mathbf{V}_p)} dt' \quad (158b)$$

where the notation $\langle \cdot \rangle_{(\mathbf{y}_p, \mathbf{V}_p)}$ indicates the averaged value conditioned on the particle trajectory that ‘arrive’ at $(\mathbf{y}_p, \mathbf{V}_p)$ at time t , which explains that the dispersion tensors are functions of $(\mathbf{y}_p, \mathbf{V}_p)$ even if the eventual dependence on \mathbf{V}_p is often neglected. In these equations, $\Gamma_{jk}(t, t')$ stands for the response function

$$\Gamma_{jk}(t, t') = \frac{\delta \mathbf{x}_{p,j}(t)}{\delta u_{f,k}(t', \mathbf{x}_p(t'))} \quad (159)$$

that measures the effect of a perturbation of the fluctuating fluid velocity seen at an earlier time on the particle position $\mathbf{x}_p(t)$ at time t , and $\dot{\Gamma} = \frac{\partial}{\partial t} \Gamma$. By plugging the flux given by Eq. (157) into Eq. (156), the closed form of the kinetic PDF equation is:

$$\begin{aligned} \frac{\partial p_p^{L,r}}{\partial t} + \frac{\partial [V_{p,i} p_p^{L,r}]}{\partial y_{p,i}} &= - \frac{\partial [F_{ext,i} p_p^{L,r}]}{\partial V_{p,i}} + \frac{\partial}{\partial V_{p,i}} \left[\frac{V_{p,i}}{\tau_p^{st}} p_p^{L,r} \right] - \frac{\partial}{\partial V_{p,i}} \left[\left(\kappa_i + \frac{1}{\tau_p^{st}} \langle U_{f,i} \rangle \right) p_p^{L,r} \right] \\ &\quad + \frac{\partial^2 [\lambda_{ij} p_p^{L,r}]}{\partial V_{p,i} \partial y_{p,j}} + \frac{\partial^2 [\mu_{ij} p_p^{L,r}]}{\partial V_{p,i} \partial V_{p,j}}. \end{aligned} \quad (160)$$

Some points can be noted:

- (i) The derivation handles both a Lagrangian PDF $p_p^{L,r}$ and an external field since the velocity of the fluid seen is treated as the value of $\mathbf{u}_f(t, \mathbf{x})$ at the particle location;
- (ii) The derivation is made only in sample space without equivalent in physical space;
- (iii) Even with the reduced set of variables for a one-particle PDF model, the kinetic PDF equation is an one equation in a 6-dimensional space, making a direct solution of Eq. (160) by classical numerical techniques (e.g. Finite Volume) intractable;
- (iv) The closed PDF equation in Eq. (160) looks like a Fokker–Planck equation but the study of this equation requires further attention (see Sections 9.2 and 10.1).

7.3.3. The dynamic PDF model

The dynamic PDF approach follows a different road in that the velocity of the fluid seen is included in the description. In physical space, this means that we are considering the evolution equations for the extended set of variables $\mathbf{Z}_p = (\mathbf{x}_p, \mathbf{U}_p, \mathbf{U}_s)$, with the form

$$\frac{d\mathbf{x}_p}{dt} = \mathbf{U}_p, \quad (161a)$$

$$\frac{d\mathbf{U}_p}{dt} = \frac{1}{\tau_p} (\mathbf{U}_s - \mathbf{U}_p) + \mathbf{F}_{ext}, \quad (161b)$$

$$\frac{d\mathbf{U}_s}{dt} = \Theta_s(t), \quad (161c)$$

where Θ_s stands for the acceleration of \mathbf{U}_s . This extended set of variables implies that the particle momentum equation Eq. (154b) is now treated without approximation even with the complete formula for the particle relaxation time in Eq. (12). In sample space, the Lagrangian PDF is $p_p^L(t; \mathbf{y}_p, \mathbf{V}_p, \mathbf{V}_s)$ where \mathbf{V}_s is used to denote the sample space variable corresponding to the stochastic process \mathbf{U}_s . With the extended set of variables, the drag force term appears now in closed form and the PDF equation is (see [1]):

$$\frac{\partial p_p^L}{\partial t} + \frac{\partial [V_{p,i} p_p^L]}{\partial y_{p,i}} = - \frac{\partial}{\partial V_{p,i}} \left[\left(\frac{V_{s,i} - V_{p,i}}{\tau_p} \right) p_p^L \right] - \frac{\partial}{\partial V_{s,i}} \left[\langle \Theta_{s,i} | (\mathbf{y}_p, \mathbf{V}_p, \mathbf{V}_s) \rangle p_p^L \right] \quad (162)$$

which is still an unclosed equation but where the closure issue has been shifted to the conditional average of the acceleration of the fluid seen Θ_s which is now to be modeled.

The modeling step consists in decomposing the acceleration into slow and fast variations

$$\Theta_s(t) = \mathbf{A}_s + \mathbf{B}_s \xi_s(t) \quad (163)$$

with \mathbf{A}_s and \mathbf{B}_s functions of the system and where ξ_s stands for a rapidly-varying process which is replaced by a white-noise term when the system is observed at times larger than the Kolmogorov timescale τ_K . The rational behind the model can be found in previous articles [1,4,5,153,154] and the main ideas will resurface in Section 10.1.4 in the course of the analysis of dynamical systems with colored or white noises. For our present purpose, we can simply represent the modeling step by the shift from the exact particle equations in Eqs. (161) to the Langevin represented by the following SDEs

$$d\mathbf{x}_p = \mathbf{U}_p dt \quad (164a)$$

$$d\mathbf{U}_p = \frac{1}{\tau_p}(\mathbf{U}_s - \mathbf{U}_p) dt + \mathbf{F}_{ext} dt \quad (164b)$$

$$d\mathbf{U}_s = \mathbf{A}_s(t, \mathbf{Z}_p, \langle \mathcal{F}[\mathbf{Z}_p] \rangle) dt + \mathbf{B}_s(t, \mathbf{Z}_p, \langle \mathcal{G}[\mathbf{Z}_p] \rangle) d\mathbf{W} \quad (164c)$$

where $d\mathbf{W}$ is a vector of independent Wiener processes and where a complete notation has been introduced in the drift vector \mathbf{A}_s and the diffusion matrix \mathbf{B}_s to indicate that, in general, these coefficients depend not only on the particle state vector but also on some statistics of the process (this is an example of McKean SDEs introduced in Section 4.3.2). Correspondingly, the PDF equation in Eq. (162) becomes a FPE

$$\frac{\partial p_p^L}{\partial t} + \frac{\partial [V_{p,i} p_p^L]}{\partial y_{p,i}} = -\frac{\partial}{\partial V_{p,i}} \left[\left(\frac{V_{s,i} - V_{p,i}}{\tau_p} \right) p_p^L \right] - \frac{\partial [A_{s,i} p_p^L]}{\partial V_{s,i}} + \frac{1}{2} \frac{\partial^2 [(B_s B_s^T)_{ij} p_p^L]}{\partial V_{s,i} \partial V_{s,j}}. \quad (165)$$

With respect to this Langevin model, one point has been a source of repeated confusion. If the increments of the Wiener process are normally distributed (see Section 4.3.1), it is important to note that it is only the conditional acceleration of the velocity of the fluid seen, which we can write as $d\mathbf{U}_s | (\mathbf{Z}_p(t) = \mathbf{z}_p)$, that is assumed to be Gaussian [1,5,60]. As a result, the stochastic process $(\mathbf{x}_p, \mathbf{U}_p, \mathbf{U}_s)$ can deviate from Gaussianity when the drift is non linear or when the diffusion matrix \mathbf{B}_s is non-constant. In that sense, the dynamic PDF approach predicts non-Gaussian statistics in inhomogeneous turbulent flows, contrary to the kinetic PDF approach which assumes Gaussian distributions for fluid velocities.

To illustrate the dependence of the drift and diffusion terms in Eq. (164c) and for later discussions in Section 10, it is useful to give the form of the state-of-the-art Langevin model for the velocity of the fluid seen (see complementary accounts in [4,5,154]). This model is an extension of the GLM for fluid particles (see Section 6.5.1) and takes the form

$$dU_{s,i} = -\frac{1}{\rho_f} \frac{\partial \langle P_f \rangle}{\partial x_i} dt + (\langle U_{p,j} \rangle - \langle U_{f,j} \rangle) \frac{\partial \langle U_{f,i} \rangle}{\partial x_j} dt + G_{ij}^* (U_{s,j} - \langle U_{f,j} \rangle) dt + B_{s,ij} dW_j. \quad (166)$$

The matrix G_{ij}^* is built on the matrix G_{ij} of the GLM (cf. Eqs. (128)–(129)) and is given by

$$G_{ij}^* = -\left(\frac{1}{2} + \frac{3}{4}C_0\right) \frac{\langle \epsilon_f \rangle}{k_f} H_{ij}, \quad (167)$$

where the matrix H_{ij} accounts for the crossing-trajectory effect and can be expressed as

$$H_{ij} = b_\perp \delta_{ij} + [b_{||} - b_\perp] r_i r_j, \quad (168)$$

with $(r_i)_{i=1,3}$ the components of the unit vector \mathbf{r} aligned with the mean relative velocity, $\mathbf{r} = \langle \mathbf{U}_r \rangle / |\langle \mathbf{U}_r \rangle|$. The coefficients $b_{||}$ and b_\perp represent the Csanady factors which stand for the ratio between the timescale of fluid particle velocities T_L and the timescale of the fluid velocities seen by discrete particles $T_{L,||}^*$ and $T_{L,\perp}^*$, in the direction parallel to the mean relative velocity or transverse to it, respectively. Using the Csanady formulas for these timescales (see [1,5,154])

$$T_{L,||}^* = \frac{T_L}{\sqrt{1 + \beta^2 \frac{|\langle \mathbf{U}_r \rangle|^2}{2k_f/3}}}, \quad T_{L,\perp}^* = \frac{T_L}{\sqrt{1 + 4\beta^2 \frac{|\langle \mathbf{U}_r \rangle|^2}{2k_f/3}}}, \quad (169)$$

(with $\beta = T_L/T_E$ the ratio of the Lagrangian timescale to the Eulerian one taken as a constant), the Csanady factors are directly obtained as $b_{||} = T_L/T_{L,||}^*$ and $b_\perp = T_L/T_{L,\perp}^*$. Using Eq. (129) for T_L , the matrix G_{ij}^* can be re-expressed as

$$G_{ik}^* = -\frac{1}{T_{L,\perp}^*} \delta_{ik} - \left[\frac{1}{T_{L,||}^*} - \frac{1}{T_{L,\perp}^*} \right] r_i r_k. \quad (170)$$

In Eq. (166), the diffusion matrix $B_{s,ij}$ is obtained as the square root of the matrix L_{ij} (i.e. $\mathbf{B}_s \mathbf{B}_s^T = \mathbf{L}$) given by

$$L_{ij} = L_\perp \delta_{ij} + [L_{||} - L_\perp] r_i r_j, \quad (171)$$

where the coefficients $L_{||}$ and L_\perp are

$$L_{||} = \langle \epsilon_f \rangle \left(C_0 b_{||} \tilde{k}_f / k_f + \frac{2}{3} (b_{||} \tilde{k}_f / k_f - 1) \right), \quad (172a)$$

$$L_{\perp} = \langle \epsilon_f \rangle \left(C_0 b_{\perp} \tilde{k}_f / k_f + \frac{2}{3} (b_{\perp} \tilde{k}_f / k_f - 1) \right). \quad (172b)$$

In these expressions, a new kinetic energy \tilde{k}_f is introduced and is defined as

$$\tilde{k}_f = \frac{3}{2} \frac{\text{Tr}(\mathbf{H} \cdot \mathbf{R}_f)}{\text{Tr}(\mathbf{H})}, \quad (173)$$

where $\text{Tr}(\mathbf{H}) = H_{ii}$ denotes the trace of the matrix \mathbf{H} and where \mathbf{R}_f is the Reynolds-stress tensor. The matrix equation $\mathbf{B}_s = \mathbf{L}^{1/2}$ does not yield a unique solution but, as we are only interested in weak solutions, different solutions \mathbf{B}_s give the same statistics and, in a weak sense, are therefore equivalent.

A few remarks can be made:

- (i) The Langevin models for the velocity of the fluid seen (cf. Eq. (166)) in two-phase flow and the one for the velocity of fluid particles (cf. Eq. (126b)) have forms which are similar to the ones used in several particle-based mesoscopic methods (e.g. DPD, SDPD, etc.) with the sum of a pressure-like mean term, a dissipative force and a random term;
- (ii) In single- and two-phase turbulent flows, the dissipative forces are written as return-to-a-mean-velocity terms, $\mathbf{A} \sim -(\mathbf{U} - \langle \mathbf{U}_f \rangle)/T$ with T a timescale that represents kinetic energy transfer, while the diffusion term are expressed as functions of the fluid kinetic energy dissipation rate, $\mathbf{B} \sim \sqrt{\langle \epsilon_f \rangle}$;
- (iii) The closure of the diffusion term is not due to the classical form of the fluctuation–dissipation relation since there is no conservation of the fluctuating kinetic energy but is worked out by using an extended version. This was introduced in [1] and has been used recently as a specific criterion to assess modeling proposals for single- and two-phase PDF models (see the analysis in [4]);
- (iv) In spite of many attempts, there is at the moment only one well-established formulation of such Langevin models (see [4]) which is a clear indication that much well-oriented research work remains to be done.

7.4. Summary and important points

The kinetic and dynamic PDF models represent different approaches to the construction of probabilistic descriptions of particles in turbulent flows. In the kinetic PDF model, particle dynamics is described in terms of particle position and velocity, *i.e.* with the variables $\mathbf{Z}_p^r = (\mathbf{x}_p, \mathbf{U}_p)$. This choice is obviously made to copy the formulations presented in Section 5, as well as the approaches developed below or at the FR-hydrodynamical level in Sections 7.1 and 7.2. The dynamic PDF model follows a more flexible approach in which the choice of the variables corresponds to a separation between slow and fast variables. This leads to selecting an extended set of variables, *i.e.* $\mathbf{Z}_p = (\mathbf{x}_p, \mathbf{U}_p, \mathbf{U}_s)$, to describe particle dynamics in high Reynolds-number turbulent flows simulated with RANS methods.

These differences do not constitute a moot point and, to understand the issue at stake, we can take up the remarks made at the end of Section 6.7 about the two ways to look at one-particle PDF models. In single-phase flow modeling, PDF models can be developed with a top-down view as in (nearly) all the mesoscopic methods in classical statistical physics, with RANS models playing the same ‘reference role’ as the hydrodynamical description for the methods in Section 5. This corresponds to the standpoint (i) at the end of Section 6.7. However, this is not so for turbulent disperse two-phase flows since there is no previously-established set of moment equations for averaged particle quantities to use as a reference description. We are in the situation illustrated by the examples put forward in Section 3.2.2 which showed that mesoscopic models are precisely needed to derive closed macroscopic descriptions. Phrased differently, *there is no alternative to using a bottom-up approach in turbulent polydisperse two-phase flow modeling*.

The consequence is that the validity of the macroscopic descriptions rests upon the mathematical and physical foundations of these PDF formulations. This explains, in particular, the two criteria introduced in Sections 4.5.1 and 4.5.2 to assess whether a PDF model forms an acceptable probabilistic description. It also points to the need to study the different techniques with which PDF models are obtained and to analyze the physical content of current modeling closures. This is done in detail in Sections 9 and 10. In Section 7.3, we have limited ourselves to two different one-particle PDF models. There are however other possible choices whose analysis requires to consider both the fluid and the particle description, before proposing a hierarchy between different methods. This is addressed in Section 8.

8. The challenges of statistical closures for polydisperse turbulent flows

The formulation of dynamic PDF models in Section 7.3.3 introduces new elements in that some characteristics of the carrier fluid flow are included in the description and treated as particle-attached variables. This is a first hint of the differences compared to formulations based on kinetic variables only and the question ‘what are the variables to associate to a particle?’ turns out to be a central one. To account for this notion, it proves useful to define the state vector as the set of variables that are explicitly modeled and attached to the particles. In other words, the state vector characterizes the information that is resolved.

The hierarchies related to the choice of the state vector are presented in Section 8.1. This helps to clarify the information available in statistical descriptions, as discussed in Section 8.2, and to emphasize the importance of consistent fluid and particle descriptions in Section 8.3. Then, classifications of the different modeling approaches are proposed in Section 8.4.

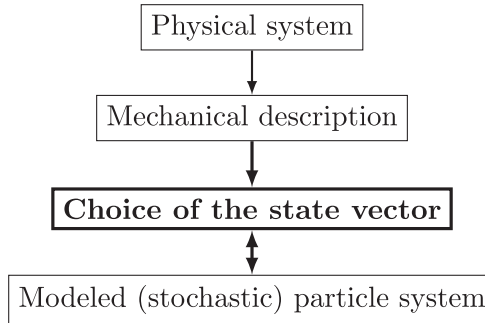


Fig. 48. Sketch of the relation between the mechanical description of a physical system, the selection of the state vector and the following modeling steps.

8.1. A double hierarchy for two-phase flow models

As shown in Fig. 48, the selection of the state-vector variables follows from the choice of the mechanical description of a physical situation and precedes the development of a model.

With the introduction of Lagrangian PDF models for the description of fields at the hydrodynamical level (see Section 6.5), we are essentially adopting a particle point of view in single-phase as well as in disperse two-phase turbulent flows and the state vector is therefore referred to as the particle state vector (with the caveat that it can correspond to a description in terms of a set of N particles, as will be exemplified in Section 8.1.1). In some cases, the definition of the particle state vector is obvious. There are, however, situations where its selection is an important step with the practical consequence that it can either facilitate or hinder the formulation of a model (this is the meaning of the double arrow in Fig. 48).

In connection with the fluid-particle and particle-particle interactions put forward in Section 2.2 are two hierarchies of the particle state vector that can be explained with a general form of the particle momentum equation written, for a particle labeled $[i]$ ($i = 1, \dots, N$), as

$$\frac{d\mathbf{x}_p^{[i]}}{dt} = \mathbf{U}_p^{[i]}, \quad (174a)$$

$$\frac{d\mathbf{U}_p^{[i]}}{dt} = \underbrace{\mathbf{F}_{f \rightarrow p}(t; \mathbf{x}_p^{[i]}, \mathbf{U}_p^{[i]}, \mathcal{F}_{\mathbf{x}_p^{[i]}}[\mathbf{U}_f(t; \mathbf{x})])}_{\text{fluid-particle interaction}} + \underbrace{\sum_{j \neq i}^N \mathbf{F}_{p \rightarrow p}^{[j] \rightarrow [i]}(t; \mathbf{x}_p^{[i]}, \mathbf{U}_p^{[i]}, \mathbf{x}_p^{[j]}, \mathbf{U}_p^{[j]}, \mathcal{G}[\mathbf{U}_f(t; \mathbf{x})])}_{\text{particle-particle interaction}}. \quad (174b)$$

In Eq. (174b), the fluid-particle interaction is formulated to express its local nature (in physical space) and with a dependence on the local fluid flow properties indicated by the index of the functional $\mathcal{F}_{\mathbf{x}_p^{[i]}}[\mathbf{U}_f(t; \mathbf{x})]$. The second term on the rhs of Eq. (174b) accounts for particle-particle interactions and is a sum over all the forces due to other particles (labeled as $[j]$) that depend on these particle locations and velocities (i.e. $(\mathbf{x}_p^{[j]}, \mathbf{U}_p^{[j]})$) as well as a possible mediation through the whole velocity field indicated by the presence of the functional $\mathcal{G}[\mathbf{U}_f(t; \mathbf{x})]$ (for example, hydrodynamical influences between particles fall in that category).

Since the BBGKY hierarchy is a classical feature of statistical physics and the hierarchy of one-particle descriptions has been emphasized in several works (see [1,4,5,52,60,153]), the following presentation is limited to the relevant elements for the discussions to come. Furthermore, since we are considering the stochastic process made up by the variables selected in the state vector, we can use the notations already introduced in Section 4 and, from now on, discrete particle state vectors are written as \mathbf{Z}_p . Note that, since we are operating at or above the FR-hydrodynamical level of description, an index p or f is used for the state vector when we are referring to discrete or fluid particles, respectively, while no index is used when developments valid for ‘general particle approaches’ are made. This switch from general particle systems to fluid and discrete particle ones is at play in Sections 9 and 10.

8.1.1. Classical BBGKY-like hierarchies

The first hierarchy is related to the particle-particle interaction $\mathbf{F}_{p \rightarrow p}$ in Eq. (174b) which involves a sum over all the N particles. When the forces $\mathbf{F}_{p \rightarrow p}^{[j] \rightarrow [i]}$ are assumed to derive from a potential, whereby $\mathbf{F}_{p \rightarrow p}^{[j] \rightarrow [i]} = -\nabla\phi(t, |\mathbf{x}_p^{[j]} - \mathbf{x}_p^{[i]}|)$ with $\phi(t, \mathbf{r})$ the potential, we are in the well-addressed situation of classical mechanics (one example is MD described in Section 5.1). It is then known that, if the problem is closed when the N particles are treated simultaneously, a reduced description in terms of a subset of s particles is unclosed since the dynamics of the s particles depends on the $N - s$ other particles (which are now external to the reduced description). This is the well-known BBGKY hierarchy, usually developed in sample space, and whose detailed presentation can be found in every textbook on classical statistical physics (see, among others, [47–49]).

From this brief account, it can be seen that this first hierarchy unfolds in terms of the number of particles retained in the probabilistic description. More precisely, we can select a one-particle PDF description in which the particle state vector

is $\mathbf{Z}_p = (\mathbf{x}_p, \mathbf{U}_p)$, or a two-particle PDF description corresponding to $\mathbf{Z}_p = (\mathbf{x}_p^{[1]}, \mathbf{U}_p^{[1]}, \mathbf{x}_p^{[2]}, \mathbf{U}_p^{[2]})$, or a s -particle PDF one corresponding to $\mathbf{Z}_p = (\mathbf{x}_p^{[1]}, \mathbf{U}_p^{[1]}, \dots, \mathbf{x}_p^{[s]}, \mathbf{U}_p^{[s]})$, etc.

For our purpose, the important element is that this choice is limited here to the number of particles retained in the state vector, while the variables attached to each particle are (nearly always) only made up by their position and velocity, *i.e.* $\mathbf{Z}_p^{[i]} = (\mathbf{x}_p^{[i]}, \mathbf{U}_p^{[i]})$. In classical statistical physics, this can be understood since particle–particle interactions are expressed in terms of their relative positions (for conservative forces) or, at most, in terms of relative positions and velocities. However, fluid–particle interactions raises new questions.

8.1.2. Hierarchies with respect to one-particle state vectors

The first hierarchy is compounded by a second one that manifests a specific characteristic of particles in non-fully resolved turbulent flows in relation to the fluid–particle interaction $\mathbf{F}_{f \rightarrow p}$ in Eq. (174b). If we consider, for example, that this term is represented by the drag force, we have $\mathbf{F}_{f \rightarrow p} = (\mathbf{U}_s - \mathbf{U}_p)/\tau_p$ where the velocity of the fluid seen is $\mathbf{U}_s(t) = \mathbf{U}_f(t, \mathbf{x}_p(t))$ (note that we have left out the particle label $[i]$, as we are now dealing with a one-particle description since these forces are local in space).

If the whole instantaneous fluid velocity field $\mathbf{U}_f(t, \mathbf{x})$ is known, then $\mathbf{U}_s(t)$ is fully determined by the particle location $\mathbf{x}_p(t)$ at each time and a particle state vector limited to the kinetic variables, $\mathbf{Z}_p = (\mathbf{x}_p, \mathbf{U}_p)$, is enough to determine particle dynamics. This is similar to the classical (kinetic) situation analyzed in the first hierarchy. However, if the fluid velocity field is partially resolved, we have only limited information on $\mathbf{U}_f(t, \mathbf{x})$. This means that \mathbf{U}_s is not known and is external to the particle kinetic description. In that case, it makes sense to include the velocity of the fluid seen as an additional variable and consider the extended state vector $\mathbf{Z}_p = (\mathbf{x}_p, \mathbf{U}_p, \mathbf{U}_s)$. This procedure can be continued by including successive derivatives, *i.e.* $\mathbf{Z}_p = (\mathbf{x}_p, \mathbf{U}_p, \mathbf{U}_s, \dot{\mathbf{U}}_s)$, or $\mathbf{Z}_p = (\mathbf{x}_p, \mathbf{U}_p, \mathbf{U}_s, \dot{\mathbf{U}}_s, \ddot{\mathbf{U}}_s)$, etc., which characterizes the second hierarchy in terms of one-particle state vectors. It is readily seen that a similar reasoning holds if we consider other fluid–particle forces, such as the added-mass force.

It is worth noting that, although specific to the case of particles in partially-resolved turbulent flows, this infinite hierarchy of one-particle state vectors is an extension of the two historical descriptions of Brownian particles. Indeed, Brownian motion was first modeled in terms of particle positions, *i.e.* $\mathbf{Z}_p = (\mathbf{x}_p)$, in Einstein's landmark study and later addressed in terms of particle position and velocity, *i.e.* $\mathbf{Z}_p = (\mathbf{x}_p, \mathbf{U}_p)$, in Langevin's approach.

Once the central role played by the definition of the particle state vector has been demonstrated by the results given throughout Section 9 and by the specific analysis in Section 10.1, further examples of how to select relevant state vectors are provided in Section 10.2.

8.2. The available information: what can and cannot be calculated

When a mesoscopic or macroscopic description is chosen, it is important to be aware of the information that can be extracted as well as the one irreversibly lost in the coarse-graining procedure leading to that formulation. In classical statistical physics, information is, of course, limited. For example, at the hydrodynamical level, one has access only to mean molecular properties, such as the fluid density and velocity fields. Yet, given the large separation of scales and the principles of equipartition of energy and molecular chaos, some information on molecular fluctuations can be retrieved. This is more difficult in single-phase and disperse two-phase flow turbulence, since there is no scale separation and no equilibrium principles. Furthermore, the mixed formulations in terms of fields and particles (translated into the differences between Lagrangian and Eulerian PDFs) compounded by the use of stochastic models can make probabilistic descriptions of particles in turbulent flows more confusing.

To illustrate the available information corresponding to the choice of a probabilistic description, we can take up the examples of Section 3.2.2 using the notions of the particle state vector introduced in Section 8.1 and of the Lagrangian and Eulerian PDFs given in Section 4.4

- (1) For the first example presented in Section 3.2.2, the choice of a (fluid) particle state vector $\mathbf{Z}_f = (\mathbf{x}_f, \phi_f) = (\mathbf{x}_f, (\phi_l)_{l=0,N_s})$ (noting $\phi_0 = \phi_f$) means that the chemical source terms are closed but that the turbulent fluxes are still unclosed. This is in line with the second hierarchy described above in Section 8.1.2. If this description is retained, then all the one-point moments of the state-vector variables are accessible since they derive from the known Eulerian PDF $p_f^E(t, \mathbf{x}; \psi_f)$, and the relation between the simulated PDF and the available information can be expressed as

$$\underbrace{\langle \phi_{f,l}^m \rangle(t, \mathbf{x})}_{\text{available}} = \int \psi_{f,l}^m \underbrace{p_f^E(t, \mathbf{x}; \psi_f)}_{\text{known}} d\psi_f, \quad \forall m \in \mathbb{N}. \quad (175)$$

However, spatial correlations, such as the two-point correlation, cannot be calculated since they depend on the two-point PDFs which cannot be retrieved from the one-point one. This can be written as

$$\underbrace{\langle \phi_{f,l}(t, \mathbf{x}^{[1]}) \phi_{f,l}(t, \mathbf{x}^{[2]}) \rangle}_{\text{unavailable}} = \int \psi_{f,l}^{[1]} \psi_{f,l}^{[2]} \underbrace{p_f^E(t, \mathbf{x}^{[1]}, \mathbf{x}^{[2]}; \psi_f^{[1]}, \psi_f^{[2]})}_{\text{unknown}} d\psi_f^{[1]} d\psi_f^{[2]}, \quad (176)$$

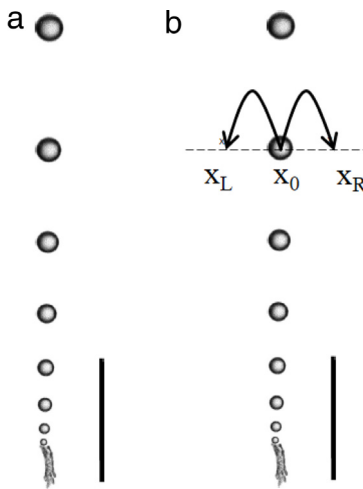


Fig. 49. A string of individual bubbles rising in a liquid flow (a); Representation of the mean volumetric fraction induced by lateral fluctuations (b).

which translates that there is no length information (and no instantaneous field) in one-point (Eulerian) PDFs deriving from one-particle (Lagrangian) PDFs. Therefore, it is not possible to extract scalar spectra from a one-point approach. The same is true for velocities, showing that one-point PDF methods can predict the infinite hierarchy of one-point velocity moments but do not contain information about the kinetic energy spectrum or about instantaneous velocity-gradients (as a consequence, the fluid dissipation is external to a one-point velocity PDF formulation). Naturally, two-point PDFs are obtained from two-particle PDFs, in line with the first hierarchy of state vector put forward in Section 8.1.1, and the kinetic energy spectrum is available at this level of description. It can be noted that these limitations are not intrinsic to the PDF approach but reflect the choice of a specific reduced description. Though these points are clear when properly addressed, this is not an aspect that should be passed over too quickly as there are still unfortunate but major mistakes being made where a kinetic energy spectrum is “calculated” from one-particle PDF models (see an example of such a pitfall in [155]).

- (2) Similar considerations hold for the macroscopic description of particle dynamics limited to the particle volumetric fraction $\alpha_p(t, \mathbf{x})$ and the first two velocity moments, *i.e.* the mean particle velocity $\langle U_{p,i}(t, \mathbf{x}) \rangle$ and the kinetic tensor $\langle u_{p,i} u_{p,j}(t, \mathbf{x}) \rangle$, cf. Eqs. (29) (cf. the second example presented in Section 3.2.2). These moments can be extracted from the one-point (Eulerian) MDF $F_p^E(t, \mathbf{x}; \mathbf{V}_s, \mathbf{V}_p)$ obtained from a one-particle (Lagrangian) PDF model that includes the velocity of the fluid seen in the particle state vector $p_p^L(t; \mathbf{y}_p, \mathbf{V}_s, \mathbf{V}_p)$, following the methodology recalled in Section 4.4. For instance, the mean drag force is given by

$$\alpha_p \rho_p \left\langle \left(\frac{U_{s,i} - U_{p,i}}{\tau_p} \right) \right\rangle = \int \left[\frac{V_{s,i} - V_{p,i}}{\tau_p(\mathbf{V}_s, \mathbf{V}_p, d_p)} \right] F_p^E(t, \mathbf{x}; \mathbf{V}_s, \mathbf{V}_p) d\mathbf{V}_s d\mathbf{V}_p \quad (177)$$

while the other terms are also obtained from the MDF $F_p^E(t, \mathbf{x}; \mathbf{V}_s, \mathbf{V}_p)$.

However, an unfortunate mistake consists in trying to calculate the effects of interactions at distance from that sole information. To exemplify this point, consider the situation represented in Fig. 49(a) which shows a string of small bubbles detaching continuously, but sequentially, from the bottom wall (which is acting as a nucleation site) and rising in a liquid. Let us now imagine that the liquid flow is turbulent and that, in an horizontal cross-section, there are lateral fluctuations around a zero mean value. As a result, the string of bubbles is not rising along a strict vertical line driven by the buoyancy force only but is sometimes shifted to the right of the point x_0 (located at the intersection between the vertical line and the horizontal plane we are considering) and sometimes to its left (see Fig. 49(b)). For the sake of a simple presentation of the argument, we can use a very simple model where there is a one-half probability that the bubbles cross the plane at a point on the right x_R and a one-half probability that the bubbles cross the plane at a point on the left x_L . Then, in a statistical one-point formulation, we get that $\alpha_b(t, \mathbf{x}_L) = \alpha_b(t, \mathbf{x}_R) = 0.5$ which is an exact result for this simple model.

Based on that information, it is however a mistake to consider that bubbles located in two adjacent cells coalesce and form larger bubbles, since it is clear that bubbles are never present in \mathbf{x}_L and in \mathbf{x}_R at the same time.

- (3) The previous example is a manifestation that coalescence rates cannot be calculated when only one-point information is available. This reflects again that there is no length information in one-point descriptions derived from one-particle PDFs, as in the case of the kinetic energy spectrum or the scalar spectra mentioned above. In that sense, the case of the rising bubbles shown in Fig. 49 serves to illustrate the difference between what can be calculated from a one-particle PDF approach and what cannot: the complex growth process of champagne bubbles (see the illustration in Fig. 6(b))

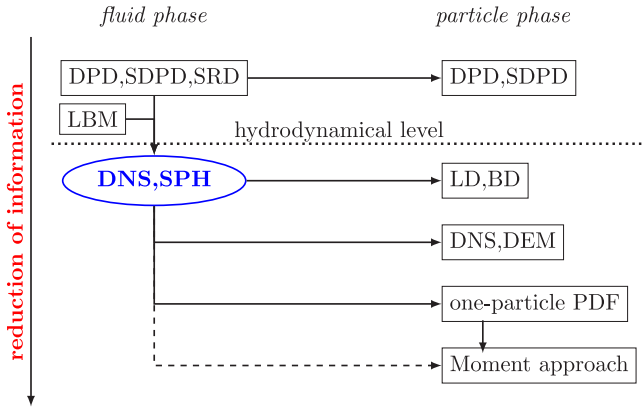


Fig. 50. Sketch of consistent descriptions for the particle phase when a microscopic description (DNS) is available for the turbulent fluid flow as a function of decreasing information content.

that depends on local variables (especially, the local amount of excess carbon dioxide) can be calculated by introducing the relevant variables in the bubble state vector and simulating the corresponding processes but coalescence rates cannot.

In consequence, to calculate collision rates, a fully-microscopic N -particle formulation is needed (or, at the very least, a fine-enough mesoscopic formulation consisting in two-particle PDF approaches). In one-particle PDF models, particle collisions must be accounted for by using predefined collision rates. This is an interesting example of the relation between microscopic, mesoscopic and macroscopic formulations. How externally-provided collision/agglomeration rates are used in present one-particle PDF models for turbulent disperse two-phase flows has been recently discussed (see [5, section 6.2]) and is recalled at the beginning of Section 10.6. Whether we consider a one-particle or a N -particle PDF formulation, there are, however, several challenging issues related to particle collisions in turbulent flows, which are addressed in Sections 10.6.1–10.6.3.

8.3. The importance of consistent fluid and particle descriptions

The preceding analysis of the information content is not limited to the particle phase and must be applied to the complete fluid and particle system. This brings out the importance of the consistency between the descriptions retained for the fluid and particle phases.

To clarify this point, imagine a N -particle PDF formulation where N discrete particles are tracked simultaneously in a turbulent flow. Such a microscopic description of particle dynamics requires the knowledge of the instantaneous fluid velocity field since particles can be at different locations at a given time. In other words, a microscopic approach is possible but provided that we have also a similar microscopic approach for the fluid phase, typically through a Direct Numerical Simulation (DNS). Similarly, a two-particle PDF formulation requires that we have a two-point PDF model for the fluid phase, for the complete approach to the fluid and particle system to be meaningful. However, when the information available for the fluid phase is limited to one-point moments, in classical models (cf. the $k-\epsilon$ and RANS models described in Section 6.3), considering two-particle PDF models for the particle phase becomes inconsistent since there is no length information on the carrier fluid.

8.4. Summary and relations between present statistical models

The potential lack of spatial information on the carrier fluid flow is one of the characteristic challenges when modeling particles in turbulent flows. Therefore, classifications of the various formulations depend on the resolution of the fluid phase.

More precisely, if the turbulent fluid flow is fully resolved (that is with a microscopic, or DNS, approach where all the degrees of freedom are explicitly calculated), the different approaches described in Section 7 can be considered. These approaches are organized in Fig. 50 as a function of the reduction of information where the aim is to propose a general picture with respect to the information content and not an assessment with regard to the specific quality of each method (as for the formulations of classical physics discussed in Section 5).

On the other hand, when only limited information is available for the fluid phase, the consistency issues raised in the precedent section modify the picture. For example, if only one-point moments are resolved for the turbulent fluid flows, as when typical RANS formulations are used (see Section 6), then models for particles can only be developed in the context of one-particle PDF approaches and ‘down the information ladder’. This is represented by the modified classification shown in Fig. 51.

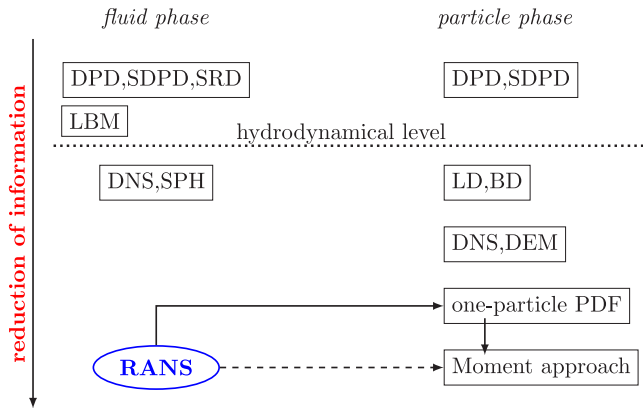


Fig. 51. Sketch of consistent descriptions for the particle phase when only limited information (RANS approach) is available for the turbulent fluid flow as a function of decreasing information content.

The analyses developed in this section have pointed out the central role played by one-particle PDF approaches, especially in the context of partially-resolved turbulent fluid flows. In keeping with the issue of the choice of the variables in the particle state vector, the formulation of these models is now studied in detail in Sections 9 and 10.

9. General modeling tools and statistical closures

In this section, we present modeling tools before studying probabilistic models for particles in turbulent flows in Section 10. In that sense, these discussions pave the way for the developments to come. It is however important to realize that some of the points discussed in the analyses of these probabilistic models are common to a wide class of dynamical systems. For that reason, these modeling tools are presented in general terms but are also developed with a view towards the case of particle dynamics in turbulent flows.

The elimination of Gaussian noise is first considered in Section 9.1 before addressing the probabilistic descriptions of dynamical systems under external colored or white noises in Section 9.2. Then, a detailed presentation of the important technique of fast-variable elimination is proposed in Section 9.3. Drawing on these results, the role of the particle state vector is brought out in Section 9.4.

9.1. Functional approaches and the Furutsu–Novikov–Donsker theorem

As often in probability, analytical formulas can be worked out for Gaussian random variables or stochastic processes. One such formula is the Furutsu–Novikov–Donsker (FND) relation [150–152] which is useful to express the statistical effects of Gaussian signals on random variables or dynamical systems. This relation can be found under several alternative forms and is presented here in three steps: first, for a Gaussian random variable, then for a Gaussian time process and, finally, for a Gaussian random field.

For random variables, we consider a vector-valued centered Gaussian variable $(X_i)_{i=1,N}$ and a differentiable function $f(x_1, x_2, \dots, x_N)$ of N variables. Then, the correlation between one component X_k and the function $f(X_1, X_2, \dots, X_N)$ of the Gaussian random variable is:

$$\langle X_k f(X_1, X_2, \dots, X_N) \rangle = \langle X_k X_l \rangle \left\langle \frac{\partial f}{\partial X_l} \right\rangle. \quad (178)$$

This is the form given, for example in [39, section 4.1], where it is presented under the meaningful name of Gaussian integration by parts. This formulation has the further merit of opening the way for the interpretation of the two other forms of the FND relation.

In the second formulation, we consider a Gaussian centered stochastic process ξ , where the trajectories are therefore random functions in time, and a function F of these trajectories. This is expressed by using functional notations and writing $F[t; \xi]$ to denote a function of present and past values of ξ , that is $F[t; \xi] = F(t; \xi(t'))$, with $t' \leq t$. In that case, the general formulation of the FND relation states that

$$\langle \xi_k(t) F[t; \xi] \rangle = \int_0^t \langle \xi_k(t) \xi_l(t') \rangle \left\langle \frac{\delta F[t; \xi]}{\delta \xi_l(t')} \right\rangle dt', \quad (179)$$

where $\delta F[t; \xi]/\delta \xi_l(t')$ is to be understood as the functional derivative of F with respect to ξ_l at the time t' . In spite of the (slightly) more complicated reference to functional derivatives, it is seen that Eq. (179) is basically an extension of Eq. (178) to the context of continuous time signals and implies the two-time correlations $\langle \xi_k(t) \xi_l(t') \rangle$ which ‘propagate’ the influence

of the different past ‘impulses’ $\delta F[t; \xi]/\delta\xi_l(t')$ to build the correlation at time t . This is also seen by considering a discrete time setting where the vector-valued centered random variable in Eq. (178) would typically be $(X(\Delta t), X(2\Delta t), \dots, X(N\Delta t))$ and $X_k = X(N\Delta t)$.

The FND relation for time signals in Eq. (179) has an extended form for an arbitrary functional $R[t; \Psi]$ of a Gaussian random field $\Psi(t, \mathbf{x})$ with zero mean. It writes

$$\langle \Psi_k(t, \mathbf{x}) R[t; \Psi] \rangle = \int_0^t \int_{\mathbf{x}'} \langle \Psi_k(t, \mathbf{x}) \Psi_l(t', \mathbf{x}') \rangle \left\langle \frac{\delta R[t; \Psi]}{\delta \Psi_l(t', \mathbf{x}')} \right\rangle dt', \quad (180)$$

where the integration is over all past times and all point \mathbf{x}' of the Gaussian random field and involves therefore the two-time two-point correlations $\langle \Psi_k(t, \mathbf{x}) \Psi_l(t', \mathbf{x}') \rangle$.

When applicable, the FND relation is useful to derive closed PDF equations for dynamical systems. However, the status of such formulations with respect to the criteria introduced in Sections 4.5.1 and 4.5.2 can be wondered. This aspect is now analyzed.

9.2. Probabilistic descriptions of dynamical systems subject to white or colored noises

How to handle the fluid velocity seen by particles in probabilistic descriptions of particles in turbulent flows is one example of a general issue, which is the formulation of proper probabilistic descriptions of dynamical systems under the influence of external noises. This is of wide applicability for the construction of statistical models and there has been continuous debate over this question [59,62,68,156]. It is therefore of interest to address the question of complete and well-posed probabilistic descriptions for a generic form of dynamical systems.

Dynamical systems under white or colored noises. We consider a general dynamical system characterized by a set of n variables gathered in the state vector $\mathbf{Z} = (Z_1, Z_2, \dots, Z_n)$ with evolution equations

$$\frac{dZ_i(t)}{dt} = A_i(t, \mathbf{Z}(t), \mathcal{F}[\mathbf{Z}]) + B_{ij}(t, \mathbf{Z}(t), \mathcal{F}[\mathbf{Z}]) \xi_j(t) \quad (181)$$

where $\xi = (\xi_j)_{j=1,n}$ represents an ‘external noise’. In this equation, $\mathcal{F}[\mathbf{Z}]$ accounts for a possible dependence of the vector \mathbf{A} and of the matrix \mathbf{B} on statistics of the stochastic process \mathbf{Z} . However, for the sake of simplicity, the dependence of \mathbf{A} and \mathbf{B} is written as $\mathbf{A}(t, \mathbf{Z})$ and $\mathbf{B}(t, \mathbf{Z})$ in the following. With these simplifications, the issue is to build a consistent probabilistic description of the stochastic process \mathbf{Z} . There are two different situations.

First, if the external noise ξ is a Gaussian process with independent values, we are evolving within a well-established framework. Indeed, ξ is a delta-correlated Gaussian process $\langle \xi_k(t) \xi_l(s) \rangle = \delta_{kl} \delta(t - s)$, that is a ‘Gaussian white-noise’, and by integration over small time increments we get the SDEs, written as

$$d\mathbf{Z}(t) = \mathbf{A}(t, \mathbf{Z}(t)) dt + \mathbf{B}(t, \mathbf{Z}(t)) d\mathbf{W}(t) \quad (182)$$

with $d\mathbf{W} = (dW_l)_{l=1,n}$ a vector of independent Wiener processes and where, for instance, the stochastic integrals are defined according to the Ito rule (see Section 4.3). As discussed in Section 4.2, \mathbf{Z} defines a Markov process which implies that the complete law of the stochastic process is reconstructed from the knowledge of only two functions: the initial and transition PDFs [43,50,55,59,61,62]. This means that the SDE in Eq. (182), supplemented with an initial condition $\mathbf{Z}(t_0) = \mathbf{Z}_0$, guarantees that a complete probabilistic description is obtained (see Section 4.5.1). In sample space, the corresponding FPE for the transition PDF $p(t, \mathbf{z} | (t_0, \mathbf{z}_0))$ (cf. Eq. (53)) is

$$\frac{\partial p(t, \mathbf{z} | (t_0, \mathbf{z}_0))}{\partial t} = - \frac{\partial [A_i(t, \mathbf{z}) p(t, \mathbf{z} | (t_0, \mathbf{z}_0))] }{\partial z_i} + \frac{1}{2} \frac{\partial^2 [D_{ij}(t, \mathbf{z}) p(t, \mathbf{z} | (t_0, \mathbf{z}_0))] }{\partial z_i \partial z_j} \quad (183)$$

where $\mathbf{D} = (D_{ij})_{i,j=1,n} = (\mathbf{B}\mathbf{B}^\top)_{ij}$ is a definite-positive diffusion matrix. As recalled in Section 4.5.2, there is now a well-established body of work that ensures that the SDEs in Eq. (182) and the FPE in Eq. (183) are well-posed for sufficiently smooth drift vectors and diffusion matrices [61,70]. In these analyses, a central point is that $D_{ij}(t, \mathbf{z})$ is definite-positive for all sample space values \mathbf{z} , whatever the choice of A_i and B_{ij} .

Second, the situation is different for ‘colored noises’ when ξ has a non-zero correlation timescale. This is found, for example, for stationary Gaussian processes simulated as a set of independent stationary Ornstein–Uhlenbeck processes with trajectory equations

$$d\xi_k(t) = -\frac{\xi_k(t)}{\tau} dt + \sigma dW_k(t), \quad (184)$$

where τ is the timescale of ξ_k and σ a constant equal to $\sigma^2 = 2\langle \xi_k^2 \rangle / \tau$ from the classical fluctuation–dissipation theorem [43]. For the sake of simplicity, τ and σ are retained for each component ξ_k (differences can be accounted for through the choice of \mathbf{B}). The auto-correlation of this process is an exponential function $\langle \xi_k(t) \xi_l(s) \rangle = \langle \xi^2 \rangle \exp(-|t - s|/\tau) \delta_{kl}$ and is not delta-correlated when $\tau \neq 0$. For such external noises, the process \mathbf{Z} in Eq. (181) is no longer Markovian [59,61,62] although, as put forward in Section 4.2, a classical remark is to note that Markovianity is retrieved by considered the extended process (\mathbf{Z}, ξ) [59,61,62].

The issue of well-posed PDF equations Whether a description is Markovian or not does not prevent to consider the equation satisfied by the one-time PDF of the process $p(t; \mathbf{z})$ (and its corresponding DF). This is the equation of interest to derive a set of partial-differential equations in physical space for some statistical moments, such as the first and second-order moments, $\langle Z_i(t) \rangle$ and $\langle Z_i(t) Z_j(t) \rangle$, respectively. However, it is essential that this equation be mathematically well-posed for the resulting macroscopic descriptions to be regarded as acceptable. This is basically the criterion put forward in Section 4.5.2 and this question is addressed here for the system in Eq. (181) when ξ is a set of OU processes given by Eq. (184). It is worth emphasizing that the objective is to study whether the formulation of well-based PDF equations can be obtained for the general class represented by Eq. (181), regardless of the choices of \mathbf{A} and \mathbf{B} .

Derivation of the PDF equation. To address the general issue of the well-posed nature of probabilistic approaches and, therefore, of the resulting macroscopic descriptions, the PDF equation is first derived for a Gaussian colored noise. For this purpose, we consider the equation satisfied by the one-time PDF $p(t; \mathbf{z})$ for a dynamical system represented by the evolution equation Eq. (181). Starting from the ‘fine-grained PDF’ $\mathcal{P}(t; \mathbf{z})$ defined as $\mathcal{P}(t; \mathbf{z}) = \delta(\mathbf{Z}(t) - \mathbf{z})$ and using that $p(t; \mathbf{z}) = \langle \mathcal{P}(t; \mathbf{z}) \rangle$ (see Section 4.5), the exact but unclosed PDF equation for $p(t; \mathbf{z})$ is

$$\frac{\partial p}{\partial t} = -\frac{\partial}{\partial z_i} [A_i(t, \mathbf{z}) p] - \frac{\partial}{\partial z_i} [B_{ik}(t, \mathbf{z}) \langle \xi_k |(t, \mathbf{z}) \rangle p] \quad (185)$$

which, with $\langle X \mathcal{P} \rangle = \langle X |(t, \mathbf{z}) \rangle p(t, \mathbf{z})$, is given by

$$\frac{\partial p}{\partial t} = -\frac{\partial}{\partial z_i} [A_i(t, \mathbf{z}) p] - \frac{\partial}{\partial z_i} [B_{ik}(t, \mathbf{z}) \langle \xi_k \mathcal{P} \rangle]. \quad (186)$$

In Eq. (186), the open flux $\langle \xi_k \mathcal{P} \rangle$ can be written as $\langle \xi_k \mathcal{F}[t; \xi] \rangle$, where $\mathcal{F}[\cdot]$ stands for a functional dependence since \mathcal{P} is a functional of the Gaussian centered process ξ . We can apply the FND relation introduced in Section 9.1 and Eq. (179) which reads

$$\langle \xi_k(t) \mathcal{P}[t; \xi] \rangle = \int_0^t \langle \xi_k(t) \xi_l(t') \rangle \left\langle \frac{\delta \mathcal{P}[t; \xi]}{\delta \xi_l(t')} \right\rangle dt'. \quad (187)$$

Then, using

$$\frac{\delta \mathcal{P}(t; \mathbf{z})}{\delta \xi_l(t')} = -\frac{\delta Z_j(t)}{\delta \xi_l(t')} \frac{\partial \mathcal{P}(t; \mathbf{z})}{\partial z_j}, \quad (188a)$$

$$= -\frac{\partial}{\partial z_j} \left[\frac{\delta Z_j(t)}{\delta \xi_l(t')} \mathcal{P} \right] + \left(\frac{\partial}{\partial z_j} \left[\frac{\delta Z_j(t)}{\delta \xi_l(t')} \right] \right) \mathcal{P}, \quad (188b)$$

and applying the averaging operator, we obtain

$$\langle \xi_k \mathcal{P} \rangle = \alpha_k(t, \mathbf{z}) p(t, \mathbf{z}) - \frac{\partial \left[\lambda_{kj}(t, \mathbf{z}) p(t, \mathbf{z}) \right]}{\partial z_j}, \quad (189)$$

with

$$\alpha_k(t, \mathbf{z}) = \int_0^t \langle \xi_k(t) \xi_l(t') \rangle \left\langle \frac{\partial}{\partial z_j} \left[\frac{\delta Z_j(t)}{\delta \xi_l(t')} \right] |(t, \mathbf{z}) \right\rangle dt', \quad (190)$$

and where the important coefficient λ_{kj} is given by

$$\lambda_{kj}(t, \mathbf{z}) = \int_0^t \langle \xi_k(t) \xi_l(t') \rangle \left\langle \frac{\delta Z_j(t)}{\delta \xi_l(t')} |(t, \mathbf{z}) \right\rangle dt'. \quad (191)$$

From these expressions, it follows that the averaged value of λ_{kj} is

$$\int \lambda_{kj}(t, \mathbf{z}) p(t, \mathbf{z}) d\mathbf{z} = \int_0^t \langle \xi_k(t) \xi_l(t') \rangle \left\langle \frac{\delta Z_j(t)}{\delta \xi_l(t')} \right\rangle dt'. \quad (192)$$

On the other hand, applying directly the FND relation to $Z_j(t)$ in Eq. (179) leads to the important result that

$$\langle \xi_k Z_j(t) \rangle = \int \lambda_{kj}(t, \mathbf{z}) p(t, \mathbf{z}) d\mathbf{z}. \quad (193)$$

Combining Eqs. (189) and Eq. (186) gives the closed form for the equation satisfied by the one-time PDF $p(t; \mathbf{z})$

$$\frac{\partial p}{\partial t} = -\frac{\partial}{\partial z_i} [(A_i + B_{ik} \alpha_k) p] + \frac{\partial}{\partial z_i} \left[B_{ik} \frac{\partial (\lambda_{kj} p)}{\partial z_j} \right], \quad (194)$$

which can be re-arranged as

$$\frac{\partial p}{\partial t} = -\frac{\partial}{\partial z_i} [\widetilde{A}_i p] + \frac{1}{2} \frac{\partial^2}{\partial z_i \partial z_j} [\widetilde{D}_{ij} p], \quad (195)$$

with $\tilde{A}_i = A_i + B_{ik}\alpha_k + \lambda_{kj}\partial B_{ik}/\partial z_j$ and

$$\tilde{D}_{ij}(t, \mathbf{z}) = B_{ik}(t, \mathbf{z})\lambda_{kj}(t, \mathbf{z}) + B_{jk}(t, \mathbf{z})\lambda_{ki}(t, \mathbf{z}). \quad (196)$$

We now consider the nature of the one-time PDF equation for the limited aim of deriving statistical moments.

The well-posed nature of PDF equations. The well-posed property of the closed PDF equation, Eq. (195), is governed by the symmetrical matrix \tilde{D}_{ij} . Indeed, if \tilde{D}_{ij} is not positive definite (there is at least one negative eigenvalue), this implies that a marginal of the one-time PDF appears as the ‘solution’ of an ‘anti-diffusion’ PDE. This question is studied in detail in [52] for kinetic models of particles in turbulent flows where it is proved that such equations are ill-posed in the sense that they can only be solved for very special initial conditions. It is thus required that $\tilde{D}_{ij}(t, \mathbf{z})$ have only positive (or null) eigenvalues, $\forall \mathbf{z}$, for this equation to correspond to a proper probabilistic description.

This mathematical formulation should not hide the physical issues related to that question. For example, in thermodynamical terms, the existence of a negative eigenvalue means that one is trying to describe as a closed system a system whose contact with the ‘external world’ cannot be treated as a contact with a heat bath since it contains a (negative) correlation and, thus, an underlying order that needs to be taken into account in the description. In other words, this is similar to treating what is basically a return-to-equilibrium-like term as a diffusion-like one. On the other hand, positive eigenvalues of the second-order matrix \tilde{D}_{ij} means that the corresponding effects can truly be regarded as the sum of uncorrelated ‘pure noise’ perturbations, leading to real diffusive and disorder actions on the system that is considered. Furthermore, it must be stressed that only well-based PDF, or DF, equations guarantee that the resulting set of moment equations forms realizable models.

We now address two simple situations but which are of a wide interest.

Analysis of the linear case. The first situation corresponds to the case where the drift vector is linear in $\mathbf{Z}(t)$ (or is linearized around a given point in sample space). Then, Eq. (181) becomes

$$\frac{dZ_i(t)}{dt} = -G_{ik}Z_k(t) + B_{ik}\xi_k(t) \quad (197)$$

where \mathbf{G} is a constant matrix representing return-to-equilibrium effects and where the colored noise ξ is still a set of independent stationary OU processes as in Eq. (184). In the linear case, the ‘response functions’ $\delta Z_j(t)/\delta \xi_i(t')$ in Eq. (191) are independent of the sample space value \mathbf{z} , showing that $\lambda_{ji} = \langle Z_i \xi_j \rangle$. In the stationary state where λ_{ij} reach constant values the correlations are easily derived through the relations

$$\frac{d\lambda_{ji}}{dt} = 0 \implies (\delta_{ik} + \tau G_{ik}) \langle Z_k \xi_j \rangle = B_{ij} \tau \langle \xi^2 \rangle, \quad (198)$$

which can be inverted to give $\lambda_{ji} = \tau \langle \xi^2 \rangle \tilde{G}_{ik}^{-1} B_{kj}$ with $\tilde{\mathbf{G}} = \mathbb{1} + \tau \mathbf{G}$.

To show that the positive-definite property of \tilde{D}_{ij} is not automatically satisfied, it is sufficient to consider a specific counter-example, for instance a simple two-dimensional situation where $\mathbf{Z} = (Z_1, Z_2)$ and evolution equations having the form

$$dZ_1(t) = -Z_1(t) + \kappa Z_2 + B dW_1(t), \quad (199a)$$

$$dZ_2(t) = -Z_2(t) + \kappa Z_1 + B dW_2(t). \quad (199b)$$

This corresponds to a return-to-equilibrium matrix \mathbf{G} given by

$$\mathbf{G} = \begin{pmatrix} 1 & -\kappa \\ -\kappa & 1 \end{pmatrix} \quad (200)$$

and an isotropic noise term *i.e.* $\mathbf{B} = B\mathbb{1}$, which entails that the determinant of the (2×2) matrix \tilde{D}_{ij} is

$$\det(\tilde{\mathbf{D}}) = \frac{4B^2 \tau^2 (\langle \xi^2 \rangle)^2}{(1 + \tau)^2 - \tau^2 \kappa^2}. \quad (201)$$

Then, as soon as $\tau \neq 0$, this determinant is negative for large values of κ and, hence, such a system is ill-posed. In other words, as soon as the two components Z_1 and Z_2 are strongly coupled, the resulting probabilistic description becomes ill-based even for such a trivial system.

Note that for the general formulation in Eq. (197) and for small values of τ , the inverse matrix can be approximated by $\tilde{\mathbf{G}}^{-1} = \mathbb{1} - \tau \mathbf{G} + \mathcal{O}(\tau^2)$. Then, the correlations λ_{ji} can be written as

$$\lambda_{ji} = \tau \langle \xi^2 \rangle B_{ij} - \tau^2 \langle \xi^2 \rangle G_{ik} B_{kj} + \mathcal{O}(\tau^2). \quad (202)$$

Using this approximation in Eq. (196), the symmetrical matrix \tilde{D}_{ij} is obtained after straightforward algebra as

$$\tilde{D}_{ij} = 2\tau \langle \xi^2 \rangle (BB^\perp)_{ij} - \tau^2 \langle \xi^2 \rangle C_{ij} + \mathcal{O}(\tau^2), \quad (203)$$

where $\mathbf{C} = (BB^\perp)G^\perp + G(BB^\perp)$ is a symmetrical matrix. The first term on the right-hand side (rhs) of Eq. (203) constitutes a positive-definite matrix but the second one is unsure. The important point is that this second term is explicitly dependent

upon \mathbf{G} . The only possibility to ensure that the resulting matrix \tilde{D}_{ij} remains definite positive whatever the choice of \mathbf{G} is to take the limit $\tau \rightarrow 0$. To retain a non-zero \tilde{D}_{ij} matrix, this limit must be taken as:

$$\tau \rightarrow 0 \text{ and } \langle \xi^2 \rangle \rightarrow \infty, \text{ such that } \lim_{\tau \rightarrow 0} (\tau \langle \xi^2 \rangle) = K \quad (204)$$

where K is a positive constant. This corresponds to the white-noise limit and we can approximate the integration of the noise term over a small time interval dt by writing that [1,43]

$$\xi_j(t) dt \simeq \sqrt{2K} dW_j(t), \quad (205)$$

with W_j a Wiener process. This leads to the expression

$$\lambda_{ji} \simeq \sqrt{2K} \langle Z_i(t) \circ dW_j(t) \rangle / dt, \quad (206)$$

where the symbol \circ indicates that stochastic integrals are to be taken in the Stratonovich interpretation since we are considering white-noises as the limit of differentiable processes [55]. Classical rules of stochastic calculus give that $\lambda_{ji} \simeq KB_{ij}$ (this is the result of the conversion from the Stratonovich to the Ito definition), from which we retrieve that $\tilde{D}_{ij} = 2K(BB^\perp)_{ij}$.

Thus, in that white-noise limit, the PDF equation becomes a FPE as in Eq. (194) corresponding to the FPE in the Stratonovich sense while the one in Eq. (195) corresponds to the traditional FPE in the Ito sense. It is well-known that both forms are well-based equations.

Analysis of general kinetic PDF descriptions. In the second situation, we consider a specific structure where $dZ_1/dt = Z_2$ and where the external noises are acting only on the variables (Z_2, \dots, Z_n) , so that we have

$$\frac{dZ_1(t)}{dt} = Z_2(t), \quad (207a)$$

$$\frac{dZ_i(t)}{dt} = A_i(t, Z_1(t), \dots, Z_n(t)) + B_i(t, Z_1(t), \dots, Z_n(t)), \quad \text{for } i \geq 2. \quad (207b)$$

This corresponds, for example, to descriptions where Z_1 is a particle position (i.e. $Z_1 = x_p$) while Z_2 represents its velocity (i.e. $Z_2 = U_p$), its temperature (i.e. $Z_2 = T_p$) or any particle-attached variable that is of importance for the physical case considered. In consequence, this situation includes the probabilistic description of particle dynamics in turbulent flows from a kinetic point of view, as described in Section 7.3.2. Indeed, if we consider a simple particle momentum equation with only a drag force term, we have (using a one-dimensional setting for the sake of simplicity)

$$\frac{dx_p(t)}{dt} = U_p(t), \quad (208a)$$

$$\frac{dU_p(t)}{dt} = -\frac{U_p(t)}{\tau_p} + \frac{1}{\tau_p} U_f(t, x_p(t)). \quad (208b)$$

The important characteristic of kinetic PDF approaches is to treat the second term on the rhs of Eq. (208b), which is the velocity of the fluid at the particle position, as an external noise term. Using present notations, this means that we have $Z_1 = x_p$, $Z_2 = U_p$, $A_2 = -Z_2/\tau_p$ and $\xi_2(t) = U_f(t, x_p(t))$ with $B_{22} = 1/\tau_p$. It is thus seen that the specific structure considered in this section is fairly general and encompasses kinetic approaches to particle systems in random media which model particles as a dynamical system influenced by external Gaussian colored noises representing the effects of these random media.

In the present case, the matrix \mathbf{B} has the form

$$\mathbf{B} = \begin{pmatrix} 0 & 0 & \dots & 0 \\ 0 & B_{11}^r & \dots & B_{1,n-1}^r \\ \vdots & \vdots & & \vdots \\ 0 & B_{n-1,1}^r & \dots & B_{n-1,n-1}^r \end{pmatrix} \quad (209)$$

where B_{kl}^r denotes the reduced matrix whose components are not necessarily zero. Using Eq. (196), \tilde{D}_{ij} becomes

$$\tilde{\mathbf{D}} = \begin{pmatrix} 0 & \tilde{D}_{21} & \dots & \tilde{D}_{n1} \\ \tilde{D}_{21} & \tilde{D}_{22} & \dots & \tilde{D}_{2n} \\ \vdots & \vdots & & \vdots \\ \tilde{D}_{n1} & \tilde{D}_{n2} & \dots & \tilde{D}_{nn} \end{pmatrix} \quad (210)$$

where we have $\tilde{D}_{11} = 0$. If \tilde{D}_{ij} is to be definite positive, all the symmetrical sub-matrices

$$\tilde{\mathbf{D}}_i^r = \begin{pmatrix} 0 & \tilde{D}_{i1} \\ \tilde{D}_{i1} & \tilde{D}_{ii} \end{pmatrix} \quad (211)$$

must also be positive definite. Yet, their determinant is negative, $\det(\tilde{\mathbf{D}}_i^r) = -(\tilde{D}_{i1})^2 \leq 0$, showing that they have always one negative eigenvalue. For the definite positive property to be satisfied, we must be in the degenerate situation where these

negative eigenvalues become zero. This imposes that we must have $\tilde{D}_{i1}(t, \mathbf{z}) = B_{ik}(t, \mathbf{z})\lambda_{k1}(t, \mathbf{z}) = 0, \forall i = 2, \dots, n, \forall \mathbf{z}$, and regardless of the matrix coefficients $B_{ik}(t, \mathbf{z})$. On the other hand, when the coefficients of \mathbf{B} are independent of \mathbf{z} , we get from Eq. (196) and Eq. (193),

$$\langle \tilde{D}_{i1}(t, \mathbf{z}) \rangle = \langle Z_1 (B_{il}\xi_l) \rangle \quad (212)$$

which represent the correlations between the (position-like) variable Z_1 on which there is no explicit noise with the combined noises $\tilde{\xi}_i = B_{il}\xi_l$ acting on the various (velocity-like) variables Z_i with $i \geq 2$. Note that since $dZ_1/dt = Z_2$, all the variables Z_i with $i \geq 2$ appear as the ‘derivatives’ of Z_1 , which explains this terminology. Each combined noise $\tilde{\xi}_i$ is also given by a OU process

$$d\tilde{\xi}_i(t) = -\frac{\tilde{\xi}_i(t)}{\tau} dt + \sigma B_{il} dW_l(t), \quad (213)$$

with $(W_l)_{l=1,n}$ the same Wiener processes as in Eq. (184). At equilibrium where we have $d\langle Z_1 \tilde{\xi}_i \rangle / dt = 0$, the correlations are easily derived as $\langle Z_1 \tilde{\xi}_i \rangle = \tau \langle Z_2 \tilde{\xi}_i \rangle (i \geq 2)$ and further equilibrium estimations of $\langle Z_2 \tilde{\xi}_i \rangle$ lead to

$$\langle Z_1 \tilde{\xi}_i \rangle = \tau^2 [\langle A_2 \tilde{\xi}_i \rangle + \langle \tilde{\xi}_2 \tilde{\xi}_i \rangle] \quad (214)$$

where the term in brackets on the rhs is only dependent on the state variables (Z_2, \dots, Z_n) on which the external noises are acting through the (reduced) matrix \mathbf{B}^r . Since $\langle \tilde{\xi}_2 \tilde{\xi}_i \rangle = (BB^\perp)_{2i} \langle \xi^2 \rangle$, we can estimate that this term scales as the noise energy $\langle \xi^2 \rangle$, from which it follows that

$$\langle Z_1 \tilde{\xi}_i \rangle = \tau^2 \langle \xi^2 \rangle \times \mathcal{O}(1), \quad \forall i \geq 2. \quad (215)$$

To avoid considering only equilibrium states, it is possible to work out a direct estimation. The condition $\tilde{D}_{i1}(t, \mathbf{z}) = B_{ik}(t, \mathbf{z})\lambda_{k1}(t, \mathbf{z}) = 0, \forall i = 2, \dots, n$ and $\forall B_{ik}$ implies that we must have $\lambda_{k1} = 0, \forall k = 2, \dots, n$. Going back to the expression in Eq. (191), this means that

$$\int_0^t \langle \xi_k(t) \tilde{\xi}_k(t') \rangle \left\langle \frac{\delta Z_1(t)}{\delta \xi_k(t')} \right\rangle |(t, \mathbf{z}) dt' = 0, \quad (216)$$

(no summation on k), $\forall k \geq 2$ and $\forall i \geq 2$. Since $dZ_1/dt = Z_2$, we can expect the functional derivatives to be dominated by the noises entering the evolution equation of Z_2 . Then, as physical systems have generally relaxation terms, we introduce T_2 the characteristic correlation timescale of Z_2 . As the result must be obtained regardless of the coefficients $B_{k1}(t, \mathbf{z})$ and $B_{2k}(t', \mathbf{z}')$, this shows that we must have

$$\forall k, \quad \langle \xi^2 \rangle \int_0^t e^{-(t-t')/\tau} \left\langle \frac{\delta Z_1(t)}{\delta \xi_k(t')} \right\rangle dt' = 0. \quad (217)$$

The ‘faster’ response term can be estimated as

$$\left\langle \frac{\delta Z_1(t)}{\delta \xi_k(t')} \right\rangle \simeq T_2 [1 - \exp(-(t-t')/T_2)] \quad (218)$$

which yields again the same scaling since

$$\langle \xi^2 \rangle \int_0^t e^{-(t-t')/\tau} \left\langle \frac{\delta Z_1(t)}{\delta \xi_k(t')} \right\rangle dt' \simeq \tau^2 \langle \xi^2 \rangle \times \frac{T_2}{T_2 + \tau}. \quad (219)$$

As a result, we obtain from these direct estimations that the coefficients λ_{k1} scale as

$$\lambda_{k1} \sim \tau^{m(k)} \langle \xi^2 \rangle \quad (220)$$

where $m(k)$ is an integer whose value depend on k and on the characteristics of the dynamical system (that is the specific choices of \mathbf{A} and \mathbf{B}) but is such that $m(k) \geq 2, \forall k$.

From all these estimations, it is concluded that to ensure that \tilde{D}_{ij} has only positive or null eigenvalues, we must again take the white-noise limit, $\tau \rightarrow 0$ with $\tau \langle \xi^2 \rangle$ being constant, as in the first case studied above.

Summary. From the developments of this section, it follows that white-noise processes play a central role in the formulation of complete and well-posed probabilistic descriptions of dynamical systems. Since white noises are mathematical idealizations of stochastic processes whose fluctuations become infinitely rapid, this is connected to the notion of fast variables and, in particular, to what is referred to as ‘the elimination of fast variables’. The consequences on the selection of the variables retained to properly describe a dynamical system in a probabilistic sense are addressed in Section 9.4 but the technical aspects and the physical ideas that underlie this notion of fast-variable elimination must be first investigated.

9.3. Adiabatic elimination of fast variables

For the simple Langevin (or OU) process considered in Eq. (184), a key aspect of the fast-variable elimination is already manifested by the special limit given by Eq. (204). This is in line with the general but heuristic formulation of fast-variable elimination proposed, for example, in [1, section 4] and whose outline is worth recalling in order to introduce the more detailed developments described below. To that effect, we consider a stochastic process X whose time-rate of change is a stationary stochastic process Y with an integral timescale noted T_Y . This means that we have

$$\frac{dX(t)}{dt} = Y(t), \quad \text{with} \quad \langle Y(t)Y(t+s) \rangle = \langle Y^2 \rangle R_Y(s) \quad (221)$$

where the variance $\langle Y^2 \rangle$ is constant in time and $R_Y(s)$ is the auto-correlation function of Y . Then, straightforward manipulations show that (see [1, section 4])

$$\langle X^2(t) \rangle \simeq \langle Y^2 \rangle \times t^2 \quad \text{if } t \ll T_Y \quad (222a)$$

$$\langle X^2(t) \rangle \simeq 2(\langle Y^2 \rangle T_Y) \times t \quad \text{if } t \gg T_Y \quad (222b)$$

while the behavior of $\langle X^2(t) \rangle$ in the intermediate time range (*i.e.* when $t \sim T_Y$) is dependent upon the specific form of the auto-correlation function $R_Y(s)$. As in Eq. (204), the manifestation of the white-noise limit is translated here into the condition that $T_Y \rightarrow 0$ while $\langle Y^2 \rangle \rightarrow \infty$ in such a way that $\lim(\langle Y^2 \rangle T_Y)$ is a finite and positive constant K , so that the modeling step consists in approximating the increments of X by a random-walk

$$dX(t) \simeq \sqrt{2K} dW(t). \quad (223)$$

From an intuitive point of view, this summary corresponds to the approach put forward in [1] to apply the notions of synergetics (see [157]) and fast-variable elimination to fluid- and discrete-particle PDF modeling. Yet, in a more formal approach, it is best to express these ideas by introducing a precise parametrization of the basic equations in order to give a rigorous sense to the above limit. Such a mathematically well-defined parametrization is also needed to obtain the correct diffusive limit in the case of space-dependent drift and diffusion coefficients, as will be shown below. However, various parametrizations have been proposed in the literature and, at first sight, it is not clear whether these formulations lead to the same result or correspond to intrinsically different formulations of rapidly-varying stochastic processes. It is thus useful to take up the question of the fast-variable elimination and to address in detail the meaning of the above limits. This is the purpose of the present section. More precisely, the aims of this section are:

- (1) To bring out the meaning of the fast-variable elimination;
- (2) To clarify the relations between the different ways to parametrize dynamical systems;
- (3) To show that, in the general case of non-homogeneous stochastic processes, only one approach remains valid and therefore should be used;
- (4) To pave the way for the discussions of PDF models of disperse two-phase flows that are developed in Section 10.

To express the main ideas in a physically-meaningful approach, it is best to consider a practical situation and, for that purpose, the important notions are illustrated with the canonical Langevin model of discrete particle dynamics. Then, the two typical formulations of the white-noise limit that can be found in the literature are discussed: first, for the over-damped Langevin model in the simple constant-coefficient case in Section 9.3.1 and, second, for an extended case in Section 9.3.2. The most general form of the over-damped Langevin limit is worked out in Section 9.3.3 with a new formulation that does not make use of the operator formalism. In Section 9.3.4, the important consequence of the fluid incompressibility on the over-damped limit model is analyzed while a detailed study of how such ideas can be applied for the general case of non-homogeneous turbulent flows is developed in Section 9.3.5.

9.3.1. Canonical overdamped Langevin model

The simplest Langevin model for particle transport corresponds to a kinematic approach where particles are described by their position X and velocity U which, in a one-dimensional setting, are the solutions of the following equations of motion:

$$dX(t) = U(t) dt, \quad (224a)$$

$$dU(t) = -\frac{U(t)}{T} dt + \sigma dW(t). \quad (224b)$$

In Eq. (224b), the drift coefficient is a return-to-equilibrium term written with a constant timescale T and σ is the constant diffusion coefficient of the OU process used to simulate particle velocities. This corresponds to the classical Langevin model for colloidal or Brownian particles in a fluid at rest, in which case T is the particle relaxation timescale τ_p in the Stokes regime and σ is easily obtained from the equipartition of energy and the usual fluctuation-dissipation relation as $\sigma = \sqrt{2k_B \Theta_f / (m_p \tau_p)}$. This corresponds also to the formulation of the simple Langevin model for (notional) fluid particles in the PDF approach to single-phase flow turbulence (see Section 6), considered here for a stationary isotropic turbulent flow, in which case T is the Lagrangian timescale T_L and σ is expressed as $\sigma = \sqrt{2\langle u^2 \rangle / T_L}$ from the same application of

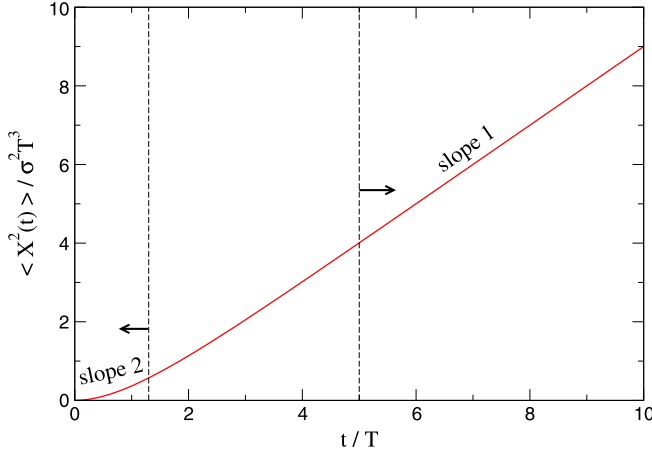


Fig. 52. Profile of the position normalized variance $\langle X^2(t) \rangle / (\sigma^2 T^3)$ for the canonical model as a function of the normalized time t/T , showing the initial scaling as t^2 in the short-time limit (i.e. $t \ll T$) and the linear behavior in t in the long-time limit (i.e. $t \gg T$).

the fluctuation-dissipation relation with $\langle u^2 \rangle$ the constant value of the fluid kinetic energy in one direction. More generally, Eqs. (224) can be seen as representing a class of models where the process of interest, here X , is governed by a colored noise, here U , whose timescale is T and whose energy becomes equal to the constant value $\langle U(t)^2 \rangle = \sigma^2 T/2$ after a possible transient time.

The expression of the second-order moments of the joint process (X, U) can be found in [44, section 4.1] for the general case when there is a transient period depending on the initial conditions $(X(0), U(0))$. However, for the sake of simplicity and without any loss of generality for the present analysis, it is sufficient to consider that the initial conditions are such that statistical equilibrium is reached right from the outset. This is simply done by choosing $U(0)$ as a centered Gaussian random variable with a variance equal to $\langle U(0)^2 \rangle = \sigma^2 T/2$, while $X(0)$ can be taken as the origin (i.e. $X(0) = 0$), which means that $X(t)$ stands now for particle increments or displacements. This represents a classical point-source dispersion problem. Then, simple manipulations of the stochastic integrals, or integration of the velocity auto-correlation function (see [30, section 12.4]), show that the particle position variance is

$$\langle X^2(t) \rangle = (\sigma T)^2 \{t - T[1 - \exp(-t/T)]\} \quad (225)$$

or, in terms of non-dimensional quantities,

$$\frac{\langle X^2(t) \rangle}{\sigma^2 T^3} = \frac{t}{T} - [1 - \exp(-t/T)] \quad (226)$$

whose profile as a function of t/T is plotted in Fig. 52.

In Fig. 52, it is seen that, for small time intervals (the short-time limit when $t \ll T$), there is always a regime where the increments of particle positions vary as $\langle X^2(t) \rangle \sim t^2$, which is an indication that the particle velocity is still a finite-variance process (loosely speaking, particle velocities still ‘exists’). It is also seen in Fig. 52 that, for long time intervals (the long-time limit when $t \gg T$), there is always a regime where the increments of particle positions vary as $\langle X^2(t) \rangle \sim t$, which is the statistical signature of a white-noise behavior of particle velocities. This is in keeping with the general limits expressed in Eqs. (222). The leading idea is that, for small values of the characteristic timescale T , the diffusive limit (or ‘long-time limit’) is reached very quickly so that the random-walk approximation already given in Eq. (223) should be valid for nearly all values of t . Note that we have here $(\sigma T)^2 = 2\langle U(t)^2 \rangle T$, with U playing the role of the general process Y in Eq. (221) and thus with $T = T_Y$, in line with the notations in Eq. (223).

The issue is to formalize these ideas by a proper parametrization of the basic equations, Eqs. (224), and, in particular, to indicate how particle velocities behave when their integral timescale becomes very small. In the literature, this can be found under two apparently-different formulations which are now presented.

Finite velocity variance and time rescaling. In the first formulation, a small parameter χ is introduced in the equations of the canonical Langevin model, Eqs. (224), under the form:

$$dX^{(\chi)}(t) = U^{(\chi)}(t) dt, \quad (227a)$$

$$dU^{(\chi)}(t) = -\frac{U^{(\chi)}(t)}{\chi T} dt + \frac{\sigma}{\sqrt{\chi}} dW(t). \quad (227b)$$

This parametrization is referred to as (P1) and is the formulation usually found in the literature dedicated to the study of the over-damped Langevin limit. Since the coefficients are constant, the trajectories of the process $(X^{(\chi)}, U^{(\chi)})$ are easily

integrated, which gives

$$U^{(\chi)}(t) = U(0)e^{-t/\chi T} + \frac{\sigma}{\sqrt{\chi}} e^{-t/\chi T} \int_0^t e^{s/\chi T} dW(s), \quad (228a)$$

$$X^{(\chi)}(t) = X(0) + \chi U(0)T [1 - e^{-t/\chi T}] + \sqrt{\chi} \sigma T \int_0^t [1 - e^{-(t-s)/\chi T}] dW(s), \quad (228b)$$

with $(X(0), U(0))$ the initial conditions. From these integrated forms, several limits can be taken. First, it is readily seen that, if we take the limit $\chi \rightarrow 0$ in real time t , we have

$$X^{(\chi)}(t) \xrightarrow{\chi \rightarrow 0} X(0), \quad (229)$$

showing that the effects of the fluctuating velocities have completely vanished and that particles remain at a standstill at their initial positions. At the same time, it is interesting to note that the parametrization of the drift and diffusion coefficients chosen in Eqs. (227) implies that particle velocities remain at the same energetic level. Indeed, applying Ito's calculus to Eq. (227b) gives that

$$\frac{d \langle (U^{(\chi)}(t))^2 \rangle}{dt} = \frac{1}{\chi} \left(-\frac{2 \langle (U^{(\chi)}(t))^2 \rangle}{T} + \sigma^2 \right) = 0. \quad (230)$$

Therefore, $\langle (U^{(\chi)}(t))^2 \rangle$ has the same value as $\langle (U(t))^2 \rangle$ in the original Langevin model in Eq. (224b), namely $\langle (U^{(\chi)}(t))^2 \rangle = \langle (U(t))^2 \rangle = \sigma^2 T/2$. In other words, if the fluctuation-dissipation relation is satisfied by the initial model in Eqs. (224), it remains valid for its parametrized version (P1), whatever the choice of the parameter χ . In the limit $\chi \rightarrow 0$, it is seen that $U^{(\chi)}(t)$ tends towards a process having a finite variance independent of χ but with a vanishing timescale χT . It is thus not surprising that, in this limit, the uncorrelated but with-a-fixed-thermostat-valued fluctuations of $U^{(\chi)}(t)$ have a vanishing effect on $X^{(\chi)}(t)$. However, a second limit of the integrated trajectory equations in Eqs. (228) can be taken once time is rescaled. Indeed, if we consider particle positions at the rescaled time $t/\chi, X^{(\chi)}(t/\chi)$, then we have

$$\begin{aligned} X^{(\chi)}(t/\chi) &= X(0) + \chi U(0)T [1 - e^{-t/\chi^2 T}] + \sqrt{\chi} \sigma T \int_0^{t/\chi} [1 - e^{-(t-\chi s)/\chi^2 T}] dW(s), \\ &= X(0) + \chi U(0)T [1 - e^{-t/\chi^2 T}] + \sqrt{\chi} \sigma T \int_0^t [1 - e^{-(t-u)/\chi^2 T}] dW(u/\chi). \end{aligned} \quad (231)$$

Since we are essentially concerned with weak approximations, or convergence of stochastic processes in law, we can use that $\sqrt{\chi} W(u/\chi)$ is also a Wiener process, that is $\sqrt{\chi} dW(u/\chi) \equiv d\tilde{W}(u)$ where $\tilde{W}(u)$ is another Wiener process. This gives for the particle positions (keeping the notation $dW(u)$ instead of $d\tilde{W}(u)$ for the sake of simplicity)

$$X^{(\chi)}(t/\chi) = X(0) + \chi U(0)T [1 - e^{-t/\chi^2 T}] + \sigma T \int_0^t [1 - e^{-(t-u)/\chi^2 T}] dW(u), \quad (232)$$

which shows that we retrieve the pure diffusive limit for particle positions, since

$$X^{(\chi)}(t/\chi) \xrightarrow{\chi \rightarrow 0} X(0) + (\sigma T) W(t), \quad (233)$$

also expressed by the random-walk approximation

$$\lim_{\chi \rightarrow 0} dX^{(\chi)}(t/\chi) = (\sigma T) dW(t). \quad (234)$$

This is the classical result put forward in the literature. Using the same approximation in law, it is interesting to note that

$$U^{(\chi)}(t/\chi) = U(0)e^{-t/\chi^2} + \frac{\sigma T}{\chi} \int_0^t e^{-(t-u)/\chi^2 T} dW(u), \quad (235)$$

from which it results that $U^{(\chi)}(t/\chi)$ has a vanishing correlation timescale, i.e. $\chi^2 T$ (compared to χT for $U^{(\chi)}(t)$) and a finite variance, $\sigma^2 T/2$, which is consistent with the reasoning above.

There is, however, another possibility for the parametrization of the equations of the canonical Langevin model. *Infinite velocity variance in real time.* In the second formulation, a small parameter χ is still introduced in the equations of the same Langevin model, Eqs. (224), but with a different scaling of the diffusion coefficient. For this second parametrization, referred to as (P2), we consider the following equations:

$$dX^{(\chi)}(t) = U^{(\chi)}(t) dt, \quad (236a)$$

$$dU^{(\chi)}(t) = -\frac{U^{(\chi)}(t)}{\chi T} dt + \frac{\sigma}{\chi} dW(t). \quad (236b)$$

The integrated trajectories of the process $(X^{(\chi)}, U^{(\chi)})$ are now given by

$$U^{(\chi)}(t) = U(0)e^{-t/\chi T} + \frac{\sigma}{\chi} e^{-t/\chi T} \int_0^t e^{s/\chi T} dW(s), \quad (237a)$$

$$X^{(\chi)}(t) = X(0) + \chi U(0)T [1 - e^{-t/\chi T}] + \sigma T \int_0^t [1 - e^{-(t-s)/\chi T}] dW_s. \quad (237b)$$

When $\chi \rightarrow 0$, we can take the limit in real time t (that is without any time rescaling operation), which yields directly that

$$X^{(\chi)}(t) \xrightarrow{\chi \rightarrow 0} X(0) + (\sigma T) W(t), \quad (238)$$

or, in terms of the SDE for particle positions, that we can write

$$\lim_{\chi \rightarrow 0} dX^{(\chi)}(t) = (\sigma T) dW(t). \quad (239)$$

It is also immediate that the particle velocity variance has a stationary value (in time) that depends explicitly on the chosen parameter χ . This is obtained, for example, by writing the evolution equation for $\langle (U^{(\chi)}(t))^2 \rangle$

$$\frac{d \langle (U^{(\chi)}(t))^2 \rangle}{dt} = -\frac{2 \langle (U^{(\chi)}(t))^2 \rangle}{\chi T} + \frac{\sigma^2}{\chi^2}, \quad (240)$$

which shows that, at equilibrium, $\langle (U^{(\chi)}(t))^2 \rangle = \sigma^2 T/(2\chi)$. In that sense, the particle kinetic energy grows unbounded as $\chi \rightarrow 0$ and behaves as $1/\chi$ in that limit. However, the auto-correlation timescale of $U^{(\chi)}(t)$ is $T_{U^{(\chi)}} = \chi T$ showing that

$$\lim_{\chi \rightarrow 0} \langle (U^{(\chi)}(t))^2 \rangle \times T_{U^{(\chi)}} = \frac{1}{2} \sigma^2 T^2 \quad (241)$$

which remains finite. This result reveals that the parametrization (P2) is in line with the general ideas recalled at the beginning of Section 9.3.

If we compare the end result on particle positions, that is Eq. (234) with Eq. (239), it is seen that the same diffusive limit is retrieved. More precisely, if we note $X^{(P1,\chi)}(t)$ and $X^{(P2,\chi)}(t)$ the solutions of the parametrization (P1) and (P2) respectively, we have

$$\lim_{\chi \rightarrow 0} X^{(P1,\chi)}(t/\chi) = \lim_{\chi \rightarrow 0} X^{(P2,\chi)}(t), \quad (242)$$

where, once again, the identity is to be understood as an identity in law. However, in the two formulations, the roads towards that limit appear as rather different and it is worth clarifying whether (P1) and (P2) are equivalent for all situations.

9.3.2. Relations and differences between various parametrizations

From a more qualitative standpoint, the different ideas behind the two parametrizations (P1) and (P2) can be understood by looking at Fig. 52.

For (P1), the choice is to keep particle velocities at a constant energy level (with respect to variations of χ), in line with the usual notions of classical (equilibrium) statistical physics and the equipartition of energy at a given temperature. Then, the decrease of the velocity auto-correlation timescale of the parametrized process (P1) is compensated by stretching time: in a way, this time rescaling allows us to step over the intermediate regime and be directly in the ‘long-time limit’, as explained at the beginning of Section 9.3.

For (P2), we observe the process in real time t but expect the ‘long-time limit’ to be reached before that time t . This implies that particle velocity becomes a white-noise process with unbounded energy (when $\chi \rightarrow 0$) but whose cumulative effects on particle position gives a diffusive behavior as soon as $t > 0$, for sufficiently small values of χ .

For the canonical Langevin model in Eqs. (224), this reasoning can be given a more quantitative flavor. Indeed, from the developments above, it appears that there are two important combinations of the drift and diffusion coefficients of Eq. (224b): the first one is $\sigma^2 T$, which governs the equilibrium level of the particle kinetic energy; the second one is σT , which governs the particle diffusion coefficient (that is the diffusion of particle positions). When both T and σ are parametrized and become functions of a small parameter χ , it is not possible to keep both factors constant. It can be seen that (P1) is based on the respect of the first combination, yielding a constant particle energy (with regard to χ) and requiring time rescaling, while for (P2) the emphasis is put on the respect of the second combination, leading to a proper diffusion limit behavior for particle positions in real time but with a resulting unbounded particle kinetic energy level.

In spite of the different philosophies behind (P1) and (P2), it can be shown that, for special evolution equations, the two approaches are equivalent. To demonstrate this correspondence, we consider a more realistic particle system whose form is (still using a one-dimensional setting for the sake of simplicity and without loss of generality):

$$dX(t) = U(t) dt, \quad (243a)$$

$$dU(t) = F(X(t)) dt - \frac{U(t)}{T(X(t))} dt + \sigma(X(t)) dW(t). \quad (243b)$$

This system refers, for example, to a particle transport model in inhomogeneous fluid flows where the friction term and the diffusion coefficient are space dependent. A deterministic force, $F(X_t)$, has been added but it is worth noting that, if all these terms are variable in space, there is no explicit dependence on time. In other words, we are considering a particle transport model in stationary environments. This point will resurface below.

Directly extending what was done for the canonical Langevin model, the parametrization (P1) consists in introducing a small parameter χ and in considering the solution $(X^{(\chi)}, U^{(\chi)})$ of the following SDEs:

$$dX^{(\chi)}(t) = U^{(\chi)}(t) dt, \quad (244a)$$

$$dU^{(\chi)}(t) = F(X^{(\chi)}(t)) dt - \frac{U^{(\chi)}(t)}{\chi T(X^{(\chi)}(t))} dt + \frac{\sigma(X^{(\chi)}(t))}{\sqrt{\chi}} dW_t. \quad (244b)$$

Then, the time-stretching operation is applied by defining $X_{(\chi)}(t) = X^{(\chi)}(t/\chi)$ and $U_{(\chi)}(t) = U^{(\chi)}(t/\chi)$. It follows that the rescaled joint process $(X_{(\chi)}, U_{(\chi)})$ is the solution of

$$dX_{(\chi)}(t) = \frac{1}{\chi} U_{(\chi)}(t) dt, \quad (245a)$$

$$dU_{(\chi)}(t) = \frac{1}{\chi} F(X_{(\chi)}(t)) dt - \frac{U_{(\chi)}(t)}{\chi^2 T(X_{(\chi)}(t))} dt + \frac{\sigma(X_{(\chi)}(t))}{\sqrt{\chi}} dW_{t/\chi}, \quad (245b)$$

which, using the same equivalence in law $\sqrt{\chi} W_{t/\chi} \equiv W_t$, can be written as

$$dX_{(\chi)}(t) = \frac{1}{\chi} U_{(\chi)}(t) dt, \quad (246a)$$

$$dU_{(\chi)}(t) = \frac{1}{\chi} F(X_{(\chi)}(t)) dt - \frac{U_{(\chi)}(t)}{\chi^2 T(X_{(\chi)}(t))} dt + \frac{\sigma(X_{(\chi)}(t))}{\chi} dW_t. \quad (246b)$$

Then, we define the new particle velocity $\tilde{U}_{(\chi)}(t) = 1/\chi U_{(\chi)}(t)$ to obtain

$$dX_{(\chi)}(t) = \tilde{U}_{(\chi)}(t) dt, \quad (247a)$$

$$d\tilde{U}_{(\chi)}(t) = \frac{1}{\chi^2} F(X_{(\chi)}(t)) dt - \frac{\tilde{U}_{(\chi)}(t)}{\chi^2 T(X_{(\chi)}(t))} dt + \frac{\sigma(X_{(\chi)}(t))}{\chi^2} dW_t. \quad (247b)$$

On the other hand, the parametrization (P2) consists in multiplying all the terms on the rhs of Eq. (243b) by the inverse of a small parameter. This means that we are now handling the solution $(X^{(\chi)}, U^{(\chi)})$ of the system equations

$$dX^{(\chi)}(t) = U^{(\chi)}(t) dt, \quad (248a)$$

$$dU^{(\chi)}(t) = \frac{1}{\chi} F(X^{(\chi)}(t)) dt - \frac{U^{(\chi)}(t)}{\chi T(X^{(\chi)}(t))} dt + \frac{\sigma(X^{(\chi)}(t))}{\chi} dW_t. \quad (248b)$$

Comparing Eqs. (247) to Eqs. (248), it is obvious that the two parametrizations are equivalent and that there is an explicit correspondence between $(X_{(\chi)}, 1/\chi U_{(\chi)})$ in (P1) and $(X^{(\chi)}, U^{(\chi)})$ for (P2). Using notations similar to the ones introduced in Eq. (242) for the limit process on particle positions, we can express this link by writing

$$\lim_{\chi \rightarrow 0} X_{(P1, \chi)}(t) = \lim_{\chi \rightarrow 0} X^{(P1, \chi)}(t/\chi) = \lim_{\chi \rightarrow 0} X_t^{(P2, \chi^2)}, \quad (249)$$

accounting for the fact that χ in the (P1) formulation appears as χ^2 in the (P2) one.

This correspondence brings out that the apparent manipulation of particle velocities with a constant energy level (with respect to χ) in (P1), for example in the canonical Langevin model in Section 9.3.1, is something of an artifact. Indeed, Eq. (247a) reveals that the effective convective velocity is actually $\tilde{U}_{(\chi)}$, which depends explicitly on χ . Therefore, we have $\langle (\tilde{U}_{(\chi)})^2 \rangle \sim 1/\chi^2$ while the ‘real’ auto-correlation timescale is $T_{\tilde{U}_{(\chi)}} \sim \chi^2$ and we find again that the ‘real-velocity’ variance grows unbounded (in χ) while its timescale goes to zero in such a way that the product, $\langle (\tilde{U}_{(\chi)})^2 \rangle \times T_{\tilde{U}_{(\chi)}}$, remains a constant which is the transport coefficient and, in the present case, the particle diffusion coefficient. Consequently, there is actually only one way to take the limit.

Differences in the general case. At this point, it can be thought that, whatever the basic particle model, the two formulations are equivalent and result in the same over-damped limit through different manipulations. This is true but insofar as systems such as the one in Eqs. (243) are considered. It is, however, essential to note that this represents an homogeneous stochastic model where the drift and diffusion coefficients are space dependent but time invariant, whereas a more general system is

$$dX(t) = U(t) dt, \quad (250a)$$

$$dU(t) = F(t, X(t)) dt - \frac{U(t)}{T(t, X(t))} dt + \sigma(t, X(t)) dW(t), \quad (250b)$$

where the drift and diffusion coefficients in Eq. (250b) depend not only on particle location but also on time. In that case, the parametrization (P1) implies to handle terms such as $F(t/\chi, X_{(\chi)})$, which become meaningless when $\chi \rightarrow 0$ or amounts to considering only infinite-time limits, such as $F(+\infty, X(t))$, provided that such limits exist. Clearly, the approach (P1) cannot be applied for these general space- and time-dependent particle systems. However, it was shown in Sections 6 and 7 that this is precisely the form under which particle statistical models are developed for general turbulent single- and two-phase flows. For example, the GLM introduced in Section 6.5.1 means that $F(t, X(t)) = \langle U_f(t, X(t)) \rangle / T(t, X(t))$ in Eq. (250b).

This situation is an illustration of the new issues brought by statistical models for particles in turbulent flows and exemplifies the need to extend the techniques used for classical (equilibrium) statistical physics. In practice, this leaves only the formulation (P2) as the correct approach to work out the limit of general over-damped Langevin models.

9.3.3. General over-damped Langevin model

We consider a particle system for the joint process (\mathbf{X}, \mathbf{U}) in a multi-dimensional space (typically, a three-dimensional space) with a Langevin form, that is

$$dX_i(t) = U_i(t) dt, \quad (251a)$$

$$dU_i(t) = G_{ij}(t, \mathbf{X}(t)) [U_j - \Phi_j(t, \mathbf{X}(t))] dt + \sigma_{ij}(t, \mathbf{X}(t)) dW_j \quad (251b)$$

where $\Phi(t, \mathbf{x})$ is a known, time- and space-dependent field and with the assumption that the ‘friction matrix’ G_{ij} can be inverted. Then, applying (P2), we introduce the system

$$dX_i^{(\chi)}(t) = U_i^{(\chi)}(t) dt, \quad (252a)$$

$$dU_i^{(\chi)}(t) = \frac{1}{\chi} G_{ij}(t, \mathbf{X}^{(\chi)}(t)) [U_j^{(\chi)}(t) - \Phi_j(t, \mathbf{X}^{(\chi)}(t))] dt + \frac{1}{\chi} \sigma_{ij}(t, \mathbf{X}^{(\chi)}(t)) dW_j, \quad (252b)$$

and the aim is to derive the resulting model on particle positions when $\chi \rightarrow 0$.

By applying the inverse matrix \mathbf{G}^{-1} to Eq. (252b) and using Eq. (252a), we get

$$\chi G_{ik}^{-1} dU_k = dX_i - \Phi_i dt + (G^{-1} \sigma)_{il} dW_l, \quad (253)$$

where the explicit dependence on $(t, \mathbf{X}^{(\chi)}(t))$ is skipped in the notations of \mathbf{G} , Φ and σ , for the sake of simplicity. Then, by integrating Eq. (253) by parts, we obtain

$$\chi G_{ik}^{-1} dU_k^{(\chi)} = \chi d(G_{ik}^{-1} U_k^{(\chi)}) - \chi U_k^{(\chi)} d(G_{ik}^{-1}), \quad (254)$$

$$= \chi d(G_{ik}^{-1} U_k^{(\chi)}) - \chi U_k^{(\chi)} \frac{\partial G_{ik}^{-1}}{\partial t} dt - \chi U_k^{(\chi)} \frac{\partial G_{ik}^{-1}}{\partial x_j} dX_j^{(\chi)}, \quad (255)$$

$$= \chi d(G_{ik}^{-1} U_k^{(\chi)}) - \chi U_k^{(\chi)} \frac{\partial G_{ik}^{-1}}{\partial t} dt - \chi \frac{\partial G_{ik}^{-1}}{\partial x_j} U_k^{(\chi)} U_j^{(\chi)} dt, \quad (256)$$

and we have to study the limits of χU_k and $\chi U_k U_j$. Note that there are no additional Ito terms in the expression of $d(G_{ik}^{-1})$ as there is no explicit white-noise terms entering Eq. (252a). On the other hand, the derivation of $d(U_k U_j)$ does require Ito’s calculus, which yields that

$$\begin{aligned} \chi^2 d(U_k^{(\chi)} U_j^{(\chi)}) &= \chi G_{kl} (U_l^{(\chi)} - \Phi_l) U_j^{(\chi)} dt + \chi G_{jl} (U_l^{(\chi)} - \Phi_l) U_k^{(\chi)} dt \\ &\quad + (\sigma \sigma^\perp)_{kj} dt + \chi U_j^{(\chi)} \sigma_{kl} dW_l + \chi U_k^{(\chi)} \sigma_{jl} dW_l, \end{aligned} \quad (257)$$

and which, by re-organizing the different terms in terms of the successive products of the particle velocities, is rewritten as

$$\begin{aligned} \chi^2 d(U_k^{(\chi)} U_j^{(\chi)}) &= (\sigma \sigma^\perp)_{kj} dt + \chi G_{kl} U_l^{(\chi)} U_j^{(\chi)} dt + \chi G_{jl} U_l^{(\chi)} U_k^{(\chi)} dt \\ &\quad - \chi U_j^{(\chi)} G_{kl} \Phi_l dt - \chi U_k^{(\chi)} G_{jl} \Phi_l dt + \chi U_j^{(\chi)} \sigma_{kl} dW_l + \chi U_k^{(\chi)} \sigma_{jl} dW_l. \end{aligned} \quad (258)$$

When $\chi \rightarrow 0$, the only meaningful limit in Eq. (258) is obtained when, apart from the constant diffusion term (i.e. $(\sigma \sigma^\perp)_{kj}$), $\lim_{\chi \rightarrow 0} (\chi U_k^{(\chi)} U_j^{(\chi)})$ tend towards finite and non-necessarily zero values. This means that $U_k^{(\chi)} \sim 1/\sqrt{\chi}$ and, thus, that $\chi U_k^{(\chi)} \rightarrow 0$ and $\chi^2 U_k^{(\chi)} U_j^{(\chi)} \rightarrow 0$. Note that this is, of course, the scaling of the parametrization (P2) for the canonical Langevin model in Section 9.3.1. This suggests to define the matrix A_{ij} by

$$A_{ij} = \lim_{\chi \rightarrow 0} (\chi U_k^{(\chi)} U_j^{(\chi)}). \quad (259)$$

Then, by taking the limit $\chi \rightarrow 0$, it follows that Eq. (258) becomes an algebraic equation, written in matrix notation as

$$\mathbf{GA} + \mathbf{AG}^\perp = -\sigma \sigma^\perp \quad (260)$$

which can have several solutions if no additional constraints are brought in. By taking the limit $\chi \rightarrow 0$ in Eq. (256), it is seen that

$$\lim_{\chi \rightarrow 0} \chi G_{ik}^{-1} dU_k^{(\chi)} = -\frac{\partial G_{ik}^{-1}}{\partial x_j} A_{kj} dt, \quad (261)$$

and, from Eq. (253), we obtain the over-damped Langevin limit model, which consists in a diffusion stochastic model for particle positions, as

$$dX_i = \Phi_i dt - \frac{\partial G_{ij}^{-1}}{\partial x_k} A_{kj} dt - (G^{-1}\sigma)_{ij} dW_j. \quad (262)$$

From Eq. (262), it follows that the diffusion matrix for \mathbf{X} in the corresponding Fokker–Planck equation is, in matrix notation,

$$\mathbf{D} = \frac{1}{2} (\mathbf{G}^{-1}\sigma) (\mathbf{G}^{-1}\sigma)^\perp = \frac{1}{2} \mathbf{G}^{-1}\sigma\sigma^\perp (\mathbf{G}^\perp)^{-1}. \quad (263)$$

Since we are only concerned with weak approximations of stochastic processes, there is no difference between SDEs having different diffusion coefficients corresponding to the same diffusion matrix \mathbf{D} . For this reason, the SDE in Eq. (262) is equivalent to

$$dX_i = \Phi_i dt - \frac{\partial G_{ij}^{-1}}{\partial x_k} A_{kj} dt + (G^{-1}\sigma)_{ij} dW_j. \quad (264)$$

The form in Eq. (264) represents the fast-variable-elimination result for the general system considered in Eqs. (251) with space- and time-dependent drift and diffusion coefficients. It embodies the notions of slow and fast variables since, in the limit when $G_{ij} \rightarrow 0$ (properly expressed with the small parameter χ), the fast-variable $\mathbf{U}(t)$ is eliminated and the noise (represented by $d\mathbf{W}(t)$) is ‘shifted upward’ to the resulting equation of the slow variable $\mathbf{X}(t)$. Note that, in line with the slaving principle where fast variables are governed by slow ones, all the terms appearing on the rhs of Eq. (264) are to be understood as functions of (t, \mathbf{X}) : in other words, the elimination of fast-variables is local in time and in space. At this stage, three remarks are in order.

- (a) The complete expression in Eq. (264) differs from the one derived with the loose approach which consists in directly writing that $dU_i \simeq 0$ in Eq. (251b) and reporting the expression of $U_i dt$ in the particle position equation in Eq. (251a). This intuitive formulation of the ideas of slow and fast variables gives immediately the correct result for constant relaxation timescales and is, therefore, quite attractive. Yet, in the general situation represented by the model in Eqs. (251), this would give

$$dX_i = \Phi_i dt + (G^{-1}\sigma)_{ij} dW_j, \quad (265)$$

and, thus, would miss the second term on the rhs of Eq. (264) that is essential when the incompressibility is taken into account, as will be shown below.

- (b) The second remark is that variants of the above result can be obtained if additional assumptions are made on the system. For example, if we assume that \mathbf{GA} is a symmetrical matrix, then Eq. (260) gives $2\mathbf{GA} = -\sigma\sigma^\perp$ from which we get that $A = -1/2\mathbf{G}^{-1}\sigma\sigma^\perp$ and which also implies that the matrix $\mathbf{G}^{-1}\sigma\sigma^\perp$ should be symmetrical. From the expression of the diffusion matrix \mathbf{D} in Eq. (263), we have then $\mathbf{A} = -\mathbf{DG}^\perp$, which gives

$$dX_i = \Phi_i dt + \frac{\partial G_{ij}^{-1}}{\partial x_k} D_{kl} G_{lj} dt + (G^{-1}\sigma)_{il} dW_l. \quad (266)$$

This is the form derived recently in [158]. Further tedious but straightforward algebraic manipulations lead to the alternative form

$$dX_i = \Phi_i dt + G_{ij}^{-1} \frac{\partial A_{kj}}{\partial x_k} dt + \frac{\partial D_{ik}}{\partial x_k} dt + B_{ij} dW_j, \quad (267)$$

where \mathbf{B} is a matrix such that $\mathbf{BB}^\perp = 2\mathbf{D}$ and is loosely written as $\mathbf{B} = (2\mathbf{D})^{1/2}$. This form is interesting to reveal the special structure of the last two terms on the rhs and this point is addressed in more details in the next two subsections.

- (c) The third remark is the matrix $A_{ij} = \lim_{\chi \rightarrow 0} (\chi U_i^{(\chi)} U_j^{(\chi)})$, which is a solution of Eq. (260), is only a function of time and space and, therefore, is not random at a given time t and at a given location \mathbf{x} . In other words, in this limit of $\chi \rightarrow 0$, there is no intrinsic randomness due to velocities left in A_{ij} and $(A_{ij} | \mathbf{X}(t) = \mathbf{x})$ is a fixed number at a given time and location. As can be seen by applying the conditional averaging operator (conditioned on particles being at a given position) to Eq. (258), this means that we can also write that

$$A_{ij}(t, \mathbf{x}) = \lim_{\chi \rightarrow 0} \langle \chi U_i^{(\chi)} U_j^{(\chi)} | \mathbf{X}^{(\chi)}(t) = \mathbf{x} \rangle \quad (268)$$

which allows A_{ij} to be associated to the Reynolds stress tensor (see Sections 6 and 7), as will appear in the developments below.

9.3.4. The incompressibility constraint in the tracer-particle limit

Particle systems represented by Eqs. (251) are of direct significance for the simulation of colloidal particles as well as for PDF models for single-phase flow turbulence. For colloidal particles having negligible inertia, the elimination of particle velocities corresponds to Brownian dynamics while for fluid PDF models this corresponds to composition PDF models (see [30, section 12.7]). Based on this not-well-known but interesting similarity between the two applications, aspects which have been investigated for one problem can be used to shed new light into other situations. In particular, the fluid incompressibility induces a constraint that has been developed for PDF models but is of general interest.

To understand the issue raised by the fluid incompressibility constraint, it is sufficient to consider the limit model for particle positions written as a general diffusion stochastic process

$$dX_i = C_i(t, X) dt + B_{ij}(t, X) dW_j. \quad (269)$$

Then, the Fokker–Planck equation for the particle-position density $p_X(t, \mathbf{x})$ is

$$\frac{\partial p_X}{\partial t} = -\frac{\partial}{\partial x_i} [C_i(t, \mathbf{x}) p_X] + \frac{\partial^2}{\partial x_i \partial x_j} [D_{ij}(t, \mathbf{x}) p_X], \quad (270)$$

with, as usual, $D_{ij} = 1/2B_{ik}B_{jk}$. When the fluid is incompressible, an initially uniform particle distribution should remain uniform. This can be easily understood by considering that each particle represents a small amount of fluid mass and, consequently, that a local accumulation of particles (and, thus, a deviation of particle concentration from uniformity) would be equivalent to mass not being uniformly distributed and, therefore, would be at variance with the fluid incompressible condition. With the present particle stochastic model, this condition is respected provided that the drift and diffusion coefficients of the Fokker–Planck equation, Eq. (270), satisfy the following relation:

$$\frac{\partial C_i(t, \mathbf{x})}{\partial x_i} = \frac{\partial^2 D_{ij}(t, \mathbf{x})}{\partial x_i \partial x_j}. \quad (271)$$

Colloids and polymers. For colloids and polymers (in the free-draining approximation), the situation is actually simple. In that case, the matrix $-G_{ij}$ in Eq. (251b) corresponds to the friction matrix and $\Phi_i(t, \mathbf{x})$ to the local fluid velocity, that is $\Phi(t, \mathbf{x}) = \mathbf{U}_f(t, \mathbf{x})$. Furthermore, the matrix equation in Eq. (260) reflects the classical fluctuation–dissipation relation which, with the use of the equipartition of energy, shows that $A_{ij} = k_B \Theta_f \delta_{ij}$ and, thus, that $G_{ij} = -(\sigma \sigma^\perp)_{ij}/(k_B \Theta_f)$. This is the usual result of the Ermak–McCammon model (see [50,140]) and we can use the simplified relation in Eq. (267) which takes the form

$$dX_i = U_{f,i}(t, \mathbf{X}) dt + G_{ij}^{-1} \frac{\partial A_{kj}}{\partial x_k} dt + \frac{\partial D_{ik}}{\partial x_k} dt + (2D)_{ij}^{1/2} dW_j. \quad (272)$$

The condition in Eq. (271) becomes

$$\frac{\partial U_{f,i}}{\partial x_i} + \frac{\partial}{\partial x_i} \left[G_{ij}^{-1} \frac{\partial A_{kj}}{\partial x_k} \right] + \frac{\partial^2 D_{ij}(t, \mathbf{x})}{\partial x_i \partial x_j} = \frac{\partial^2 D_{ij}(t, \mathbf{x})}{\partial x_i \partial x_j}. \quad (273)$$

From the fluid incompressibility constraint, we have $\partial U_{f,i}/\partial x_i = 0$ and the last two terms obviously cancel out. This leaves only the divergence of the second term on the rhs of Eq. (272) but, given the present form of the matrix A_{ij} , this term is zero in isothermal fluid flows. In short, the incompressibility constraint is always satisfied at the level of particle-position distributions in isothermal flows, thanks to the simplified form of the particle energies (translated into A_{ij} being proportional to the identity matrix).

It can then be noted that the incompressible condition is violated in non-isothermal flows where $\Theta_f(t, \mathbf{x})$ becomes space dependent, since $\partial A_{kj}/\partial x_k = k_B (\partial \Theta_f/\partial x_k) \delta_{kj} \neq 0$. However, in that case, the concentration of inertia-less particles does not have to be constant and is governed by the thermo-phoresis process. To further develop that example, a one-dimensional formulation is sufficient with $G^{-1} = -\tau_p$ and $D_p = \tau_p k_B \Theta_f$ the Einstein diffusion coefficient for a unit-mass particle (cf. Eq. (24)). Then, the limit model in Eq. (272) becomes

$$dX = U_f(t, X) dt + (2D_p)^{1/2} dW. \quad (274)$$

However, this resulting form does not reproduce the exponential profile of particle concentrations along temperature gradients. This is why the initial particle equation of motion has to be extended to account for the molecular-based phenomenon of thermo-phoresis and the form proposed in [5, section 2.3] corresponds here to having

$$\Phi(t, \mathbf{x}) = \mathbf{U}_f(t, \mathbf{x}) - \frac{D_p}{\tau_p} \left(S_T - \frac{1}{\Theta_f} \right) \nabla \Theta_f, \quad (275)$$

where S_T is the Soret coefficient. In our simplified one-dimensional setting, this gives

$$dX = U_f(t, X) dt - D_p \left(S_T - \frac{1}{\Theta_f(t, X)} \right) (\nabla \Theta_f)(t, X) dt + (2D_p)^{1/2} dW. \quad (276)$$

In a one-dimensional view, the velocity of an incompressible fluid is constant while, in the general three-dimensional one, it does not create any accumulation. Therefore, any such deviations from a uniform distribution can only be due to the last two terms on the rhs of Eq. (276). The resulting stationary PDF equation can be worked out in sample space from the balance between these drift and diffusion terms, giving

$$\frac{\partial}{\partial x} \left[D_p \left(S_T - \frac{1}{\Theta_f} \right) \nabla \Theta_f p_X(x) \right] + \frac{\partial^2}{\partial x^2} [D_p p_X(x)] = 0, \quad (277)$$

which can be developed into

$$D_p S_T \nabla \Theta_f p_X(x) - \frac{D_p}{\Theta_f} \nabla \Theta_f p_X(x) + \frac{\partial D_p}{\partial x} p_X(x) + D_p \frac{\partial p_X(x)}{\partial x} = 0. \quad (278)$$

Given the expression of the diffusion coefficient, the second and third terms on the rhs of Eq. (278) cancel out, leaving

$$S_T \nabla \Theta_f p_X(x) + \frac{\partial p_X(x)}{\partial x} = 0, \quad (279)$$

from which we retrieve the correct result that the particle concentration (or the particle-position density) follows an exponential profile: $p_X(x) = c_0 \exp(-S_T(\Theta_f - \Theta_{f,0}))$. Further details and discussions on the account of thermo-phoresis and similar molecular-induced phenomena can be found in [5]. These considerations illustrate the interplay between microscopic (i.e. here, molecular-based effects), mesoscopic (i.e. here, the formulation of the Lagrangian stochastic model in Eqs. (251)) and macroscopic (i.e. here, the resulting uniform or non-uniform concentrations) levels of description.

Fluid particles for turbulent flows. Though the ideas are basically the same, the situation becomes more intricate for the statistical analysis of fluid-particle systems representing PDF models for single-phase turbulent flow, due to the absence of equipartition of energy or similar simplified equilibrium context in fluid dynamics. Thus, this requires to delve deeper into the question of how fast-variable-elimination techniques should be applied.

As presented in Section 6.5.1, we consider a Langevin model for fluid particles in single-phase turbulent flows. This still corresponds to the particle system in Eqs. (251) but with a matrix G_{ij} on which no special assumptions are made (apart from being invertible) and with a proper account of the mean pressure-gradient term. We have therefore

$$\Phi_i(t, \mathbf{x}) = \langle U_{f,i} \rangle(t, \mathbf{x}) + G_{ij}^{-1} \left(\frac{1}{\rho_f} \frac{\partial \langle P_f \rangle(t, \mathbf{x})}{\partial x_j} \right). \quad (280)$$

Following the technique described above, the elimination of the fast-variable $\mathbf{U}(t)$ gives a limit model for $\mathbf{X}(t)$ which, from Eq. (264), takes the form (leaving out again the dependences of field quantities on (t, \mathbf{x}) for the sake of simplicity but writing \mathbf{X}_f and \mathbf{U}_f as we are now dealing only with fluid particles), using $A_{kj} = A_{jk}$

$$dX_{f,i} = \langle U_{f,i} \rangle dt + G_{ij}^{-1} \left(\frac{1}{\rho_f} \frac{\partial \langle P_f \rangle}{\partial x_j} \right) dt - \frac{\partial G_{ij}^{-1}}{\partial x_k} A_{jk} dt + (G^{-1} \sigma)_{ij} dW_j, \quad (281)$$

which can be rewritten as

$$dX_{f,i} = \langle U_{f,i} \rangle dt + G_{ij}^{-1} \left\{ \frac{1}{\rho_f} \frac{\partial \langle P_f \rangle}{\partial x_j} + \frac{\partial A_{jk}}{\partial x_k} \right\} dt - \frac{\partial}{\partial x_k} [G_{ij}^{-1} A_{jk}] dt + (G^{-1} \sigma)_{ij} dW_j, \quad (282)$$

where A_{jk} is a solution of the matrix equation in Eq. (260). Since the fluid is incompressible, we have that $\partial \langle U_{f,i} \rangle / \partial x_i = 0$ and the first term on the rhs of Eq. (282) respects the incompressible condition in Eq. (271). We consider then the contributions coming from the last two terms on the rhs of Eq. (282). Using Eqs. (263) and (260), we have

$$\mathbf{D} = -\frac{1}{2} \mathbf{G}^{-1} (\mathbf{G}\mathbf{A} + \mathbf{A}\mathbf{G}^\perp) (\mathbf{G}^\perp)^{-1} = -\frac{1}{2} \mathbf{G}^{-1} \mathbf{A} - \frac{1}{2} \mathbf{A} (\mathbf{G}^\perp)^{-1}. \quad (283)$$

For the condition in Eq. (271), this implies that

$$\frac{\partial^2 D_{ik}}{\partial x_i \partial x_k} = -\frac{1}{2} \frac{\partial^2}{\partial x_i \partial x_k} (G_{ij}^{-1} A_{jk}) - \frac{1}{2} \frac{\partial^2}{\partial x_i \partial x_k} (A_{ij} G_{kj}^{-1}) = -\frac{\partial}{\partial x_i} \left(\frac{\partial}{\partial x_k} (G_{ij}^{-1} A_{jk}) \right) \quad (284)$$

where the last step follows from the symmetry between the summation indexes i and k and from the symmetry of the matrix A_{ij} . This shows that the incompressibility condition is always satisfied by the last two terms on the rhs of Eq. (282). For the complete model in Eq. (282) and given that G_{ij}^{-1} is invertible, this implies that the resulting model of the fast-elimination technique respects the incompressibility constraint provided that

$$\frac{1}{\rho_f} \frac{\partial \langle P_f \rangle}{\partial x_j} + \frac{\partial A_{jk}}{\partial x_k} = 0 \quad (285)$$

with A_{jk} defined in Eq. (259) and a solution of Eq. (260). At first sight, it is not immediate to check that this condition is met and, if so, what the precise meaning of this new equilibrium relation can be. These aspects are now investigated.

9.3.5. Applications for single-phase turbulent flows

To analyze the application of the idea of fast-variable elimination for fluid-particle velocities in PDF models, we refer to the GLM introduced in Section 6.5.1. This corresponds to the generic form used in Eqs. (251) with Φ_i given in Eq. (280). Following the leading principle of the parametrization (P2), we introduce a small parameter χ and consider the limit of the following equations (leaving out the dependences on $(t, \mathbf{X}^{(\chi)}(t))$ of the field quantities)

$$dX_{f,i}^{(\chi)} = U_{f,i}^{(\chi)} dt, \quad (286a)$$

$$dU_{f,i}^{(\chi)} = -\frac{1}{\chi} \frac{1}{\rho_f} \frac{\partial \langle P_f \rangle}{\partial x_i} dt + \frac{1}{\chi} G_{ij} \left[U_{f,j}^{(\chi)} - \langle U_{f,j} \rangle \right] dt + \frac{1}{\chi} \sigma_{ij} dW_j. \quad (286b)$$

It is seen that the return-to-equilibrium term in Eq. (286b) is expressed with respect to the unchanged mean fluid velocity field. Therefore, these equations indicate that the physical idea underlying this parametrization is that, as χ becomes smaller, we are considering velocity fields that fluctuates more and more rapidly but around the same mean one $\langle \mathbf{U}_f(t, \mathbf{x}) \rangle$. The first-order moment, that is the Reynolds equation, is easily obtained from Eqs. (286) and has the form (see derivations in [1,4,30])

$$\frac{\partial}{\partial t} \left[\langle U_{f,i}^{(\chi)} | \mathbf{X}_f^{(\chi)}(t) = \mathbf{x} \rangle \right] = -\frac{1}{\chi} \frac{1}{\rho_f} \frac{\partial \langle P_f \rangle}{\partial x_i}(t, \mathbf{x}) - \frac{\partial}{\partial x_k} \left[\langle U_{f,i}^{(\chi)} U_{f,k}^{(\chi)} | \mathbf{X}_f^{(\chi)}(t) = \mathbf{x} \rangle \right], \quad (287)$$

which can also be written as

$$\frac{\partial \langle U_{f,i} \rangle}{\partial t} + \langle U_{f,k} \rangle \frac{\partial \langle U_{f,i} \rangle}{\partial x_k} = -\frac{1}{\chi} \frac{1}{\rho_f} \frac{\partial \langle P_f \rangle}{\partial x_i} - \frac{\partial}{\partial x_k} \left[\langle u_{f,i}^{(\chi)} u_{f,k}^{(\chi)} | \mathbf{X}_f^{(\chi)}(t) = \mathbf{x} \rangle \right], \quad (288)$$

where $u_{f,i}^{(\chi)} = U_{f,i}^{(\chi)} - \langle U_{f,i} \rangle(t, \mathbf{X}_f^{(\chi)}(t))$ is the fluctuating particle velocity with respect to the local mean fluid value. By multiplying Eq. (287) with χ and taking the limit $\chi \rightarrow 0$, we get, with the help of the characterization of A_{ij} in Eq. (268), that

$$\frac{1}{\rho_f} \frac{\partial \langle P_f \rangle}{\partial x_i} + \frac{\partial A_{ik}}{\partial x_k} = 0 \quad (289)$$

which is the same as Eq. (285), showing that the incompressibility constraint studied in Section 9.3.4 is indeed satisfied. Note that, for small χ , we can approximate A_{ij} by

$$A_{ij}(t, \mathbf{x}) \simeq \chi \langle u_i^{(\chi)} u_j^{(\chi)} | \mathbf{X}^{(\chi)}(t) = \mathbf{x} \rangle \quad (290)$$

and the same result is therefore obtained from the alternative form of the Reynolds equation in Eq. (288). In physical terms, this means that A_{ij}/χ is the local fluid kinetic energy which is dominated by its fluctuating component (the fluctuating kinetic energy) and, thus, that $A_{ij} \simeq \chi R_{f,ij}^{(\chi)}$ where $R_{f,ij}^{(\chi)}$ is the Reynolds stress tensor introduced in Section 6. When $\chi \rightarrow 0$, the fluctuating kinetic energy and the Reynolds tensor grow unbounded (as $1/\chi$) but their contributions are compensated by a equally-large mean-pressure-gradient term. Crudely speaking, this is in line with Bernoulli's law where the sum of the fluid pressure and its kinetic energy remains constant. This remark provides further support to the parametrization (P2) and for the fact that the mean-pressure gradient is parametrized as in Eq. (286b).

If the incompressibility constraint is satisfied whatever the form of the matrix G_{ij} , there are further questions with respect to Eq. (260). Indeed, Eq. (260) expresses a fluctuation-dissipation type of relation and, therefore, describes an equilibrium situation. It can then be wondered how an equilibrium condition can be applied to a non-equilibrium phenomenon such as fluid turbulence. More precisely, since A_{ij} is directly related to the Reynolds stress tensor, the issue is to work out in what sense an equilibrium is reached when there is a continuous, and potentially unbalanced, production and dissipation of turbulent kinetic energy.

To outline this difficulty with the parametrization in Eqs. (286), we consider the equations for the second-order moments, $R_{f,ij}^{(\chi)}(t, \mathbf{x}) = \langle u_{f,i}^{(\chi)} u_{f,j}^{(\chi)} | \mathbf{X}_f^{(\chi)}(t) = \mathbf{x} \rangle$, obtained by applying the PDF methodology to the Lagrangian stochastic description (see [1,4,5,30,111]):

$$\begin{aligned} \frac{\partial R_{f,ij}^{(\chi)}}{\partial t} + \langle U_{f,k} \rangle \frac{\partial R_{f,ij}^{(\chi)}}{\partial x_k} &= -\frac{\partial}{\partial x_k} \left[\langle u_i^{(\chi)} u_j^{(\chi)} u_k^{(\chi)} | \mathbf{X}^{(\chi)}(t) = \mathbf{x} \rangle \right] \\ &\quad - R_{f,kj}^{(\chi)} \frac{\partial \langle U_{f,i} \rangle}{\partial x_k} - R_{f,ik}^{(\chi)} \frac{\partial \langle U_{f,j} \rangle}{\partial x_k} \\ &\quad + \frac{1}{\chi} G_{ik} R_{f,kj}^{(\chi)} + \frac{1}{\chi} G_{jk} R_{f,ik}^{(\chi)} + \frac{1}{\chi^2} (\sigma \sigma^\perp)_{ij}. \end{aligned} \quad (291)$$

Then, multiplying both sides of Eq. (291) by χ^2 and taking the limit $\chi \rightarrow 0$, we retrieve the matrix equation in Eq. (260) (recalling that $u_i^{(\chi)} \sim 1/\sqrt{\chi}$ and using that $A_{ij} = \chi R_{f,ij}^{(\chi)}$)

$$G_{ik} A_{kj} + A_{ik} G_{jk} = -(\sigma \sigma^\perp)_{ij}. \quad (292)$$

The above developments are, of course, similar to the ones presented at the beginning of Section 9.3.3. In particular, Eq. (291) is the Eulerian counterpart of Eqs. (257)–(258) (actually, Eq. (291) is derived by taking the average of Eq. (258) conditioned on a given spatial location).

However, Eq. (292) contradicts the constraint that Langevin models should respect in their application to single-phase turbulent flows, namely that the budget of turbulent kinetic energy be satisfied. This means that we should have

$$\text{Tr}(\mathbf{G}\mathbf{R}_f) + \frac{1}{2}\text{Tr}(\boldsymbol{\sigma}\boldsymbol{\sigma}^\perp) = -\langle\epsilon_f\rangle \quad (293)$$

whereas Eq. (292) predicts obviously that $2\text{Tr}(\mathbf{G}\mathbf{R}_f) + \text{Tr}(\boldsymbol{\sigma}\boldsymbol{\sigma}^\perp) = 0$. At this stage, it could be wondered whether the requirement in Eq. (293), which is met by the ‘original’ model (simply retrieved by putting $\chi = 1$ in Eqs. (286)), should necessarily be respected in the limit $\chi \rightarrow 0$. This point can be addressed with scaling arguments, using a one-dimensional formulation for the sake of simplicity. From Section 6.5.1, we know that σ is typically modeled as $\sigma \simeq \sqrt{\langle\epsilon_f\rangle}$, while G is usually expressed as $G \simeq -\langle\epsilon_f\rangle/k_f$. Writing $k_f^{(1)}$, $G^{(1)}$, R_f^1 and $\sigma^{(1)}$ for quantities related to the original velocity field, we have then that

$$G^{(1)}R_f^{(1)} + \frac{1}{2}(\sigma^{(1)})^2 = -\langle\epsilon_f^{(1)}\rangle. \quad (294)$$

For the fast-velocity version of the original velocity field obtained by introducing the small parameter χ , we are actually handling $\langle\epsilon_f^{(\chi)}\rangle \simeq \langle\epsilon_f^{(1)}\rangle/\chi^2$ and $k_f^{(\chi)} \simeq k_f^{(1)}/\chi$. This means that $\sigma^{(\chi)} \simeq \sigma^{(1)}/\chi$ and $G^{(\chi)} \simeq G^{(1)}/\chi$, in agreement with the choice of the parametrization (P2) made in Eqs. (286). By dividing both sides of Eq. (294) by χ^2 , we obtain

$$\frac{G^{(1)}R_f^{(1)}}{\chi} + \frac{1}{2}\left(\frac{\sigma^{(1)}}{\chi}\right)^2 = -\frac{\langle\epsilon_f^{(1)}\rangle}{\chi^2}, \quad (295)$$

and, thus, that

$$G^{(\chi)}R_f^{(\chi)} + \frac{1}{2}(\sigma^{(\chi)})^2 = -\langle\epsilon_f^{(\chi)}\rangle. \quad (296)$$

On the contrary, if we start with Eq. (292) and divide both sides by χ^2 , we get that

$$G^{(\chi)}R_f^{(\chi)} + \frac{1}{2}(\sigma^{(\chi)})^2 = 0, \quad (297)$$

which is, obviously, at variance with Eq. (296) and shows that this approach to the limit of rapidly-varying velocities is, in fact, equivalent to assuming that there is no dissipation. Moreover, there is an inconsistency between the scaling of the production term $P_f^{(\chi)} = R_{f,ik}^{(\chi)} \partial\langle U_{f,i}\rangle/\partial x_k$ and of the dissipation terms, since $P_f^{(\chi)} \sim 1/\chi$ while $\langle\epsilon_f^{(\chi)}\rangle \sim 1/\chi^2$. This does not invalidate the analysis of Eq. (291) that led to Eq. (294) but reveals that the rapidly-fluctuating velocities $u_{f,i}^{(\chi)}$ do not seem to possess the typical behavior expected for a turbulent flow even when they are rescaled. To give a precise example, it is interesting to consider a simple case, *i.e.* when G_{ij} and σ_{ij} are given by the Simplified Langevin Model, noted SLM (this corresponds to the GLM described in Section 6.5.1, cf. Eq. (128), with $G_{ij}^a = 0$), which means that we have

$$G_{ij} = -\left(\frac{1}{2} + \frac{3}{4}C_0\right) \frac{\langle\epsilon_f^{(1)}\rangle}{k_f^{(1)}} \delta_{ij}, \quad \text{and} \quad \sigma_{ij} = \sqrt{C_0\langle\epsilon_f^{(1)}\rangle} \delta_{ij}. \quad (298)$$

Then, Eq. (292) yields that $R_{f,ik}^{(\chi)} \simeq A_{ij}/\chi$ is given by

$$\chi R_{f,ij}^{(\chi)} = k_f^{(1)} \frac{C_0}{1 + 3/2C_0} \delta_{ij} \quad (299)$$

and, consequently, that $\chi k_f^{(\chi)} = k_f^{(1)}3/2C_0/(1 + 3/2C_0)$. It can be noted that $k_f^{(\chi)}$ has the expected scaling (*i.e.* $k_f^{(\chi)} \sim k_f^{(1)}/\chi$), but this result is nevertheless surprising as we would expect an exact relation of the form $\chi k_f^{(\chi)} = k_f^{(1)}$ to hold for this simple Langevin model.

The origin of these difficulties can be traced back to the existence of only one timescale in the formulations of classical macroscopic models for single-phase turbulence. Indeed, it is generally assumed that $k_f/\langle\epsilon_f\rangle$, which stands for the timescale at which turbulent kinetic energy is being dissipated by viscous motions (*i.e.* by internal friction), is also the timescale at which energy is being transferred between the different components of the Reynolds stress tensor (*i.e.* by conservative exchanges). This is represented in Fig. 53, which indicates that the different energy transfers (redistribution and dissipation) are assumed to take place at the same rate.

It is, however, possible to relax this hypothesis by considering that there are not one but two timescales involved: the first one is still $k_f/\langle\epsilon_f\rangle$ for the rate of turbulent kinetic dissipation but we can introduce a separate timescale to account for the rate at which energy is being transferred between the components. This second situation is sketched in Fig. 54.

From a physical standpoint, these ideas are translated into Langevin formulations where the dissipation and redistribution terms are modeled with different timescales. As an illustration, we propose the following example where we have

$$dX_{f,i} = U_{f,i} dt, \quad (300a)$$

$$dU_{f,i} = -\frac{1}{\rho_f} \frac{\partial\langle P_f\rangle}{\partial x_i} dt - \frac{1}{2} \frac{\langle\epsilon_f\rangle}{k_f} [U_{f,i} - \langle U_{f,i}\rangle] dt + \tilde{G}_{ij} [U_{f,j} - \langle U_{f,j}\rangle] dt + \tilde{\sigma}_{ij} dW_j. \quad (300b)$$

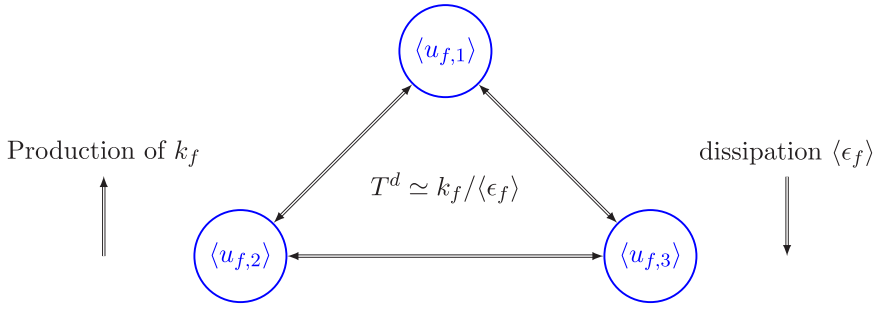


Fig. 53. Description of classical models where one timescale is used to describe both energy dissipation and redistribution, as indicated by the same thickness of the arrows representing these various energy transfers.

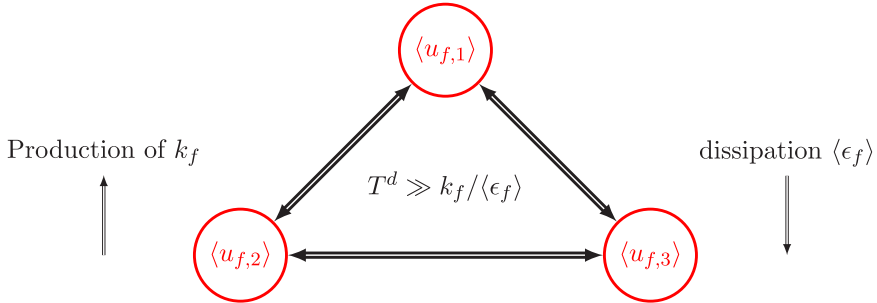


Fig. 54. Description of the new model where two timescales are used to describe separately the energy dissipation and the energy redistribution between the components of the Reynolds stress tensor, as indicated by the different thickness of the arrows representing these various energy transfers.

It is seen that the terms on the rhs of Eq. (300b) account respectively for the mean continuity equation (the incompressible condition), the dissipative behavior (the sink of turbulent kinetic energy represented by $\langle \epsilon_f \rangle$), while the sum of the last two terms represent essentially the redistribution terms between the components of the Reynolds stress tensor (with neither energy production nor dissipation). This distinction between the dissipation and redistribution terms is not as clear-cut since the complete redistribution term $\mathcal{R}_{f,ij}^d$ appearing in the Reynolds stress equation corresponding to the model in Eqs. (300) is

$$\mathcal{R}_{f,ij}^d = -\frac{\langle \epsilon_f \rangle}{k_f} \left(R_{f,ij} - \frac{2}{3} k_f \delta_{ij} \right) + \tilde{G}_{ik} R_{f,kj} + \tilde{G}_{jk} R_{f,ki} \quad (301)$$

showing that the second term on the rhs side of Eq. (300b) leads not only to the correct sink term, $-2/3 \langle \epsilon_f \rangle \delta_{ij}$, in the Reynolds stress equation but contributes also to $\mathcal{R}_{f,ij}^d$ with a Rotta (or return-to-equilibrium) term.

Actually, it can be noted that present Lagrangian stochastic models are not obtained as the sum of distinct stochastic submodels that represent the separate effects of the fluctuating pressure-gradient (which redistributes kinetic energy) and of the viscous term (which dissipates kinetic energy) entering the fundamental Navier–Stokes equation, but rather as one model for the sum of the two physical phenomena. To the author knowledge, only one work has addressed this question in detail and has derived a Langevin model by modeling the separate effects, using ideas from statistical physics such as Onsager's hypothesis (see [119]). However, this requires to switch continuously between the SDE and the Fokker–Planck descriptions or use informal notations with complex diffusion coefficients, which would unnecessarily obscure the description to come. Indeed, with the choice of the timescales retained for the different terms on the rhs side of Eq. (300b), it will be seen that this Rotta contribution does not play a significant role in the following analysis. For that reason, we therefore loosely identify the second term on the rhs side of Eq. (300b) as the energy sink term while the last two terms are referred to as the redistribution ones.

The drift and diffusion coefficients of the redistribution model, \tilde{G}_{ij} and $\tilde{\sigma}_{ij}$, can be expressed in terms of a redistribution timescale written as $T^d = k_f/\tilde{\epsilon}_f$, with the caveat that $\tilde{\epsilon}_f$ is not an energy dissipation but rather an energy transfer rate: thus $\tilde{G}_{ij} \sim -\tilde{\epsilon}_f/k_f$ while $\tilde{\sigma}_{ij} \sim \sqrt{\tilde{\epsilon}_f}$. We can then choose $\tilde{\epsilon}_f$ so that $\langle \epsilon_f \rangle \ll \tilde{\epsilon}_f$, which implies that $k_f/\tilde{\epsilon}_f \ll k_f/\langle \epsilon_f \rangle$. This expresses the idea that the (conservative) energy transfer rate between the components of the Reynolds stress tensor is much faster than the rate at which turbulent kinetic energy is being dissipated. Note that this justifies to neglect the Rotta term on the rhs of Eq. (301) and, therefore, to speak of the separate dissipation and redistribution terms, as done in the previous paragraph.

In terms of a proper (P2) of parametrization, the above ideas are formalized by introducing a small parameter χ and by considering the following system of equations:

$$dX_{f,i}^{(\chi)} = U_{f,i}^{(\chi)} dt, \quad (302a)$$

$$dU_{f,i}^{(\chi)} = -\frac{1}{\chi} \frac{1}{\rho_f} \frac{\partial \langle P_f \rangle}{\partial x_i} dt - \frac{1}{2} \frac{\langle \epsilon_f^{(\chi)} \rangle}{k_f^{(\chi)}} \left[U_{f,i}^{(\chi)} - \langle U_{f,i} \rangle \right] dt + \frac{1}{\chi} \tilde{G}_{ij}^{(1)} \left[U_{f,j}^{(\chi)} - \langle U_{f,j} \rangle \right] dt + \frac{1}{\chi} \tilde{\sigma}_{ij}^{(1)} dW_j. \quad (302b)$$

This system is obtained with the same scaling as in the previous attempt, cf. Eqs. (286) and (291), that is by choosing $\tilde{\epsilon}_f \sim 1/\chi^2$ which, with $k_f^{(\chi)} \sim 1/\chi$, gives the $1/\chi$ terms of the parametrized redistribution model. The difference with the first parametrization in Eqs. (286) comes from the second term on the rhs of Eq. (302b), where we can choose $\langle \epsilon_f^{(\chi)} \rangle$ so that $\langle \epsilon_f^{(\chi)} \rangle \sim 1/\chi$. This gives that $\langle \epsilon_f^{(\chi)} \rangle / k_f^{(\chi)} \sim 1$ and the system in Eqs. (302) can also be written as:

$$dX_{f,i}^{(\chi)} = U_{f,i}^{(\chi)} dt, \quad (303a)$$

$$dU_{f,i}^{(\chi)} = -\frac{1}{\chi} \frac{1}{\rho_f} \frac{\partial \langle P_f \rangle}{\partial x_i} dt - \frac{1}{2} \frac{\langle \epsilon_f^{(1)} \rangle}{k_f^{(1)}} \left[U_{f,i}^{(\chi)} - \langle U_{f,i} \rangle \right] dt + \frac{1}{\chi} \tilde{G}_{ij}^{(1)} \left[U_{f,j}^{(\chi)} - \langle U_{f,j} \rangle \right] dt + \frac{1}{\chi} \tilde{\sigma}_{ij}^{(1)} dW_j. \quad (303b)$$

Interesting properties are obtained from this formulation. For the equation satisfied by the turbulent kinetic energy, the redistribution terms play no role and we retrieve the form

$$\frac{D_f k_f^{(\chi)}}{Dt} + \frac{\partial T(k_f)_l}{\partial x_l} = \mathcal{P}_{k_f}^{(\chi)} - \langle \epsilon_f^{(\chi)} \rangle \quad (304)$$

where $T(k_f)_l = \langle u_l^{(\chi)} 1/2 \sum_i (u_i^{(\chi)})^2 \rangle$ represents the flux due to the triple velocity correlations. The important point is that we have now a consistent scaling of the different terms since both $\mathcal{P}_{k_f}^{(\chi)} = -R_{f,ij}^{(\chi)} \partial \langle U_{f,i} \rangle / \partial x_j$ and $\langle \epsilon_f^{(\chi)} \rangle$ vary as $1/\chi$, contrary to what was obtained with the first parametrization. On the other hand, when we analyze the limit of the complete Reynolds-stress-tensor equations, as in Eqs. (291), the dissipation term plays no significant role and its effects disappear in the limit $\chi \rightarrow 0$. This leads to the same result as in Eq. (260), or Eq. (292), for the matrix $A_{ij} = \chi R_{f,ij}^{(\chi)}$ but with the essential difference that these equations involve the redistribution matrix \tilde{G}_{ij} and not G_{ij}

$$\tilde{G}_{ik} A_{kj} + \tilde{G}_{jk} A_{ik} = -(\tilde{\sigma} \tilde{\sigma}^\perp)_{ij}. \quad (305)$$

As a consequence, there is no conflict anymore between Eq. (305) and the turbulent kinetic energy budget since this one is now expressed by $2\text{Tr}(\mathbf{GR}_f) + \text{Tr}(\tilde{\sigma} \tilde{\sigma}^\perp) = 0$ by construction of the redistribution model. To illustrate the difference in a specific situation, we can consider the same example of the SLM, where

$$\tilde{G}_{ij}^{(1)} = -\frac{3}{4} C_0 \frac{\langle \epsilon_f^{(1)} \rangle}{k_f^{(1)}} \delta_{ij}, \quad \text{and} \quad \tilde{\sigma}_{ij}^{(1)} = \sqrt{C_0 \langle \epsilon_f^{(1)} \rangle} \delta_{ij} \quad (306)$$

which yields immediately that we have now

$$\chi R_{f,ij}^{(\chi)} = \frac{2}{3} k_f^{(1)} \delta_{ij} \quad (307)$$

and, consequently, that $\chi k_f^{(\chi)} = k_f^{(1)}$, in line with what we expected right from the outset.

This result for the SLM helps to bring out the main idea of the present application of the notion of fast variables in a non-equilibrium situation. While turbulence is produced and dissipated at rates which are not necessarily identical (which means that the turbulence is not considered at equilibrium in terms of the second-order velocity moments), the redistribution of energy between the components of the Reynolds stress tensor is much faster than the potentially-unbalanced production and dissipation rates. This is indeed consistent with the notion of slow and fast variables: k_f can evolve and, for instance, decay but at a rate which is much slower than the one governing the exchanges between the components of the Reynolds stress tensor. For example, the principle of the Rotta model of the SLM is precisely to act as a return-to-isotropy driving force. Applied in the context of fast-variable elimination, it is not surprising to find that its action consists in pulling ‘immediately’ these components to their local isotropic form. Finally, in terms of the usual mean quantities handled in classical models for turbulence, it is seen that the approach developed with Eqs. (300)–(305) is a consistent formulation to have $\mathcal{R}_{f,ij}^d = 0$ while turbulence can still be evolving (i.e. $D_f k_f / Dt \neq 0$).

Applications for composition-PDF models. These developments are immediately applicable for composition-PDF models in single-phase turbulence. Going back to Eq. (282) and making use of the following results when particle velocities become fast variables, the limit model obtained for particle positions is

$$dX_{f,i} = \langle U_{f,i} \rangle dt - \frac{\partial}{\partial x_k} [\tilde{G}_{ij}^{-1} A_{jk}] dt + (\tilde{G}^{-1} \tilde{\sigma})_{ij} dW_j, \quad (308)$$

with A_{ij} the solution of Eq. (305).

When the redistribution model leads to an isotropic form in the infinite-relaxation limit, as with the SLM, the limit model has the simple form (with $\tilde{T} = -\tilde{G}^{-1}$)

$$dX_{f,i} = \langle U_{f,i} \rangle dt + \frac{\partial}{\partial x_i} \left[\tilde{T} \left(\frac{1}{2} \tilde{T} \tilde{\sigma}^2 \right) \right] dt + (\tilde{T} \tilde{\sigma}) dW_i. \quad (309)$$

It is worth recalling that, in line with the principles formalized with the (P2) parametrization, this is achieved locally in time and space. This means that Eq. (309) holds for the general case when $\tilde{T} = \tilde{T}(t, \mathbf{x})$ and $\tilde{\sigma} = \tilde{\sigma}(t, \mathbf{x})$. Note that we find again the interplay between the two combinations of the drift and diffusion coefficients, namely $\tilde{T}\tilde{\sigma}$ and $\tilde{T}(\tilde{\sigma})^2/2$, mentioned at the beginning of Section 9.3.2. Then, by defining $\Gamma_{f,t}(t, \mathbf{x}) = (\tilde{T}\tilde{\sigma})^2/2$, we get that

$$dX_{f,i} = \langle U_{f,i} \rangle dt + \frac{\partial \Gamma_{f,t}}{\partial x_i} dt + \sqrt{2 \Gamma_{f,t}} dW_i. \quad (310)$$

To bring out the physical meaning of this limit model, it is sufficient to consider the simplest case when a perfectly-conserved scalar, say ϕ_f , is attached to each particle. Along a particle trajectory we have $d\phi_f = 0$ and the position-scalar PDF $p_f^L(t; \mathbf{y}, \psi)$ is the solution of the FPE

$$\frac{\partial p_f^L}{\partial t} + \langle U_{f,k} \rangle \frac{\partial p_f^L}{\partial y_k} = -\frac{\partial}{\partial y_k} \left[\left(\frac{\partial \Gamma_{f,t}}{\partial x_i} \right) p_f^L \right] + \frac{\partial^2}{\partial y_k^2} [\Gamma_{f,t} p_f^L] \quad (311)$$

which is also satisfied by the Eulerian position-scalar PDF $p_f^E(t; \mathbf{x}, \psi)$ from which we obtain, by integration over all possible values of ψ_f , that the mean scalar field $\langle \phi_f \rangle(t, \mathbf{x})$ evolves as

$$\frac{\partial \langle \phi_f \rangle}{\partial t} + \langle U_{f,k} \rangle \frac{\partial \langle \phi_f \rangle}{\partial x_k} = \frac{\partial}{\partial x_k} \left[\Gamma_{f,t} \left(\frac{\partial \langle \phi_f \rangle}{\partial x_k} \right) \right]. \quad (312)$$

This reveals that the mean-scalar field is the solution of a convection-diffusion equation with $\Gamma_{f,t}$ the diffusion coefficient, referred to as the ‘turbulent diffusivity’. For obvious reasons, this description is called a composition-PDF model, and is represented by either the PDF equation in sample space in Eq. (311) or by the Lagrangian stochastic formulation in terms of particle position and scalar (\mathbf{X}, ϕ) in Eq. (310). An introduction to these methods can be found in [30, section 12.7].

At this stage, one remark is in order. The composition-PDF model expressed by Eq. (311) is traditionally derived from the velocity-composition-PDF equation by resorting to a gradient-diffusion hypothesis for the integrated effects of the fluctuating velocity (see a precise account in [30, section 12.7]). This is obtained, first, by proposing a closed form for the turbulent convective flux of the Eulerian distribution in sample space as

$$\langle v_{f,k} | \psi_f \rangle p_f^E(t, \mathbf{x}; \psi_f) = -\Gamma_{f,t} \frac{\partial p_f^E(t, \mathbf{x}; \psi_f)}{\partial x_k} \quad (313)$$

and, second, by formulating the Lagrangian stochastic model from the resulting closed form of the composition-PDF equation with the particle SDE as in Eq. (310). However, in this section, the same result is directly obtained from the fast-variable elimination technique applied to fluid-particle velocities using only a Lagrangian stochastic formulation. This is useful to provide insights into the gradient-diffusion hypothesis which expresses a clear physical picture: at the level of one macroscopic quantity (represented here, for example, by the mean-scalar field $\langle \phi_f \rangle(t, \mathbf{x})$), a gradient-diffusion model for ‘convective fluxes’ is justified when the underlying microscopic or mesoscopic ‘convective variable’ is a rapidly-varying variable that can be treated as a fast variable. This physically-important notion will resurface in Section 10.4.

Drawing on the latter point, it is seen that the elimination of fast-variables applied to fluid-particle velocities in a velocity-composition-PDF model provides a consistent method to extract a composition-PDF model based on the concept of turbulent diffusivity tensors (also called algebraic stress or non-linear viscosity models, see [30, section 11.9]). Indeed, by the same reasoning as in the isotropic case, we can use the general limit model for particle positions in Eq. (310) to show that the mean scalar field is, in the high Peclet-number limit, the solution of the following convection-diffusion equation

$$\frac{\partial \langle \phi_f \rangle}{\partial t} + \langle U_{f,k} \rangle \frac{\partial \langle \phi_f \rangle}{\partial x_k} = \frac{\partial}{\partial x_k} \left[\Gamma_{ft,kl} \left(\frac{\partial \langle \phi_f \rangle}{\partial x_l} \right) \right] \quad (314)$$

where the turbulent diffusivity tensor is directly given by $\Gamma_{ft,kl} = 1/2 (\tilde{G}^{-1} \tilde{\sigma} \tilde{\sigma}^\perp (\tilde{G}^\perp)^{-1})_{kl}$ (note that, of course, Γ_{ft} plays the same role as the diffusion matrix \mathbf{D} in Eq. (283)).

9.3.6. Applications for disperse two-phase turbulent flows

Up to now, we have essentially considered the fluid-particle case which is useful to introduce the fast-variable elimination technique. Yet, since the purpose of the present work is on disperse two-phase flows, it is important to generalize the above results to the case of discrete particles embedded in a turbulent flows. To that effect, we consider a dynamic PDF model, developed for the standard state vector $\mathbf{Z}_p = (\mathbf{x}_p, \mathbf{U}_p, \mathbf{U}_s)$, and with evolution equations that are similar to Eqs. (164) but are written here as

$$dx_{p,i} = U_{p,i} dt, \quad (315a)$$

$$dU_{p,i} = \frac{1}{\tau_p} (U_{s,i} - U_{p,i}) dt, \quad (315b)$$

$$dU_{s,i} = G_{ij}^*(t, \mathbf{x}_p(t)) [U_{s,j} - \Phi_j^*(t, \mathbf{x}_p(t))] dt + \sigma_{ij}^*(t, \mathbf{x}_p(t)) dW_j, \quad (315c)$$

where the SDE for the velocity of the fluid seen is expressed with a form corresponding to the one in Eq. (251b). From the presentation of the reference formulation, which is the Langevin model presented in Section 7.3.3 (cf. Eqs. (166)–(173)), it is seen that $G_{ij}^* \sim -1/T_L^*$ with the Csanady timescales given in Eqs. (169) while $\sigma_{ij}^* \sim \sqrt{\langle \epsilon_f \rangle}$. In Eq. (315c), $\Phi_j^*(t, \mathbf{x}_p(t))$ is typically given by an expression alike the one in Eq. (280) and which can be written as

$$\Phi_i^*(t, \mathbf{x}) = \langle U_{f,i} \rangle(t, \mathbf{x}) + G_{ij}^{-1} \left(\frac{1}{\rho_f} \frac{\partial \langle P_f \rangle(t, \mathbf{x})}{\partial x_j} + \Pi_j \right), \quad (316)$$

where Π_j can represent additional terms, such as the mean drift term appearing on the rhs of Eq. (166). It is however useful to retain the general expression in Eq. (315c) to indicate that present results are valid for a class of models and are not dependent on the specifics of one particular formulation. With these notations and the above derivations, the limit cases of the particle stochastic system in Eqs. (315) can be directly stated.

Compared to the fluid-particle case, it is seen that there are now two timescales: the particle relaxation timescale τ_p and the timescale of the velocity of the fluid seen T_L^* (leaving out the differences between the longitudinal and transverse ones for the sake of simplicity, as they are not relevant for the present discussion). Correspondingly, there are different ways with which the limit of vanishing timescales can be taken.

First of all, when $\tau_p \rightarrow 0$, this is the tracer-particle limit since the (stiff) particle momentum equation in Eq. (315b) yields that the particle velocity relaxes instantaneously to the velocity of the fluid one, *i.e.* $\mathbf{U}_p \rightarrow \mathbf{U}_s$. In that case, as mentioned in Section 7.3.3, the model for the velocity of the fluid seen reverts to the GLM used for fluid particles. In other words, when $\tau_p \rightarrow 0$, the limit system of Eqs. (315) is the one already given in Eq. (251), showing that the previous results are directly applicable. In particular, when the timescale T_L^* (equal to T_L in the tracer-particle limit) becomes much smaller than the chosen observation timescale Δt , the limit diffusive equation for the positions of the tracer particles is the one given in Eq. (308) and used above to derive closed forms for composition-PDF models.

The second limit consists in keeping a non-zero value of the particle relaxation timescale τ_p while $T_L^* \rightarrow 0$ and \mathbf{U}_s becomes a rapidly-varying variable. Then, the steps detailed with the derivations from Eqs. (253) to (264) can be followed. There is, however, an important difference since the derivations yield the product $U_{p,k} U_{s,j}$ instead of $U_{s,k} U_{s,j}$ (for example in the last term on the rhs of Eq. (256)). Due to the fact that \mathbf{U}_p remains a process with finite total variance whereas \mathbf{U}_p has an infinite total variance in the white-noise limit, there are no additional contributions coming from the Ito-like terms. Therefore, when $T_L^* \rightarrow 0$ while τ_p is kept at a finite and non-zero value, the limit particle system of Eqs. (315) becomes

$$d\mathbf{x}_{p,i} = U_{p,i} dt, \quad (317a)$$

$$dU_{p,i} = -\frac{1}{\tau_p} U_{p,i} dt + \frac{1}{\tau_p} \Phi_j^*(t, \mathbf{x}_p(t)) dt + \frac{1}{\tau_p} ((G^*)^{-1} \sigma^*)_{ij} dW_j, \quad (317b)$$

where the discrete particle velocity \mathbf{U}_p is now a stochastic diffusion process and where the white-noise term has been moved upward in the hierarchy of the variables (from \mathbf{U}_s to \mathbf{U}_p).

When the particle relaxation timescale τ_p is then taken to zero, it is interesting to note that the elimination of the particle velocity does not yield the same diffusive limit model for the tracer-particle position as in Eq. (308) since the second term on the rhs is missing. In other words, this means that $\lim_{\tau_p \rightarrow 0} \lim_{T_L^* \rightarrow 0} \neq \lim_{T_L^* \rightarrow 0} \lim_{\tau_p \rightarrow 0}$. In physical terms, keeping a non-zero finite value of τ_p filters out some information on the fast variable \mathbf{U}_s which cannot be retrieved and the proper way to take the successive limits is therefore to consider first the tracer-particle limit and, then, the diffusive limit when the velocity is eliminated in order to avoid creating spurious drifts in non-homogeneous situations.

9.3.7. Comments on the fast-variable elimination technique

Throughout Section 9.3, the discussions have mostly concerned the technical aspects of the fast-variable elimination method to fulfill the list of objectives set forth at the beginning. These accounts were detailed on purpose for two main reasons.

The first one was to clarify specific points, such as how the limit of infinitely-fast variables should be taken (cf. the (P2) parametrization) and about the meaning of ‘equilibrium limits’ in the context of non-equilibrium phenomena (*i.e.* when it is said that a fast variable reaches its equilibrium and becomes a white-noise, conditioned by the frozen values of slow variables). In that sense, the present formulation has introduced new material, such as the correct limits of over-damped Langevin models and their applications to turbulent models.

The second reason was to demonstrate that a comprehensive and rigorous treatment of fast-variable elimination can be achieved using only a formulation in terms of SDEs. Indeed, classical presentations of this technique are generally based on an operator formalism in sample space, following the Mori-Zwanzig approach (see for example [43,61]). It is shown here that, though this projector operator formalism is useful, this formulation is not mandatory and that all results can also be derived from the manipulations of the trajectories of the stochastic processes. This is believed to shed new light on the notion of fast-variable elimination.

9.4. The significance of the choice of the particle state vector

From the analyses in Section 9.2, it appears that, even for the limited goal of deriving the one-time PDF equation from which statistical moments are extracted, we must manipulate only white-noise terms as ‘external noises’. With the notations

used in Section 9.2, this means that, to come up with a proper probabilistic description of a dynamical system \mathbf{Z} subject to a noise ξ , we must handle the extended state vector (\mathbf{Z}, ξ) but not the single process \mathbf{Z} when ξ is not a white-noise. This extended point of view retrieves the Markovian characteristic with all the advantages that go with this property but is also needed to ensure that the PDF and DF equations remain well-posed. This result is of significance for kinetic descriptions of particles, or any ‘mechanical object’, in random media with non-zero time and space correlations.

A second outcome of the study in Section 9.2 is to point out the interest of a flexible modeling standpoint which consists in selecting tailor-made particle state vectors based on a physical analysis of each system and a distinction between slow and fast variables [1,5,52]. It is essential to realize that it is the interplay between the choice of a mechanical description, its physical analysis and the application of the fast-variable elimination technique that leads to physically-consistent and mathematically-well-posed probabilistic formulations.

These first conclusions are directly relevant for the development of probabilistic descriptions of particles carried by turbulent flows which are now studied in Section 10.

10. Probabilistic models for polydisperse two-phase turbulent flows

The two cornerstones of classical non-equilibrium statistical physics are Brownian motion (through Einstein/Langevin/Fokker–Planck equations) and kinetic theory (through the Boltzmann equation). Mirroring these themes, the two main issues for statistical descriptions of particles in turbulent flows are how to account for particle dispersion and particle collisions. The first one reflects particle–fluid interactions while the second issue is related to particle–particle interactions. With the presentations of general modeling tools in Section 9, we are ready to analyze the modeling approaches presented in Section 7, concentrating essentially on mesoscopic models that link the hydrodynamical level of description to averaged formulations (in the sense of the terminology introduced in Section 3). This means that we consider more specifically PDF methods. The purposes of this section are:

- (i) To assess whether present models form acceptable probabilistic descriptions in the sense of the criteria introduced in Section 4.5;
- (ii) To show the continuity with classical statistical physics as well as the key differences that create specific challenges;
- (iii) To bring out open questions where new ideas or formulations are needed.

As mentioned in the introduction of Section 9, some results have an interest for general dynamical systems and, whenever possible, such a broader perspective is adopted. Following classical formulations of particle-based approaches (see Section 5) where particle transport and collisions are treated sequentially in fractional-time-step methods, we study first particle transport without collisions before considering particle collisions without transport but in the presence of a carrier fluid. Thus, particle dispersion issues are discussed in Section 10.1 through the importance of retaining dynamic PDF descriptions. Drawing on this result, tailored selections of particle state vector is further elaborated in Section 10.2. The important, but less well-known, connection between white-noise terms and local/non-local closures in macroscopic formulations is presented in Section 10.3. This leads naturally to a discussion of gradient-diffusion models in Section 10.4 and of the notion of fast and slow variables through discrete formulations in Section 10.5. Finally, the challenges raised by the introduction of particle–particle interactions are considered in Section 10.6.

10.1. Analysis of the kinetic and dynamic PDF models

In this section, we analyze the two classes of PDF approaches represented by the kinetic PDF description (see Section 7.3.2) and the dynamic PDF model (see Section 7.3.3). The terminology of ‘classes of approaches’ indicates that we are more concerned with the characteristic properties of each family of models than with the details of variants within each class. A comprehensive study of the status of the kinetic and dynamic PDF models has recently been published (see [52]) and, in the following, we present directly the main results and emphasize the conclusions that are relevant to the construction of physically-sound statistical models of particle dynamics in turbulent flows.

10.1.1. Kinetic PDF descriptions are incomplete and ill posed

Under the assumption of a Gaussian distribution for the velocity of the fluid seen, it is demonstrated in [52] that the integration of a dynamic PDF model over the velocity of the fluid seen yields exactly the same equation for the reduced density $p_p^{L,r}(t; \mathbf{y}_p, \mathbf{V}_p)$ as in kinetic PDF formulations. This proves that kinetic PDF models are directly recovered from dynamic ones or, in other words, that the reduced PDF $p_p^{L,r}(t; \mathbf{y}_p, \mathbf{V}_p)$ is the marginal of the dynamic one $p_p^{L,r}(t; \mathbf{y}_p, \mathbf{V}_p, \mathbf{V}_s)$, i.e. that $p_p^{L,r}(t; \mathbf{y}_p, \mathbf{V}_p) = \int p_p^L(t; \mathbf{y}_p, \mathbf{V}_p, \mathbf{V}_s) d\mathbf{V}_s$. In the following, we use the notation $\mathbf{Z}_p^r = (\mathbf{x}_p, \mathbf{U}_p)$ for the reduced state vector limited to particle kinetic variables and \mathbf{z}_p^r for the corresponding variables in sample space.

An important outcome of the new derivation given in [52] is that the tensors λ_{ij} and μ_{ij} can be written as

$$\lambda_{ij}(t; \mathbf{z}_p^r) = \frac{1}{\tau_p^{st}} \left\langle \langle u_{f,i}(t, \mathbf{y}_p) (\delta x_{p,j})^{\omega[t, \mathbf{z}_p^r]}(t) \rangle \right\rangle_{\omega[t, \mathbf{z}_p^r]}, \quad (318a)$$

$$\mu_{ij}(t; \mathbf{z}_p^r) = \frac{1}{\tau_p^{st}} \left\langle \langle u_{f,i}(t, \mathbf{y}_p) (\delta U_{p,j})^{\omega[t, \mathbf{z}_p^r]}(t) \rangle \right\rangle_{\omega[t, \mathbf{z}_p^r]}. \quad (318b)$$

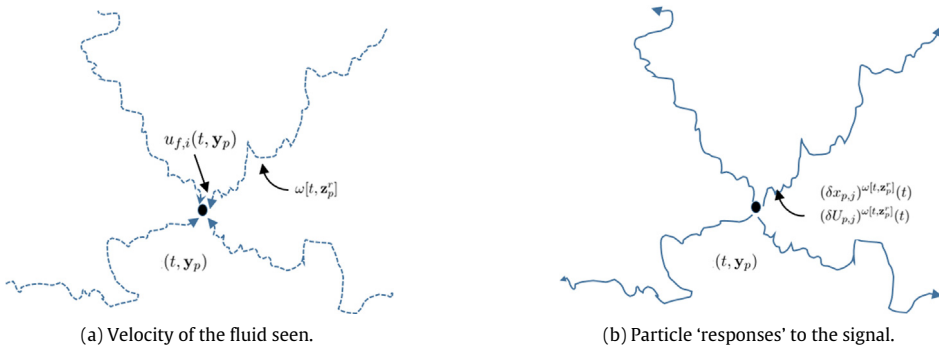


Fig. 55. Illustration of the mixed time-forward and time-backward formulation of kinetic PDF methods: (a) The velocity of the fluid seen is recorded along the particle trajectories arriving at $(t, \mathbf{x}_p(t))$ in a time-backward vision; (b) The dispersion tensors represent the correlation between that signal and the ‘responses’ $\delta\mathbf{x}_p(t)$ and $\delta\mathbf{U}_p(t)$ that would result from in a time-forward view.

In these expressions, $\omega[t, \mathbf{z}_p^r]$ represents a particle path in sample space arriving at $\mathbf{z}_p^r = (\mathbf{y}_p, \mathbf{V}_p)$ at time t and the double averaging operator means that we average first over the turbulent fluctuations of the velocity of the fluid seen along a given sample path and then over all the sample paths (see Fig. 55(a)). The particle relaxation timescale is written as τ_p^{st} to recall that kinetic PDF model can only handle constant particle relaxation timescales, thus typically limited to their expression in the Stokes regime. Furthermore, the notations $(\delta\mathbf{x}_p)^{\omega[t, \mathbf{z}_p^r]}$ and $(\delta\mathbf{U}_p)^{\omega[t, \mathbf{z}_p^r]}$ stand for the positions and velocities that particles would have when subject to the driving forces represented by the velocity of the fluid seen along the sample paths (see Fig. 55(b)). In that sense, the formulas in Eqs. (318) correspond to a prediction–correction scheme and the tensors λ_{ij} and μ_{ij} appear as ‘response functions’. From the sketches in Fig. 55, it is also seen that kinetic PDF models are a mixed combination of time-forward approaches (for $(\mathbf{x}_p, \mathbf{U}_p)$) and time-backward ones (for \mathbf{U}_s).

In homogeneous situations where the statistics of the velocity of the fluid seen are not space dependent, the physics embodied by the formulas in Eqs. (318) is clearly revealed since the above correlations become

$$\lambda_{ij} = \frac{1}{\tau_p^{st}} \langle u_{s,i}(t) x_{p,j}(t) \rangle, \quad (319a)$$

$$\mu_{ij} = \frac{1}{\tau_p^{st}} \langle u_{s,i}(t) U_{p,j}(t) \rangle, \quad (319b)$$

where there is no difference anymore between the true particle paths and the responses ones (see further details and explanations in [52]). Note that these expressions are examples of a general result for dynamical systems under colored noises, as shown in Section 9.2 with, for instance, Eq. (193). They bring out that *the tensors appearing in closed PDF formulations represent the correlations between the variables kept in the state vector and the eliminated noises*. This result plays an important role in the developments to follow in Section 10.1.4.

The first criterion to consider is whether the reduced state vector \mathbf{Z}_p^r retained in kinetic PDF approaches form a Markov process, as discussed in Section 4.5.1. There are three possibilities. The first one corresponds to the case of a ‘deterministic fluid velocity field’, that is a fully-resolved turbulent flow, where the velocity of the fluid seen at particle positions, $\mathbf{U}_s(t) = \mathbf{U}_f(t, \mathbf{x}_p(t))$, is completely determined. In that case, the information needed to update particle positions and velocities is accessible and the description is closed. Note that the PDF equation is simply given by a Liouville equation

$$\frac{\partial p_{p,r}^L}{\partial t} + V_{p,k} \frac{\partial p_{p,r}^L}{\partial y_{p,k}} = \frac{\partial}{\partial V_{p,k}} \left[\frac{1}{\tau_p^{st}} (U_{f,k}(t, \mathbf{y}_p) - V_{p,k}) p_{p,r}^L \right]. \quad (320)$$

The second possibility is when the velocity of the fluid seen is regarded as a rapidly-varying process with respect to particle velocities. This happens only if $T_L^* \ll \tau_p^{st}$, that is for ‘bullet-like particles’ for which the fluid is seen as an underlying noise and is the only case where a parallel with Brownian motion exists. This corresponds to the second limit considered in Section 9.3.6 with Eqs. (317), which taking $\Phi_i^*(t, \mathbf{x}_p(t)) = \langle U_{f,i}(t, \mathbf{x}_p) \rangle$ (and leaving out possible additional terms used to avoid spurious drifts, for the sake of a simple presentation), leads to the simplified particle system of equations

$$dx_{p,i} = U_{p,i} dt, \quad (321a)$$

$$dU_{p,i} = -\frac{U_{p,i}}{\tau_p^{st}} dt + \frac{1}{\tau_p^{st}} \langle U_{f,i}(t, \mathbf{x}_p) \rangle dt + \frac{1}{\tau_p^{st}} ((G^*)^{-1} B_s)_{ij} dW_j. \quad (321b)$$

Then, we obtain a proper system of SDEs with external noises as white-noises and \mathbf{Z}_p^r is therefore a Markov process described either by the Langevin equations in Eqs. (321) or by its equivalent Fokker–Planck equation in sample space

$$\frac{\partial p_{p,r}^L}{\partial t} + V_{p,k} \frac{\partial p_{p,r}^L}{\partial y_{p,k}} = \frac{\partial}{\partial V_{p,k}} \left[\frac{1}{\tau_p^{st}} \left(\langle U_{f,k} \rangle(t, \mathbf{y}_p) - V_{p,k} \right) p_{p,r}^L \right] + \frac{1}{2} \frac{\partial^2}{\partial V_{p,k} \partial V_{p,l}} [D_{s,kl} p_{p,r}^L], \quad (322)$$

with \mathbf{D}_s the diffusion matrix given by $\mathbf{D}_s = 1/(\tau_p^{st})^2 ((\mathbf{G}^*)^{-1} \mathbf{B}_s) ((\mathbf{G}^*)^{-1} \mathbf{B}_s)^\perp$. This corresponds to the case where $\mu_{kl} = D_{s,kl}$ but with $\lambda_{kl} = 0$ which, apart from the deterministic case mentioned above, turns out to be the only situation where \mathbf{Z}_p^r makes up a Markov process. Indeed, if we leave out these two asymptotic cases, it is clear from the classical example recalled in Section 4.2 that \mathbf{Z}_p^r is not a Markov process, since the fluid velocity seen has a non-zero correlation timescale. In other words, the reduced state vector \mathbf{Z}_p^r is non-Markovian due to the characteristic features of turbulence, namely the existence of length and time correlations. From the presentation of probabilistic approaches in Section 4.5.1, it follows immediately that the law of \mathbf{Z}_p^r cannot be retrieved from the sole knowledge of the transitional PDF, which proves that kinetic PDF formulations are incomplete probabilistic descriptions of particles in non-fully resolved (or non-white-noise) turbulent flows.

As mentioned in Section 4, the non-Markovian nature of the reduced state vector \mathbf{Z}_p^r does not prevent the formulation of kinetic PDF equations if we are only interested in using these equations to derive macroscopic (i.e. moment) descriptions. It represents, however, an early warning sign of more difficulties to come when the second criterion introduced in Section 4.5.2 is considered. Indeed, the real shortcoming is that the kinetic PDF equation, represented by the generic form in Eq. (160), is an ill-posed equation. This is investigated in details in [52] where it is proved that, if the kinetic PDF equation is exact when the velocity of the fluid seen is Gaussian, it cannot be applied outside of this Gaussian context and is, therefore, irrelevant as a general model proposal. As analyzed in [52], this is due to the existence of negative eigenvalues in the so-called ‘diffusion matrix’ entering the kinetic PDF equation. In the context of the present review, this failure can also be understood as reflecting the analysis developed in Section 9.2, in particular with the specific ‘kinetic form’ considered with Eqs. (207)–(220). In effect, casting the closed form of the kinetic PDF model as in Eq. (195), it is seen that the matrix $\tilde{\mathbf{D}}$ is (using a bloc notation with $i, j = 1, 3$)

$$\tilde{\mathbf{D}} = \begin{pmatrix} 0 & | & (\lambda_{ij}) \\ -- & | & --- \\ (\lambda_{ji}) & | & (\mu_{ij}) + (\mu_{ji}) \end{pmatrix}. \quad (323)$$

As soon as $\lambda_{ji} \neq 0$, it is immediate that the symmetrical matrix $\tilde{\mathbf{D}}$ has at least one negative eigenvalue since its determinant, $\det(\tilde{\mathbf{D}}) = -(\det(\lambda))^2$, is always negative [153]. Detailed discussions are provided in [52] but, in the scope of the present analysis, it is worth emphasizing that the central problem is rooted in the treatment of the velocity of the fluid seen as an external noise to the chosen (kinetic) description. As a further hint, it can be noted that when $\lambda_{ji} = 0$, we have a complete and well-posed probabilistic description. Since the ratio λ/μ represents the timescale of the velocity of the fluid seen T_L^* , this is the second limit case described above, where the fluid seen is regarded as a white-noise compared to particle inertia, cf. Eqs. (321)–(322) and is the only situation where a kinetic description is acceptable.

In short, all these results point to the key physical issue which is how to account for the coherence of the carrier fluid in the choice of the particle state vector. This is clarified below in Sections 10.1.3 and 10.1.4.

10.1.2. Dynamic PDF descriptions are complete and well posed

For dynamic PDF descriptions, the situation is quite straightforward. Indeed, given the choice of the extended state vector $\mathbf{Z}_p = (\mathbf{x}_p, \mathbf{U}_p, \mathbf{U}_s)$ and the formulation of \mathbf{U}_s as a stochastic diffusion process, we are in a well-established situation. The trajectory of the process \mathbf{Z}_p are proper SDEs and, since external noises are white-noises, \mathbf{Z}_p is a Markov process. The by-now-well-oiled mathematical machinery of stochastic diffusion processes (see Section 4) guarantees that the probabilistic description is complete and that the PDF equation, which is a Fokker–Planck equation, is well posed. In a nutshell, all criteria related to realizability, completeness, well-posedness, etc., are automatically satisfied in dynamic PDF approaches. This allows to concentrate on the physical relevance of the chosen description.

From the sketch in Fig. 56, it is seen that, contrary to kinetic-based methods, dynamic PDF models are purely time-forward approaches using only local statistics of the variable eliminated (here the time rate of change of the velocity of the fluid seen). These differences and the notions of local and non-local properties of corresponding macroscopic formulations are addressed later in Section 10.3.

10.1.3. The need of new statistical approaches for particle dispersion

Summing up the preceding developments, a clear picture emerges. The kinetic PDF description is the marginal of the dynamic PDF one. Yet, the kinetic PDF model is an incomplete probabilistic description with an ill-posed PDF equation while the dynamic PDF model constitutes a complete and well-posed PDF formulation. Apart from its interest for the development of stochastic models for particles in turbulent flows (cf. point (i) in the introduction of Section 10), this brings out a more

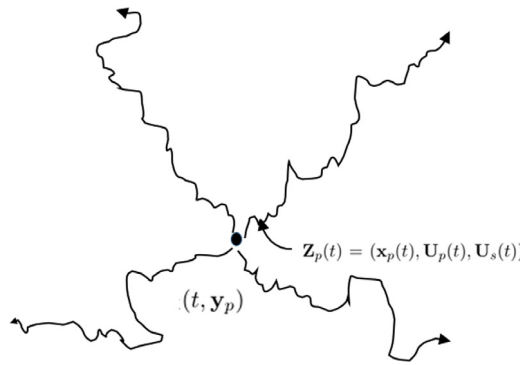


Fig. 56. Illustration of the purely time-forward formulation in dynamic PDF methods. Since the complete state vector $Z_p = (x_p, U_p, U_s)$ is a Markov process driven by white-noise, the process is marched forward in time from the local values existing at $(t, x_p(t))$.

general result in line with point (ii). The important outcome is that kinetic-based descriptions of particle dispersion in continuous media can be retained only if the underlying media are either fully resolved (that is, all their degrees of freedom are explicitly simulated) or are so rapidly changing that they can be regarded as the equivalent of ‘heat bathes’. In the general case, kinetic formulations are ill suited to build probabilistic descriptions of particles in random media (*i.e.* non-fully resolved media) and must be extended by including additional variables related to the characteristics of these random media. This supports the argument put forward in Section 9.4 and brings out the key difference between particle dispersion in turbulent flows and Brownian motion (see point (iii)). Compared to classical statistical approaches, the specific challenge is now to select new variables to form well-based dynamic PDF descriptions.

10.1.4. Colored noises must be included in the description

In [52], it is demonstrated that the introduction of the velocity of the fluid seen in the particle state vector does not change the ill-based nature of the PDF equation if the acceleration of the fluid seen (strictly speaking, the time rate of change of the velocity of the fluid seen) does not contain rapid terms that can be eliminated and replaced by white-noise effects. The demonstration is, in fact, valid for general dynamical systems influenced by colored noises.

To complement the analysis provided in [52] and to confirm that this is a general result, we consider a dynamical system where, using the notations of Section 9.2, the evolution equations for the state vector $\mathbf{Z} = (Z_1, Z_2, \dots, Z_N)$ have the following structure

$$\frac{dZ_1}{dt} = Z_2, \quad (324a)$$

$$\frac{dZ_2}{dt} = -\frac{Z_2}{\tau_2} + Z_3, \quad (324b)$$

$$\vdots$$

$$\frac{dZ_N}{dt} = -\frac{Z_N}{\tau_N} + Z_{N+1}, \quad (324c)$$

where τ_k ($k = 2, \dots, N$) are (constant) timescales and where Z_{N+1} is an external colored noise that we take as being an OU process

$$dZ_{N+1} = -\frac{Z_{N+1}}{\tau_{N+1}} dt + \sigma_{N+1} dW, \quad (325)$$

with τ_{N+1} its (constant) timescale and σ_{N+1} its diffusion coefficient that, for the sake of simplicity, is given by the fluctuation-dissipation theorem for Z_{N+1} , *i.e.* $\sigma_{N+1}^2 = 2\langle Z_{N+1}^2 \rangle / \tau_{N+1}$. It is seen that this structure is the one obtained from the initial kinetic choice ($Z_1 = x_p$, $Z_2 = U_p$ and $\tau_2 = \tau_p$) when $N-2$ successive time derivatives are included, in line with the second hierarchy mentioned in Section 8.1.2. In the present case, application of the FND relation yields that

$$\langle Z_{N+1} | \mathbf{Z} \rangle p(t; \mathbf{z}) = -\beta_{N+1-i} \frac{\partial p}{\partial z_i} \quad (326)$$

where the $\beta_{N+1-i} = \langle Z_i Z_{N+1} \rangle$, with $i = 1, \dots, N$, stand for the correlation between the eliminated variable (*i.e.* Z_{N+1}) and the variables kept in the state vector \mathbf{Z} (*i.e.* $(Z_i)_{i=1,N}$). This entails that the resulting equation for the one-particle PDF $p(t; \mathbf{z})$

is as in Eq. (195) with the matrix $(\tilde{D}_{ij})_{i,j=1,N}$ entering the second-order derivative given by

$$\tilde{D}_{ij} = \begin{pmatrix} 0 & 0 & \dots & 0 & \dots & 0 & \beta_N \\ 0 & 0 & \dots & 0 & \dots & 0 & \beta_{N-1} \\ \vdots & \vdots & & \vdots & & \vdots & \vdots \\ 0 & 0 & \dots & 0 & \dots & 0 & \beta_{N+1-i} \\ \vdots & \vdots & & \vdots & & \vdots & \vdots \\ 0 & 0 & \dots & 0 & \dots & 0 & \beta_2 \\ \beta_N & \beta_{N-1} & \dots & \beta_{N+1-i} & \dots & \beta_2 & 2\beta_1 \end{pmatrix}. \quad (327)$$

By recurrence, it is straightforward to show that $\mathbb{P}_{\tilde{D}}(x) = \det(x\mathbb{1} - \tilde{\mathbf{D}})$, the characteristic polynomial of the matrix $\tilde{\mathbf{D}}$, is

$$\mathbb{P}_{\tilde{D}}(x) = x^{N-2} \left(x^2 - 2\beta_1 x - \sum_{k=2}^N \beta_k^2 \right), \quad (328)$$

from which it follows that the N eigenvalues of the symmetrical matrix \tilde{D} are

$$e_1 = \beta_1 + \sqrt{\beta_1^2 + \sum_{k=2}^N \beta_k^2} \geq 0, \quad (329a)$$

$$e_2 = \beta_1 - \sqrt{\beta_1^2 + \sum_{k=2}^N \beta_k^2} \leq 0, \quad (329b)$$

$$e_i = 0 \quad (i = 2, \dots, N). \quad (329c)$$

Therefore, the situation is basically the same as for $N = 2$. As soon as $\beta_k \neq 0$ (for $k = 2, \dots, N$), there is always one negative eigenvalue, resulting in an anti-diffusive behavior and an ill-posed PDF equation. It can even be noted that adding more variables (*i.e.* for increasing values of N) only makes the situation worse since the negative eigenvalue, here e_2 , becomes more important. The only possibility to have a well-posed PDF equation is $\beta_k = 0, \forall k = 2, \dots, N$. With the system in Eqs. (324), it follows that the correlations between the eliminated variable and the ones kept in the state vector scale as successive powers in the timescale τ_{N+1} (this is an example of the result stated in Section 9.2),

$$\beta_i = \tau_{N+1}^i \langle (Z_{N+1})^2 \rangle \times \mathcal{O}(1), \quad \forall i = 1, \dots, N \quad (330)$$

and we find again that the only meaningful limit corresponds to $\tau_{N+1} \rightarrow 0$ and $\langle (Z_{N+1})^2 \rangle \rightarrow +\infty$, with $\tau_{N+1} \langle (Z_{N+1})^2 \rangle \simeq \beta_1$ a constant, which is the white-noise limit for Z_{N+1} . In that case, the matrix \mathbf{D} has only positive or null eigenvalues and the system in Eqs. (324) becomes a true system of SDEs for $\mathbf{Z} = (Z_1, \dots, Z_N)$ with the white-noise term entering at the level of the evolution equation for the last variable Z_N .

Summary. The conclusion is that adding more variables in the state vector, by including successive time derivatives, does not remedy the ill-posed nature of the PDF equation unless a white-noise limit is taken for one of these derivatives. This result reveals that the real issue is not about the use of the FND relation, or any other similar formulas, but is related to the application of the fast-variable elimination technique guided by physical analyses. It demonstrates that the essential modeling step is the selection of relevant particle state vectors so that external noises can be physically regarded as white noises.

Timescale separation and stochastic model for the fluid seen. To be physically justified, a clear distinction between slow and fast variables requires a separation of scales. From the applications of Kolmogorov theory recalled in Section 6.1, we know that such a separation exists between a fluid-particle velocity and its acceleration. Indeed, fluid-particle acceleration has a timescale of the order of the Kolmogorov timescale τ_K , cf. Eqs. (94), while the timescale of its velocity is governed by $T_L \simeq T_f$. Then, it derives from Eq. (95) that fluid-particle acceleration is a rapid process with respect to its velocity. Furthermore, as $Re \rightarrow +\infty$, when $v_f \rightarrow 0$ with a non-vanishing energy dissipation rate $\langle \epsilon_f \rangle$, we have

$$\tau_K \rightarrow 0, \quad \langle \mathbf{A}_f^2 \rangle \rightarrow +\infty \quad \text{with} \quad \langle \mathbf{A}_f^2 \rangle \times \tau_K \simeq \langle \epsilon_f \rangle, \quad (331)$$

which suggests that \mathbf{A}_f is the proper variable to be treated as the one to eliminate.

In practice, the fast-variable-elimination approach is applied to the fast part of the fluid-particle acceleration (in the single-phase flow case) and of the time rate of change of the velocity of the fluid seen (in the disperse two-phase flow case). Note that this is in line with the decomposition in Eq. (324c) and the elimination of Z_{N+1} which is the fast part of the acceleration of Z_N . Considering the more general case of disperse two-phase turbulent flows, this is formalized by considering an evolution equation of \mathbf{U}_s written as

$$\frac{d\mathbf{U}_s(t)}{dt} = \mathbf{A}_s(t, \mathbf{Z}_p(t), \mathcal{F}[\mathbf{Z}_p]) + \mathbf{B}_s(t, \mathbf{Z}_p(t), \mathcal{G}[\mathbf{Z}_p]) \boldsymbol{\xi}_s(t). \quad (332)$$

In Eq. (332), the terms \mathbf{A}_s and \mathbf{B}_s are governed by the fluid large-scale motions and are varying slowly (of the order of T_L), while the centered process ξ_s accounts for the rapidly-varying part of the acceleration of the fluid seen and has, therefore, a timescale τ_{ξ_s} of the order of the Kolmogorov timescale $\tau_{\xi_s} \simeq \tau_K$. Leaving out the possible dependence on functionals of the process \mathbf{Z}_p (represented by $\mathcal{F}[\mathbf{Z}_p]$ and $\mathcal{G}[\mathbf{Z}_p]$ in \mathbf{A}_s and \mathbf{B}_s) for the sake of keeping simple notations and introducing an observation timescale Δt , the increments of $\mathbf{U}_s(t)$ are

$$\mathbf{U}_s(t + \Delta t) - \mathbf{U}_s(t) = \int_t^{t+\Delta t} \mathbf{A}_s(t', \mathbf{Z}_p(t')) dt' + \int_t^{t+\Delta t} \mathbf{B}_s(t', \mathbf{Z}_p(t')) \xi_s(t') dt'. \quad (333)$$

When $\Delta t \gg \tau_K$, the integral of the rapid part can be split into the sum of several integrals, using a partition $(t_i)_{i=1,M}$ of the interval $[t; t + \Delta t]$ such that $t_1 = t$, $t_M = t + \Delta t$ and $t_{i+1} - t_i = k\tau_K$ (with $k \gg 1$, for $i = 1, \dots, M - 1$)

$$\int_t^{t+\Delta t} \mathbf{B}_s(t', \mathbf{Z}_p(t')) \xi_s(t') dt' = \sum_{i=1}^{M-1} \int_{t_i}^{t_{i+1}} \mathbf{B}_s(t', \mathbf{Z}_p(t')) \xi_s(t') dt'. \quad (334)$$

In a Lagrangian time-forward formulation at the scale of the chosen observation time Δt , what is needed is to express the conditional increments $d_{\Delta t} \mathbf{U}_s$ which represent

$$d_{\Delta t} \mathbf{U}_s | (\mathbf{Z}_p(t) = \mathbf{z}_p) = (\mathbf{U}_s(t + \Delta t) - \mathbf{U}_s(t)) | (\mathbf{Z}_p(t) = \mathbf{z}_p). \quad (335)$$

A closed dynamic PDF model is built in two modeling steps. The first one consists in freezing the slowly-varying functions $\mathbf{A}_s(t', \mathbf{Z}_p(t'))$ and $\mathbf{B}_s(t', \mathbf{Z}_p(t'))$ at the value at the beginning of the observation time interval in Eq. (333) (since $\Delta t \ll T_L$), which gives

$$d_{\Delta t} \mathbf{U}_s | (\mathbf{Z}_p(t) = \mathbf{z}_p) = \mathbf{A}_s(t, \mathbf{z}_p(t)) \Delta t + \mathbf{B}_s(t, \mathbf{z}_p(t)) \sum_{i=1}^{M-1} \int_{t_i}^{t_{i+1}} \xi_s(t') dt'. \quad (336)$$

The second step consists in considering that the $(M - 1)$ integrals entering the sum on the rhs of Eq. (336) are nearly independent, since each of them is an integration of the fast process ξ_s over time intervals which are much larger than its correlation timescale. From the Central Limit Theorem (CLT) for $M \gg 1$ (since $\Delta t \gg \tau_K$), we can then replace the sum on the rhs of Eq. (336) by a Gaussian centered variable. This provides the rationale behind the Gaussian character of the conditional increments $d_{\Delta t} \mathbf{U}_s | (\mathbf{Z}_p(t) = \mathbf{z}_p)$. Then, the fast-variable elimination of the acceleration is applied to ξ_s (since $\langle \mathbf{A}_s^2 \rangle \simeq \langle \xi_s^2 \rangle$) which gives

$$\int_t^{t+\Delta t} \xi_s(t') dt' \simeq \sqrt{\langle \epsilon_f \rangle} d\mathbf{W}. \quad (337)$$

Switching back to expressions in terms of small time increments written as dt (and re-introducing the complete notation with possible dependences on functional of the process \mathbf{Z}_p), we get that \mathbf{U}_s is modeled as a stochastic diffusion process

$$d\mathbf{U}_s(t) = \mathbf{A}_s(t, \mathbf{Z}_p(t), \mathcal{F}[\mathbf{Z}_p]) dt + \tilde{\mathbf{B}}_s(t, \mathbf{Z}_p(t), \mathcal{G}[\mathbf{Z}_p]) d\mathbf{W}, \quad (338)$$

where $\tilde{\mathbf{B}}_s = \mathbf{B}_s \sqrt{\langle \epsilon_f \rangle}$. It is therefore not surprising that the diffusion coefficients in the modeled evolution equations for \mathbf{U}_f (see Section 6.5) and for \mathbf{U}_s (see Section 7.3.3) present such a dependence on $\sqrt{\langle \epsilon_f \rangle}$. It is worth emphasizing that, in the construction of the stochastic model for \mathbf{U}_s , the notion of scale separation is manifested by the use of the two simultaneous limits (*i.e.* $\Delta t \ll T_L$ and $\Delta t \gg \tau_K$) and also by the introduction of an observation timescale Δt . This notion will resurface on several occasions throughout Section 10.

10.2. Selection of the particle state vector

The results of Section 10.1 demonstrate that the relevant choice of the particle state vector is $\mathbf{Z}_p = (\mathbf{x}_p, \mathbf{U}_p, \mathbf{U}_s)$ for particles in turbulent flows. This is in line with the guidelines set forth in Section 9.4 but insofar as we consider small, nearly pointwise, particles in high Reynolds-number turbulent flows described by statistical approaches (*i.e.* not fully resolved).

In order to get a better understanding of the interplay between mechanical descriptions, fast variables and modeling issues in the selection of particle state vectors, it is illustrative to consider another application, for example fibers in turbulent flows. This is a typical situation involving non-spherical particles and which bears similarities with the physics of polymeric fluids discussed earlier in this paper (see Section 7). An introduction to fibers in the context of Fluid Mechanics and the paper-making industry is provided in [159] and there is a growing activity dedicated to studying fiber dynamics through DNS approaches [160,161], as well as first attempts at building mesoscopic models based on simple versions of the Langevin models discussed in Section 7.3.3 or on basic Fokker–Planck formulations [162–164]. There is also an unabated activity devoted to the formulation of rheological laws. Fiber modeling can thus be cast into the framework of microscopic, mesoscopic and macroscopic approaches, with stochastic (or mesoscopic) descriptions bridging the gap between DNS studies (microscopic) and averaged rheological relations (macroscopic). In that sense, the present discussion is of interest to show how particle state vectors are defined.

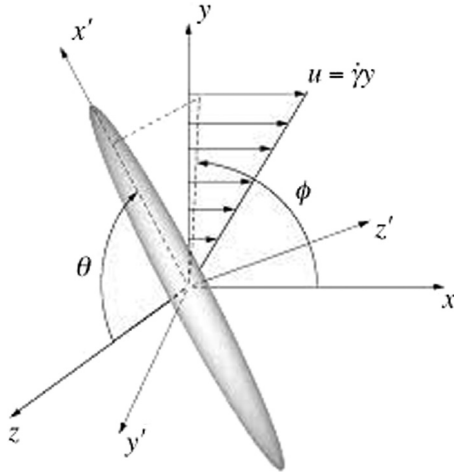


Fig. 57. Representation of a fiber as a rigid rod in a linear shear flow.

The question ‘how do we write a practical model for fibers in turbulent flows?’ involves three steps: (a) ‘how do we describe a fiber?'; (b) ‘what are the variables that we select in the particle (i.e. fiber) state-vector?’; (c) ‘what are the corresponding models?’. For the present purpose, we are concerned with the connection between the first two questions. Two descriptions can be proposed:

- (1) A first idea is to describe fibers as rigid, elongated, ellipsoids characterized by two dimensions (the lengths l_a and l_b along the major and minor axis of the ellipsoid). It is then possible to write the evolution equations of such rod-like fibers in a fluid flow, which correspond to the Jeffrey’s equations [159–161], see the sketch in Fig. 57. For our purpose, it is sufficient to express the general form of these equations as

$$\frac{d\mathbf{U}_p}{dt} = \underline{\mathbf{K}} \cdot (\mathbf{U}_s - \mathbf{U}_p) \quad (339a)$$

$$\frac{d\boldsymbol{\omega}_p}{dt} = \mathcal{F}(\boldsymbol{\omega}_p, S_{ij}^f, \Omega_{ij}^f) \quad (339b)$$

where $\boldsymbol{\omega}_p$ is the particle rotation, \mathcal{F} a function that expresses the torque acting on the fiber divided by its inertia moment, while S_{ij}^f and Ω_{ij}^f represent the symmetrical and rotational parts of the fluid velocity-gradient tensor ($S_{ij}^f = 1/2 (\mathcal{G}_{f,ij} + \mathcal{G}_{f,ji})$ and $\Omega_{ij}^f = 1/2 (\mathcal{G}_{f,ij} - \mathcal{G}_{f,ji})$ respectively, with $\mathcal{G}_{f,ij} = \partial U_{f,i} / \partial x_j$). In Eq. (339a), $\underline{\mathbf{K}}$ stands for the matrix of drag coefficients. Indeed, the different cross-sections of the rigid fiber imply that anisotropic drag coefficients must be used in the directions corresponding to the axis of the ellipsoid. This means that the fiber orientation \mathbf{p} (or the defining Euler angles) must be tracked in time and, therefore, that obtaining $\boldsymbol{\omega}_p$ (with $\boldsymbol{\omega}_p = \dot{\mathbf{p}}$) from Eq. (339b) is a requirement.

If the Jeffrey’s equations are applied with the velocity and the velocity-gradients of the fluid evaluated at the fiber center-of-mass, a relevant fiber state vector is $\mathbf{Z}_{r-f} = (\mathbf{x}_p, \mathbf{U}_p, \boldsymbol{\omega}_p, \mathbf{U}_s, \mathcal{G}_{s,ij})$ where $\mathcal{G}_{s,ij} = \mathcal{G}_{f,ij}(t, \mathbf{x}_p(t))$ are the fluid velocity-gradients at the fiber center-of-mass location. Compared to the spherical-particle case, it is seen that the fiber state vector is supplemented with the particle rotation $\boldsymbol{\omega}_p$ (or its orientation) and the fluid velocity-gradients seen $\mathcal{G}_{s,ij}$. This has modeling consequences since $\mathcal{G}_{s,ij}$ are small-scale turbulent quantities and modeling both \mathbf{U}_s and $\mathcal{G}_{s,ij}$ in turbulent flows is a challenging, even daunting, task [165]. If a large enough observation time Δt is chosen to describe the rigid fiber motion, for example such that $\Delta t \gg \tau_G$ where τ_G is the correlation timescale of velocity gradients, then $\mathcal{G}_{s,ij}$ can be regarded as fast processes and replaced by white-noises so that \mathbf{Z}_{r-f} is reduced to $\mathbf{Z}_{r-f} = (\mathbf{x}_p, \mathbf{U}_p, \boldsymbol{\omega}_p, \mathbf{U}_s)$. This assumption is made in some studies where fiber orientations are modeled with simple diffusive laws or, conversely, with a Fokker–Planck equation with constant diffusion coefficients (see [163,164]), which is acceptable only for stationary isotropic fluids and in the long-time limit where a diffusive regime is always reached (see the discussions in Section 9.3.1). On the other hand, if the observation time is not large enough, $\mathcal{G}_{s,ij}$ must be kept in the state-vector. Note, however, that Jeffrey’s equations assume a linear shear flow along the entire fiber length or, in other words, that the fluid velocity-gradients are constant over that region. If the fiber length l_a is much larger than the Kolmogorov length scale η_K , this assumption raises doubts and the averaged value of the fluid velocity gradients over l_a should be used. This implies now that a spatial information on $\mathcal{G}_{s,ij}$ has to be included in the description and, thus, in the fiber state-vector.

- (2) When flexible fibers are involved, a different mechanical description is needed, as represented for example in Fig. 58. This approach is used in some numerical simulations [162] and consists in a chain-rod model where each fiber is

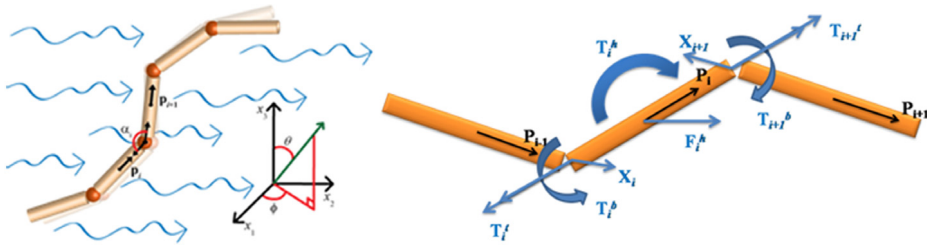


Fig. 58. A chain-rod description for flexible fibers. Each rod is subject to a force and a torque and relations must be enforced between the elementary segments to ensure the integrity of the fiber.

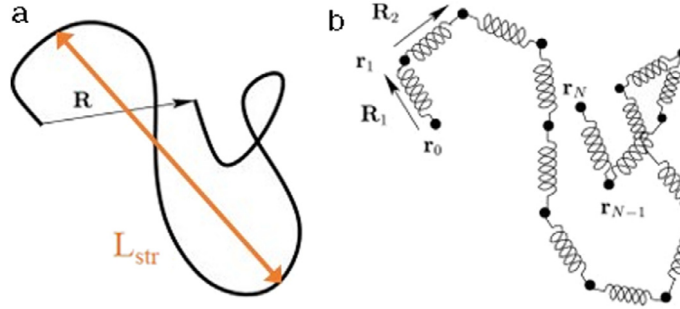


Fig. 59. A chain-spring model for flexible fibers (b), or large polymers, in a turbulent flow with L_{str} the characteristic length (cf. (a)) representing the typical elongation or stretching of the fiber/polymer in the flow.

made up by a chain of m segments of interconnected rods (see the zoom on the right in Fig. 58). The interest of such a description is that bending and twisting fiber motions can now be captured [162]. Basically, each of the elementary rods are treated as in the first approach with equations alike Jeffrey's but proper constraints must be written (and numerically enforced) to represent the connectivity between each rod. Since each rod is described by the translation of its center of mass and the rotation around it, the previous reasoning that led to the choice of \mathbf{Z}_{r-f} applies for each segment. This means that, if we denote by m the number of rigid rods used to describe one fiber, the corresponding flexible-fiber state vector becomes $\mathbf{Z}_{f-f} = (\mathbf{Z}_{r-f}^{(l)})_{l=1,M}$ to which the connectivity constraints are applied (the total number of degrees of freedom is therefore less than $M \times N_{r-f}$ where N_{r-f} is the number of degrees of freedom entering the rigid fiber state-vector). This description leads therefore to a much-extended state vector with a high-dimension (noting that \mathbf{Z}_{r-f} involves already $N_{r-f} = 18$ variables). For the present discussion, the important point is that this description requires the simulation of the vector made up by the fluid velocity seen at the center of mass of each rod at the same time, as well as the joint generation of the fluid velocity-gradients.

Similar considerations hold even if we adopt the same description as for polymers, or consider a large-scale polymer in a turbulent flows described only by its mean velocity field, (see Fig. 59). In that case, one fiber is fully described by the positions of the N beads which make up the chain, since the spring forces between consecutive beads depend only on their relative positions. However, advancing the N bead positions requires to know the fluid velocities at these N points and, therefore, to reconstruct a multi-point information on the instantaneous fluid flow.

In consequence and regardless of their specific details, these descriptions rely on a multi-time and -point information on the fluid flow. Depending on the length of these fibers with respect to the turbulent scales (Kolmogorov, Taylor and integral scales), several hypothesis can be proposed. If the length scale representing the typical fiber/polymer elongation L_{str} is of the order of the local value of the Kolmogorov length scale or even smaller, the local fluid field around the fiber center-of-mass position can be approximated by an instantaneous shear flow with a shear rate whose orientation and intensity fluctuate in time. This is equivalent to having to reconstruct the local fluid gradients around the fiber-polymer center-of-mass $\mathcal{G}_{s,ij}$, using their norm which is related to the local value of the turbulent energy dissipation (for example $\mathcal{G}_s \sim \sqrt{(\epsilon_f)/(v_f)}$ in a locally isotropic flow) and a random orientation. Even in the inertia-less limit where the bead velocities are eliminated as fast variables, this implies to select a state vector of the form $\mathbf{Z}_{f-p} = ((\mathbf{x}_p^{(l)})_{l=1,N}, \mathbf{U}_s, \mathcal{G}_{s,ij})$, which can be further reduced to $\mathbf{Z}_{f-p} = ((\mathbf{x}_p^{(l)})_{l=1,N}, \mathbf{U}_s)$ for large observation times compared to the timescale of the velocity-gradient timescale (i.e. $\Delta t \gg \tau_G$) where the effects of the variations of these velocity-gradients can be also replaced by white-noises (or diffusive) terms.

From these discussions on relevant state vectors for rigid or flexible fibers and large-scale polymers, as representing the class of ‘elongated mechanical objects’ in not-fully-resolved turbulent flows, two remarks can be made:

- (i) If the typical length scale of the elongated object is not too large ($L_{\text{str}} \simeq \eta_K$), it is possible to develop models in the frame of one-point PDF descriptions of the fluid flow. This is exemplified by the introduction of \mathbf{U}_s , or $(\mathbf{U}_s, \mathcal{G}_{s,ij})$, in

the preceding analyses. However, if their length is large compared to a length scale over which fluid velocities or its gradients vary significantly, a description in terms of the velocity and gradients seen at the fiber center-of-mass is not sufficient and a multi-point information on the fluid flow is needed. In other words, this implies that a two-point, or N -point, PDF model is required for the fluid to derive a closed one-particle PDF description for the fibers;

- (ii) The hierarchy of particle/fiber state vectors corresponds to probabilistic descriptions with a system of SDEs having more or less components due to the elimination of the fast variables. Since any mesoscopic model yields a macroscopic constitutive relation, this means that there is also a hierarchy between the corresponding macroscopic closures. Using a different terminology, this translates the fact that the hierarchy of state vectors corresponds to a hierarchy between rheological laws.

Drawing on the second remark, it is important to realize that, if the hierarchy between state vectors is expressed in terms of slow and fast variables, the corresponding hierarchy between the rheological laws is unraveled in terms of local and non-local constitutive relations. This correspondence is now studied.

10.3. Stochastic closures and local/non-local macroscopic constitutive relations

In Sections 6 and 7, the connection between Lagrangian stochastic models and the transport equations for the second-order moments of the variables contained in the state vector was emphasized. This link is natural for particle-based approaches since the particle state vector usually contains the particle position and velocity at minimum. This can be formalized with a general expression of the particle state vector written as $\mathbf{Z} = (\mathbf{x}, \mathbf{U}, (\mathbf{Z}_l^{add})_{l=1,N})$ where $(\mathbf{Z}_l^{add})_{l=1,N}$ represents a set of additional variables depending on each physical situation and by considering evolution equations written under the simple form

$$dx_i = U_i dt \quad (340a)$$

$$dU_i = F_i dt \quad (340b)$$

where \mathbf{F} on the rhs of Eq. (340b) stands for the time rate of change of the particle velocity and the incremental notation $F_i dt$ is used to loosely denote the fact that \mathbf{F} can contain white-noise terms. If $\mathbf{F} = \mathbf{F}(t, \mathbf{x})$ then the system is closed, while if $\mathbf{F} = \mathbf{F}(t, \mathbf{x}, (\mathbf{Z}_l^{add})_{l=1,N})$ the corresponding SDEs for the additional variables $(\mathbf{Z}_l^{add})_{l=1,N}$ have to be included in the description. The important point is that, as soon as the particle velocity is included in the state vector, then Eq. (340a) indicates that transport is treated without approximation. As shown in Sections 6 and 7, this is enough to ensure that we obtain the correct structure for the first two moments of the velocity field in the mean equations

$$\frac{\partial \langle U_i \rangle}{\partial t} + \langle U_k \rangle \frac{\partial \langle U_i \rangle}{\partial x_k} + \frac{\partial \langle u_i u_k \rangle}{\partial x_k} = \langle F_i \rangle, \quad (341a)$$

$$\frac{\partial \langle u_i u_j \rangle}{\partial t} + \langle U_k \rangle \frac{\partial \langle u_i u_j \rangle}{\partial x_k} + \frac{\partial \langle u_i u_j u_k \rangle}{\partial x_k} + \langle u_i u_k \rangle \frac{\partial \langle U_j \rangle}{\partial x_k} + \langle u_j u_k \rangle \frac{\partial \langle U_i \rangle}{\partial x_k} = \langle u_i \circ F_j \rangle + \langle u_j \circ F_i \rangle, \quad (341b)$$

where all the convective terms have been written on the lhs of Eqs. (341) and where the symbol in $\langle u_i \circ F_j \rangle$ designates Stratonovich calculus which allows a more compact notation to be used. In Sections 6 and 7, we have seen that various Lagrangian stochastic models can be devised where white-noise terms enter at different levels in the equations for $(\mathbf{Z}_l^{add})_{l=1,N}$ and that such modeling steps are related to local closures in the mean equations.

These examples translate a general link between the choice of a white-noise term (in time) in the particle stochastic equations and the existence of local or non-local closures (in space) in the corresponding mean equations. At this point, it is worth remembering that, in each situation, the particle state vector must be chosen so as to ensure that ‘external noises’ are treated as white-noises (see the conclusions of Section 9.4). In practice, it is therefore natural to consider stochastic models where white-noise terms appear at various levels in the set of modeled equations. Consequently, the second hierarchy of state vectors described in Section 8.1 is in correspondence with a hierarchy of local/non-local source terms in the average equations.

This correspondence can be made explicit by considering first the case of single-phase fluid turbulence and, thus, the tracer-particle limit:

- (i) If we choose to retain only the particle velocity in the state vector, i.e. $\mathbf{Z}_f = (\mathbf{x}_f, \mathbf{U}_f)$, with a description that includes a white-noise term in the stochastic equation for the particle velocity, as in the GLM introduced in Section 6.5.1 (cf. Eqs. (126))

$$dx_{f,i} = U_{f,i} dt, \quad (342a)$$

$$dU_{f,i} = -\frac{1}{\rho_f} \frac{\partial \langle P_f \rangle}{\partial x_i} dt + D_i dt + \underbrace{\sqrt{C_0 \langle \epsilon_f \rangle(t, \mathbf{x}_f)} dW_i}_{\text{fast term}}. \quad (342b)$$

Then, the high-Reynolds form of the Reynolds equation (cf. Eq. (103)) is satisfied and is re-written here as

$$\frac{D_f \langle U_{f,i} \rangle}{Dt} + \frac{\partial}{\partial x_j} [\underbrace{\langle u_{f,i} u_{f,j} \rangle}_{\text{non local}}] = -\frac{1}{\rho_f} \frac{\partial \langle P_f \rangle}{\partial x_i} \quad (343)$$

to emphasize that the components of the Reynolds-stress tensor, $\langle u_{f,i} u_{f,j} \rangle$, are not given by a local closure expression in space, as with the eddy-viscosity concept discussed in Section 6.3.1 (see further discussions in Section 10.4), but are the solutions of the second-order equations (cf. Eq. (130)):

$$\frac{D_f \langle u_{f,i} u_{f,j} \rangle}{Dt} = -\frac{\partial \langle u_{f,i} u_{f,j} u_{f,k} \rangle}{\partial x_k} + \mathcal{P}_{ij} + \langle u_{f,i} D_j \rangle + \langle u_{f,j} D_i \rangle + \underbrace{C_0 \langle \epsilon_f \rangle(t, \mathbf{x}_f)}_{\text{local term}} \delta_{ij}. \quad (344)$$

This shows that $\langle u_{f,i} u_{f,j} \rangle(t, \mathbf{x})$ is influenced by the past history of the fluid elements arriving at (t, \mathbf{x}) but that its rate of change, manifested by the terms on the rhs of Eq. (344), is local in space due to the choice of the fast term in Eq. (342b). This can be further explained by considering particle accelerations. As such, particle acceleration does not exist anymore as a regular process since its fast part is replaced by a white-noise, but its integrated value over a small time interval dt can be written as

$$A_{f,i} dt = -\frac{1}{\rho_f} \frac{\partial \langle P_f \rangle}{\partial x_i} dt + D_i dt + \underbrace{\sqrt{C_0 \langle \epsilon_f \rangle(t, \mathbf{x}_f)}}_{\text{no time-memory}} dW_i. \quad (345)$$

For the present discussion, the important element is that the fast part of particle acceleration is modeled as a process with a zero-correlation timescale. It is then seen that the “*memory-less*” term in the particle velocity stochastic equation induces a “*transport-less*”, or *local term*, in the corresponding mean equation. This closure is important for the correspondence with classical Reynolds-stress equations and to identify $\langle \epsilon_f \rangle(t, \mathbf{x})$ as the (local) value of the turbulent kinetic energy dissipation. Indeed, using the decomposition of the drift term D_i in Eqs. (127)–(128) (see Section 6.5.1), the RSM for $\langle u_{f,i} u_{f,j} \rangle$ given by Eq. (131) is retrieved where the contributions of both the drift and diffusion terms yield the local estimations of the redistribution and dissipation contributions.

- (ii) If we want to have a well-defined particle acceleration, the fast-acceleration term used above can be regularized with a ‘colored noise’, for example by writing

$$dx_{f,i} = U_{f,i} dt, \quad (346a)$$

$$dU_{f,i} = -\frac{1}{\rho_f} \frac{\partial \langle P_f \rangle}{\partial x_i} dt + D_i dt + \underbrace{\gamma_{f,i} dt}_{\text{colored}}. \quad (346b)$$

The particle acceleration is now a proper variable entering the extended particle state vector, $\mathbf{Z}_f = (\mathbf{x}_f, \mathbf{U}_f, \mathbf{A}_f)$, and we have a meaningful definition

$$A_{f,i} = -\frac{1}{\rho_f} \frac{\partial \langle P_f \rangle}{\partial x_i} + D_i dt + \gamma_{f,i} \quad (347)$$

where $\gamma_{f,i}$ is a stochastic process with $\langle \gamma_{f,i} \rangle = 0$ but a non-zero integral timescale. Then, the corresponding mean Reynolds-stress equations have the following form

$$\frac{D_f \langle u_{f,i} u_{f,j} \rangle}{Dt} = -\frac{\partial \langle u_{f,i} u_{f,j} u_{f,k} \rangle}{\partial x_k} + \mathcal{P}_{ij} + \langle u_{f,i} D_j \rangle + \langle u_{f,j} D_i \rangle + \underbrace{\langle u_{f,i} \gamma_{f,j} \rangle + \langle u_{f,j} \gamma_{f,i} \rangle}_{\text{non-local}}. \quad (348)$$

Therefore, a *non-white-noise term* for the rapid part of particle velocities results in a *non-local closure* in the corresponding mean equations. Indeed, the source terms, such as $\langle u_{f,i} \gamma_{f,j} \rangle$, are not determined only by the local flow properties but are, in turn, the solutions of transport equations which express a spatial ‘upwind’ dependence. For example, if $\gamma_{f,i}$ is given by a Langevin model with τ its integral timescale

$$d\gamma_{f,i} = -\frac{\gamma_{f,i}}{\tau} dt + K_{(i)} dW_i \quad (349)$$

(no summation on i in the last term), then $\langle u_{f,i} \gamma_{f,j} \rangle$ is the solution of the transport equation

$$\frac{D_f \langle u_{f,i} \gamma_{f,j} \rangle}{Dt} + \frac{\partial \langle u_{f,k} u_{f,i} \gamma_{f,j} \rangle}{\partial x_k} = -\langle u_{f,k} \gamma_{f,j} \rangle \frac{\partial \langle U_{f,i} \rangle}{\partial x_k} + \langle D_i \gamma_{f,j} \rangle - \frac{\langle u_{f,i} \gamma_{f,j} \rangle}{\tau} + \langle (\gamma_{f,i})^2 \rangle \delta_{ij}, \quad (350)$$

which depends on $\langle (\gamma_{f,i})^2 \rangle$ which, in turn, is the solution of

$$\frac{D_f \langle (\gamma_{f,i})^2 \rangle}{Dt} + \frac{\partial \langle u_{f,k} (\gamma_{f,i})^2 \rangle}{\partial x_k} = -2 \frac{\langle (\gamma_{f,i})^2 \rangle}{\tau} + \underbrace{K_{(i)}^2}_{\text{local term}}. \quad (351)$$

Once again, locality is present in the hierarchy but has been shifted ‘upward’ to the mean equation corresponding to the white-noise term in the stochastic model retained for $\gamma_{f,i}$ (here through the coefficient $K_{(i)}$). Such stochastic models based on particle acceleration have been proposed for homogeneous isotropic turbulence [166] and also for general inhomogeneous turbulent flows [167].

There is, however, an another interesting element due to non-locality: whereas the drift and diffusion terms in Eqs. (342b) are expressed with the local value of the turbulent kinetic energy dissipation rate, $\langle \epsilon_f \rangle(t, \mathbf{x})$, we are now handling a non-local estimation of the dissipation. Furthermore, anisotropy is potentially re-introduced since $\epsilon_{f,ij} \sim \langle u_{f,i} \gamma_{f,j} \rangle + \langle u_{f,j} \gamma_{f,i} \rangle$, which is now dependent on the flow behavior in a small domain area upstream of (t, \mathbf{x}) .

So far, the link between white-noise terms in the SDEs and local closures in the mean equations has been presented in an ‘upward’ description by considering extended state vectors, for example by going from $\mathbf{Z}_f = (\mathbf{x}_f, \mathbf{U}_f)$ to $\mathbf{Z}_f = (\mathbf{x}_f, \mathbf{U}_f, \mathbf{A}_f)$. It is also possible to move ‘downward’. Taking for instance the description in terms of particle accelerations as a starting point, the description at the level of particle location and velocity can be retrieved. This is seen from Eqs. (350) by taking the limit when $\tau \rightarrow 0$: the transport equations become stiff and the solutions are obtained by equating the terms on the rhs of the equations. Clearly, the only meaningful limit is obtained when $K_{(i)} \rightarrow \infty$ and $\tau \rightarrow 0$ in such a way that $K_{(i)} \times \tau$ tends towards a finite constant value. Thus, $\langle (\gamma_{f,i})^2 \rangle \rightarrow \infty$ but with $\langle (\gamma_{f,i})^2 \rangle \times \tau$ remaining finite. The estimation of that limit value is provided by Kolmogorov hypothesis [30], as already used in Eq. (331) in Section 10.1.4. In the limit of vanishing τ , we have therefore that $\langle u_{f,i} \gamma_{f,j} \rangle \sim [\langle (\gamma_{f,i})^2 \rangle \times \tau] \delta_{ij}$ and this result is consistent with the white-noise term in Eq. (342b) which states that $\lim_{\tau \rightarrow 0} [\langle (\gamma_{f,i})^2 \rangle \times \tau] = C_0 \langle \epsilon_f \rangle$.

This interplay between white-noise terms in the SDEs and local closures in constitutive relations is of direct concern for two-phase flow modeling. To bring out the main physical ideas and avoid cumbersome tensorial notations with complex stochastic models for the standard particle state vector $\mathbf{Z}_p = (\mathbf{x}_p, \mathbf{U}_p, \mathbf{U}_s)$, we limit ourselves to a simple isotropic formulation

$$d\mathbf{x}_{p,i} = U_{p,i} dt, \quad (352a)$$

$$dU_{p,i} = \frac{U_{s,i} - U_{p,i}}{\tau_p} dt, \quad (352b)$$

$$dU_{s,i} = -\frac{U_{s,i} - \Phi_i}{T_L^*} dt + \underbrace{\sigma_{s,ij} dW_j}_{\text{fast term}}, \quad (352c)$$

where τ_p and $T_L^*(t, \mathbf{x})$ are the same relaxation timescales in each direction, $\Phi(t, \mathbf{x})$ a field quantity (containing typically the mean fluid velocity at the particle location and additional terms depending on the choice of the stochastic model for \mathbf{U}_s), and $\sigma_s(t, \mathbf{x})$ the diffusion matrix retained in the model of \mathbf{U}_s . Then, the corresponding set of second-order moments is also governed by a hierarchy of local and non-local terms. The complete equations can be found in [1,54] but, for our purpose, it is sufficient to write the transport equations of the simplified model given in Eqs. (352) which, using a compact notation, are

$$\frac{D_p \langle u_{p,i} u_{p,j} \rangle}{Dt} = \mathcal{D}_{u_{p,i} u_{p,j}} + \mathcal{P}_{u_{p,i} u_{p,j}} + \frac{1}{\tau_p} \underbrace{[\langle u_{p,i} u_{s,j} \rangle + \langle u_{p,j} u_{s,i} \rangle - 2 \langle u_{p,i} u_{p,j} \rangle]}_{\text{non-local term}}, \quad (353a)$$

$$\frac{D_p \langle u_{s,i} u_{p,j} \rangle}{Dt} = \mathcal{D}_{u_{p,i} u_{s,j}} + \mathcal{P}_{u_{p,i} u_{s,j}} + \frac{1}{\tau_p} \underbrace{\langle u_{s,i} u_{s,j} \rangle}_{\text{non-local term}} - \left(\frac{1}{\tau_p} + \frac{1}{T_L^*} \right) \langle u_{s,i} u_{p,j} \rangle, \quad (353b)$$

$$\frac{D_p \langle u_{s,i} u_{s,j} \rangle}{Dt} = \mathcal{D}_{u_{s,i} u_{s,j}} + \mathcal{P}_{u_{s,i} u_{s,j}} - \frac{2}{T_L^*} \langle u_{s,i} u_{s,j} \rangle + \underbrace{(\sigma_s \sigma_s^\perp)_{ij}}_{\text{local term}}, \quad (353c)$$

where $\mathcal{D}_{u_{k,i} u_{l,j}}$ and $\mathcal{P}_{u_{k,i} u_{l,j}}$ (with $k, l \in \{p, s\}$) stand for the diffusion and production terms entering each mean second-order equations and whose details are not relevant for the present discussion (see the complete formulations in [1, section 8.3.1] or in [54] for example). The important point is manifested by the structure of the second-order equations. It is seen that the complete system in Eqs. (353) is closed but exhibits a typical hierarchical structure in terms of the local and non-local source terms appearing on the rhs of Eqs. (353). More specifically, the particle kinetic tensor $\langle u_{p,i} u_{p,j} \rangle$ is non-locally dependent on $\langle u_{p,i} u_{s,j} \rangle$ which, in turn, is non-locally dependent on $\langle u_{s,i} u_{s,j} \rangle$ whose closure is also non-local since it is given by the solution of the transport equation in Eq. (353c). Only the last term on the rhs of Eq. (353c) is local, since this is the first level at which the white-noise term of Eq. (352c) manifests itself for second-order moments.

A different structure results when white-noise terms enter the particle system of equation at another level. For instance, when the velocity of the fluid seen \mathbf{U}_s is regarded as a rapidly-varying variable with respect to particle inertia (i.e. $T_L^* \ll \tau_p$), we can use the fast-variable elimination techniques presented in Section 9.3 and the system in Eqs. (352) is reduced to

$$d\mathbf{x}_{p,i} = U_{p,i} dt, \quad (354a)$$

$$dU_{p,i} = -\frac{U_{p,i}}{\tau_p} dt + \frac{1}{\tau_p} \Phi_i(t, \mathbf{x}_p) dt + \frac{1}{\tau_p} \underbrace{(T_L^* \sigma_{s,ij}) dW_j}_{\text{fast term}}. \quad (354b)$$

The transport equations for the particle kinetic tensor has then the following form

$$\frac{D_p \langle u_{p,i} u_{p,j} \rangle}{Dt} = \mathcal{D}_{u_{p,i} u_{p,j}} + \mathcal{P}_{u_{p,i} u_{p,j}} - \frac{2}{\tau_p} \langle u_{p,i} u_{p,j} \rangle + \underbrace{(\sigma_p \sigma_p^\perp)_{ij}}_{\text{local term}}, \quad (355)$$

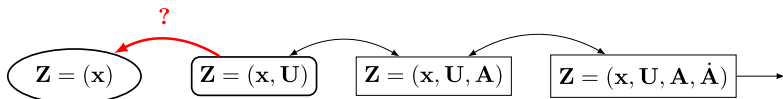


Fig. 60. Hierarchy of one-particle state vectors and the issue of stochastic formulations in terms of $\mathbf{Z} = (\mathbf{x})$.

with σ_p the diffusion matrix in the SDE for \mathbf{U}_p given by $\sigma_p(t, \mathbf{x}_p) = 1/\tau_p(T_L^* \sigma_s)(t, \mathbf{x}_p)$. Since the fast-variable elimination is local in time and space, it is seen that the white-noise term in the evolution equation of \mathbf{U}_s in Eq. (352c) has been shifted upward to the equation of \mathbf{U}_p . In correspondence, the transport equation for the particle kinetic tensor is now closed with the rhs of Eq. (355) involving only local terms.

Obviously, solving the 6 coupled PDEs of Eqs. (355) is less daunting than trying to do so for the 21 coupled PDEs of Eqs. (353) (for each class of particle diameter) and such forms are often considered in two-fluid models. From the very structure of Eqs. (353), it is however evident that, in a general non-homogeneous flow, using local closures for the correlations $\langle u_{s,i} u_{p,j} \rangle$ and $\langle u_{s,i} u_{j,l} \rangle$ amounts to assuming that the fluid velocity seen relaxes quickly to a local value, which is the notion embodied by the formulation above with \mathbf{U}_s as a fast variable to eliminate. From a physical point of view, neglecting transport effects for \mathbf{U}_s , while keeping track of those for \mathbf{U}_p , is equivalent to considering that there is a marked separation between the timescales or, in other words, that we have $T_L^* \ll \tau_p$. This is indeed the assumption made to derive the system in Eqs. (354). It is also clear that this is a stringent limitation of such models since this can be done only for high-inertia particles for which turbulent fluctuations can be regarded as noise. It is interesting to remark that we are then in the same situation as for Brownian particles with respect to fluid molecules whose ‘fluctuations’ are properly simulated by white-noise driving terms. This is, however, a very poor approach for discrete particles when we are not in the limit of high Stokes numbers. Note that a form similar to the one in Eq. (355) is obtained with the kinetic PDF approach (see [168]). However, we know from the study in Section 10.1 that the ratio of the dispersion coefficients λ and μ represents the timescale of the variable that has been eliminated from the description (here \mathbf{U}_s). This implies that $\lambda/\mu = T_L^*$ which, in the present case, is negligible (with respect to τ_p), showing that we have $\lambda = 0$. This is the only situation where the kinetic PDF description is well-posed and an acceptable PDF description for particles in high Reynolds-number turbulent flows. In that case, the kinetic PDF description is identical to the Fokker–Planck equation corresponding to the stochastic system in Eq. (354) and is, thus, limited to discrete particles in a ballistic regime (*i.e.* to the description of ‘bullet particles’).

10.4. A physical analysis of gradient-diffusion models

In the preceding sub-section, the connection between white-noises in SDEs and local source terms in constitutive relations was illustrated by considering extensions of the ‘elementary’ state vector made up by the particle position and location $\mathbf{Z} = (\mathbf{x}, \mathbf{U})$. It is however also interesting to explore the opposite direction when the particle velocity is eliminated (see the sketch in Fig. 60). In relation with this problem is the question of the physical meaning of gradient-diffusion hypotheses.

At first sight, this creates a puzzle when addressed from the kinetic variables $\mathbf{Z} = (\mathbf{x}, \mathbf{U})$ in the state vector. Indeed, using Eqs. (340) and (341), it is seen that, as soon as particle velocity exists as a proper stochastic process, the second-order velocity moments are the solution of transport equations (the same is, of course, also valid for the kinetic stress tensor in the two-phase flow situation). As it transpires from the name of transport equation, there is little chance for a second-order moment to be given by a gradient-diffusion relation (*i.e.* by a local formulation) in a general non-homogeneous turbulent flows unless some hypotheses are made on the relevant timescales.

To investigate this issue, it is best to start by considering the case of a passive scalar ϕ_f in single-phase flows. A simple evolution equation such as

$$d\phi_f = -\frac{\phi_f - \langle \phi_f \rangle}{\tau_{\phi_f}} dt \quad (356)$$

can be retained and added to the description to make up the extended particle state vector $\mathbf{Z}_f = (\mathbf{x}_f, \mathbf{U}_f, \phi_f)$. The rhs of Eq. (356) represents a basic model accounting for scalar dissipation, written as an interaction by exchange with the mean (IEM) scalar value $\langle \phi_f \rangle(t, \mathbf{x})$ and where the scalar dissipation timescale τ_{ϕ_f} is proportional to the timescale of turbulent kinetic energy decay, *i.e.* $\tau_{\phi_f} = 2 C_{\phi_f} k_f / \langle \epsilon_f \rangle$ (with C_{ϕ_f} a constant). This IEM model is used here for the sake of completeness but could also be left out since it does not play any role in the following (for instance, this simplification was used at the end of Section 9.3). With the SDEs for particle position and velocity as in Eqs. (342), the corresponding second-order moment equations are the Reynolds equations in Eq. (343) and the transport equations for the Reynolds stress tensor components in Eq. (344) to which the mean scalar equation is added. This equation for the mean scalar field is easily derived (see [30,111]) as

$$\frac{D_f \langle \phi_f \rangle}{Dt} + \frac{\partial \langle u_{f,i} \phi_f' \rangle}{\partial x_i} = 0, \quad (357)$$

where $\langle u_{f,i} \phi'_f \rangle$ is the turbulent scalar flux (see Section 3.2.2 and Eq. (27)). In turn, $\langle u_{f,i} \phi'_f \rangle$ is the solution of a transport equation which, using the GLM model, cf. Eqs. (126) in Section 6.5.1, and the usual decomposition of D_i given in Eq. (127), is

$$\frac{D_f \langle u_{f,i} \phi'_f \rangle}{Dt} + \frac{\partial \langle u_{f,k} u_{f,i} \phi'_f \rangle}{\partial x_k} = -\langle u_{f,k} \phi'_f \rangle \frac{\partial \langle U_{f,i} \rangle}{\partial x_k} - \langle u_{f,i} u_{f,k} \rangle \frac{\partial \langle \phi_f \rangle}{\partial x_k} - \left(G_{ik} - \frac{1}{2} C_{\phi_f} \frac{\langle \epsilon_f \rangle}{k_f} \delta_{ik} \right) \langle u_{f,k} \phi'_f \rangle. \quad (358)$$

Note that we retrieve the same structure in terms of local and non-local closures: $\langle u_{f,i} \phi'_f \rangle$ is non-local in Eq. (357) and is the solution of a transport equation where locality enters only through the last two (modeled) terms on the rhs of Eq. (358).

In traditional turbulence modeling, turbulent-diffusivity models are obtained by neglecting all convective terms and equating the source terms on the rhs of Eq. (358) (see [30,111]). This leads to algebraic expressions where scalar fluxes are proportional to the mean scalar gradients

$$\langle u_{f,i} \phi'_f \rangle = -\Gamma_{ft,ik} \left(\frac{\partial \langle \phi_f \rangle}{\partial x_k} \right), \quad (359)$$

which is identical to the one obtained in Eq. (314). From the results of Section 9.3, it is seen that such a gradient-diffusion model requires fluid-particle velocities to become fast-variables for this closure to remain valid in general non-homogeneous turbulent flows. This is physically unjustified since the timescale of velocity fluctuations is not negligible with respect to those of the mean velocity or scalar gradients and is even generally larger.

If one cannot expect the fluid velocity correlation timescale T_L to be much smaller than an observation timescale Δt with which a turbulent flow is analyzed, there are, however, some situations where gradient-diffusion formulas can work. One typical example is provided by the case of a scalar point-source dispersion (as represented in Fig. 61(a)). From the analysis developed in Section 9.3, we know that, if the turbulence intensities $\langle u_{f,i} u_{f,j} \rangle \sim u_f^2$ and timescales T_L do not change significantly downstream of the source injection, a diffusion regime for the particle positions (and, therefore, for the scalar concentration) is always reached in the long-time limit (see the discussion with the canonical Langevin transport model in Section 9.3.1). It is thus not a surprise that a gradient-diffusion model becomes applicable in this limit. Since fluid particles are convected downstream with the mean fluid flow, this long-time limit corresponds to the far-field region, that is the region sufficiently far downstream (the precise spatial location where this region is considered to begin depends on the mean fluid velocity in each case). This explains the classical result that turbulent-diffusivity models work well in the far-field region downstream of the injection but give poor predictions near the source, which corresponds to the short-time limit where a diffusive law is not yet reached.

This reasoning is illustrated in Fig. 61 for the spread of a thermal plume in grid-generated turbulence (see details and analyses in [30,169]). In that situation, the passive scalar is heat (not high enough to modify the fluid density and induce buoyancy effects) injected from a point source downstream of a grid which generates an isotropic but decaying turbulent flow (see Fig. 61(a)). The decay of the turbulent kinetic energy is given by $u_f^2 \sim U_f^2 (x_w/M)^{-m}$, with x_w the distance from the injection, U_f the free-stream fluid velocity, m the mesh size of the grid and where m is typically equal to $m \simeq 1.32$. Turbulence is thus spatially uniform in the directions normal to the mean flow and slowly decaying downstream of the injection.

Experimental measurements (from [170]) and numerical predictions of the evolution of the thickness of the thermal plume are shown in Fig. 61(b) as a function of x_w (with $x_w \simeq U_f t$). It is seen that there are three regimes in the profile of the normalized thermal plume thickness σ_{th}/M in Fig. 61(b). The first one, immediately after the injection, is due to molecular diffusion. It was not explicitly considered in the example of the canonical Langevin model in Section 9.3.1 but is easily included (by adding a white-noise term in Eq. (224a)). The other two regimes, where $\sigma_{th} \sim x_w$ and $\sigma_{th} \sim x_w^{0.34}$ respectively, correspond to the short- and long-time limits analyzed in Section 9.3.1. The scaling as $x_w^{0.34}$ in the diffusive limit, instead of $x_w^{0.5}$, is due to the fact that turbulence is decaying. From the profiles in Fig. 61(b), it is seen that particle models based on simple Langevin models (cf. the GLM with $G_{ij}^a = 0$) predict correctly the evolution of the plume thickness in the three regimes. On the contrary, gradient-diffusion models (in that case, a diffusivity model based on the $k-\epsilon$ model) are in poor agreement, especially in the near-field region corresponding to the short-time limit after the injection. This is in line with the above analysis. Only in the far-field region, corresponding to the long-time (diffusive) limit, do these models start to be acceptable in the sense that the slope of the predicted plume spread is in line with experimental reality. In the initial stages of the plume spread, gradient-diffusion models are clearly performing poorly.

This analysis is directly applicable to the large-scale examples of volcanic eruptions discussed in Section 2.1. As shown in Fig. 62, the evolution of a volcanic cloud can only be properly captured by approaches that treat transport without approximation, especially in the near-field region, whereas the traditional random-walk models should not be retained until the far-field region is reached.

This reasoning for the convective scalar flux and about the validity (or the lack of it) of turbulent-diffusivity assumptions can be directly extended to the Reynolds-stress tensor and to the physical analysis of the concept of a turbulent viscosity. In that category, the reference closure is, of course, the $k-\epsilon$ model in Eq. (105) which is obviously an attempt to reproduce, at the level of the mean equations, Newton's law for the effects of molecular fluctuations in the hydrodynamical equations. In the context of the previous discussion in terms of local and non-local closures, the key point is that a turbulent-viscosity model is a local expression for the Reynolds stress components which are, by nature, convective terms and, thus, intrinsically non-local. Answers to the question of the physical validity of such gradient-diffusion hypothesis are provided by the developments presented in Section 9.3.5, which demonstrate that locality is retrieved when velocities become fast-variables.

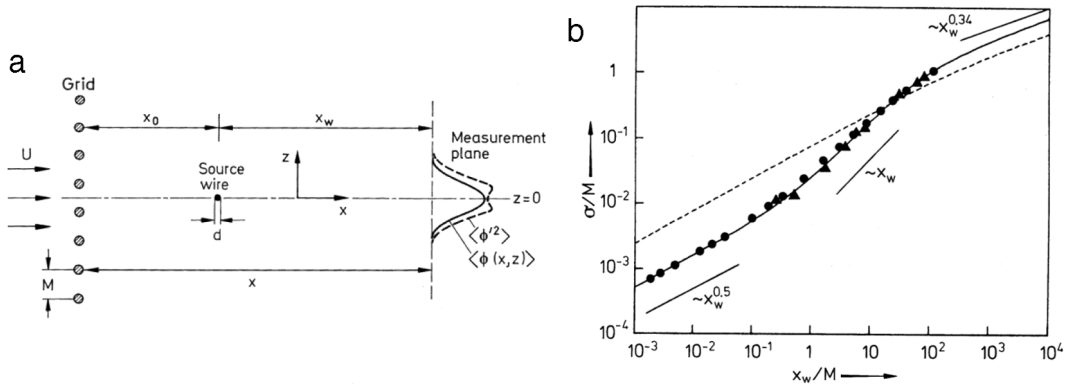


Fig. 61. A scalar point-source dispersion problem: (a) Sketch of a heated wire downstream of a grid creating a decaying isotropic turbulent flow; (b) Evolution of the thermal wire thickness as a function of the distance from the wire with predictions obtained with a gradient-diffusion hypothesis from the $k - \epsilon$ model (—), from a particle PDF model (— and ●) and experimental measurements ▲ from [170].
Source: Results from [169].

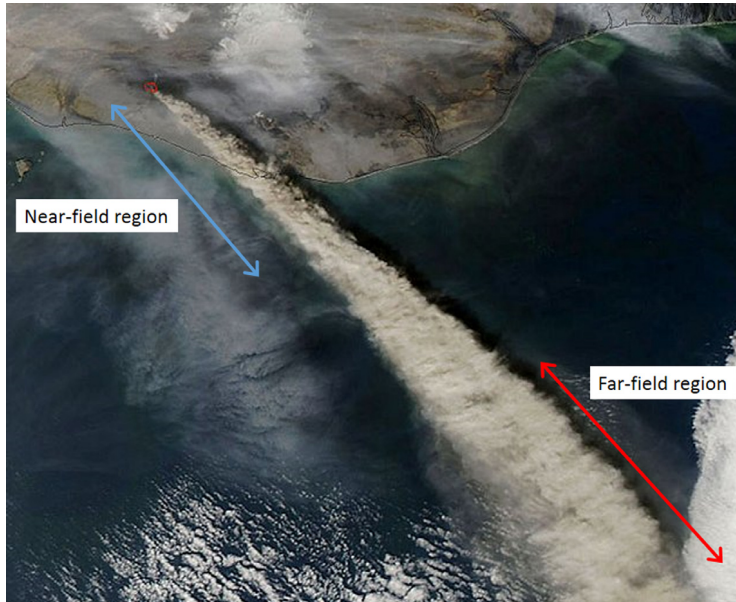


Fig. 62. Spread of a volcanic ash plume with a qualitative indication of the near-field region where gradient-diffusion hypothesis cannot be used and of the far-field zone where it may be used (credit: NASA).

At first sight, this seems to create a technical difficulty as the energy of fast variables becomes infinite in the white-noise limit. In Section 9.3, this white-noise limit is taken since the ideas of infinitely-fast variables are developed in continuous time (that is by taking the limit of the observation time as $\Delta t \rightarrow 0$) but it is possible to handle the tensor $A_{ij} = \lim_{\chi \rightarrow 0} \langle \chi u_{f,i} u_{f,j} \rangle$ as a surrogate for the Reynolds stress tensor in the parametrization (P2) or resort to the parametrization (P1) which has the advantage of keeping energy finite. As already done above, it is also possible to introduce an observation timescale Δt and regard a fast variable as being a process whose auto-correlation timescale becomes very small with respect to Δt . This is the simple version of the very-fast-relaxation ideas used in Section 9.3.5 and is in anticipation of discrete formulations which are helpful for these notions (see Section 10.5).

Based on the discussions in Sections 9.3 and 10.3, it is clear that a local closure of the Reynolds stress tensor as in Eq. (105) can only hold true when velocities have vanishing relaxation timescales and are rapidly varying (see the discussion about the introduction of two timescales in Section 9.3.5).

This discussion is applicable to the two-phase flow situation and is directly relevant for the analysis of two-fluid models where similar assumptions are often made for the particle kinetic tensor $\langle u_{p,i} u_{p,j} \rangle$ expressed by

$$\langle u_{p,i} u_{p,j} \rangle = \frac{1}{3} \langle u_{p,k} u_{p,k} \rangle \delta_{ij} - v_{p,t} \left(\frac{\partial \langle U_{p,i} \rangle}{\partial x_j} + \frac{\partial \langle U_{p,j} \rangle}{\partial x_i} - \frac{2}{3} \frac{\partial \langle U_{p,k} \rangle}{\partial x_k} \delta_{ij} \right). \quad (360)$$

In the present context, we are not concerned with the specific choices put forward for the expression of the ‘particle turbulent viscosity’ $\nu_{p,t}$ but mostly with the formulation of a local closure for $\langle u_{p,i} u_{p,j} \rangle$ in terms of the local values of the gradients of the particle mean velocity field. As for the fluid scalar situation, there are cases where such relations can work relatively well. As a mirror of the scalar point-source dispersion problem, a typical example is provided by the point-source dispersion of solid particles in a turbulent fluid flow, for example a jet flow in the middle of which small discrete particles are released. In this situation, the physical analysis follows the one already developed for the scalar concentration: when the turbulent fluid flow characteristics do not vary too much downstream of the particle injection, there is always a diffusive regime that, for the particles, is reached sufficiently long after the time of their injection and which corresponds to a region sufficiently far downstream of the position of the injection. In that case also, a particle turbulent viscosity concept does not work too badly, although the near-field (close to the injection location) is typically poorly captured.

Apart from these special situations, the notion of a particle turbulent viscosity raises even more doubts and concerns than in the fluid case. Indeed, in the fluid situation, the driving force of a fluid element is due to the pressure-gradient and viscous terms and it can sometimes be assumed that a part of the pressure-gradient acts as a fast-relaxation term. In the two-phase case, the situation is different. Using the simple model version in Eqs. (352) for the sake of the present argument (this simple formulation contains all the key physical characteristics of a two-phase flow situation), it is seen that the driving force of the particle velocity (*i.e.* its acceleration) is governed both by τ_p and by the (large-scale) fluid turbulent velocity \mathbf{U}_s whose timescale is T_L^* . It is easy to show that, in homogeneous situations, the resulting characteristic timescale of \mathbf{U}_p is given by $\tau_p + T_L^*$ which we can use as a reference timescale. Then, for a local closure expression such as the one in Eq. (360) to have a chance to be approximately valid, we must be in a situation where $\tau_p + T_L^* \ll \Delta t$ but also with an observation time Δt is still small enough to capture the evolution of the particle mean-velocity gradients $\Delta t (\partial \langle U_{p,i} \rangle / \partial x_j) \ll 1$. Clearly, this is a very strong limitation for the validity of local closures for the particle kinetic tensor. It not only implies that the fluid velocities be rapid variables but also that we limit ourselves to small-inertia particles.

In summary, there is no escaping that one must consider the complete set of transport equations in Eqs. (353), except for very special cases that are of little interest (there is no need of a two-phase treatment for purely diffusive, small-inertia, Brownian particles). Given the daunting numerical task generated by this coupled system of PDEs (which has, furthermore, to be written for each particle class when particles are polydispersed), it is seen that the particle stochastic system in Eqs. (352) (which contains much more information than the first and second-order moments) is the most attractive formulation not only to respect the key aspects of the physics of dispersed two-phase flows but also as a numerical approach. Some details on this numerical formulation, which are helpful to bring out the practical meaning of rapidly-varying variables, are now outlined.

10.5. Slow and fast variables in numerical formulations

In Section 9.3, the fast-variable elimination principles were presented in continuous time. This means that, for example in the (P2) parametrization which allows the fast-variable elimination to be carried out in real time, the time increments dt are infinitesimally small quantities. Thus, obtaining a meaningful limit result requires the variance of the eliminated variable to become infinite. From a physical point of view, this infinite-variance limit raises questions since it corresponds to handling infinite-energy processes. It is however possible to reconcile the elimination of fast variables in real time with finite-energy processes by considering time-discrete formulations. This approach was already hinted to in Sections 10.2 and 10.3 when an ‘observation time’ was introduced to distinguish between slow and fast variables. This notion stands obviously for a numerical time step but, as it follows from its name, an observation time Δt is useful to introduce a physically-meaningful scale which corresponds to the timescale at which we decide to observe a given phenomenon.

To bring out the physical meaning of the fast-variable elimination procedure, it is sufficient to consider the canonical Langevin model given in Eqs. (224a,b) in Section 9.3 with only the particle position and velocity (X, U). Since the timescale T and the diffusion coefficient σ are constant, the trajectories of the process between a time t and a time $t + \Delta t$ can be exactly integrated. A straightforward application of the rules of stochastic calculus gives

$$X(t + \Delta t) = X(t) + U(t)T [1 - \exp(-\Delta t/T)] + I_X(\Delta t), \quad (361a)$$

$$U(t + \Delta t) = U(t) \exp(-\Delta t/T) + I_U(\Delta t), \quad (361b)$$

where the stochastic integrals are defined by

$$I_X(\Delta t) = \sigma T \int_t^{t+\Delta t} dW(s) - \sigma T \exp(-(t + \Delta t)/T) \int_t^{t+\Delta t} \exp(s/T) dW(s), \quad (362a)$$

$$I_U(\Delta t) = \sigma \exp(-(t + \Delta t)/T) \int_t^{t+\Delta t} \exp(s/T) dW(s). \quad (362b)$$

In these equations, $(I_X(\Delta t), I_U(\Delta t))$ is a vector composed by two joint, centered Gaussian random variables which, using Cholesky algorithm, can be simulated as

$$I_X(\Delta t) = \left(\langle I_X I_U \rangle / \sqrt{\langle I_U^2 \rangle} \right) \xi_U + \sqrt{\langle I_X^2 \rangle - \langle I_X I_U \rangle^2 / \langle I_U^2 \rangle} \xi_X, \quad (363a)$$

$$I_U(\Delta t) = \sqrt{\langle I_U^2 \rangle} \xi_U, \quad (363b)$$

where ξ_X and ξ_U are two independent normalized Gaussian random variables. The components of the covariance matrix are given by (see [44, section 4.1]):

$$\langle I_X^2 \rangle = (\sigma T)^2 \{ \Delta t - T[1 - \exp(-\Delta t/T)][3 - \exp(-\Delta t/T)]/2 \}, \quad (364a)$$

$$\langle I_U^2 \rangle = \sigma^2 T[1 - \exp(-2\Delta t/T)]/2, \quad (364b)$$

$$\langle I_X I_U \rangle = \{ \sigma T[1 - \exp(-\Delta t/T)] \}^2/2. \quad (364c)$$

In the continuous sense, the fast-variable limit corresponds to $T \rightarrow 0$. However, in a discrete sense, this limit is translated by the condition $T \ll \Delta t$, which means that the fast variable $U(t)$ has a characteristic timescale which becomes negligible *with respect to the one we have chosen to observe our phenomenon*. In this limit, the discrete formulation of the canonical Langevin model is obtained by using $\Delta t/T \gg 1$ in the above equations, which gives

$$X(t + \Delta t) \simeq X(t) + (\sigma T) \sqrt{\Delta t} \xi_X, \quad (365a)$$

$$U(t + \Delta t) \simeq \sqrt{\frac{\sigma^2 T}{2}} \xi_U. \quad (365b)$$

It is seen that the two processes X and U are now decoupled, with the positions governed by the combination (σT) while velocities are driven by the combination $(\sigma^2 T)$. These are the right coefficients to reproduce the correct rate of diffusion and level of kinetic energy (see the discussion in Section 9.3.2). Eq. (365a) is, of course, the first-order Euler scheme for the integration of the diffusive regime, that is of the random-walk approximation given in Eq. (234). Note that the correct diffusive contribution on the rhs of Eq. (365a) is due to the last term on the rhs of Eq. (363a) which, when the classical Taylor expansion is performed with $\Delta t \ll T$, is first-order negligible.

The noteworthy element is that, in the discrete limit formulation, the particle velocity does not ‘disappear’ (whereas, in the continuous sense, it becomes a Gaussian white-noise). As seen from Eq. (365b), particle velocities are now simulated as a series of independent Gaussian random variables. This is physically correct since we are observing particle velocities with an observation time Δt much larger than its memory (or its auto-correlation timescale T). In short, the discrete formulation is helpful to provide further light on the fast-variable elimination procedure. Provided that the stochastic integrals which express the influence of the fast variables on the slow ones are properly manipulated (which means here that all the terms on the rhs of Eq. (363a) are simulated), fast variables are represented by a series of independent Gaussian random variables while their integrated effects (over their numerous fluctuations within each time span Δt) are expressed by diffusion coefficients in the resulting evolution equations for the slow variables.

These notions are used for instance in some derivations of the limit of the over-damped Langevin model (see [158]). They have been extended and applied for the analysis of asymptotic cases for the complete Lagrangian stochastic model for two-phase flow presented in Section 7.3.3, where they are used for the development of first- and second-order numerical schemes in a comprehensive work on these aspects [44].

10.6. Particle collision and agglomeration rates

When considering the statistical effects of particle collisions, the reference framework is made up by the kinetic theory and the Boltzmann equation [171] for the distribution function $f(t; \mathbf{y}_p, \mathbf{V}_p, d_p)$ which retains only particle location, velocity and diameter (or volume) in the particle state vector. It was originally developed in sample space and, in the absence of forces acting on particles between collisions, has the following form

$$\frac{\partial f}{\partial t} + V_{p,k} \frac{\partial f}{\partial y_k} = Q_{coll}(f) \quad (366)$$

where $Q_{coll}(f)$ is the collision source term given by

$$Q_{coll}(f) = \int_{\mathbb{R}^3} d\mathbf{V}_{c,p} \int_{S^2} d\mathbf{e} B(\mathbf{V}_p, \mathbf{V}_{c,p}, \mathbf{e}) [f(t; \mathbf{y}_p, \mathbf{V}_p^{ac}, d_p) f(t; \mathbf{y}_p, \mathbf{V}_{c,p}^{ac}, d_{c,p}) - f(t; \mathbf{y}_p, \mathbf{V}_p, d_p) f(t; \mathbf{y}_p, \mathbf{V}_{c,p}, d_{c,p})]. \quad (367)$$

The gain and loss terms in Eq. (367) correspond to the result of possible collisions with all other particles and are expressed as sums over potential collisional partners whose velocity before the collision event is written $\mathbf{V}_{c,p}$. In the integrals in Eq. (367), S^2 denotes the unit sphere in \mathbb{R}^3 and \mathbf{e} is a unit vector on S^2 representing the orientation of the collision event. The likelihood of collisions is measured by the collision kernel $B(\mathbf{V}_p, \mathbf{V}_{c,p}, \mathbf{e})$ involving the collision cross-section which, in the kinetic theory, is given by

$$B(\mathbf{V}_p, \mathbf{V}_{c,p}, \mathbf{e}) = \pi \left(\frac{d_p}{2} + \frac{d_{c,p}}{2} \right)^2 |(\mathbf{V}_p - \mathbf{V}_{c,p}, \mathbf{e})| \quad (368)$$

where d_p and $d_{c,p}$ are the diameters of the particle and its collisional partner and (\cdot, \cdot) denotes the scalar product. In physical space, the transformation relations that express the collision event and relate the two colliding particles are given by

$$\mathbf{U}_p^{ac} = \mathbf{U}_p - \frac{2m_{c,p}}{m_p + m_{c,p}} (\mathbf{U}_p - \mathbf{U}_{c,p}, \mathbf{e}) \cdot \mathbf{e}, \quad (369a)$$

$$\mathbf{U}_{c,p}^{ac} = \mathbf{U}_{c,p} + \frac{2m_p}{m_p + m_{c,p}} (\mathbf{U}_p - \mathbf{U}_{c,p}, \mathbf{e}) \cdot \mathbf{e} \quad (369b)$$

where m_p and $m_{c,p}$ are the masses of the target particle and its collisional partner (with $m_p = \rho_p \pi d_p^3 / 6$ and $m_{c,p} = \rho_{c,p} \pi d_{c,p}^3 / 6$, respectively) and \mathbf{U}_p^{ac} and $\mathbf{U}_{c,p}^{ac}$ their velocities after an elastic collision. The effects of particle collisions are therefore expressed by two main characteristics: first, the selection of an appropriate collision kernel $B(\mathbf{V}_p, \mathbf{V}_{c,p}, \mathbf{e})$ (or $\tilde{B}(\mathbf{V}_p, \mathbf{V}_{c,p}) = \int_{S^2} B(\mathbf{V}_p, \mathbf{V}_{c,p}, \mathbf{e}) d\mathbf{e}$ its average over all directions) and, second, by the determination of an elementary collision event given by the transformation relations in Eqs. (369). This implies that the mass of each particle is preserved and that the total number of particles, as well as the total momentum and kinetic energy (due to elastic bouncing) are conserved. Therefore, (elastic) collisions are essentially redistributing kinetic energy between particles, which explains the usual reference to a ‘thermalization effect’.

Stochastic particle systems for collision events. From an historical perspective, the Boltzmann equation was first established before stochastic particle systems, where a set of N particles interact through a random mechanism, were introduced and studied later on. These formulations in terms of stochastic particle systems are attractive to bring out the physical mechanisms in a more intuitive manner and to provide convergence studies for solutions of the Boltzmann equation [85]. They also allow extensions to agglomeration/fragmentation to be easily included and are, therefore, helpful to extend the range of applications of Lagrangian stochastic methods [5]. Some of the methods reviewed in Section 5, for instance SRD, are of course related to such formulations, although it was mentioned that the SRD approach is ‘more mesoscopic’ in the sense that it introduces a simple random mechanism based on hydrodynamical conservations laws. In the present section, we refer to stochastic particle systems such as the well-known DSMC method [84] as well as to the ones analyzed in mathematically-oriented works [172–175]. An excellent overview of these formulations is provided in a recent article by Wagner [85].

As indicated in [85], stochastic particle systems are essentially built on jump processes (cf. Section 4.3) and can be represented by the generic algorithm for N particles contained in a small volume \mathcal{V} and described with a reduced particle state vector $\mathbf{Z}_p^{(N)} = (\mathbf{U}_p^{(1)}, \dots, \mathbf{U}_p^{(N)})$ limited to particle velocities when a locally homogeneous hypothesis is made inside the volume \mathcal{V} . The N particles interact through the following generalized Poisson process:

- (1) The system waits in the same state during a time which is an exponentially-distributed random variable whose parameter is

$$\lambda_c(\mathbf{Z}_p^{(N)}) = \frac{1}{2N\mathcal{V}} \sum_{\substack{k,l=1 \\ k \neq l}}^N \int_{S^2} B(\mathbf{U}_p^{(k)}, \mathbf{U}_p^{(l)}, \mathbf{e}) d\mathbf{e}. \quad (370)$$

- (2) At the time of a jump, two indices i and j corresponding to two particles in the volume \mathcal{V} are chosen as well as a direction \mathbf{e} on the unit sphere S^2 according to the probability

$$p_c(i, j, \mathbf{e}) = \frac{B(\mathbf{U}_p^{(i)}, \mathbf{U}_p^{(j)}, \mathbf{e})}{2N\mathcal{V}\lambda_c(\mathbf{Z}_p^{(N)})} = \frac{B(\mathbf{U}_p^{(i)}, \mathbf{U}_p^{(j)}, \mathbf{e})}{\sum_{\substack{k,l=1 \\ k \neq l}}^N \int_{S^2} B(\mathbf{U}_p^{(k)}, \mathbf{U}_p^{(l)}, \mathbf{e}) d\mathbf{e}}. \quad (371)$$

- (3) For the selected particle pair, the transformations representing the collision event in Eqs. (369), are applied to modify the particle velocities.

Note that this corresponds basically to the collision step of the DSMC approach which uses a time-splitting algorithm with the transport and collision steps treated sequentially and where the above stochastic particle model is applied within each cell. It is also evident that, based on a somewhat cruder picture, the SRD method is following the same ideas and the same steps. There is a detailed literature on these aspects with a fruitful cross-fertilization between physical and mathematical studies [85,171,172]. For our purpose, it is worth underlying that stochastic particle systems correspond in physical space to the Boltzmann equation in sample space. In that sense, they appear as the counterparts of the correspondence between Langevin SDEs and the Fokker–Planck equation (cf. Section 4.3).

10.6.1. Remarks on kinetic-based approaches and open issues

For molecules undergoing free flights and collisions, the Boltzmann equation is undoubtedly the reference framework. For particles (either solid particles or droplets) carried in a fluid flow, its extension leads to the Williams equation, particularly used for sprays [176], and which can be written as

$$\frac{\partial f}{\partial t} + V_{p,k} \frac{\partial f}{\partial y_k} + \frac{\partial [F_k f]}{\partial V_{p,k}} + \frac{\partial [R_p f]}{\partial \theta_p} = Q_{coll}(f) \quad (372)$$

for a distribution $f(t; \mathbf{y}_p, \mathbf{V}_p, \theta_p)$ where θ_p is the sample space variable corresponding to the particle volume ϑ_p (other choices can be made and the distribution can be expressed as a function of the particle diameter d_p but this is not relevant for the present discussion). The third term on the lhs of Eq. (372) involves a force \mathbf{F} acting on particles and R_p stands for the time rate of the particle volume, such as an evaporation term for droplets, and where the collisional term on the rhs of Eq. (372) is still given by Eq. (367). There are, however, two major difficulties with the Williams approach for particles (either solid particles or droplets) in turbulent flows that call for revised formulations.

- (1) The first issue concerns the formulation of the transport step and is related to the limitation to the reduced particle state vector $\mathbf{Z}_p^r = (\mathbf{x}_p, \mathbf{U}_p, \mathbf{d}_p)$. Comparing the lhs of Eq. (372) to the lhs of the Boltzmann equation Eq. (366), it is seen that the Williams equation has two additional terms which account for particle momentum and volume changes during the transport step due to exchanges with the carrier fluid flow. It is also seen that these two terms are treated as purely deterministic terms. Consequently, these two effects appear as first-order derivatives in sample space, corresponding to a Liouville formulation when $Q_{coll}(f) = 0$. As such, the Williams description is strictly limited to either laminar flows or fully-resolved turbulent flows (*i.e.* obtained through a DNS). When only limited information is available on turbulent flows, such as with a LES or a moment approach, the choice of the formulation in Eq. (372) in terms of the reduced state vector \mathbf{Z}_p^r implies that the effects due to the unresolved degrees of freedom of a turbulent flow are either completely neglected or have to be represented through a kinetic-based closure model. However, it follows from the general analysis of Section 9.2 as well as from the developments of Section 10.1, and more specifically of Section 10.1.1, that any such generalizations to partially-resolved turbulent fluid flows result in ill-based formulations and are, therefore, inappropriate to the general case of particles/droplets in the vast majority of practical situations of interest.

The first conclusion is therefore that the Williams description must be extended to a dynamic PDF description to obtain a complete and well-posed formulation of the transport step in (partially-resolved) turbulent fluid flows. If we consider the monodisperse case to simplify the way relations are expressed, the kinetic-based NDFs are the marginals of the MDFs of a dynamic description (see Section 7.3.3), so that we have

$$f(t; \mathbf{y}_p, \mathbf{V}_p, \theta_p) \equiv \int F_p^L(t; \mathbf{y}_p, \mathbf{V}_p, \theta_p, \mathbf{V}_s) d\mathbf{V}_s, \quad (373a)$$

$$f(t, \mathbf{x}; \mathbf{V}_p, \theta_p) \equiv \int F_p^E(t; \mathbf{y}_p, \mathbf{V}_p, \theta_p, \mathbf{V}_s) d\mathbf{V}_s. \quad (373b)$$

When the velocity of the fluid seen is re-introduced and the standard particle state vector $\mathbf{Z}_p = (\mathbf{x}_p, \mathbf{U}_p, \mathbf{U}_s, d_p)$ retained, the transformation rules for collision events must be supplemented with conditions for \mathbf{U}_s . Considering the case of elastic particle rebound, the extended transformation relations that supersede Eqs. (369) and define the complete collision event are

$$\mathbf{U}_p^{ac} = \mathbf{U}_p - \frac{2m_{c,p}}{m_p + m_{c,p}} (\mathbf{U}_p - \mathbf{U}_{c,p}, \mathbf{e}) \cdot \mathbf{e}, \quad (374a)$$

$$\mathbf{U}_{c,p}^{ac} = \mathbf{U}_{c,p} + \frac{2m_p}{m_p + m_{c,p}} (\mathbf{U}_p - \mathbf{U}_{c,p}, \mathbf{e}) \cdot \mathbf{e}, \quad (374b)$$

$$\mathbf{U}_s^{ac} = \mathbf{U}_{c,s}^{ac} = \mathbf{U}_s^{new}, \quad (374c)$$

where \mathbf{U}_s^{new} is a new value assigned to the two fluid velocities seen by the colliding particles at the time of collision, as they are located at the same point (the same condition for \mathbf{U}_s would apply for the case of agglomeration). This is true in the approximation of point-wise particles and remains valid provided that the distance between the two particle centers of mass remains small with respect to the Kolmogorov scale (or to a scale taken as representing the distance below which fluid velocities are strongly correlated).

- (2) The second issue concerns the collision step and is related to the molecular chaos hypothesis. The derivation of the gain/loss balance term in Eq. (367) involves handling the joint velocities $(\mathbf{V}_p, \mathbf{V}_{c,p})$ and $(\mathbf{V}_p^{ac}, \mathbf{V}_{c,p}^{ac})$ of the target particle and its collisional partner before and after the collision event, and is originally given by

$$Q_{coll}(f) = \int_{\mathbb{R}^3} d\mathbf{V}_{c,p} \int_{S^2} d\mathbf{e} B(\mathbf{V}_p, \mathbf{V}_{c,p}, \mathbf{e}) [f_2(t; \mathbf{y}_p, \mathbf{V}_p^{ac}, d_p, \mathbf{V}_{c,p}^{ac}, d_{c,p}) - f_2(t; \mathbf{y}_p, \mathbf{V}_p, d_p, \mathbf{V}_{c,p}, d_{c,p})], \quad (375)$$

where f_2 is used to denote the two-particle PDF, expressed here at the same location (using a point-particle approximation for the sake of simplicity to avoid cumbersome notations to indicate that $|\mathbf{y}_p - \mathbf{y}_{c,p}| = (d_p + d_{c,p})/2$). With the expression of the collision term in Eq. (375), the Boltzmann equation in Eq. (366) is unclosed, involving a BBGKY-like hierarchy [48,49]. The closed form of the (highly non-linear) Boltzmann equation in Eqs. (366)–(367) is obtained by applying the molecular chaos hypothesis

$$f_2(t; \mathbf{y}_p, \mathbf{V}_p, d_p, \mathbf{V}_{c,p}, d_{c,p}) = f(t; \mathbf{y}_p, \mathbf{V}_p, d_p) \times f(t; \mathbf{y}_p, \mathbf{V}_{c,p}, d_{c,p}) \quad (376)$$

which states that, upon collision, the velocities of the colliding partners are uncorrelated (the notation f is kept for the distribution function as in Eq. (366) to indicate that we are referring to the Molecular Dynamics context).

In Molecular Dynamics, the molecular chaos assumption is central to express marginal densities of the N -particle distribution in terms of the one-particle distribution (see Section 5.4) and has, in consequence, the status of a founding principle. Yet, can we simply transpose it to the case of discrete particles embedded in turbulent flows without second thoughts? Indeed, particles transported by a fluid flow have velocities which are correlated to the fluid velocity seen by each of them. In a small fluid region when particles converge to a same location, these fluid velocities seen are correlated and it then can be expected that, upon contact, discrete particles have also correlated velocities. In other

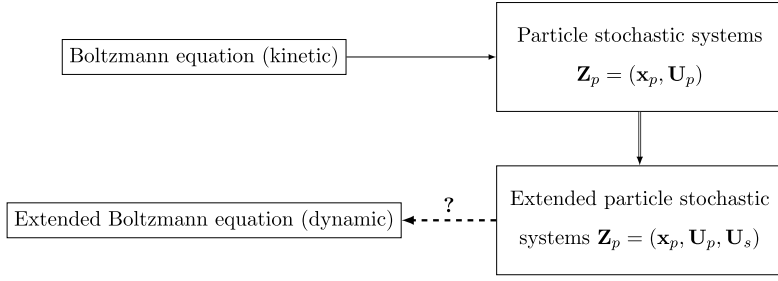


Fig. 63. Representation of the correspondences between Boltzmann equation and particle stochastic systems.

words, discrete particle velocities are correlated by the spatial coherence of the underlying carrier fluid flow, which means that in the general case

$$p_{p,(2)}^L(t; \mathbf{y}_p, \mathbf{V}_p, d_p, \mathbf{V}_s, \mathbf{V}_{c,p}, d_{c,p}, \mathbf{V}_{c,s}) \neq p_{p,(1)}^L(t; \mathbf{y}_p, \mathbf{V}_p, d_p, \mathbf{V}_s) \times p_{p,(1)}^L(t; \mathbf{y}_p, \mathbf{V}_{c,p}, d_{c,p}, \mathbf{V}_{c,s}), \quad (377)$$

where the notations $p_{p,(1)}^L$ and $p_{p,(2)}^L$ are used here for the one- and two-particle Lagrangian PDFs to distinguish the case of particles in turbulent flows from the MD case. There are some situations where we can expect the molecular chaos assumption to remain valid. For example, very small particles (say, with diameters $d_p \leq 0.1 \mu\text{m}$) are sensitive to fluid Brownian effects and, since the Brownian ‘forces’ are independent at each location (in an hydrodynamical description, small distances are much larger than the fluid mean free path), we can expect particle velocities to be nearly uncorrelated. At the other extreme, high-inertia (or high Stokes-number) particles are not very sensitive to fluid motion and the effects of previous collisions and of the ballistic regime can be assumed to produce nearly uncorrelated velocities upon particle contact. This can be also the case in dense regimes when collisions are dominant and where the inherent randomness associated to the interaction mechanisms keeps particles in the realm of the molecular chaos property. However, for intermediate Stokes numbers and for intermediate particle loads, collisions can take place with particle velocities that are still correlated.

As already indicated, the first issue is overcome by using a dynamic PDF description to describe particle transport in partially-resolved turbulent flows. Using a compact notation to represent a reference Langevin model for the evolution of the velocity of the fluid seen as

$$dU_{s,i} = A_{s,i} dt + B_{s,ij} dW_j, \quad (378)$$

the extended description is expressed, in sample space, by a Fokker–Planck–Boltzmann equation for the PDF $p_p^L(t; \mathbf{y}_p, \mathbf{V}_p, \theta_p, \mathbf{V}_s)$

$$\frac{\partial p_p^L}{\partial t} + V_{p,k} \frac{\partial p_p^L}{\partial y_k} + \frac{\partial [F_k p_p^L]}{\partial V_{p,k}} + \frac{\partial [R_p p_p^L]}{\partial \theta_p} + \frac{\partial [A_{s,k} p_p^L]}{\partial V_{s,k}} = \frac{1}{2} \frac{\partial [(B_s B^\perp)_{kl} p_p^L]}{\partial V_{s,k} \partial V_{s,l}} + Q_{coll}(p_p^L). \quad (379)$$

In this equation, F_k typically stands for the drag force whose contribution is closed at the level of a dynamic PDF formulation. Conversely, the evolution of particle diameters, or volumes, generally involves fluid temperature, compositions, etc. with their own evolution equations that can also be expressed as stochastic processes. Yet, for the sake of simplicity and without limiting the present discussion, only a deterministic term R_p is retained in Eq. (379).

The second issue is more intricate and is present whether the turbulent fluid flow is fully-resolved or not. Due to the constraint that the velocities of the fluid seen by colliding particles are identical, it is essential that such an information be contained in the overall approach. In other words, this requires also that a dynamic PDF description be used with the further consequence that a revisited formulation of the collisional terms is needed. It is interesting to note that the translation of the original Boltzmann equation in terms of particle stochastic systems allows extensions to be easily implemented and that we are faced with the task of reverting to formulations in sample space (see the sketch in Fig. 63).

One such possibility would be to restrict the collision kernel from the kinetic theory, cf. Eq. (368), to particle pairs having the same value of the velocity of the fluid seen, for example with simple criteria such as

$$B(\mathbf{V}_p, \mathbf{V}_s, \mathbf{V}_{c,p}, \mathbf{V}_{c,s}, \mathbf{e}) = \begin{cases} \pi \left(\frac{d_p}{2} + \frac{d_{c,p}}{2} \right)^2 |(\mathbf{V}_p - \mathbf{V}_{c,p}, \mathbf{e})| & \text{if } \mathbf{V}_s = \mathbf{V}_{c,s}, \\ B(\mathbf{V}_p, \mathbf{V}_{c,p}, \mathbf{e}) = 0 & \text{if not.} \end{cases} \quad (380)$$

This represents, of course, a very crude estimation, still relying on the notion of a particle ballistic regime, and whose purpose is essentially to exemplify the importance of introducing the velocity of the fluid seen, and/or the fluid gradients, in the particle-collisional picture. In particular, kernels should depend on the value of the local correlation between particles and the fluid $\langle U_{p,i} U_{s,j} \rangle$: for example, high-inertia particles are nearly uncorrelated with the underlying fluid flow and the kernel

should revert to the classical estimation from kinetic theory while Brownian effects may have to be included for small-inertia particles.

Summary From these discussions, the conclusion is that descriptions that include the velocity of the fluid seen or, more generally, characteristic variables of the fluid flow (e.g. temperature, compositions, etc.), are needed and that representations of particle collisions in turbulent flows must be extended to account for fluid-induced particle velocity correlations.

Along the same line, recent research has demonstrated that reduced kinetic descriptions of coalescence, i.e. the Smoluchowski coagulation-kinetic model, break down for relatively dilute suspensions due to correlations between successive collisions induced by fluid turbulence [177]. It is then important to include particle transport and fluid intermittency effects in the picture (see conclusions in [177]). In particular, particle stochastic systems of the form given with Eqs. (370)–(371) (see also the discussions on the explicit forms of particle stochastic systems used for agglomeration applications in [5]) are possible but with a generalized, or non-homogeneous, Poisson process (even in homogeneous turbulence conditions) where the waiting times are not longer exponentially distributed but follows a power-law decay that is dependent on the fluid turbulence characteristics [177].

10.6.2. Revisiting the estimation of particle collision rates

In the methods for particle–particle interactions, the collision and/or agglomeration kernels are central quantities but still contained several open issues. A great body of work has been devoted to the derivation of these kernels in various situations and typical formulas are available in classical textbooks [21,178,179]. The expression of the Brownian agglomeration kernel goes back to the beginning of the 20th century with Smoluchowski's work while others were developed later. One example is the collision kernel in stationary isotropic turbulence [180]. Analysis are still dedicated to the study of some of these kernels and, for instance, improvements were proposed for the Saffman's formula in isotropic turbulence (see [181,182]).

Yet, the available kernel expressions are valid in idealized situations and the separate formulas correspond to distinct situations: the Brownian kernel is derived by considering that particles are only subjected to Brownian-diffusion motion; the isotropic turbulence collision kernel by assuming that particle relative motion is governed entirely by the fluid local shear-rate (which varies randomly with a rms equal to $\sqrt{\langle \epsilon_f \rangle / v_f}$); while the gravitational kernel is obtained by considering only gravity-induced differential velocities for particles with different diameters (implying that monodisperse particles do not collide).

In a practical situation, where all these effects are potentially present, it is not clear if a new collision kernel has to be found, if one of the previously-mentioned expressions should prevail or if we should add them all. Small particles with diameters ranging from 0.1 μm (Brownian) to a few tenths of microns (thus subject to fluid turbulence conditions) in a near-wall boundary layer where the fluid flow is highly anisotropic are one example of such situations. Another example is the interplay between gravity and turbulent structures, whereby fluid turbulence can concentrate particles in some structures of the fluid (this is referred to as the preferential concentration effect) but also reduce the relative velocity of nearby particles, leading to a competition between these correlated effects that cannot be treated independently (see recent works on gravity-enhanced settling in [183]). We find again that the turbulence of the underlying carrier fluid plays a significant role and needs to be included to capture the interplay between various effects.

Even in some apparently well-established situations, known results can be limited by assumptions made in the derivation of the kernels. This is the case for the Brownian collision kernel whose derivation can be found in textbooks (see, for example, the presentation in [179, chapter 7]). The classical approach is to consider the interactions of particles with a target one before generalizing to particle relative motion and the reasoning is based on the profile of the particle concentration c_p . In spherical coordinates, the governing equation for particle concentration is

$$\frac{\partial c_p}{\partial t} = D_p \frac{\partial}{r^2 \partial r} \left[r^2 \left(\frac{\partial c_p}{\partial r} \right) \right] = 2D_p \left(\frac{1}{r} \frac{\partial c_p}{\partial r} + \frac{1}{2} \frac{\partial^2 c_p}{\partial r^2} \right) \quad (381)$$

where D_p is the Einstein–Stokes diffusion coefficient (see Eq. (24)) and where the last part on the rhs of Eq. (381) is the infinitesimal generator of the Bessel process in dimension 3 governing particle distances. However, the essential assumption in the derivation is to consider that the surface of the target particle is a perfect sink [179], so that the perfectly-absorbing boundary condition $c_p = 0$ applies at the distance of contact $R_{p,ij}^{\min} = a_{p,i} + a_{p,j}$ (where $a_{p,i}$ and $a_{p,j}$ are the radius of the diffusive particle and the target one, respectively). The disappearance of particles on the surface of the target one (particles are ‘killed’ there) creates a concentration profile whose gradient gives the flux of incoming particles and, therefore, the collision rate (or, more accurately, the pure agglomeration rate).

It is important to realize that the perfect-sink assumption at the surface of the target particles allows to relate the number of collisions (and, thus, the collision rate) to the particle concentration. This can be explained by considering a sketch of a trajectory of the relative distance, as in Fig. 64, and introducing the first-passage time of the process for a threshold equal to the contact distance $R_{p,ij}^{\min}$

$$T_{R_{p,ij}^{\min}} = \inf\{t \geq 0 ; R_{p,ij}(t) = R_{p,ij}^{\min}\} \quad (382)$$

where $R_{p,ij}(t)$ is the distance between the two particles.

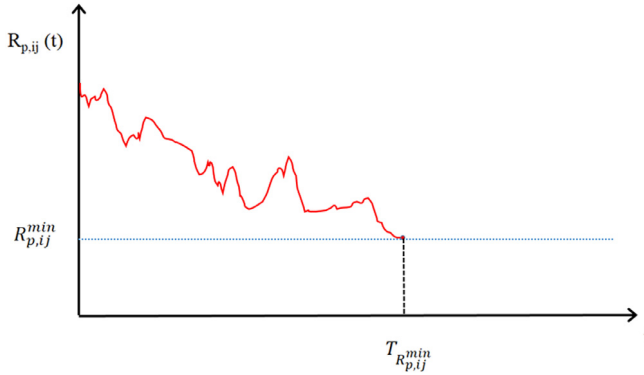


Fig. 64. Illustration of the perfectly-absorbing condition used in the classical derivation of collision/agglomeration kernels: each trajectory for the relative distance reaching the threshold corresponding to the contact is killed and the first-passage instant is a stopping time.

The perfect-absorbing condition means that the first-passage time is actually a stopping time and that, if we start with N particles, the number of ‘living’ particles at a time t is

$$\sum_{i=1}^N \mathbb{1}_{\{T_{R_{p,ij}^{min}} > t\}}. \quad (383)$$

By normalizing over the number of particles released from an initial position r , we get that

$$n_p(t, r) = \lim_{N \rightarrow +\infty} \frac{1}{N} \sum_{i=1}^N \mathbb{1}_{\{T_{R_{p,ij}^{min}} > 0\}} = \mathbb{P}_r(T_{R_{p,ij}^{min}} > t) \quad (384)$$

which gives the concentration of the remaining particles at time t that started at a distance r . The (Eulerian) field concentration $c_p(t, \mathbf{x})$ is easily deduced but it is already clear from the above that the perfect-sink boundary condition provides a direct relation between particle concentration and the number of collisions on the target particle. Furthermore, particle concentration is assumed to remain constant by a constant influx (or feeding) of new particles. Classical manipulations show then that the collision kernel β_{ij} between particles of classes i and j , corresponding to diameters $d_{p,i}$ and $d_{p,j}$ respectively, is given by

$$\beta_{ij} = \frac{2k_B \Theta_f (d_{p,i} + d_{p,j})^2}{3\mu_f (d_{p,i} + d_{p,j})}. \quad (385)$$

This analysis has led to a classical numerical approach in particle collision studies in which, upon detection between two particles, one of the colliding particles is removed and re-initialized randomly within the simulation box (see [181,184]).

If this derivation is a well-justified short-cut method to obtain the pure-agglomeration rate, it can be wondered whether it remains valid when, for example, elastic rebound or any mixed (absorption/rebound) conditions apply at the surface of the target particle. If an elastic rebound condition is enforced, the approach in terms of the particle-concentration profile is not applicable anymore since we have that $c(t, \mathbf{x})$ remains a constant value throughout the small homogeneous box that is considered. In other words, the above derivation of collision kernels would yield that $\beta_{ij} = 0$ and that no interaction takes place whatever the particle concentration. A more direct approach in terms of the trajectories of the relative distance between a particle and a given target brings out an even more puzzling outcome. Indeed, it is known from mathematical studies of Brownian motion (and of related processes such as the Bessel process), that, if a Brownian particle hits a boundary and is reflected, there is a near-one probability that this particle will hit again the boundary an infinite number of times in any small time interval after the time of first contact before drifting away (see Fig. 65 where the boundary indicates the surface of the target particle). In other words, there is no escaping that this direct estimation of the number of collisions gives an infinite collision rate, i.e. $\beta_{ij} = +\infty$. Clearly, a new formulation is needed to reconcile a proper mathematical treatment combined to realistic and general boundary conditions with the expected physical result of a non-zero but finite collision rate.

One idea is to introduce the notion of the ‘local time’ of the stochastic process driving the relative distance between particles (Christophe Profeta, personal communication). For a one-dimensional stochastic process X , the local time at $x = x_0$ is defined as

$$L_t^{(x_0)}[X] = \lim_{\epsilon \rightarrow 0} \frac{1}{\epsilon} \int_0^t \mathbb{1}_{\{|X(s) - x_0| \leq \epsilon\}} ds \quad (386)$$

which is a way to express the time spent by the process ‘at the boundary $x = 0$ ’. It is proposed to use this local time as a measure of the number of collisions between a set of particles and a target one (whose surface represents the boundary),

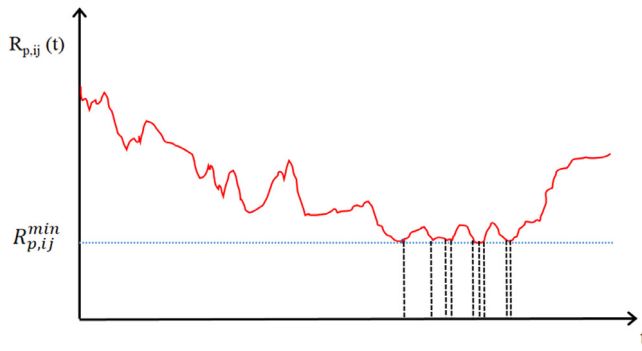


Fig. 65. Illustration of a more realistic situation in the case of non perfectly-absorbing conditions at the point of contact. The trajectory representing the relative distance between a target particle and an incoming one continues to live after the first-contact time. In the case of Brownian motion, there is even an infinite number of contacts before the trajectory eventually drifts away.

which suggests that the collision rate can be calculated as

$$\beta_{ij} = \frac{d}{dt} \langle L_t^{(d_{ij}^{\min})} \rangle. \quad (387)$$

In the case where there is a well-defined particle velocity process, the manipulation of the so-called Rice formula gives the usual expression from statistical physics (still using, for the sake of simplicity of the presentation, a one-dimensional formulation with V_p the particle normal velocities to a unit surface taken as $x = 0$), that is

$$\frac{d}{dt} \langle L_t^{(d_{ij}^{\min})} \rangle(t) = \int_0^{+\infty} V_p p_p^L(t; 0, V_p) dV_p. \quad (388)$$

Furthermore, this expression in terms of the local time of the process has the further advantage of remaining applicable even when the particle velocity is no longer a well-defined process, as in the case of Brownian motion. To the best of the author's knowledge, this is an unexplored area and much work remains to be done to assess the interest of these research directions.

10.6.3. Calculating collision/agglomeration kernels

To derive new kernels or to assess the validity of present ones in general conditions, numerical simulations in the spirit of DNS are well-suited. Since the purpose is to detect collisions rather than to account for a given collision or agglomeration rate, the analysis of Section 8.2 indicates that the N particles must be tracked simultaneously to have information on their relative locations. Compared to the Lagrangian approaches discussed in Sections 9 and 10, which were mostly expressed in the one-particle PDF framework, we are now in the realm of N -particle PDF methods. Then, different treatments can be developed, depending on the particle diameters involved.

For high-inertia particles, say with $d_p \geq 10\text{--}20 \mu\text{m}$ (for solid particles or droplets in air with density ratios $\rho_p/\rho_f \geq 1000$), Brownian effects can be neglected. This means that the forces acting on particles are basically the ones discussed in Section 2 and that the particle momentum equation has the form described there. In that case, the task at hand is to estimate accurately the vector made up by the correlated fluid velocities seen by the N particles. This is the same issue raised in the discussion of relevant particle state vectors for fibers and polymers in turbulent flows in Section 10.2 but, since the N discrete particles are not bound together and can occupy the whole flow domain, this requires to have time and space information over the complete instantaneous fluid flow. In the point-particle approximation, this can be done with a DNS which provides full resolution of the turbulence of the single-phase flow. To capture hydrodynamic influences, whereby the wake flow behind one particle can influence neighboring ones, improved methods can be applied (superposition with Stokelets, boundary-element method, etc., see [185–187]). Then, if the time step is small enough (see further discussions below), particle collisions can be detected by classical methods, such as overlap techniques [184,188] or molecular-based algorithms [189]. For particles with high-enough inertia, the limitations imposed by classical collision-detection algorithms on the time step are not too stringent compared to the ones imposed by the DNS calculation.

For small colloidal particles, say with $d_p \leq 0.1\text{--}1 \mu\text{m}$, Brownian effects are important and must be included. This leads to considering the joint N -Langevin equations which can be written for the complete state vector $\mathbf{Z}_p^r = (\mathbf{x}_p^{[1]}, \mathbf{v}_p^{[1]}, \dots, \mathbf{x}_p^{[N]}, \mathbf{v}_p^{[N]})$ as

$$d\mathbf{x}_{p,i}^{[k]} = U_{p,i}^{[k]} dt, \quad (389a)$$

$$dU_{p,i}^{[k]} = \sum_{l=1}^N \left(-\alpha_{i,j}^{[k,l]} (U_{p,j}^{[l]} - U_{f,j}(t, \mathbf{x}_p^{[l]}(t))) dt + F_i^{[l \rightarrow k]} dt + K_{i,j}^{[k,l]} dW_j^{[l]} \right) \quad (389b)$$

where $k, l = 1, \dots, N$ denotes the particle index and where a kinetic-based description is appropriate since the fluid flow is fully resolved. The third term on the rhs of Eq. (389b) represents the non-hydrodynamical force exerted by the particle labeled $[l]$ on the particle labeled $[k]$ ($i = 1, 3$ remains the index used for space coordinates). It is seen that the drag term, which is the first term on the rhs of Eq. (389b), involves a fourth-order tensor $\alpha_{i,j}^{[k,l]}$ which corresponds to a sum over all particles. This form is meant to represent the hydrodynamic influence of a particle on surrounding ones, through a modified and generalized drag force (this was already introduced with BD equations, cf. Eq. (149b) in Section 7.2.1, and is related to the mobility tensor). Correspondingly, the diffusion term in Eq. (389b) involves a vector of independent Wiener processes for each particle and each component through another fourth-order tensor $K_{i,j}^{[k,l]}$ which is related to $\alpha_{i,j}^{[k,l]}$ by the generalized fluctuation–dissipation theorem. The drag force tensor is different between the direction aligned with the line joining the centers of two interacting particles and the two directions perpendicular to it to account for the modifications of the drag coefficient due to small-range lubrication effects between two approaching particles (this is basically the same effect as the wall-induced modifications of the drag coefficient when one has to separate the longitudinal and transverse directions [33]).

The model in Eqs. (389) is an example of the Langevin Dynamics (LD) approach mentioned in Section 7.2.1 (its over-damped limit forms a Brownian Dynamics model) and is used, for example, to study colloidal suspensions (see [190]) where the interaction forces between particles $F_i^{[l \rightarrow k]}$ are typically DLVO-like forces. The complex drag force term is applied when the fluid flow is not really treated (this model is written for a fluid at rest in [190]) and, in practice, the cross-influences manifested by the generalized drag tensor can be simplified to the usual local drag force expression. This consists in writing that $\alpha_{i,j}^{[k,l]} = 1/\tau_p \delta_{kl} \delta_{ij}$ and $K_{i,j}^{[k,l]} = K_{\text{Br}} \delta_{kl} \delta_{ij}$. Then, the classical form of the LD approach is [178]

$$d\mathbf{x}_{p,i}^{[k]} = U_{p,i}^{[k]} dt, \quad (390a)$$

$$dU_{p,i}^{[k]} = -\frac{1}{\tau_p} \left(U_{p,i}^{[k]} - U_{f,i}(t, \mathbf{x}_p^{[k]}(t)) \right) dt + \sum_{l=1}^N F_i^{[l \rightarrow k]} dt + K_{\text{Br}} dW_i^{[k]}, \quad (390b)$$

where the explicit superscript $[k]$ is kept to indicate that we are handling the joint N particle system. As mentioned, LD simulations are mostly applied for colloidal suspensions, where the macroscopic effects due to fluid flow variations are disregarded, which means that the timescale (or the time span studied) remains small. For small colloids, particle dynamics has therefore become random but the limited time span which is covered allows very small time steps to be used, with corresponding straight-line particle displacements within each time step. Then, deterministic methods to detect particle contact can still be applied.

However, for particles with diameters in the intermediate range (say for polydisperse particles with diameters ranging from $0.1 \mu\text{m}$ to $10 \mu\text{m}$) and carried by an evolving turbulent flow, the previous constraints become very severe. A larger time span has to be covered to capture the fluid flow changes while the use of deterministic methods for the detection of particle collisions imposes limits that make the whole approach inapplicable when the particle diameter is smaller than about $1 \mu\text{m}$ (see the analysis of the limit of the so-called ballistic regime in [191]). This represents a major impediment for the application of deterministic approaches since this is precisely the range of particle diameter over which the Brownian and turbulence agglomeration kernels overlap, raising the uncertainty described in Section 10.6.2.

The situation can be understood by recalling that present deterministic techniques used to detect particle collisions in fluid flows are extensions of Molecular Dynamics methods and rely on particle displacements being straight lines within each time step, as sketched in Fig. 66(a). From the particle system in Eqs. (390), it is seen that this amounts to imposing $\Delta t \ll \tau_p$ [191] since τ_p is the particle velocity integral timescale. This can be further assessed with some simple estimations from the numerical evaluations given in Section 10.5 and, in particular, with Eqs. (361): the straight-line displacement constraint means that the random term (the third term on the rhs of Eqs. (361)) must be much smaller than the free-flight one (the second term on the rhs of Eqs. (361)). Using straightforward estimations of the random integral with Eqs. (363)–(364) in the limit $\Delta t \ll T$ (with $T = \tau_p$ here), we must have $\sigma(\Delta t)^{3/2} \ll u_p \Delta t$, with u_p the order of the particle velocity (typically, $u_p = \langle U_p^2 \rangle^{1/2}$). Then, the usual estimation of σ from the fluctuation–dissipation theorem, namely $\sigma^2 = 2u_p^2/\tau_p$, yields that $\Delta t \ll \tau_p$, as mentioned above. Since colloidal particles have drag coefficients which lie in the Stokes regimes, τ_p scales with d_p^2 , which reveals that Δt collapses to very low values when d_p is in the colloidal range. This strong limitation has been brought out by discrete-in-time estimations. Yet, as pointed out in Section 10.5, Δt stands also for a physical timescale which is the observation reference time at which we wish to describe a system.

To overcome this restriction on the observation timescale Δt and introduce a new paradigm, a new approach was recently put forward [191]. The principle is to retain a non-negligible Δt (say, governed by scales such as the Kolmogorov timescale of the fluid flow) and allow collisions to become stochastic processes. The new situation is sketched in Fig. 66(b) where it is seen that, for a given pair of particles whose positions are known at time t and $t + \Delta t$, it is not possible anymore to determine with certainty whether a collision took place, or not, during the time interval $s \in [t; t + \Delta t]$. Note that we are considering here the complete N -particle system and a fully-resolved fluid flow. With respect to the discussions presented in Section 8.1, the particle+fluid system is thus closed and there is no implied randomness due to the choice of a reduced statistical description, for example in the sense of a classical BBGKY hierarchy. Nevertheless, the problem is formulated as a conditional probabilistic one: conditioned on the locations of each particle pair at the beginning and end of a time step, the probability that a collision has occurred at a time s ($t \leq s \leq t + \Delta t$) needs to be evaluated. Therefore, this approach

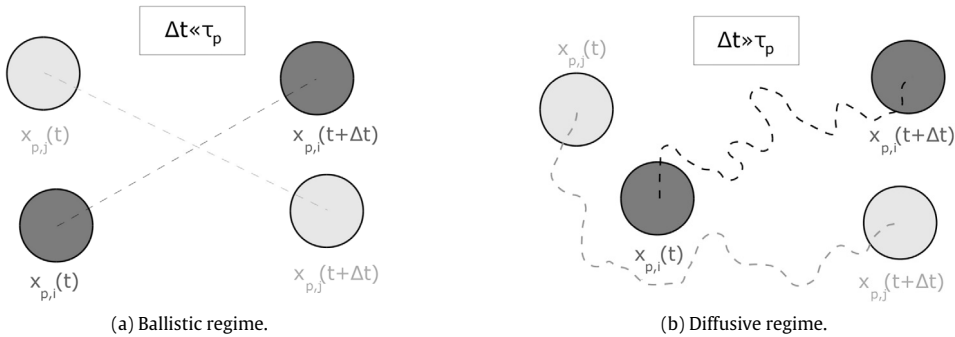


Fig. 66. Sketch of the ballistic (a) and diffusive (b) regimes for a pair of particles over a time step Δt . In the ballistic regime, particles move in straight lines allowing detection methods based on geometrical criteria (overlap, collision cylinder, etc.) to be used. In the diffusive regime, probabilistic laws must be introduced to account for the diffusive relative particle trajectory within the time step.

represents a new aspect, where randomness is not only accounted through the prediction of successive particle locations and velocities at discrete times but is based also on continuous trajectories. In other words, this is a *trajectory-based approach*.

Details on this new formulation can be found in recent publications (see [191–193]) but, in the context of the present discussion, the following points are worth mentioning:

- (1) The first applications were performed with the simple, but somewhat artificial, treatment of the collision event: when a collision is detected between a pair of particles, one of the collision partner is removed and re-initialized randomly within the homogeneous box (see [181,184]). As recalled in Section 10.6.2, this is consistent with the assumptions made in the derivation of the Brownian collision rate and excellent results are obtained whatever the choice of the observation time Δt (see results in [191]). This new approach is therefore able to reproduce the ballistic regime as well as the diffusive regime.
- (2) These results have the status of a validation test but the interest is to address more realistic interactions and one such complete treatment of the collision event, as proposed in [193], is represented in Fig. 67. When a collision between two particles occurs within a time step, the simulation consists in generating: (a) the time t_c at which the collision takes place; (b) the location of this collision; (c) the resulting new particle trajectories and locations at the end of the time step. At the moment, a proper assessment of the numerical predictions is hindered by some of the issues raised in Section 10.6.2. Indeed, if the random-walk approximation is used for particle positions, a simple estimation of the collision probability can be used (see [191]), but we are then faced with the difficulty that a pair of particles having collided once at t_c has a near-one probability to collide again in any time interval $[t_c ; t_c + \tau]$ for any value of τ . The current remedy is to introduce a time interval Δt_c during which a pair of colliding particles cannot undergo another collision (see details in [193]). This can be traced back to the fact that, just after a collision, particles have a short-time but non-negligible ballistic regime which tend to drive them apart. This free-of-collision time lapse is estimated by saying that the separation distance over Δt_c due to diffusion motion (*i.e.* due to the diffusive model for the relative position of particles $[i]$ and $[j]$, $dx^{[ij]} = B^{[ij]} d\mathbf{W}$) should be of the same order as the one induced by convective motions, which gives

$$B^{[ij]} \sqrt{\Delta t_c} \sim \left(\frac{k_B \Theta_f}{m_p} \right)^{1/2} \tau_p \quad (391)$$

for two particles with the same mass m_p and relaxation timescale τ_p . This gives for the time Δt_c during which no further collisions are allowed for a colliding pair

$$\Delta t_c \simeq C \frac{\ell_{p,f} d_p}{(B^{[ij]})^2}, \quad (392)$$

with C a constant and the characteristic length $\ell_{p,f}$ given by

$$\ell_{p,f} = \frac{\rho_p}{\rho_f} \left(\frac{k_B \Theta_f}{\rho_f v_f^2} \right). \quad (393)$$

Although this reasoning relies on a physical argument, it remains an artifact whose main merit is to point to the interest of having probability formula for the occurrence of a collision based on the complete particle dynamics in complex situations.

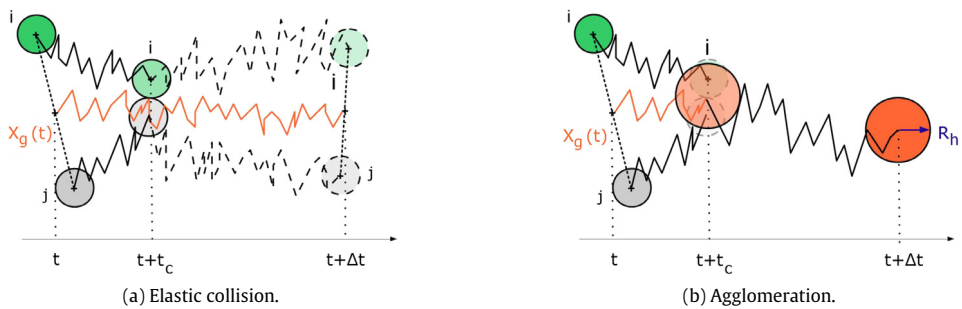


Fig. 67. New treatment of particle collision/agglomeration events based on the generation of the random time t_c of the collision event, on the prediction of its location as the position the barycenter at t_c and on the subsequent reconstruction of particle trajectories after the collision/agglomeration event in the rest of the time step $\Delta t - t_c$ [192,193].

Source: Reprinted from [192] with permission from ACS.

10.7. Summary

From the analyses developed throughout Section 10, a clear conclusion emerges: casting the dynamics of discrete particles carried by turbulent flows into a well-posed and satisfactory framework is not achieved by simply extending the methods that have been successful below the hydrodynamical level of description. New approaches and modeling principles are needed. This is true for the description of fluid-particle as well as particle-particle interactions.

The study of single-particle dynamics in non fully-resolved turbulent flows is perhaps more advanced since it benefits from the developments of the modeling tools detailed in Section 9. The main outcome is that kinetic descriptions are ill-based and that flexible modeling standpoints based on a proper definition of the particle state vector are required.

Similar questions appear for the representation of particle-particle interactions in turbulent flows and the second outcome is that classical kinetic descriptions cannot be immediately carried over to the present context due to fluid-induced correlations that need to be accounted for in Boltzmann-like probabilistic descriptions. In that sense, the present difficulties faced with the new modeling approach outlined in Section 10.6.3 illustrate the open questions related to particle collisions raised throughout Section 10.6. Indeed, the real issue is not due to modeling uncertainties but to the lack of a proper understanding of the statistical laws governing particle-particle interactions for particles subject simultaneously to Brownian motions, inertia and turbulence effects in non-homogeneous situations.

11. Conclusion

The aim of this review article was to study statistical models of particles in turbulent flows. As mentioned in Section 1, the chosen standpoint was to address this question within a general framework that includes models developed in classical statistical physics (at the meso-molecular level) as well as approaches for single-phase turbulent flows. This was done to establish links between apparently-different formulations and to bring out the specific challenges met by models for particle dynamics in turbulent flows.

With respect to this overall objective, a number of conclusions have been reached:

- (1) Most of the particle-based methods discussed in Sections 5–7 (e.g., MD, DPD, SDPD, SPH, DNS, one-particle FDF and PDF) reveal a similarity that continues across the hydrodynamical level of description;
- (2) This similarity points to the possibility to construct new formulations, such as SPH/FDF in single-phase turbulence (see Sections 6.5.3–6.6) and SPH/DNS in disperse two-phase flows at the fully-resolved hydrodynamical level (see Section 7.2.3);
- (3) One-particle PDF models for disperse two-phase turbulent flows are bottom-up formulations (see Section 7.4). Indeed, there is no equilibrium distribution or equipartition of energy in turbulence and the classical fluctuation-dissipation relation must be revisited (to account for the fluid dissipation of the turbulent kinetic energy), which constitutes the specific statistical challenges of models for particles in turbulent flows while classical macroscopic closures are inadequate in most situations (see Section 10.4);
- (4) A significant outcome is that formulations in terms of kinetic variables only are ill-based for particles in random media with non-zero space and time correlations, such as non fully-resolved turbulent flows. New approaches are called for by including variables related to the underlying turbulent flow in the particle state vector (see Sections 9.2 and 10.1);
- (5) A follow-up conclusion is that the important step in the formulation of a statistical model is the physical analysis, especially the separation between slow and fast variables leading to the selection of an appropriate state vector (see Section 9), rather than the application of special tools with ill-suited state vectors;
- (6) Similarly, extended formulations of particle collisions are needed for particles whose dynamics is correlated by the underlying fluid flow (see Section 10.6).

These points do not imply that a final state of affairs has been obtained but, simply, that a framework can be used to build bridges between different scales and modeling approaches. In that sense, this marks only a step along the modeling road. Formulated in a more straightforward language, this presentation is an invitation to devote more (modeling) energy to the challenging issues of particle dynamics in turbulent flows. Indeed, it was indicated that very few models, respecting the basic criteria that have been set forth, have been developed so far and several open issues remain that require additional investigations and new insights. Clearly, more work is needed and the author's hope is that this review has helped to attract attention towards these interesting aspects in physics.

Acknowledgments

The author would like to express his thanks to Dr. Christophe Profeta for his help with the mathematical manipulations of the fast-elimination techniques in Section 9.3. The author would like also to express special thanks to Dr. Christophe Henry for useful advice.

References

- [1] J.-P. Minier, E. Peirano, The PDF approach to turbulent and polydispersed two-phase flows, *Phys. Rep.* 352 (1–3) (2001) 1–214.
- [2] C. Henry, J.-P. Minier, G. Lefèvre, Towards a description of particulate fouling: from single-particle deposition to clogging, *Adv. Colloid Interface Sci.* 185–186 (2012) 34–76.
- [3] A. Bragg, D.C. Swailes, R. Skartlien, Drift-free kinetic equations for turbulent dispersion, *Phys. Rev. E* 86 (056306) (2012).
- [4] J.-P. Minier, S. Chibbaro, S.B. Pope, Guidelines for the formulation of Lagrangian stochastic models for particle simulations of single-phase and dispersed two-phase flows, *Phys. Fluids* 26 (2014) 113303.
- [5] J.-P. Minier, On Lagrangian stochastic methods for turbulent polydisperse two-phase reactive flows, *Prog. Energy Combust. Sci.* 50 (2015) 1–62.
- [6] M.S. Yadav, Interfacial Area Transport Across Vertical Elbows in Air-Water Two-Phase Flow, (Ph.d. thesis), The Pennsylvania State University, The Graduate School, Department of Mechanical and Nuclear Engineering, 2013.
- [7] D. Quéré, Leidenfrost dynamics, *Annu. Rev. Fluid Mech.* 45 (2013) 197–215.
- [8] P. Ahlrichs, B. Dunweg, Raindrop size distribution: Fitting performance of common theoretical models, *Adv. Water Resour.* 96 (2016) 290–305.
- [9] E. Reyssat, F. Chevy, A.-L. Biance, L. Petitjean, D. Quéré, Shape and instability of free-falling liquid globules, *Europhys. Lett.* 80 (2007) 34005.
- [10] E. Villermieux, B. Bossa, Single drop fragmentation determines size distribution of raindrops, *Nature Phys.* 5 (2009) 697702.
- [11] E. Villermieux, F. Elloï, The distribution of raindrops speeds, *Geophys. Res. Lett.* 38 (2011) L19805.
- [12] G. Liger-Belair, Uncorked. The Science of Champagne, first ed., Princeton University Press, Princeton, 2004.
- [13] G. Liger-Belair, F. Beaumont, M.-A. Vialatte, S. Jégou, P. Jeandet, G. Polidori, Kinetics and stability of the mixing flow patterns found in champagne glasses as determined by laser tomography techniques: likely impact on champagne tasting, *Anal. Chim. Acta* 621 (2008) 30–37.
- [14] F.E. Fish, P. Legac, T.M. Williams, T. Wei, Measurement of hydrodynamic force generation by swimming dolphins using bubble DPIV, *J. Exp. Biol.* 217 (2014) 252–260.
- [15] G. Liger-Belair, How many bubbles in your glass of bubbly? *J. Phys. Chem. B* 118 (11) (2014) 3156–3163.
- [16] E. Villermieux, B. Bossa, Drop fragmentation on impact, *J. Fluid Mech.* 668 (2011) 412435.
- [17] Y.S. Joung, C.R. Buie, Aerosol generation by raindrop impact on soil, *Nat. Commun.* 6 (2015) 6083. <http://dx.doi.org/10.1038/ncomms7083>.
- [18] I. Manzella, C. Bonadonna, J.C. Phillips, H. Monnard, The role of gravitational instabilities in deposition of volcanic ash, *Geology* 43 (3) (2015) 211–214.
- [19] A.R. Van Eaton, L.G. Mastin, M. herzog, H.F. Schwaiger, D.J. Scheider, K.L. Wallace, A. Clarke, Hail formation triggers rapid ash aggregation in volcanic plumes, *Nat. Commun.* 6 (2015) 7860. <http://dx.doi.org/10.1038/ncomms8860>.
- [20] J.N. Israelachvili, *Intermolecular & Surface Forces*, third ed., Academic Press, 2011.
- [21] R.J. Hunter, *Foundations of Colloid Science*, second ed., Oxford University Press, 2001.
- [22] W.D. Ristenpart, I.A. Aksay, D.A. Saville, Assembly of colloidal aggregates by electrohydrodynamic flow: Kinetic experiments and scaling analysis, *Phys. Rev. E* 69 (2004) 021405.
- [23] C. Henry, J.-P. Minier, Progress in particle resuspension from rough surfaces by turbulent flows, *Prog. Energy Combust. Sci.* 45 (2014) 1–53.
- [24] J.-P. Minier, J. Pozorski, Particles in Wall-Bounded Turbulent Flows: Deposition, Re-Suspension and Agglomeration, CISM, International Centre for Mechanical Sciences, Vol. 571, Springer Verlag, Berlin, 2017.
- [25] Y. Liang, N. Hilal, P. Langston, V. Starov, Interactions forces between colloidal particles in liquid: theory and experiment, *Adv. Colloid Interface Sci.* 134–135 (2007) 151–166.
- [26] J. Eggers, Drop formation—an overview, *Z. Angew. Math. Mech.* 85 (6) (2005) 400–410.
- [27] J. Eggers, E. Villermieux, Physics of liquid jets, *Rep. Prog. Phys.* 71 (2008) 036601.
- [28] H.P. Kavehpour, Coalescence of drops, *Annu. Rev. Fluid Mech.* 47 (2015) 245–268.
- [29] M.L. Eggersdorfer, S.E. Pratsinis, Agglomerates and aggregates of nanoparticles made in the gas phase, *Adv. Powder Technol.* 25 (2014) 71–90.
- [30] S.B. Pope, *Turbulent Flows*, Cambridge University Press, 2000.
- [31] S.B. Pope, PDF methods for turbulent reactive flows, *Prog. Energy Combust. Sci.* 11 (1985) 119–192.
- [32] D.C. Haworth, Progress in probability density function methods for turbulent reacting flows, *Prog. Energy Combust. Sci.* 36 (2010) 168–259.
- [33] R. Clift, J.R. Grace, M.E. Weber, *Bubbles, Drops and Particles*, Academic Press, 1978.
- [34] R. Gatignol, The Faxén formulae for a rigid particle in an unsteady non-uniform Stokes flow, *J. Mec. Theor. Appl.* 1 (2) (1983) 143–160.
- [35] M.R. Maxey, J.J. Riley, Equation of motion for a small rigid sphere in a nonuniform flow, *Phys. Fluids* 26 (4) (1983) 883–889.
- [36] J.P. McLaughlin, Inertial migration of a small sphere in linear shear flows, *J. Fluid Mech.* 224 (1991) 261–274.
- [37] Q. Wang, K.D. Squires, M. Chen, J.B. McLaughlin, On the role of the lift force in turbulence simulations of particle deposition, *Int. J. Multiph. Flow* 23 (4) (1997) 749–763.
- [38] A.S. Monin, A.M. Yaglom, *Statistical Fluid Mechanics: Mechanics of Turbulence*, first ed., The MIT Press, 1971.
- [39] U. Frisch, *Turbulence*, Cambridge University Press, 1995.
- [40] C.E. Brennen, *Fundamentals of Multiphase Flows*, Cambridge University Press, 2005.
- [41] T. Elperin, N. Kleerorin, V.S. L'vov, J. Rogachevski, D. Sokoloff, Clustering instability of the spatial distribution of inertial particles in turbulent flows, *Phys. Rev. E* 66 (2002) 036302.
- [42] T. Elperin, N. Kleerorin, M.A. Liberman, V.S. L'vov, J. Rogachevski, Clustering of aerosols in atmospheric turbulent flows, *Environ. Fluid Mech.* 7 (2007) 173–193.
- [43] C.W. Gardiner, *Handbook of Stochastic Methods for Physics, Chemistry and the Natural Sciences*, Springer, Berlin, 1990.

- [44] E. Peirano, S. Chibbaro, J. Pozorski, J.-P. Minier, Mean-field/PDF numerical approach for polydispersed turbulent two-phase flows, *Prog. Energy Combust. Sci.* 32 (3) (2006) 315–371.
- [45] M. Van Dyke, *Stochastic Processes in Physics and Chemistry*, first ed., Parabolic Press, 1982.
- [46] A. Vazquez-Quesada, M. Ellero, P. Espagnol, A SPH-based particle model for computational microrheology, *Microfluid Nanofluid* 13 (2012) 249260.
- [47] F. Reif, *Fundamentals of Statistical and Thermal Physics*, McGraw Hill International Editions, Singapore, 1985.
- [48] R.L. Liboff, *Kinetic Theory. Classical, Quantum, and Relativistic descriptions*, second ed., Pergamon Press, Oxford, 1998.
- [49] R. Balescu, *Statistical Dynamics: Matter Out of Equilibrium*, Imperial College Press, London, 1997.
- [50] H.C. Öttinger, *Stochastic Processes in Polymeric Fluids. Tools and Examples for Developing Simulation Algorithms*, Springer, Berlin, 1996.
- [51] R.O. Fox, Large-Eddy-Simulation tools for multiphase flows, *Annu. Rev. Fluid Mech.* 44 (2012) 47–76.
- [52] J.-P. Minier, C. Profeta, Kinetic and dynamic probability-density-function descriptions of disperse turbulent two-phase flows, *Phys. Rev. E* 92 (053020) (2015).
- [53] R.O. Fox, *Computational Models for Turbulent Reacting Flows*, Cambridge University Press, 2003.
- [54] E. Peirano, J.-P. Minier, A probabilistic formalism and hierarchy of models for polydispersed turbulent two-phase flows, *Phys. Rev. E* 65 (046301) (2002).
- [55] L. Arnold, *Stochastic Differential Equations: Theory and Applications*, Wiley, New-York, 1974.
- [56] I. Karatzas, S.E. Shreve, Brownian motion and stochastic calculus, in: *Graduate Texts in Mathematics*, second ed., Springer-Verlag, New York, 1991.
- [57] F.C. Klebaner, *Introduction to Stochastic Calculus with Applications*, Imperial College Press, London, 1998.
- [58] B. Øksendal, *Stochastic Differential Equations*, Springer, 2003.
- [59] N.G. Van Kampen, *Stochastic Processes in Physics and Chemistry*, third ed., North Holland, 2007.
- [60] S. Chibbaro, J.-P. Minier, *Stochastic Methods for Fluid Mechanics*, in: CISM, International Centre for Mechanical Sciences, Vol. 548, Springer Verlag, Berlin, 2014.
- [61] H. Risken, *The Fokker-Planck Equation. Methods of Solution and Applications*, Springer, Berlin, 1996.
- [62] N.G. Van Kampen, Remarks on non-Markov processes, *Braz. J. Phys.* 28 (2) (1998) 90–96.
- [63] P.S. Hagan, C.R. Doering, C.D. Levermore, The distribution of exit times for weakly colored noise, *J. Stat. Phys.* 54 (5–6) (1989) 1321–1352.
- [64] P.S. Hagan, C.R. Doering, C.D. Levermore, Mean exit times for particles driven by weakly colored noise, *SIAM J. Appl. Math.* 49 (5) (1989) 1480–1513.
- [65] M.M. Klosek-Dygas, B.J. Matkowsky, Z. Schuss, Colored noise in activated rate processes, *J. Stat. Phys.* 54 (5–6) (1989) 1309–1320.
- [66] J.-P. Minier, S. Chibbaro, Mathematical background on stochastic processes, in: S. Chibbaro, J.-P. Minier (Eds.), *Stochastic Methods for Fluid Mechanics*, Springer, 2014, pp. 1–38.
- [67] S.B. Pope, Lagrangian PDF Methods for Turbulent Reactive Flows, *Annu. Rev. Fluid Mech.* 26 (1994) 23–63.
- [68] P. Hanggi, P. Jung, Colored noise in dynamical systems, in: I. Prigogine, S.A. Rice (Eds.), *Advances in Chemical Physics*, vol. LXXXIX, John Wiley & Sons, 1995, pp. 239–326.
- [69] S. Kullback, *Information Theory and Statistics*, John Wiley & Sons, 1959.
- [70] P.A. Markowich, C. Villani, On the trend to equilibrium for the Fokker-Planck equation: an interplay between physics and functional analysis, *Mat. Contemp.* 19 (2000) 1–29.
- [71] A. Ullah, Entropy, divergence and distance measures with econometric applications, *J. Statist. Plann. Inference* 49 (1996) 137–162.
- [72] P.J. Hoogerbrugge, J.M.V.A. Koelman, Simulating microscopic hydrodynamics phenomena with dissipative particle dynamics, *Europhys. Lett.* 19 (1992) 155–160.
- [73] J.M.V.A. Koelman, P.J. Hoogerbrugge, Dynamic simulation of hard sphere suspensions under steady shear, *Europhys. Lett.* 21 (1993) 363–368.
- [74] P. Espagnol, P. Warren, Statistical mechanics of dissipative particle dynamics, *Europhys. Lett.* 30 (1995) 191–193.
- [75] P. Espagnol, Hydrodynamics from dissipative particle dynamics, *Phys. Rev. E* 52 (1995) 1734–1742.
- [76] E. Mooendarbary, T.Y. Ng, M. Zangeneh, *Dissipative Particle Dynamics: Introduction, Methodology and Complex Fluid Applications—A Review*, *Int. J. Appl. Math.* 1 (4) (2009) 737–763.
- [77] I.V. Pivkin, B. Caswell, G.E. Karniadakis, *Dissipative Particle Dynamics*, in: K.B. Lipkowitz (Ed.), *Reviews in Computational Chemistry*, vol. 27, John Wiley & Sons, 2011, pp. 105–110.
- [78] S. Succi, Mesoscopic particle models of fluid flows, in: S. Chibbaro, J.-P. Minier (Eds.), *Stochastic Methods in Fluid Mechanics*, Springer, 2014, pp. 137–165.
- [79] P.B. Warren, Dissipative particle dynamics, *Curr. Opin. Colloid Interface Sci.* 3 (6) (1997) 620–624.
- [80] P. Espagnol, Dissipative particle dynamics with energy conservation, *Europhys. Lett.* 40 (1997) 631–636.
- [81] Malevanets, R. Kapral, Mesoscopic Multi-particle Collision Model for Fluid Flow and Molecular Dynamics, in: M. Karttunen, I. Vattulainen, A. Lukkarine (Eds.), *Novel Methods in Soft Matter Simulations*, Springer, 2004, pp. 116–149.
- [82] R. Kapral, Multiparticle Collision Dynamics: Simulation of Complex Systems of Mesoscales, in: S.A. Rice (Ed.), *Advances in Chemical Physics*, vol. 140, John Wiley & Sons, 2008, pp. 89–146.
- [83] G. Gompper, T. Ihle, K. Kroll, R.G. Winkler, Multi-particle collision dynamics—a particle-based mesoscale simulation approach to the hydrodynamics of complex fluids, *Adv. Polym. Sci.* 221 (2009) 1–87.
- [84] G.A. Bird, *Molecular Gas Dynamics and The Direct Simulation of Gas Flows*, Clarendon Oxford, 1994.
- [85] W. Wagner, Stochastic models in kinetic theory, *Phys. Fluids* 23 (2011) 030602.
- [86] S. Succi, *The Lattice Boltzmann Equation for fluid dynamics and beyond*, first ed., Oxford University Press, 2001.
- [87] S. Chen, G.D. Doolen, Lattice Boltzmann method for fluid flows, *Annu. Rev. Fluid Mech.* 30 (1998) 329–364.
- [88] L.B. Lucy, A numerical approach to the testing of the fission hypothesis, *Astron. J.* 82 (1977) 10131024.
- [89] R.A. Gingold, J.J. Monaghan, Smoothed particle hydrodynamics: theory and application to non-spherical stars, *Mon. Not. R. Astron. Soc.* 181 (1977) 375389.
- [90] J.J. Monaghan, Smoothed particle hydrodynamics and its diverse applications, *Annu. Rev. Fluid Mech.* 44 (2012) 323–346.
- [91] D. Violeau, *Fluid Mechanics and the SPH Method. Theory and Applications*, Oxford University Press, 2012.
- [92] P. Espagnol, M. Revenga, Smoothed dissipative particle dynamics, *Phys. Rev. E* 67 (2003) 026705.
- [93] X.Y. Hu, N.A. Adams, A multi-phase SPH method for macroscopic and mesoscopic flows, *J. Comput. Phys.* 213 (2) (2006) 844–861.
- [94] K. Szewc, J. Pozorski, J.-P. Minier, Simulations of single bubbles rising through viscous liquids using Smoothed Particle Hydrodynamics, *Int. J. Multiph. Flow* 50 (2013) 98–105.
- [95] K. Szewc, J. Pozorski, J.-P. Minier, On the problem of spurious fragmentation of interfaces in the multiphase Smoothed Particle Hydrodynamics method, *Internat. J. Numer. Methods Engrg.* 103 (9) (2015) 625–649.
- [96] K. Szewc, J. Pozorski, J.-P. Minier, Analysis of the the incompressibility constraint in Smoothed Particle Hydrodynamics, *Internat. J. Numer. Methods Engrg.* 92 (4) (2012) 343–369.
- [97] P. Espagnol, Dissipative particle dynamics, in: S. Yip (Ed.), *Handbook of Materials Modeling*, Springer, 2005, pp. 2503–2512.
- [98] N.A. Gatsonis, R. Potamis, J. Yang, A smooth dissipative particle dynamics method for domains with arbitrary-geometry solid boundaries, *J. Comput. Phys.* 256 (2014) 441–464.

- [99] K. Muller, D.A. Fedosov, G. Gompper, Smoothed dissipative particle dynamics with angular momentum conservation, *J. Comput. Phys.* 281 (2015) 301–315.
- [100] H.C. Öttinger, *Beyond Equilibrium Thermodynamics*, John Wiley & Sons, 2005.
- [101] A. Vazquez-Quesada, M. Ellero, P. Espagnol, Consistent scaling of thermal fluctuations in smoothed dissipative particle dynamics, *J. Chem. Phys.* 130 (2009) 034901.
- [102] H. Tennekes, J.L. Lumley, *A First Course in Turbulence*, first ed., The MIT Press, 1972.
- [103] S.B. Pope, Self-conditioned fields for large-eddy simulations of turbulent flows, *J. Fluid Mech.* 652 (2010) 139–169.
- [104] P.J. Colucci, F.A. Jaberi, P. Givi, S.B. Pope, Filtered density function for large eddy simulation of turbulent reacting flows, *Phys. Fluids* 10 (1998) 499–515.
- [105] F.A. Jaberi, P.J. Colucci, S. James, P. Givi, S.B. Pope, Filtered mass density function for large-eddy simulation of turbulent reactive flows, *J. Fluid Mech.* 401 (1999) 85–121.
- [106] L.Y.M. Gicquel, P. Givi, F.A. Jaberi, S.B. Pope, Velocity filtered density function for large eddy simulation of turbulent flows, *Phys. Fluids* 14 (3) (2002) 1196–1213.
- [107] M.R.H. Sheikhi, T.G. Drozda, P. Givi, S.B. Pope, Velocity-scalar filtered density function for large eddy simulation of turbulent flows, *Phys. Fluids* 15 (8) (2003) 2321–2337.
- [108] M.R.H. Sheikhi, P. Givi, S.B. Pope, Velocity-scalar filtered mass density function for large eddy simulation of turbulent reactive flows, *Phys. Fluids* 19 (2007) 095106.
- [109] M.R.H. Sheikhi, P. Givi, S.B. Pope, Frequency-velocity-scalar filtered mass density function for large eddy simulation of turbulent flows, *Phys. Fluids* 21 (2009) 075102.
- [110] D.C. Haworth, S.B. Pope, A generalized Langevin model for turbulent flows, *Phys. Fluids* 30 (1986) 387.
- [111] S.B. Pope, On the relationship between stochastic Lagrangian models of turbulence and second-order closures, *Phys. Fluids* 6 (2) (1994) 973–985.
- [112] M. Muradoglu, S.B. Pope, D.A. Caughey, The hybrid method for the PDF equations of turbulent reactive flows: consistency, conditions and correction algorithms, *J. Comput. Phys.* 172 (2001) 841–878.
- [113] P. Jenny, S.B. Pope, M. Muradoglu, D.A. Caughey, A hybrid algorithm for the joint PDF equation of turbulent reactive flows, *J. Comput. Phys.* 166 (2001) 218–252.
- [114] M.H. Kalos, P.A. Whitlock, *Monte Carlo Methods*. Vol 1: Basics, Wiley-Interscience, New-York, 1986.
- [115] S. Chibbaro, J.-P. Minier, The FDF or LES/PDF method for turbulent two-phase flows, *J. Phys.: Conf. Ser.* 318 (4) (2011) 042049.
- [116] S.B. Pope, Simple models of turbulent flows, *Phys. Fluids* 23 (2011) 011301.
- [117] T.S. Lundgren, Distribution functions in the statistical theory of turbulence, *Phys. Fluids* 10 (1967) 969–975.
- [118] T.S. Lundgren, Model equation for nonhomogeneous turbulence, *Phys. Fluids* 12 (1969) 485–497.
- [119] J.-P. Minier, J. Pozorski, Derivation of a PDF model for turbulent flows based on principles from statistical physics, *Phys. Fluids* 9 (6) (1997) 1748–1753.
- [120] W. Pan, A.M. Tartakovsky, Dissipative particle dynamics models for colloid transport in porous media, *Adv. Water Resour.* 58 (2013) 41–48.
- [121] V. Pryamitsyn, V. Ganesan, A coarse-grained explicit solvent simulation of rheology of colloidal suspensions, *J. Chem. Phys.* 122 (2005) 104906.
- [122] S. Chen, N. Phan-Thien, B.C. Khoo, X.J. Fan, Flow around spheres by dissipative particle dynamics, *Phys. Fluids* 18 (10) (2006) 103605.
- [123] M. Whittle, K.P. Travis, Dynamic simulations of colloids by core-modified dissipative particle dynamics, *J. Chem. Phys.* 132 (2010) 124906.
- [124] W. Pan, D.A. Fedosov, G.E. Karniadakis, B. Caswell, Hydrodynamic interactions for single dissipative-particle-dynamics particles and their clusters and filaments, *Phys. Rev. E* 78 (4) (2008) 046706.
- [125] W. Pan, B. Caswell, G.E. Karniadakis, Rheology, microstructure and migration in Brownian colloidal suspensions, *Langmuir* 26 (1) (2010) 130–142.
- [126] N. Mai-Duy, N. Phan-Thien, B.C. Khoo, Investigation of particles size effects in Dissipative Particle Dynamics (DPD) modelling of colloidal suspensions, *Comput. Phys. Comm.* 189 (2015) 37–46.
- [127] X. Bian, S. Litvinov, M. Ellero, N.A. Adams, Multiscale modeling of particle in suspension with smoothed dissipative particle dynamics, *Phys. Fluids* 24 (2012) 012002.
- [128] D.A. Fedosov, M. Peltomaki, G. Gompper, Deformation and dynamics of red blood cells in flow through cylindrical microchannels, *Soft Matter* 10 (2014) 4258.
- [129] N.B. Martyus, Study of a dissipative particle dynamics based approach for modeling suspensions, *J. Rheol.* 49 (2005) 401–424.
- [130] W. Pan, I.V. Pivkin, G.E. Karniadakis, Single-particle hydrodynamics in DPD: A new formulation, *Europhys. Lett.* 84 (2008) 10012.
- [131] A.J.C. Ladd, Numerical simulations of particulate suspensions via a discretized Boltzmann equation. I. Theoretical foundation, *J. Fluid Mech.* 271 (1994) 285–309.
- [132] A.J.C. Ladd, Numerical simulations of particulate suspensions via a discretized Boltzmann equation. II. Numerical results, *J. Fluid Mech.* 271 (1994) 311–339.
- [133] I.V. Pivkin, B. Caswell, G.E. Karniadakis, Mesoscopic simulation methods for studying flow and transport in electric fields in micro- and nanochannels, in: R.T. Kelly (Ed.), *Advances in Microfluidics*, InTech, 2012, pp. 97–126 (Chapter 5).
- [134] E.W. Llewellin, Lbflow: An extensible lattice Boltzmann framework for the simulation of geophysical flows. Part I: theory and implementation, *Comput. Geosci.* 16 (2010) 115–122.
- [135] P. Ahlrichs, B. Dunweg, Simulation of a single polymer chain in solution by combining Lattice Boltzmann and molecular dynamics, *J. Chem. Phys.* 111 (1999) 8225.
- [136] R.B. Bird, C.F. Curtiss, R.C. Armstrong, O. Hassager, *Dynamics of Polymeric Liquids*, second ed., John Wiley and Sons, New-York, 1987.
- [137] M. Doi, S.F. Edwards, *The Theory of Polymer Dynamics*, Oxford Science Publications, New-York, 1986.
- [138] P. De Gennes, *Introduction to Polymer Dynamics*, Cambridge University Press, 1990.
- [139] S.-P. Fu, Y.-N. Young, S. Jiang, Efficient Brownian dynamics simulation of DNA molecules with hydrodynamic interactions in linear flows, *Phys. Rev. E* 91 (063008) (2015).
- [140] D.L. Ermak, J.A. McCammon, Brownian dynamics with hydrodynamic interaction, *J. Chem. Phys.* 69 (1978) 1352–1360.
- [141] J.S. Marshall, Particle aggregation and capture by walls in a particulate aerosol channel flow, *J. Aerosol Sci.* 38 (2007) 333–351.
- [142] J.S. Marshall, Discrete-element modeling of particulate aerosol flows, *J. Comput. Phys.* 228 (2009) 1541–1561.
- [143] J.S. Marshall, S. Li, *Adhesive Particle Flow. A Discrete-Element Approach*, Cambridge University Press, New-York, 2014.
- [144] C. Marchioli, Physics and Modelling of Particle Deposition and Resuspension in Wall-Bounded Turbulence, in: J.-P. Minier, J. Pozorski (Eds.), *Particles in Wall-Bounded Turbulent Flows: Deposition, Re-Suspension and Agglomeration*, Springer, 2017, pp. 151–208.
- [145] C. Marchioli, A. Soldati, Mechanisms for particle transfer and segregation in a turbulent boundary layer, *J. Fluid Mech.* 468 (2002) 283–315.
- [146] C. Marchioli, A. Giusti, M.V. Salvetti, A. Soldati, A direct numerical simulation of particle wall transfer in upward turbulent pipe flow, *Int. J. Multiph. Flow* 29 (2003) 1017–1038.
- [147] A. Soldati, C. Marchioli, Physics and modelling of turbulent particle deposition and entrainment: Review of a systematic study, *Int. J. Multiph. Flow* 35 (2009) 827–839.
- [148] J.G.M. Kuerten, Subgrid modeling in particle-laden channel flow, *Phys. Fluids* 18 (2006) 025108.
- [149] O. Simonin, Statistical and continuum modelling of turbulent reactive particulate flows, in: *Lecture Series 2000-06*, Von Karman Institute for Fluid Dynamics, 2000.

- [150] K. Furutsu, On the statistical theory of electromagnetic waves in a fluctuating medium, *J. Res. Natl. Inst. Stand. Technol.* D67 (1963) 303.
- [151] E.A. Novikov, Functionals and the random-force method in turbulence theory, *Sov. Phys. JETP* 20 (3) (1965) 1290–1294.
- [152] M.D. Donsker, On function space integrals, in: W.T. Martin, I. Segal (Eds.), *Analysis in Function Space*, the MIT Press, 1964, pp. 17–30.
- [153] J. Pozorski, J.-P. Minier, Probability density function modelling of dispersed two-phase turbulent flows, *Phys. Rev. E* 59 (1) (1998) 855–863.
- [154] J.-P. Minier, E. Peirano, S. Chibbaro, PDF model based on Langevin equation for polydispersed two-phase flows applied to a bluff-body gas-solid flow, *Phys. Fluids* 16 (7) (2004) 2419.
- [155] K. Sala, J.S. Marshall, Stochastic vortex structure method for modeling particle clustering and collisions in homogeneous turbulence, *Phys. Fluids* 25 (2013) 103301.
- [156] N.G. Van Kampen, Langevin-like equation with colored noise, *J. Stat. Phys.* 54 (5–6) (1989) 1289–1308.
- [157] H. Haken, Synergetics: an overview, *Rep. Progr. Phys.* 52 (1989) 515–533.
- [158] T. Kuroiwa, K. Miyazaki, Brownian motion with multiplicative noises revisited, *J. Phys. A* 47 (1) (2014).
- [159] F. Lundell, L.D. Söderberg, P.H. Alfredsson, Fluid Mechanics of papermaking, *Annu. Rev. Fluid Mech.* 43 (2011) 195–217.
- [160] C. Marchioli, M. Fantoni, A. Soldati, Orientation, distribution and deposition of elongated, inertial fibers in turbulent channel flow, *Phys. Fluids* 22 (2010) 033301.
- [161] L. Zhao, C. Marchioli, H.I. Andersson, Slip velocity of rigid fibers in turbulent channel flow, *Phys. Fluids* 26 (2014) 063302.
- [162] S. Sasic, A.-E. Almstedt, Dynamics of fibres in a turbulent flow field - a particle-level simulation technique, *Int. J. Multiph. Flow* 31 (2010) 1058–1064.
- [163] J.A. Olson, R.J. Kerekes, The motion of fibres in turbulent flow, *J. Fluid Mech.* 377 (1998) 47–64.
- [164] J.A. Olson, The motion of fibres in turbulent flow, stochastic simulation of isotropic homogeneous turbulence, *Int. J. Multiph. Flow* 27 (2001) 2083–2103.
- [165] S.S. Girimaji, S.B. Pope, A diffusion model for velocity gradients in turbulence, *Phys. Fluids A* 2 (1990) 242–256.
- [166] A.G. Lamorgese, S.B. Pope, P.K. Yeung, B.L. Sawford, A conditionally cubic-Gaussian stochastic Lagrangian model for acceleration in isotropic turbulence, *J. Fluid Mech.* 582 (2007) 423–448.
- [167] S.B. Pope, A stochastic Lagrangian model for acceleration in turbulent flows, *Physics of Fluids* 14 (7) (2002) 2360–2375.
- [168] A. Bragg, D.C. Swailes, R. Skartlien, Particle transport in a turbulent boundary layer: non-local closures for particle dispersion tensors accounting for particle-wall interactions, *Phys. Fluids* 24 (103304) (2012).
- [169] M.S. Anand, S.B. Pope, Diffusion behind a line source behind a grid turbulence, in: L.J.S. Bradbury et al. (Ed.), *Proceedings of Turbulent Shear Flows 4*, Springer, Berlin, 1985, pp. 46–61.
- [170] Z. Warhaft, Interference of line sources in grid turbulence, *J. Fluid Mec.* 44 (1984) 363–387.
- [171] C. Cercignani, *The Boltzmann Equation and its Applications*, Springer New-York, 1988.
- [172] W. Wagner, Stochastic models and Monte-Carlo algorithms for Boltzmann-type equations, in: *Monte Carlo and Quasi-Monte Carlo Methods 2002*, Springer Berlin, 2004, pp. 129–153.
- [173] A. Eibeck, W. Wagner, Stochastic interacting particle systems and nonlinear kinetic equations, *Ann. Appl. Probab.* 13 (2003) 845.
- [174] N. Fournier, S. Mischler, On a discrete Boltzmann-Smoluchowski equation with rates bounded in the velocity variables, *Comm. Math. Sci. Suppl.* 1 (2004).
- [175] N. Fournier, S. Mischler, A Boltzmann equation for elastic, inelastic and coalescing collisions, *J. Math. Pure Appl.* 84 (2005) 1173–1234.
- [176] F.A. Williams, *Combustion Theory*, Addison-Wesley Publishing Company, 1985.
- [177] J. Bec, S.S. Ray, E.W. Saw, H. Homann, Abrupt growth of large aggregates by correlated coalescences in turbulent flows, *Phys. Rev. E* 93 (2016) 031102(R).
- [178] M. Elimelech, J. Gregory, X. Jia, R.A. Williams, *Particle Deposition and Aggregation: Measurement, Modelling and Simulation*, Butterworth Heinemann, 1995.
- [179] S.K. Friedlander, *Smoke, Dust, and Haze. Fundamentals of Aerosol Dynamics*, second ed., Oxford University Press, 2000.
- [180] P.G. Saffman, J.S. Turner, On the collision of drops in turbulent clouds, *J. Fluid Mech.* 1 (1) (1956) 16–30.
- [181] B.K. Brunk, D.L. Koch, L.W. Lion, Hydrodynamic pair diffusion in isotropic random velocity fields with application to turbulent coagulation, *Phys. Fluids* 9 (1997) 2670–2691.
- [182] B.K. Brunk, D.L. Koch, L.W. Lion, Turbulent coagulation of colloidal particles, *J. Fluid Mech.* 364 (1998) 81–113.
- [183] J. Bec, H. Homann, S.S. Ray, Gravity-driven enhancement of heavy particle clustering in turbulent flow, *Phys. Rev. Lett.* 112 (184501) (2014).
- [184] S. Sundaram, L.R. Collins, Numerical considerations in simulating a turbulent suspension of finite-volume particles, *J. Comput. Phys.* 124 (1996) 337–350.
- [185] O. Ayala, B. Rosa, L.-P. Wang, W.W. Grabowski, Effects of turbulence on the geometric collision rate of sedimenting droplets. Part 1. Results from direct numerical simulation, *New J. Phys.* 10 (2008) 075015.
- [186] L.-P. Wang, B. Rosa, H. Gao, G. He, G. Jin, Turbulent collision of inertial particles: point-particle based, hybrid simulations and beyond, *Int. J. Multiph. Flow* 35 (2009) 854–867.
- [187] B. Rosa, H. Parishani, O. Ayala, W.W. Grabowski, L.-P. Wang, Kinematic and dynamic collision statistics of cloud droplets from high-resolution simulations, *New J. Phys.* 15 (2013) 045032.
- [188] M. Chen, K. Kontomaris, J.B. McLaughlin, Direct numerical simulation of droplet collisions in a turbulent channel flow. Part I: collision algorithm, *Int. J. Multiph. Flow* 19 (1998) 1079–1103.
- [189] H. Sigurgeirsson, A. Stuart, W.L. Wan, Algorithms for particle-field simulations with collisions, *J. Comput. Phys.* 172 (2001) 766–807.
- [190] N.M. Kovalchuk, V.M. Starov, Aggregation in colloidal suspensions: effects of colloidal forces and hydrodynamic interactions, *Adv. Colloid Interface Sci.* 179–182 (2012) 99–106.
- [191] M. Mohaupt, J.-P. Minier, A. Tanière, A new approach for the detection of particle interactions for large-inertia and colloidal particles in a turbulent flow, *Int. J. Multiph. Flow* 37 (2011) 746–755.
- [192] C. Henry, J.-P. Minier, J. Pozorski, G. Lefèvre, A new stochastic approach for the simulation of agglomeration between colloidal particles, *Langmuir* 29 (2013) 13694–13707.
- [193] C. Henry, J.-P. Minier, M. Mohaupt, C. Profeta, J. Pozorski, A. Tanière, A stochastic approach for the simulation of collisions between colloidal particles at large time steps, *Int. J. Multiph. Flow* 61 (2014) 94–107.